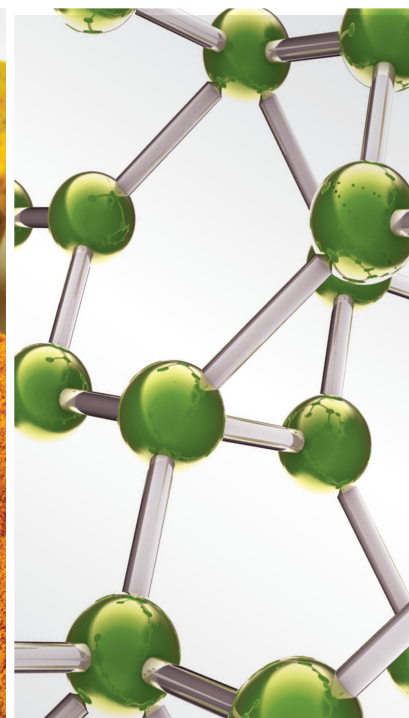
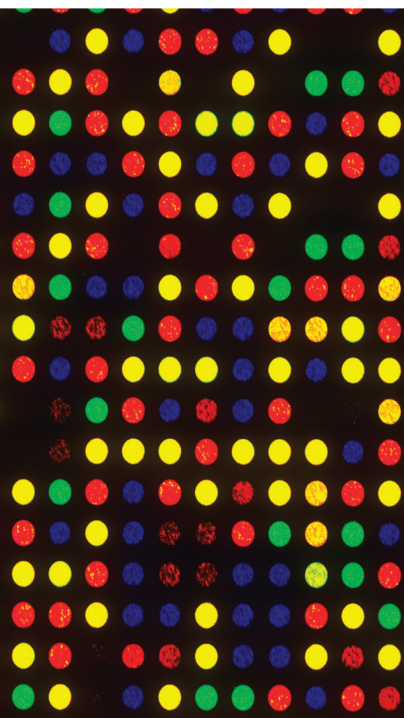


Artificial Intelligence Device Development in Complementary and Alternative Medicine 2022

Lead Guest Editor: Wen Si

Guest Editors: Lu Zhang and Lei Jiang





**Artificial Intelligence Device Development in
Complementary and Alternative Medicine 2022**

Evidence-Based Complementary and Alternative Medicine

**Artificial Intelligence Device
Development in Complementary and
Alternative Medicine 2022**

Lead Guest Editor: Wen Si

Guest Editors: Lu Zhang and Lei Jiang



Copyright © 2023 Hindawi Limited. All rights reserved.

This is a special issue published in "Evidence-Based Complementary and Alternative Medicine." All articles are open access articles distributed under the Creative Commons Attribution License, which permits unrestricted use, distribution, and reproduction in any medium, provided the original work is properly cited.

Chief Editor

Jian-Li Gao , China

Associate Editors

Hyunsu Bae , Republic of Korea
Raffaele Capasso , Italy
Jae Youl Cho , Republic of Korea
Caigan Du , Canada
Yuewen Gong , Canada
Hai-dong Guo , China
Kuzhuvelil B. Harikumar , India
Ching-Liang Hsieh , Taiwan
Cheorl-Ho Kim , Republic of Korea
Victor Kuete , Cameroon
Hajime Nakae , Japan
Yoshiji Ohta , Japan
Olumayokun A. Olajide , United Kingdom
Chang G. Son , Republic of Korea
Shan-Yu Su , Taiwan
Michał Tomczyk , Poland
Jenny M. Wilkinson , Australia

Academic Editors

Eman A. Mahmoud , Egypt
Ammar AL-Farga , Saudi Arabia
Smail Aazza , Morocco
Nahla S. Abdel-Azim, Egypt
Ana Lúcia Abreu-Silva , Brazil
Gustavo J. Acevedo-Hernández , Mexico
Mohd Adnan , Saudi Arabia
Jose C Adsuar , Spain
Sayeed Ahmad, India
Touqeer Ahmed , Pakistan
Basiru Ajiboye , Nigeria
Bushra Akhtar , Pakistan
Fahmida Alam , Malaysia
Mohammad Jahoor Alam, Saudi Arabia
Clara Albani, Argentina
Ulysses Paulino Albuquerque , Brazil
Mohammed S. Ali-Shtayeh , Palestinian Authority
Ekram Alias, Malaysia
Terje Alraek , Norway
Adolfo Andrade-Cetto , Mexico
Letizia Angiolella , Italy
Makoto Arai , Japan

Daniel Dias Rufino Arcanjo , Brazil
Duygu AĞAGÜNDÜZ , Turkey
Neda Baghban , Iran
Samra Bashir , Pakistan
Rusliza Basir , Malaysia
Jairo Kenupp Bastos , Brazil
Arpita Basu , USA
Mateus R. Beguelini , Brazil
Juana Benedí, Spain
Samira Boulbaroud, Morocco
Mohammed Bourhia , Morocco
Abdelhakim Bouyahya, Morocco
Nunzio Antonio Cacciola , Italy
Francesco Cardini , Italy
María C. Carpinella , Argentina
Harish Chandra , India
Guang Chen, China
Jianping Chen , China
Kevin Chen, USA
Mei-Chih Chen, Taiwan
Xiaojia Chen , Macau
Evan P. Cherniack , USA
Giuseppina Chianese , Italy
Kok-Yong Chin , Malaysia
Lin China, China
Salvatore Chirumbolo , Italy
Hwi-Young Cho , Republic of Korea
Jeong June Choi , Republic of Korea
Jun-Yong Choi, Republic of Korea
Kathrine Bisgaard Christensen , Denmark
Shuang-En Chuang, Taiwan
Ying-Chien Chung , Taiwan
Francisco José Cidral-Filho, Brazil
Daniel Collado-Mateo , Spain
Lisa A. Conboy , USA
Kieran Cooley , Canada
Edwin L. Cooper , USA
José Otávio do Amaral Corrêa , Brazil
Maria T. Cruz , Portugal
Huantian Cui , China
Giuseppe D'Antona , Italy
Ademar A. Da Silva Filho , Brazil
Chongshan Dai, China
Laura De Martino , Italy
Josué De Moraes , Brazil

Arthur De Sá Ferreira , Brazil
Nunziatina De Tommasi , Italy
Marinella De leo , Italy
Gourav Dey , India
Dinesh Dhamecha, USA
Claudia Di Giacomo , Italy
Antonella Di Sotto , Italy
Mario Dioguardi, Italy
Jeng-Ren Duann , USA
Thomas Efferth , Germany
Abir El-Alfy, USA
Mohamed Ahmed El-Esawi , Egypt
Mohd Ramli Elvy Suhana, Malaysia
Talha Bin Emran, Japan
Roger Engel , Australia
Karim Ennouri , Tunisia
Giuseppe Esposito , Italy
Tahereh Eteraf-Oskouei, Iran
Robson Xavier Faria , Brazil
Mohammad Fattahi , Iran
Keturah R. Faurot , USA
Piergiorgio Fedeli , Italy
Laura Ferraro , Italy
Antonella Fioravanti , Italy
Carmen Formisano , Italy
Hua-Lin Fu , China
Liz G Müller , Brazil
Gabino Garrido , Chile
Safoora Gharibzadeh, Iran
Muhammad N. Ghayur , USA
Angelica Gomes , Brazil
Elena González-Burgos, Spain
Susana Gorzalczany , Argentina
Jiangyong Gu , China
Maruti Ram Gudavalli , USA
Jian-You Guo , China
Shanshan Guo, China
Narcís Gusi , Spain
Svein Haavik, Norway
Fernando Hallwass, Brazil
Gajin Han , Republic of Korea
Ihsan Ul Haq, Pakistan
Hicham Harhar , Morocco
Mohammad Hashem Hashempur , Iran
Muhammad Ali Hashmi , Pakistan

Waseem Hassan , Pakistan
Sandrina A. Heleno , Portugal
Pablo Herrero , Spain
Soon S. Hong , Republic of Korea
Md. Akil Hossain , Republic of Korea
Muhammad Jahangir Hossen , Bangladesh
Shih-Min Hsia , Taiwan
Changmin Hu , China
Tao Hu , China
Weicheng Hu , China
Wen-Long Hu, Taiwan
Xiao-Yang (Mio) Hu, United Kingdom
Sheng-Teng Huang , Taiwan
Ciara Hughes , Ireland
Attila Hunyadi , Hungary
Liaqat Hussain , Pakistan
Maria-Carmen Iglesias-Osma , Spain
Amjad Iqbal , Pakistan
Chie Ishikawa , Japan
Angelo A. Izzo, Italy
Satveer Jagwani , USA
Rana Jamous , Palestinian Authority
Muhammad Saeed Jan , Pakistan
G. K. Jayaprakasha, USA
Kyu Shik Jeong, Republic of Korea
Leopold Jirovetz , Austria
Jeeyoun Jung , Republic of Korea
Nurkhalida Kamal , Saint Vincent and the
Grenadines
Atsushi Kameyama , Japan
Kyungsu Kang, Republic of Korea
Wenyi Kang , China
Shao-Hsuan Kao , Taiwan
Nasiara Karim , Pakistan
Morimasa Kato , Japan
Kumar Katragunta , USA
Deborah A. Kennedy , Canada
Washim Khan, USA
Bonglee Kim , Republic of Korea
Dong Hyun Kim , Republic of Korea
Junghyun Kim , Republic of Korea
Kyungho Kim, Republic of Korea
Yun Jin Kim , Malaysia
Yoshiyuki Kimura , Japan

Nebojša Kladar , Serbia
Mi Mi Ko , Republic of Korea
Toshiaki Kogure , Japan
Malcolm Koo , Taiwan
Yu-Hsiang Kuan , Taiwan
Robert Kubina , Poland
Chan-Yen Kuo , Taiwan
Kuang C. Lai , Taiwan
King Hei Stanley Lam, Hong Kong
Fanuel Lampiao, Malawi
Ilaria Lampronti , Italy
Mario Ledda , Italy
Harry Lee , China
Jeong-Sang Lee , Republic of Korea
Ju Ah Lee , Republic of Korea
Kyu Pil Lee , Republic of Korea
Namhun Lee , Republic of Korea
Sang Yeoup Lee , Republic of Korea
Ankita Leekha , USA
Christian Lehmann , Canada
George B. Lenon , Australia
Marco Leonti, Italy
Hua Li , China
Min Li , China
Xing Li , China
Xuqi Li , China
Yi-Rong Li , Taiwan
Vuanghao Lim , Malaysia
Bi-Fong Lin, Taiwan
Ho Lin , Taiwan
Shuibin Lin, China
Kuo-Tong Liou , Taiwan
I-Min Liu, Taiwan
Suhuan Liu , China
Xiaosong Liu , Australia
Yujun Liu , China
Emilio Lizarraga , Argentina
Monica Loizzo , Italy
Nguyen Phuoc Long, Republic of Korea
Zaira López, Mexico
Chunhua Lu , China
Ângelo Luís , Portugal
Anderson Luiz-Ferreira , Brazil
Ivan Luzardo Luzardo-Ocampo, Mexico

Michel Mansur Machado , Brazil
Filippo Maggi , Italy
Juraj Majtan , Slovakia
Toshiaki Makino , Japan
Nicola Malafrente, Italy
Giuseppe Malfa , Italy
Francesca Mancianti , Italy
Carmen Mannucci , Italy
Juan M. Manzanque , Spain
Fatima Martel , Portugal
Carlos H. G. Martins , Brazil
Maulidiani Maulidiani, Malaysia
Andrea Maxia , Italy
Avijit Mazumder , India
Isac Medeiros , Brazil
Ahmed Mediani , Malaysia
Lewis Mehl-Madrona, USA
Ayikoé Guy Mensah-Nyagan , France
Oliver Micke , Germany
Maria G. Miguel , Portugal
Luigi Milella , Italy
Roberto Miniero , Italy
Letteria Minutoli, Italy
Prashant Modi , India
Daniel Kam-Wah Mok, Hong Kong
Changjong Moon , Republic of Korea
Albert Moraska, USA
Mark Moss , United Kingdom
Yoshiharu Motoo , Japan
Yoshiki Mukudai , Japan
Sakthivel Muniyan , USA
Saima Muzammil , Pakistan
Benoit Banga N'guessan , Ghana
Massimo Nabissi , Italy
Siddavaram Nagini, India
Takao Namiki , Japan
Srinivas Nammi , Australia
Krishnadas Nandakumar , India
Vitaly Napadow , USA
Edoardo Napoli , Italy
Jorddy Neves Cruz , Brazil
Marcello Nicoletti , Italy
Eliud Nyaga Mwaniki Njagi , Kenya
Cristina Nogueira , Brazil

Sakineh Kazemi Noureini , Iran
Rômulo Dias Novaes, Brazil
Martin Offenbaecher , Germany
Oluwafemi Adeleke Ojo , Nigeria
Olufunmiso Olusola Olajuyigbe , Nigeria
Luís Flávio Oliveira, Brazil
Mozaniel Oliveira , Brazil
Atolani Olubunmi , Nigeria
Abimbola Peter Oluyori , Nigeria
Timothy Omara, Austria
Chiagoziem Anariochi Otuechere , Nigeria
Sokcheon Pak , Australia
Antônio Palumbo Jr, Brazil
Zongfu Pan , China
Siyaram Pandey , Canada
Niranjan Parajuli , Nepal
Gunhyuk Park , Republic of Korea
Wansu Park , Republic of Korea
Rodolfo Parreira , Brazil
Mohammad Mahdi Parvizi , Iran
Luiz Felipe Passero , Brazil
Mitesh Patel, India
Claudia Helena Pellizzon , Brazil
Cheng Peng, Australia
Weijun Peng , China
Sonia Piacente, Italy
Andrea Pieroni , Italy
Haifa Qiao , USA
Cláudia Quintino Rocha , Brazil
DANIELA RUSSO , Italy
Muralidharan Arumugam Ramachandran,
Singapore
Manzoor Rather , India
Miguel Rebollo-Hernanz , Spain
Gauhar Rehman, Pakistan
Daniela Rigano , Italy
José L. Rios, Spain
Francisca Rius Diaz, Spain
Eliana Rodrigues , Brazil
Maan Bahadur Rokaya , Czech Republic
Mariangela Rondanelli , Italy
Antonietta Rossi , Italy
Mi Heon Ryu , Republic of Korea
Bashar Saad , Palestinian Authority
Sabi Saheed, South Africa

Mohamed Z.M. Salem , Egypt
Avni Sali, Australia
Andreas Sandner-Kiesling, Austria
Manel Santafe , Spain
José Roberto Santin , Brazil
Tadaaki Satou , Japan
Roland Schoop, Switzerland
Sindy Seara-Paz, Spain
Veronique Seidel , United Kingdom
Vijayakumar Sekar , China
Terry Selfe , USA
Arham Shabbir , Pakistan
Suzana Shahar, Malaysia
Wen-Bin Shang , China
Xiaofei Shang , China
Ali Sharif , Pakistan
Karen J. Sherman , USA
San-Jun Shi , China
Insop Shim , Republic of Korea
Maria Im Hee Shin, China
Yukihiro Shoyama, Japan
Morry Silberstein , Australia
Samuel Martins Silvestre , Portugal
Preet Amol Singh, India
Rajeev K Singla , China
Kuttulebbai N. S. Sirajudeen , Malaysia
Slim Smaoui , Tunisia
Eun Jung Sohn , Republic of Korea
Maxim A. Solovchuk , Taiwan
Young-Jin Son , Republic of Korea
Chengwu Song , China
Vanessa Steenkamp , South Africa
Annarita Stringaro , Italy
Keiichiro Sugimoto , Japan
Valeria Sulsen , Argentina
Zewei Sun , China
Sharifah S. Syed Alwi , United Kingdom
Orazio Tagliatalata-Scafati , Italy
Takashi Takeda , Japan
Gianluca Tamagno , Ireland
Hongxun Tao, China
Jun-Yan Tao , China
Lay Kek Teh , Malaysia
Norman Temple , Canada

Kamani H. Tennekoon , Sri Lanka
Seong Lin Teoh, Malaysia
Menaka Thounaojam , USA
Jinhui Tian, China
Zipora Tietel, Israel
Loren Toussaint , USA
Riaz Ullah , Saudi Arabia
Philip F. Uzor , Nigeria
Luca Vanella , Italy
Antonio Vassallo , Italy
Cristian Vergallo, Italy
Miguel Vilas-Boas , Portugal
Aristo Vojdani , USA
Yun WANG , China
QIBIAO WU , Macau
Abraham Wall-Medrano , Mexico
Chong-Zhi Wang , USA
Guang-Jun Wang , China
Jinan Wang , China
Qi-Rui Wang , China
Ru-Feng Wang , China
Shu-Ming Wang , USA
Ting-Yu Wang , China
Xue-Rui Wang , China
Youhua Wang , China
Kenji Watanabe , Japan
Jintanaporn Wattanathorn , Thailand
Silvia Wein , Germany
Katarzyna Winska , Poland
Sok Kuan Wong , Malaysia
Christopher Worsnop, Australia
Jih-Huah Wu , Taiwan
Sijin Wu , China
Xian Wu, USA
Zuoqi Xiao , China
Rafael M. Ximenes , Brazil
Guoqiang Xing , USA
JiaTuo Xu , China
Mei Xue , China
Yong-Bo Xue , China
Haruki Yamada , Japan
Nobuo Yamaguchi, Japan
Junqing Yang, China
Longfei Yang , China

Mingxiao Yang , Hong Kong
Qin Yang , China
Wei-Hsiung Yang, USA
Swee Keong Yeap , Malaysia
Albert S. Yeung , USA
Ebrahim M. Yimer , Ethiopia
Yoke Keong Yong , Malaysia
Fadia S. Youssef , Egypt
Zhilong Yu, Canada
RONGJIE ZHAO , China
Sultan Zahiruddin , USA
Armando Zarrelli , Italy
Xiaobin Zeng , China
Y Zeng , China
Fangbo Zhang , China
Jianliang Zhang , China
Jiu-Liang Zhang , China
Mingbo Zhang , China
Jing Zhao , China
Zhangfeng Zhong , Macau
Guoqi Zhu , China
Yan Zhu , USA
Suzanna M. Zick , USA
Stephane Zingue , Cameroon

Contents

Toward Recognition of Easily Confused TCM Herbs on the Smartphone Using Hierarchical Clustering Convolutional Neural Network

Kun-Chan Lan , Tzu-Hao Tsai , Min-Chun Hu, Juei-Chun Weng, Jun-Xiang Zhang, and Yuan-Shiun Chang

Research Article (16 pages), Article ID 9095488, Volume 2023 (2023)

A Comparison Study of Doctor-Patient Internet Interactions in Traditional and Modern Medicine: Empirical Evidence from Online Healthcare Communities

Song Cao , Xiang Gao , Shuzhen Niu , and Qian Wei 

Research Article (13 pages), Article ID 4619914, Volume 2022 (2022)

Deep Learning Multi-label Tongue Image Analysis and Its Application in a Population Undergoing Routine Medical Checkup

Tao Jiang , Zhou Lu , Xiaojuan Hu, Lingzhi Zeng, Xuxiang Ma, Jingbin Huang, Ji Cui, Liping Tu, Changle Zhou, Xinghua Yao , and Jiatuso Xu 

Research Article (12 pages), Article ID 3384209, Volume 2022 (2022)

The Psychological Recovery of Patients in the Context of Virtual Reality Application by a Complementary Medicine Scheme Based on Visual Art

Bolin Li  and Meilin Shen 

Review Article (5 pages), Article ID 7358597, Volume 2022 (2022)

Formation Mechanism of Microbial Diversity in Artificial Intelligence Devices due to Intermediate Disturbance by Low-Dose UV Radiation for Complementary Medicine

Junjie Ye, Yang Yang, Juanyi Wang, Jingyu Han, Lihong Zhang, Tianrun Gong, Yi Zhang, Xiaodong Xing, and Chen Dong 

Research Article (11 pages), Article ID 2874835, Volume 2022 (2022)

Medication Regularity of Traditional Chinese Medicine in the Treatment of Aplastic Anemia Based on Data Mining

Nanxi Dong , Xujie Zhang , Dijiong Wu , Zhiping Hu , Wenbin Liu , Shu Deng , and Baodong Ye 

Research Article (10 pages), Article ID 1605359, Volume 2022 (2022)

An Initial Study on Automated Acupoint Positioning for Laser Acupuncture

Kun-Chan Lan, Chang-Yin Lee, Guan-Sheng Lee, Tzu-Hao Tsai, Yu-Chen Lee , and Chih-Yu Wang 

Research Article (9 pages), Article ID 8997051, Volume 2022 (2022)

Application of Virtual Reality Technology in Clinical Practice, Teaching, and Research in Complementary and Alternative Medicine

Huifang Guan , Yan Xu , and Dexi Zhao 

Review Article (12 pages), Article ID 1373170, Volume 2022 (2022)

**Establishing a Regulatory Science System for Supervising the Application of Artificial Intelligence for
Traditional Chinese Medicine: A Methodological Framework**

Ying He , Qian Wen , Ying Wang , Juan Li, Ning Li, Rongjiang Jin, Nian Li , and Yonggang Zhang 
Research Article (6 pages), Article ID 9680203, Volume 2022 (2022)

Research Article

Toward Recognition of Easily Confused TCM Herbs on the Smartphone Using Hierarchical Clustering Convolutional Neural Network

Kun-Chan Lan ¹, Tzu-Hao Tsai ¹, Min-Chun Hu,² Juei-Chun Weng,¹ Jun-Xiang Zhang,¹ and Yuan-Shiun Chang³

¹The Department of Computer Science and Information Engineering, National Cheng Kung University, Tainan 701, Taiwan

²The Department of Computer Science and Information Engineering, National Tsing Hua University, Hsinchu 300044, Taiwan

³The Department of Chinese Pharmaceutical Sciences and Chinese Medicine Resources, China Medical University, Taichung 40402, Taiwan

Correspondence should be addressed to Kun-Chan Lan; klan@csie.ncku.edu.tw

Received 9 May 2022; Revised 30 December 2022; Accepted 5 April 2023; Published 5 May 2023

Academic Editor: Ammar AL-Farga

Copyright © 2023 Kun-Chan Lan et al. This is an open access article distributed under the Creative Commons Attribution License, which permits unrestricted use, distribution, and reproduction in any medium, provided the original work is properly cited.

Background and Objective. The use of Chinese herbal medicines (CHMs) for treatment plays an important role in traditional Chinese medicine (TCM). However, some herbs are easily confused with the others because their shapes/textures look similar and they could have totally different utilities. Recently, deep learning has attracted great attention for the application of image recognition and could be useful for TCM herb identification. **Methods.** For recognizing easily-confused TCM herbs on a smartphone, we propose a CHM recognition system using hierarchical clustering convolutional neural networks (HCNNs) based on the affinity propagation clustering method. **Results.** We implement our system on the smartphone and show recognition accuracy close to 98%, based on a dataset of 65 kinds of herbs (including 12 easy-confused herbs pairs). We also investigate the effect of different parameters (e.g., selection of clustering algorithms for HCNNs, types of smartphone, and number of layers in the neural network) on the system performance. **Conclusions.** In this work, we proposed a hierarchical clustering convolutional neural network (HCNN) method to distinguish similar TCM herbs with a high accuracy. We also showed the usefulness of applying the data augmentation techniques when implementing the proposed system for a variety of smartphones.

1. Introduction

Chinese herbal medicines (CHMs) play an important role in TCM. Chinese herbs primarily come from different parts of the plants, including leaves, roots, stems, flowers, and seeds. The core idea of CHM is to restore the balance of the human body to achieve a state of health. While CHM has become an increasingly popular method of treatment globally, for most people, it is difficult to recognize different Chinese herbs and know the properties of each kind of herb. Moreover, some herbs are easily confused with the others because their shapes/textures look similar to the others but they could have totally different utilities. For example, Astragali Mongolici Radix [1] is commonly used in CHMs treatment

because of its efficacy in strengthening the immune system. However, some people will sell Hedysari Radix [2] as a replacement for Astragali Mongolici Radix because its flavor is tastier and the price is cheaper than Astragali Mongolici Radix. Hedysari Radix has similar shapes/textures as Astragali Mongolici Radix, but with lower efficacy for boosting the immune system. Other examples of easily-confused herbs are Diocoreae Rhizoma [3] and Manihot Esculenta [4]. The former is commonly used to maintain the function of the lung and kidney while the latter could be poisonous if not properly used. In Table 1, we listed some commonly-used Chinese herbs [5].

Chinese herbs are commonly used for food preparation and play a very vital role in Chinese medicine. For the

TABLE 1: Different types of Chinese herbs.

Categorization		Herb names (example)	Treating diseases
Four natures	Hot, warm	Zingiberis rhizome	Abdominal cramp, diarrhea
		Angelicae Sinensis Radix	Chronic constipation, menstrual disorders
	Cool, cold	Rehmanniae Radix	Cardiovascular diseases
		Gypsum	Bronchial asthma
Neutral	Poria	Promoting urination, edema	
Five flavors	Acrid	Gypsum	Bronchial asthma
	Sweet	Cyperis rhizoma	Emotional disorders
	Bitter	Armeniacae semen	Dissolve phlegm, relieve cough
		Atractylodis rhizoma	Palpitation, edema
	Sour	Schisandrae Fructus	Spontaneous sweating, night sweating
	Salty	Scrophulariae Radix	Chronic pharyngitis
		Pumex	Sticky sputum
	Ecklonia thallus	Goiter, scrofula	

reasons of safety and efficiency, it is important to have proper recognition of these herbs. However, given that some herbs have similar shapes/textures, most people find it difficult to recognize them without extensive experiences or expert knowledge. Therefore, it might be necessary to develop a system to facilitate people to recognize the herbs and understand the properties of these herbs.

Although there are many illustration handbooks of Chinese herbs around, it is time-consuming and inefficient to use these books to distinguish these easily-confused herbs. On the other hand, given the popularity of the smartphone, it can serve as a convenient vision-based-measurement (VBM) [6] instrument for recognizing the herbs. While a few prior studies attempted to use computer vision techniques for herb recognition [7–10], their results are generally limited in the following aspects: (1) relying on hand-crafted features, (2) based on a small data set (e.g., only 18 herbs in [7, 8]), (3) not targeting on easily-confused herbs, and (4) low recognition accuracy. In this work, we aim to build a system on top of the smartphone based on convolutional neural network (CNN) for recognition of easily confused TCM herbs. More specifically, we proposed a hierarchical CNN method to classify easily confused herbs by first clustering similar herbs into a group (using the affinity propagation algorithm [11]) and building a CNN model for these groups. We then train a CNN model for each group to classify herbs in the same group.

The contributions of this paper are in two folds. First, we set out to develop a system for automatic recognition of easily confused CHMs on the smartphone. Users just need to take pictures of CHMs and the system will show information of the herbs on the phones. The proposed system could potentially be used for the following applications: (1) knowing whether the herb is genuine or not and (2) understanding the properties of the herbs. As far as we know, this is the first TCM herb recognition App implemented on a phone. Second, we proposed a hierarchical CNN (HCNN) method for recognizing 24 easily-confused herbs. Our initial results show classification accuracy close to 98% (a 5% improvement in comparison to the naive CNN). Note that, while our proposed HCNN architecture is not entirely new, we investigate the effect of different parameters (e.g., selection of clustering algorithms for HCNN, types of

smartphone, and different CNN models) on the system performance. We believe that these insights could be of interests to readers of this journal.

2. Related Work

2.1. Herb Recognition Based on Its Smell and Taste. Luo et al. [12] developed an electronic nose that simulates biological olfactory organs to achieve the physiological function of the nose through machine learning. Their work can identify 6 types of Pungent CHMs. In addition, they proposed a method using the electronic tongue to identify taste information of five different CHMs [13]. However, these prior works have the same problem. First of all, such instruments are not easy to be built or obtain. In addition, some time-consuming preprocessing needs to be performed first before one can employ such approaches to identify different herbs (e.g., herbs need to be grinded into powders and heated for 30 minutes).

2.2. Traditional Vision Techniques for Herb Recognition. Herb recognition using computer vision techniques is generally more cost-effective than methods based on taste or smell. Some of them are based on hand-crafted features. Tao et al. [7, 8] utilized texture to classify 18 different CHMs. Cai et al. [9] and Liu et al. [10] used color, texture, and shape feature descriptors to identify 3 and 8 different CHMs, respectively. Finally, there are also some prior work on leaves and flowers recognition [14–17], using techniques such as local binary pattern (LBP) [18], histogram of oriented gradients (HOG) [19], and scale-invariant feature transform (SIFT) [20].

2.3. CNN for Herb Recognition. The problem in using traditional hand-crafted feature descriptors is that one needs to know what kinds of features are appropriate for classification. However, it might be difficult to find the representative features to identify the differences between a set of easily confused herbs. Deep learning has recently become increasingly popular, and many studies have shown that it can outperform many traditional machine learning methods for various image recognition tasks [21]. In particular, CNN has

attracted strong interest from both academia and industry since the ImageNet dataset became available. Sun and Qian [22] used CNN for CHMs recognition by collecting a total of 5,523 images from 95 categories. The average accuracy rate of their results is about 71%. They did not particularly consider the use of CNN for recognizing easily confused herbs though (e.g., as shown in Table 2, there are only two easily confused herbs pairs in their dataset). In our work, we propose a method based on HCNN to distinguish 12 pairs of easily confused herbs.

2.4. Hierarchical CNN. The concept of hierarchical CNN was introduced in some prior work. Yan et al. [23] implemented HD-CNN (hierarchical deep CNN) that breaks down an image recognition task into two levels. To separate simple classes from each other, an HD-CNN first uses a CNN classifier to classify the image data into K coarse categories. More complicated classes are redirected downstream to fine classifiers with divisions that concentrate on confusing classes. This work showed an improvement of 2.28% on the accuracy rate based on CIFAR100 and ImageNet datasets. They used spectral clustering to cluster their data into K coarse categories.

Mao et al. [24] evaluated their HCNN approach on the German traffic sign recognition benchmark (GTSRB). They proposed a CNN-oriented family clustering (CFC) algorithm to partition the traffic signs into K families. In these studies, the number of clusters (i.e., K) needs to be pre-defined which are more suitable for the fixed dataset like ImageNet. In our work, we employ affinity propagation (AP) to cluster easily confused herbs. AP does not require the number of clusters to be determined in advance. Given that currently there is no large herb image database available (the image data used in this study are all created by ourselves), AP is more suitable to us since we can then expand our database over time without worrying about changing our algorithm.

The introduction should be succinct, with no sub-headings. Limited figures may be included only if they are truly introductory, and contain no new results.

3. System Framework

We first started our experiments using a naive CNN to recognize some easily confused herbs. But then, we realized that some of these herbs look very similar and we were unable to obtain good results for these herbs. Therefore, in this work, we implement a hierarchical CNN method for these easily confused herbs.

Figure 1 shows our hierarchical clustering CNN architecture. In the training phase, we first cluster similar-looking herbs into the same group. Next, we create a two-layer CNN. The first layer is to create a model for cluster classification while the second layer is to classify herbs in the same cluster. In the testing phase, the system will first decide which cluster the input image belongs to, and then use the trained model in the second layer to recognize the herb within the identified cluster.

In this paper, we apply the AP algorithm [11] to cluster similar herbs into a group. AP is based on the concept of message passing between data points so that each data will

find the most suitable ones as its exemplars (i.e., cluster center or cluster head) and how much they are suitable as exemplars. Unlike traditional clustering algorithms such as k -means, AP does not require the number of clusters to be determined in advance. More specifically,

- (1) For our training data, we randomly sample some images from each kind of herb, and then, we extract their features to calculate the similarity matrix [11] as the input of the AP algorithm.
- (2) After performing the AP algorithm, each data point (i.e., herb) decides its exemplar. It is possible that the same kind of herb might choose different exemplars, so we adopt a majority-vote mechanism to decide the final exemplar for each kind of herb.
- (3) If the final exemplar of two kinds of the herb are the same, we cluster them into the same group.

In the first layer of our CNN-based clustering model, we utilize an open-source deep learning framework named Caffe [25], and we pretrain our CHMs model over 1 million ImageNet images of 1,000 categories. The architecture of CaffeNet is shown in Figure 2. It consists of eight layers, of which the first five layers are convolutional layers. Three max-pooling layers follow the first, second, and fifth convolutional layers, respectively. The last three layers are fully-connected layers. The number of neurons in the last fully-connected layer of our clustering model is set to the number of herb groups. The function of the first layer of our CNN-based clustering model is to decide which group the input herb belongs to.

The function of the second layer of our HCNN model is to recognize the target herb from an herb group. In the second layer, for each herb group, we train a CNN model similar to the first layer. In other words, there are multiple second-layer models, and each of them is corresponding to an herb group. Each herb group will contain at least one herb based on the clustering results.

4. Results

4.1. Experimental Environments. We evaluated our proposed hierarchical CNN model using CaffeNet [25] based on the AlexNet model [21], and all experiments were run on 64 bit Ubuntu 14.04 with an INTEL i7-4790 CPU, a GEFORCE GTX 1060 GPU, and 16 GB RAM. In particular, BLVC CaffeNet [25] is used for training the CNN model. The trained model is later ported to the phone for the testing phase.

4.2. CHM Dataset. In this work, we select 12 pairs of easily-confused CHMs from a book named “Illustrations of Commonly Misused Chinese Crude Drug Species in Taiwan” [26] for our experiments, as shown in Figure 3. The image data used for our experiments were taken by an iPhone6. One hundred images are taken for each herb so that our dataset contains 2,400 images in total. 1,440 images are used for training and the rest are used for testing. The name of the herbs is shown in Table 3. There are a total of twelve easily-confused herbs pairs in this dataset (e.g., A1/A2).

TABLE 2: Comparison of vision-based techniques for herb recognition.

	# of category	# of easily confused herbs pair	Methods	Implemented on smartphones
Tao et al. [8]	18	1	Hand-crafted	No
Liu et al. [10]	8	0	Hand-crafted	No
Sun and Qian [22]	95	2	CNN	No
Ours	65	12	Hierarchical clustering CNN	Yes

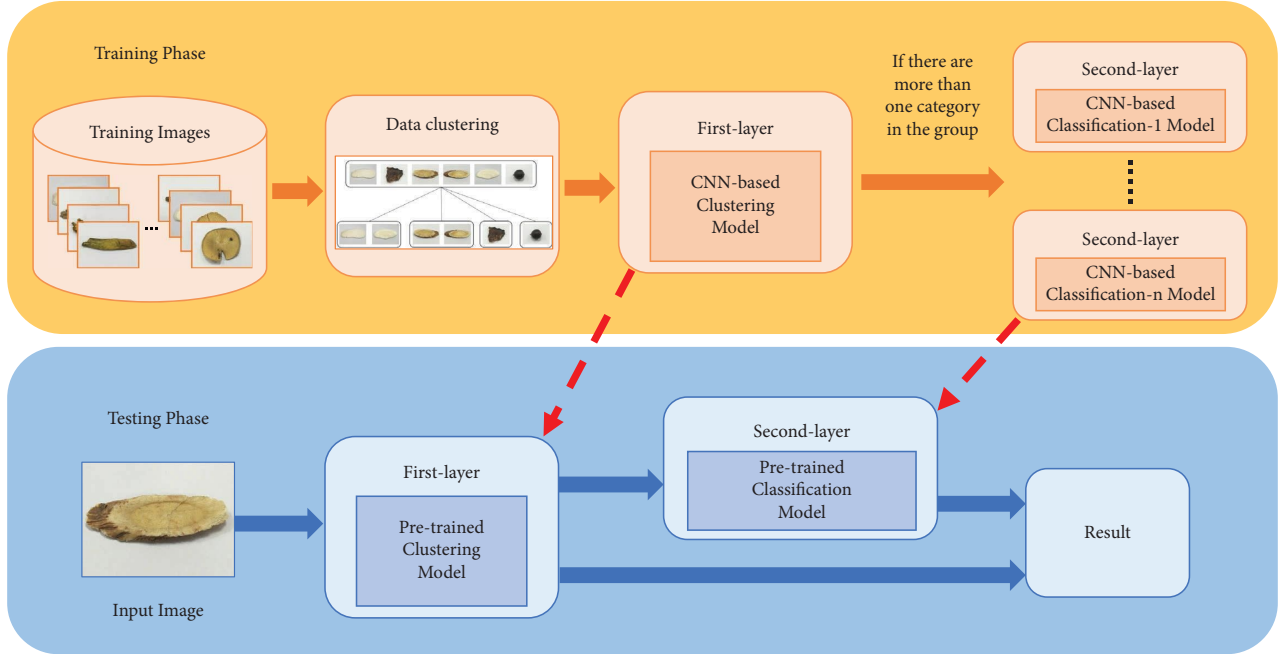


FIGURE 1: Hierarchical clustering CNN framework for CHM recognition.

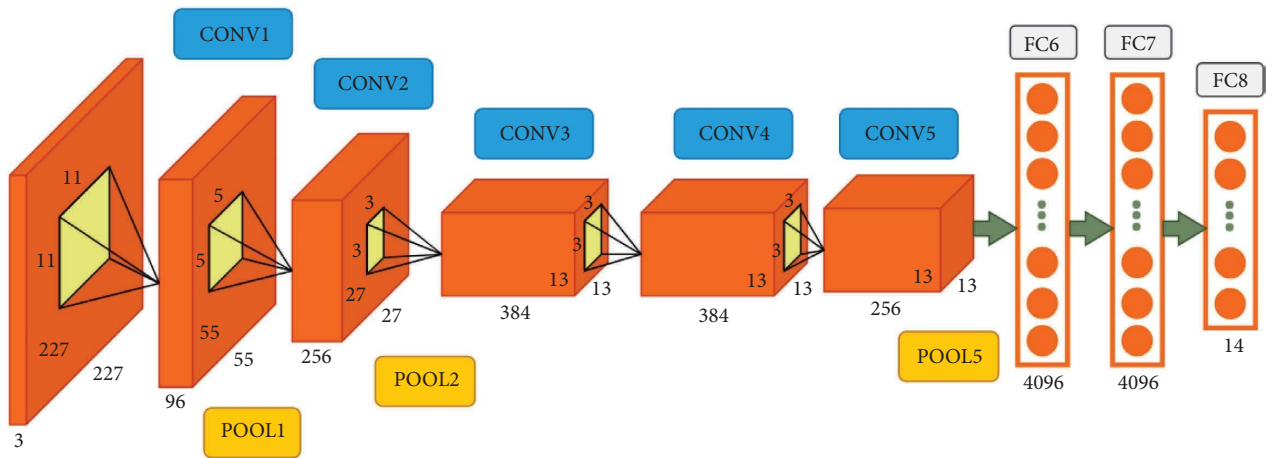


FIGURE 2: The architecture of our CaffeNet model in the first layer.

4.3. *The Benefit of Using Transfer Learning on the Accuracy of Our CNN Model.* BVLC CaffeNet provides an option called fine-tune which allows one to copy the model parameters from a pretrained CNN model (otherwise, all the parameters in the CNN model are initialized with random values). Given our dataset is small, it is expected to be beneficial from using some pretrained parameters to initialize our model.

This is known as the transfer learning method. We utilize the pretrained parameters from the model.

ImageNet work [21] is used to initialize our CHMs model. Figure 4 shows the average accuracy with and without the use of transfer learning. It clearly shows that the model can quickly converge with much higher accuracy when the fine-tune option is enabled.

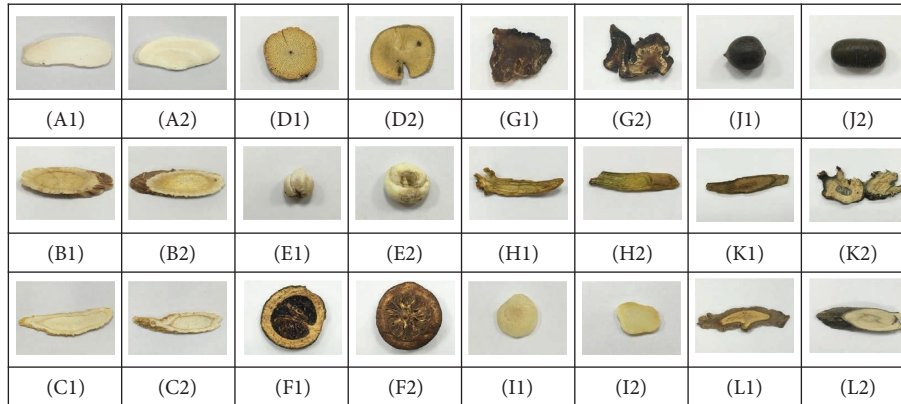


FIGURE 3: Twenty four kinds of CHMs collected by ourselves.

TABLE 3: The name of 24 kinds of herbs.

Numbers	Names
A1	Diocoreae Rhizoma
A2	Manihot esculenta
B1	Astragali Mongolici Radix
B2	Hedysari Radix
C1	Ginseng Radix
C2	Panacis Quinquefolii Radix
D1	Clematidia Armandii Caulis
D2	Aristolochia Manshuriensis Caulis
E1	Fritillariae Cirrhosae Bulbus
E2	Fritillariae Ussuriensis Bulbus
F1	Poncirus Trifoliata Fructus
F2	Aurantii Immaturus Fructus
G1	Aconiti Radix
G2	Aconiti Kusnezoffii Radix
H1	Scutellariae Baicalensis Radix
H2	Scutellariae Amoena Radix
I1	Pinelliae Rhizoma
I2	Typhonium Rhizoma
J1	Nelumbinis Fructus
J2	Caesalpinia Fructus
K1	Cyathulae Radix
K2	Strobilanthes Radix
L1	Isatis Radix
L2	Baphicacanthus Radix

4.4. Comparison of the Hand-Crafted Method with CNN for Herb Recognition. Some prior studies employed hand-crafted features for the herb recognition. In this study, we compare three different feature extraction methods, including HOG [19], LBP [18], and BOW SIFT [20], with CNN. For HOG and LBP implementation, the cell size is set to 32. Because the number of SIFT feature points in each image is not fixed, we first extract the SIFT feature points of all the training data and run them through K-means clustering (with the center set to 200) so that all images can have the same dimensional vector. Finally, a pretrained SVM [27] model to be used for herb classification.

For the CNN experiment, we first rescale the image size to $256 * 256$ and then randomly crop $224 * 224$ patches from these images to increase the number of training data and reduce overfitting. We enable the fine-tune and set the

number of neurons to be 24 in the last layer to match the number of easily confused herbs in our data. Our model is trained using stochastic gradient descent with a batch size of 60 samples (we set the momentum to 0.9, weight decay to 0.0005, and gamma to 0.1). An equal learning rate is used for all layers and the start learning rate is initialized at 0.0001.

Table 4 shows the results using hand-crafted methods and the CNN method. We employ five-fold cross-validation to calculate the accuracy. Among the traditional hand-crafted methods, LBP achieves the highest accuracy at 86.85%. This is not surprising since texture is an important feature for CHMs and LBP is powerful for texture classification. The accuracy of using CNN is 95.69%, which is much better than that of all the hand-crafted feature descriptors methods.

In addition, we compare two different CNN models, CaffeNet [25] and VGG16 [28]. The latter is used by a prior study for CHMs recognition [28]. VGG16 uses a deeper structure than CaffeNet so that it takes more time for training and testing, as shown in Table 5 (the same parameters are used for both the models). The execution time of VGG16 is about three times longer but the accuracy of both models is similar. Therefore, we decide to use a simple model like CaffeNet in this work because it runs faster with acceptable accuracy, as shown in Table 4.

Figure 5 shows the accuracy of detection for all 24 different herbs using a confusion matrix. We find that some herbs are more easily mistaken for another herb, such as B1 and B2 as well as C1 and C2. These recognition errors are reasonable though since they are easily confused even for human eyes. In the next section, we show that these classification errors can be improved with the proposed hierarchical clustering CNN method.

4.5. Performance of Hierarchical Clustering CNN Method.

In this work, we employ the use of HCNN to reduce recognition errors. We propose the use of the AP algorithm [11] to automatically cluster similar herbs into a group. In this section, we compare the performance of AP clustering and manual clustering which is based on an illustrated handbook of easily confused herbs [26]. As shown in Figure 6, twenty-

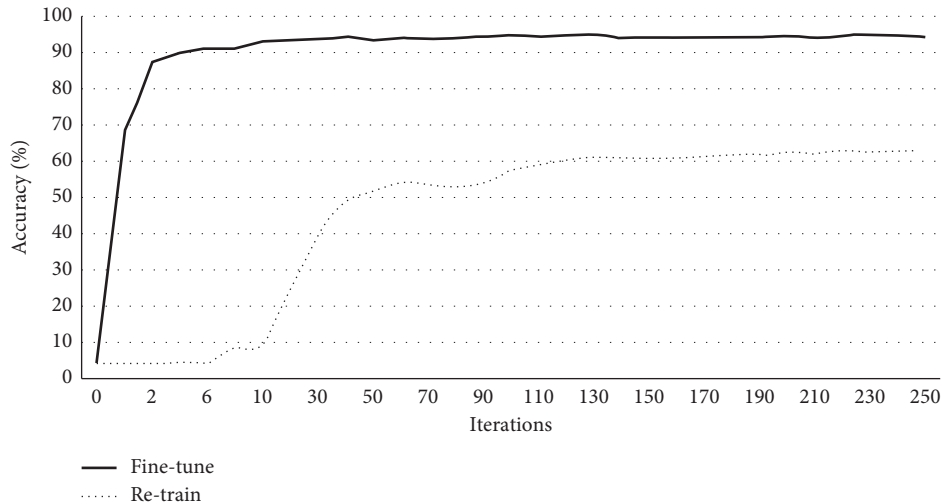


FIGURE 4: The effect of fine-tune on the performance of the CNN model.

TABLE 4: Accuracy of the hand-crafted method vs. CNN method.

Methods	Accuracy (%)
CNN (CaffeNet)	95.65
CNN (VGG16)	95.63
LBP + SVM	86.85
HOG + SVM	75.31
BOW SIFT + SVM	70.83

TABLE 5: Training and testing time of the CaffeNet and VGG16 models.

Methods	Training time (s)	Testing time (s)
CNN (CaffeNet)	408	1.9306
CNN (VGG16)	1.704	5.9577

four herbs are divided into 14 groups according to the illustrated handbook.

For the implementation of the AP algorithm, we calculate the similarity matrix based on LBP features because it has the best classification accuracy among all hand-crafted features we tried. We randomly sample 20 images for each herb to run AP. The results of AP clustering are shown in Figure 7 for comparison with the result of manual clustering in Figure 6. Figure 8 shows the confusion matrix of the cluster classification using CNN based on the AP algorithm (i.e., if a herb is classified into the correct cluster), and Figure 9 shows the confusion matrix for classifying the herb within a cluster based on the classification results shown in Figure 8.

Furthermore, we compare the performance of the AP algorithm with other clustering algorithms. Table 6 shows the herb classification accuracy from ten experiments using the other automatic clustering algorithm including k-means [29] and spectral clustering [30]. Both of them require the number of clusters to be predetermined before running the algorithm. Here, we let the number of clusters (i.e., K value) be 14 which matches with the manual clustering using the illustrated handbook. Table 6 shows that the AP algorithm

has a more stable and higher accuracy. For spectral clustering, some of the results are even worse than naive CNN (i.e., CNN without hierarchical clustering, as shown in Table 4). This is due to that spectral clustering first uses a Laplacian matrix to reduce the dimension, and then employs the k-means algorithm to do the clustering. Therefore, it might lose some information during the dimension reduction. In addition, its results are sensitive to the decision of the initial K value. A bad choice of K might lead it to a local optimal solution.

Table 7 shows a detailed comparison of the recognition accuracy for each herb between the CNN method and the proposed HCNN method. We find a significant improvement for some herbs such as B1 and H2 in addition to a general improvement of average accuracy (about 2%) when the HCNN method is employed. The results from AP clustering are very similar to that of manual clustering based on the illustrated handbook (which is considered as the ground truth for herb clustering in this study).

4.6. The Effect of the Number of CNN Layers. The above results are based on CNN architecture of 8 layers. A recent trend is to perform model compression (e.g., by reducing the number of layers of a deep neural network) for resource-limited devices like smartphones [31]. We next want to explore the use of a smaller number of layers for CNN training. Specifically,

- (1) Eight layers: 5 convolutional layers and 3 fully-connected layers (the original)
- (2) Six layers: 5 convolutional layers and 1 fully-connected layer
- (3) Four layers: 3 convolutional layers and 1 fully-connected layer.

We find that the recognition accuracy drops as we reduce the number of CNN layers. The average accuracy is about 94% for 6-layer CNN and 90% for 4-layer CNN.

	A1	A2	B1	B2	C1	C2	D1	D2	E1	E2	F1	F2	G1	G2	H1	H2	I1	I2	J1	J2	K1	K2	L1	L2	
A1	200	0	0	0	0	0	0	0	0	0	0	0	0	0	0	0	0	0	0	0	0	0	0	0	100.00%
A2	4	196	0	0	0	0	0	0	0	0	0	0	0	0	0	0	0	0	0	0	0	0	0	0	98.00%
B1	0	0	162	27	8	2	0	0	0	0	0	0	0	0	0	0	0	0	0	0	0	1	0	0	81.00%
B2	0	0	14	186	0	0	0	0	0	0	0	0	0	0	0	0	0	0	0	0	0	0	0	0	93.00%
C1	0	0	4	0	180	16	0	0	0	0	0	0	0	0	0	0	0	0	0	0	0	0	0	0	90.00%
C2	0	0	0	0	17	183	0	0	0	0	0	0	0	0	0	0	0	0	0	0	0	0	0	0	91.50%
D1	0	0	0	0	0	0	196	4	0	0	0	0	0	0	0	0	0	0	0	0	0	0	0	0	98.00%
D2	0	0	0	0	0	0	4	196	0	0	0	0	0	0	0	0	0	0	0	0	0	0	0	0	98.00%
E1	0	0	0	0	0	0	0	0	193	7	0	0	0	0	0	0	0	0	0	0	0	0	0	0	96.50%
E2	0	0	0	0	0	0	0	0	11	189	0	0	0	0	0	0	0	0	0	0	0	0	0	0	94.50%
F1	0	0	0	0	0	0	0	0	0	0	200	0	0	0	0	0	0	0	0	0	0	0	0	0	100.00%
F2	0	0	0	0	0	0	0	0	0	0	4	196	0	0	0	0	0	0	0	0	0	0	0	0	98.00%
G1	0	0	0	0	0	0	0	0	0	0	0	0	196	4	0	0	0	0	0	0	0	0	0	0	98.00%
G2	0	0	0	0	0	0	0	0	0	0	0	0	14	186	0	0	0	0	0	0	0	0	0	0	93.00%
H1	0	0	0	0	0	0	0	0	0	0	0	0	0	0	187	13	0	0	0	0	0	0	0	0	93.50%
H2	0	0	0	0	0	0	0	0	0	0	0	0	0	0	14	177	0	0	0	0	8	1	0	0	88.50%
I1	0	0	0	0	0	0	0	0	3	0	0	0	0	0	0	0	188	9	0	0	0	0	0	0	94.00%
I2	0	0	0	0	0	0	0	0	0	0	0	0	0	0	0	0	5	195	0	0	0	0	0	0	97.50%
J1	0	0	0	0	0	0	0	0	0	0	0	0	0	0	0	0	0	0	200	1	0	0	0	0	99.50%
J2	0	0	0	0	0	0	0	0	0	0	0	0	0	0	0	0	0	0	0	0	200	0	0	0	100.00%
K1	0	0	0	0	0	0	0	0	0	0	0	0	0	0	0	0	0	0	0	0	0	198	2	0	99.00%
K2	0	0	0	0	0	0	0	0	0	0	0	0	0	2	0	0	0	0	0	0	0	198	0	0	99.00%
L1	0	0	4	0	2	0	0	0	0	0	0	0	0	0	1	0	0	0	0	0	0	189	4	0	94.50%
L2	0	0	0	0	0	0	0	0	0	0	0	0	0	0	0	0	0	0	0	0	0	0	200	0	100.00%

FIGURE 5: Classification results for 24 easily-confused herbs using the naive CNN method. The ones marked in gray are classification errors. For example, 4 images of A2 are classified into A1.

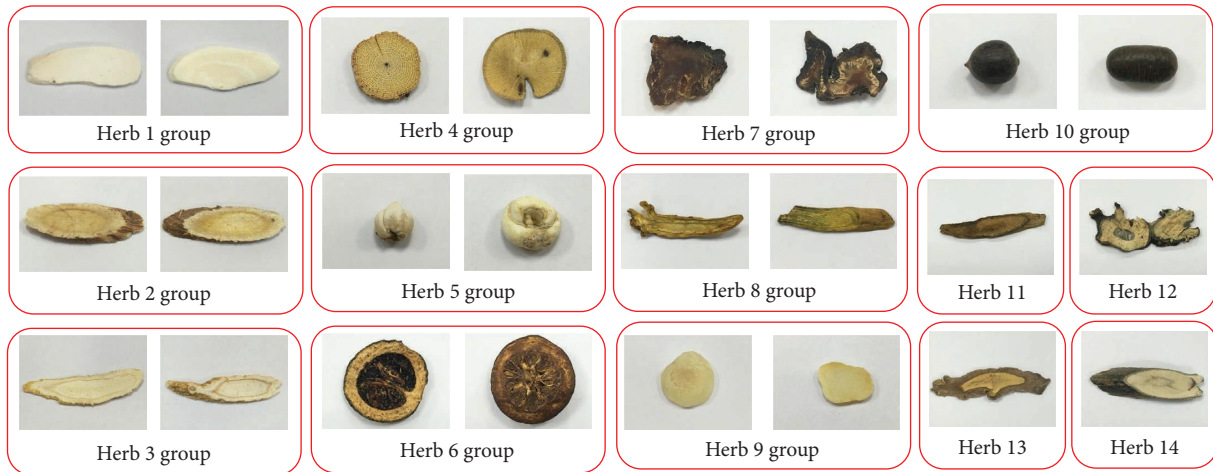


FIGURE 6: Manual clustering of 24 CHMs into 14 groups based on the illustrated handbook (group 1 to 10 are the set of easily-confused herbs, while groups 11, 12, 13, and 14 only contain a single herb).

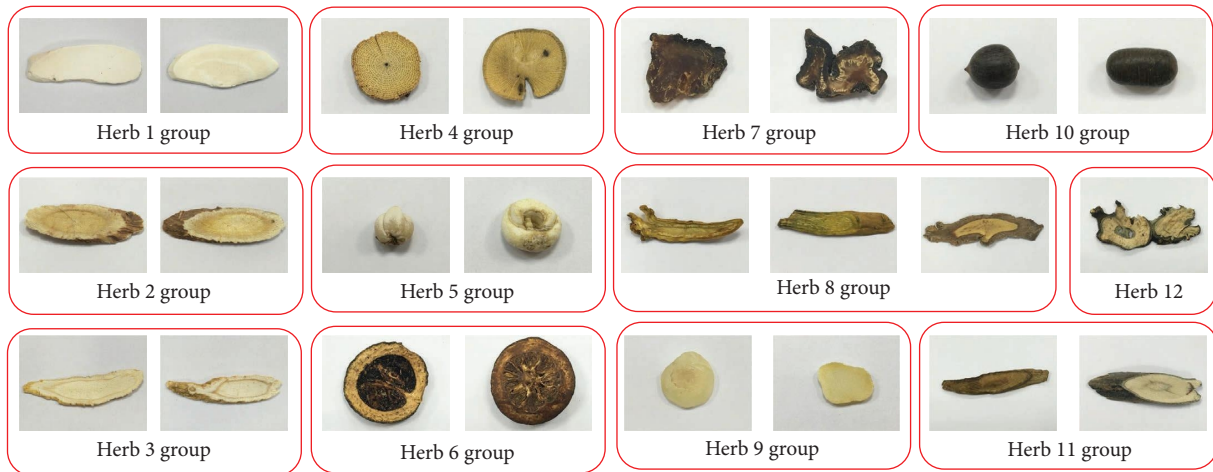


FIGURE 7: AP clusters 24 kind of CHMs into 12 groups (group 12 contains only a single herb).

	1	2	3	4	5	6	7	8	9	10	11	12
1	400	0	0	0	0	0	0	0	0	0	0	0
2	0	398	2	0	0	0	0	0	0	0	0	0
3	0	1	399	0	0	0	0	0	0	0	0	0
4	0	0	0	400	0	0	0	0	0	0	0	0
5	0	0	0	0	400	0	0	0	0	0	0	0
6	0	0	0	0	0	400	0	0	0	0	0	0
7	0	0	0	0	0	0	400	0	0	0	0	0
8	0	0	2	0	0	0	0	594	0	0	4	0
9	0	0	0	0	1	0	0	0	399	0	0	0
10	0	0	0	0	0	0	0	0	0	400	0	0
11	0	0	0	0	0	0	0	0	0	0	400	0
12	0	0	0	0	0	0	0	0	0	0	0	200

FIGURE 8: The confusion matrix for the clustering model using AP algorithm. The erroneous classification is marked in gray.

	A1	A2	B1	B2	C1	C2	D1	D2	E1	E2	F1	F2	G1	G2	H1	H2	I1	I2	J1	J2	K1	K2	L1	L2		
A1	200	0	0	0	0	0	0	0	0	0	0	0	0	0	0	0	0	0	0	0	0	0	0	0	0	100.00%
A2	0	200	0	0	0	0	0	0	0	0	0	0	0	0	0	0	0	0	0	0	0	0	0	0	0	100.00%
B1	0	0	184	14	2	0	0	0	0	0	0	0	0	0	0	0	0	0	0	0	0	0	0	0	0	92.00%
B2	0	0	10	190	0	0	0	0	0	0	0	0	0	0	0	0	0	0	0	0	0	0	0	0	0	95.00%
C1	0	0	1	0	189	10	0	0	0	0	0	0	0	0	0	0	0	0	0	0	0	0	0	0	0	94.50%
C2	0	0	0	0	14	186	0	0	0	0	0	0	0	0	0	0	0	0	0	0	0	0	0	0	0	93.00%
D1	0	0	0	0	0	0	198	2	0	0	0	0	0	0	0	0	0	0	0	0	0	0	0	0	0	99.00%
D2	0	0	0	0	0	0	1	199	0	0	0	0	0	0	0	0	0	0	0	0	0	0	0	0	0	99.50%
E1	0	0	0	0	0	0	0	0	197	3	0	0	0	0	0	0	0	0	0	0	0	0	0	0	0	98.50%
E2	0	0	0	0	0	0	0	0	4	196	0	0	0	0	0	0	0	0	0	0	0	0	0	0	0	98.00%
F1	0	0	0	0	0	0	0	0	0	0	200	0	0	0	0	0	0	0	0	0	0	0	0	0	0	100.00%
F2	0	0	0	0	0	0	0	0	0	2	198	0	0	0	0	0	0	0	0	0	0	0	0	0	0	99.00%
G1	0	0	0	0	0	0	0	0	0	0	0	0	198	2	0	0	0	0	0	0	0	0	0	0	0	99.00%
G2	0	0	0	0	0	0	0	0	0	0	0	0	5	195	0	0	0	0	0	0	0	0	0	0	0	97.50%
H1	0	0	0	0	0	0	0	0	0	0	0	0	0	0	187	13	0	0	0	0	0	0	0	0	0	93.50%
H2	0	0	0	0	0	0	0	0	0	0	0	0	0	0	12	188	0	0	0	0	0	0	0	0	0	94.00%
I1	0	0	0	0	0	0	0	0	1	0	0	0	0	0	0	0	199	0	0	0	0	0	0	0	0	99.50%
I2	0	0	0	0	0	0	0	0	0	0	0	0	0	0	0	0	4	196	0	0	0	0	0	0	0	98.00%
J1	0	0	0	0	0	0	0	0	0	0	0	0	0	0	0	0	0	0	199	1	0	0	0	0	0	99.50%
J2	0	0	0	0	0	0	0	0	0	0	0	0	0	0	0	0	0	0	0	200	0	0	0	0	0	100.00%
K1	0	0	0	0	0	0	0	0	0	0	0	0	0	0	0	0	0	0	0	0	200	0	0	0	0	100.00%
K2	0	0	0	0	0	0	0	0	0	0	0	0	0	0	0	0	0	0	0	0	0	1	199	0	0	99.50%
L1	0	0	0	0	2	0	0	0	0	0	0	0	0	0	5	0	0	0	0	0	0	0	189	4	0	94.50%
L2	0	0	0	0	0	0	0	0	0	0	0	0	0	0	0	0	0	0	0	0	0	0	0	200	0	100.00%

FIGURE 9: The confusion matrix for classifying the herb within a cluster using AP algorithm to cluster herbs. The one in gray indicates a classification error.

TABLE 6: The recognition accuracy of 10 results based on three automatic clustering algorithms.

	K-means (%)	Spectral clustering (%)	Affinity propagation (%)
1	96.83	96.29	97.65
2	96.21	95.79	97.48
3	97.38	96.21	97.85
4	96.85	95.25	97.08
5	96.96	95.48	97.85
6	96.10	95.58	97.88
7	96.15	95.25	97.48
8	96.33	96.13	97.23
9	95.77	96.08	97.65
10	96.85	95.63	97.23
Avg.	96.54	95.77	97.54

TABLE 7: The classification accuracy of CNN and the hierarchical CNN method for each herb.

	CNN (%)	HCNN by AP algorithm (average) (%)	HCNN based on manual clustering (%)
A1	100.0	100.0	100.0
A2	98.0	100.0	100.0
B1	81.0	90.8	92.0
B2	93.0	94.9	95.0
C1	90.0	93.2	94.5
C2	91.5	93.0	93.0
D1	98.0	99.0	99.0
D2	98.0	99.5	99.5
E1	96.5	98.5	98.5
E2	94.5	98.0	98.0
F1	100.0	100.0	100.0
F2	98.0	99.0	99.0
G1	98.0	98.9	99.0
G2	93.0	97.3	97.5
H1	93.5	93.5	94.5
H2	88.5	94.8	97.0
I1	94.5	98.9	99.5
I2	97.5	98.0	98.0
J1	99.5	99.6	99.5
J2	100.0	99.7	100.0
K1	99.0	99.7	99.5
K2	99.0	99.6	99.5
L1	94.5	95.3	96.0
L2	100.0	100.0	100.0
Avg.	95.65%	97.54	97.85

A significant improvement for some herbs such as B1 and H2 in addition to a general improvement of average accuracy (about 2%) when the HCNN method is employed.

Nevertheless, these results are still better than traditional methods using hand-crafted features.

4.7. The Effect of Different Brands of Smartphones. The camera parameters (e.g., resolution, image size, and color) of different smartphones can be quite different. Figure 10 shows the herb images taken by 4 different smartphones, including iPhone6, Samsung S7, Xiaomi, and Asus Pad-Phone. Figure 11 shows the color distributions from these phones. We can see that the images taken by iPhone are more similar to those from Samsung but quite different from images taken by Xiaomi and Asus phones. Therefore, if the training data are taken by iPhone and tested on other brands of phones, the recognition results could be poor, as shown in Table 8 (in this experiment, the training data and testing data were collected from different phones).

Data augmentation (DA) is a common way to improve the results of CNN by artificially creating more training data from the original dataset through various transformations of the original images. In this study, we implement four simple different data transformations on the original iPhone dataset, including rotation, resizing, and changes in brightness and histogram equalization, as shown in Figure 12.

Tables 9 and 10 show the performance of using the one single data augmentation (DA) method as well as combining multiple DA methods, respectively. By comparing Table 9 with Table 10, we can see that the data augmentation method is generally helpful to improve the recognition accuracy (up to about 9% for Asus phone) if we only have the training data

from one single type of phone (i.e., iPhone in our case). However, different types of transformations might have different effects on different phones. As shown in Table 9, providing additional data can improve the results for Xiaomi and Asus phones that does not help much for iPhone and Samsung S7. In particular, data augmentation through histogram equalization might reduce the recognition accuracy for iPhone and Samsung S7.

Finally, we consider adding additional training data from other smartphones. Specifically, 1,440 images were taken from each smartphone (60 for each herb) for training the CNN model. As shown in Table 11, introducing additional training data from all the smartphones obviously can produce a better improvement than the only use of data augmentation. However, given that it might not be feasible to collect the training data from all the smartphones in the world, data augmentation is still a good way to improve the performance of CNN. In addition, we currently are exploring the utilization of generative adversarial networks (GANs) [32] to generate synthetic herb images for data augmentation as an on-going work.

4.8. Visualization. In order to understand what features in the herb images our proposed hierarchical CNN model considers important for recognizing a herb, we employ the layer-wise relevance propagation (LRP) algorithm [33] to visualize which pixels in the input images contribute most strongly to the classification. LRP decomposes the output of the network into the sum of the relevance of the pixels in the

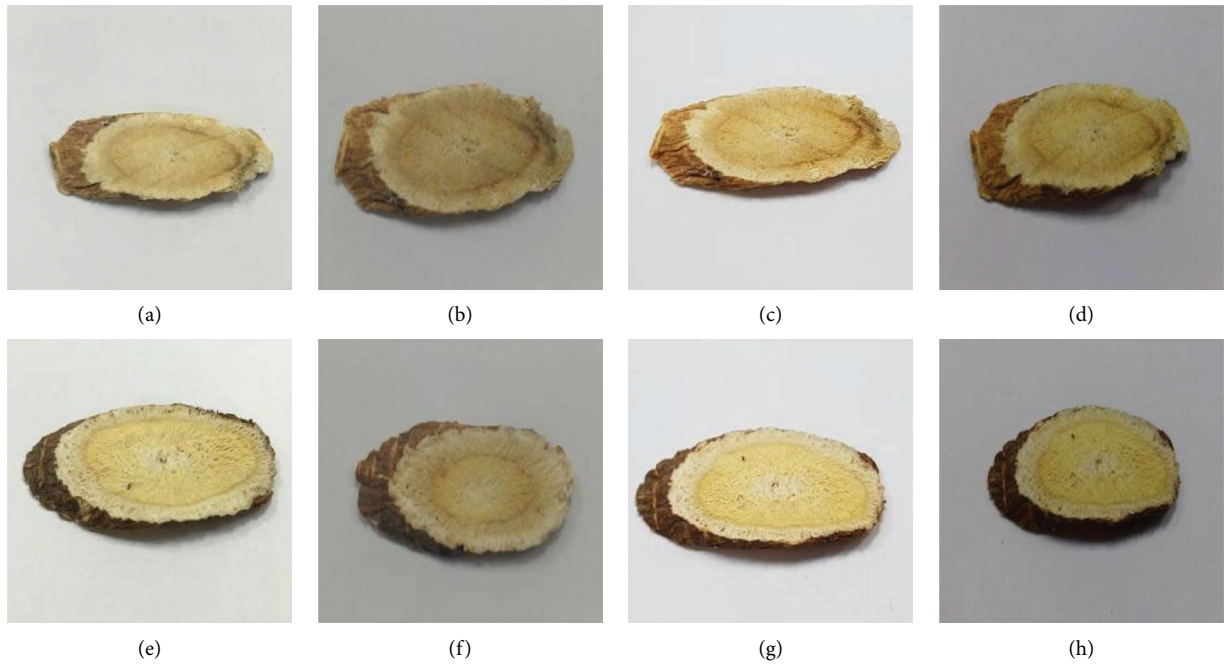


FIGURE 10: (a) and (e) are taken by iPhone6. (b) and (f) are taken by Xiaomi. (c) and (g) are taken by Samsung S7. (d) and (h) are taken by Asus PadPhone.

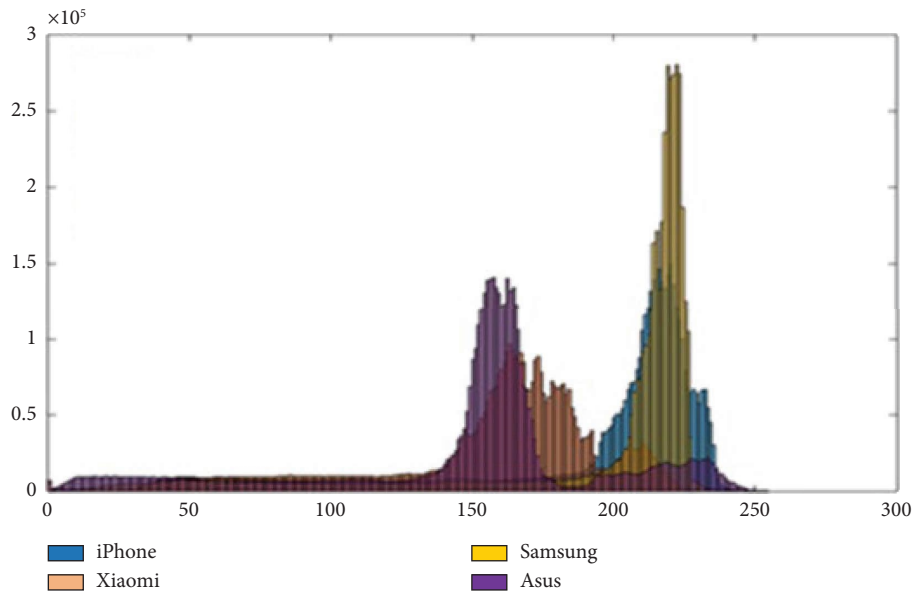


FIGURE 11: The color distribution of 4 smartphones. X axis represents the brightness of the pixel and y axis represents the number of pixels.

TABLE 8: The recognition results of 4 smartphones.

	iPhone (%)	Xiaomi (%)	Samsung (%)	Asus (%)
A1	100.0	100.0	100.0	100.0
A2	95.0	75.0	95.0	70.0
B1	85.0	95.0	85.0	90.0
B2	80.0	70.0	72.5	62.5
C1	92.5	62.5	100.0	70.0
C2	77.5	60.0	60.0	35.0
D1	95.0	82.5	100.0	87.5

TABLE 8: Continued.

	iPhone (%)	Xiaomi (%)	Samsung (%)	Asus (%)
D2	97.5	100.0	100.0	100.0
E1	97.5	87.5	67.5	100.0
E2	97.5	62.5	97.5	85.0
F1	90.0	85.0	100.0	97.5
F2	95.0	77.5	100.0	55.0
G1	92.5	100.0	95.0	100.0
G2	97.5	70.0	97.5	87.5
H1	92.5	65.0	100.0	50.0
H2	85.0	87.5	47.5	95.0
I1	80.0	100.0	97.5	82.5
I2	92.5	60.0	80.0	67.5
J1	100.0	90.0	100.0	77.5
J2	100.0	95.0	100.0	100.0
K1	100.0	87.5	100.0	100.0
K2	92.5	92.5	100.0	90.0
L1	87.5	92.5	87.5	87.5
L2	100.0	90.0	80.0	82.5
Avg.	92.60	82.81	90.10	81.77

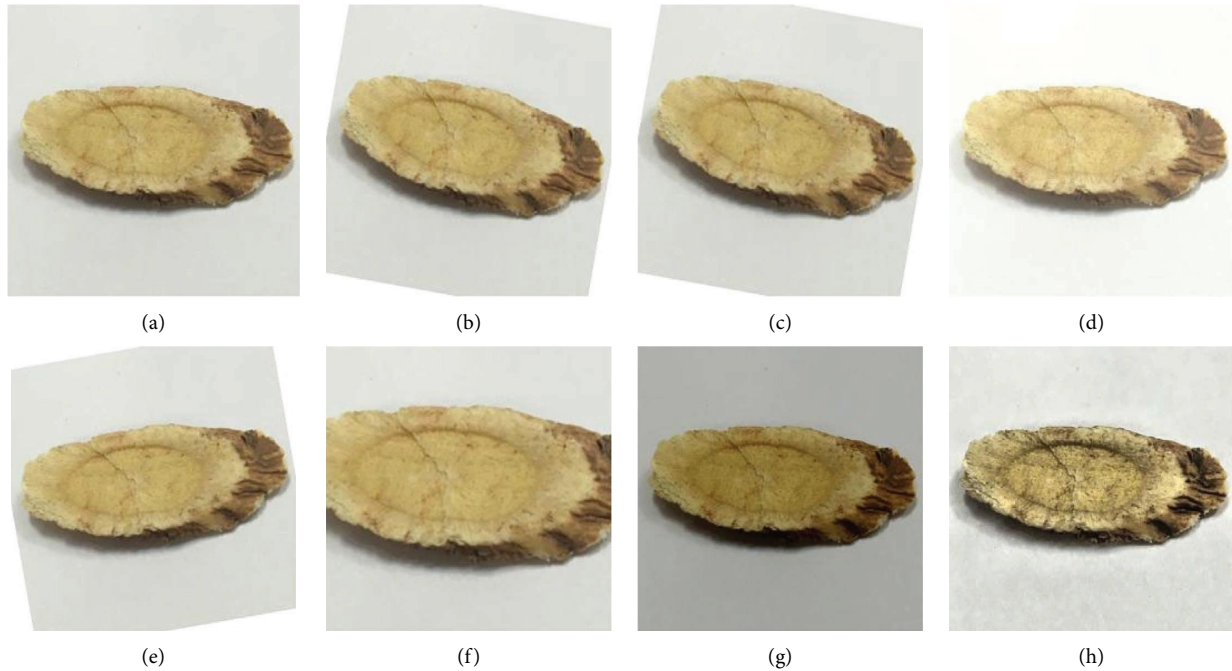


FIGURE 12: Our data augmentation method. (a) Original image, (b) rotate 10 degrees clockwise, (c) zoom-out, (d) increases the brightness, (e) histogram equalization, (f) rotate 10 degrees counterclockwise, (g) zoom-in, and (h) reduce the brightness.

TABLE 9: The result of using different data augmentation (DA) methods.

	iPhone (%)	Xiaomi (%)	Samsung (%)	Asus (%)	Avg. (%)
Without DA	92.60	82.81	90.10	81.77	86.82
(1) Rotation	92.81	84.48	88.13	84.27	87.42
(2) Size	94.58	86.25	89.17	84.79	88.70
(3) Brightness	91.88	87.92	90.31	89.17	89.82
(4) Histogram equalization	89.69	83.23	89.06	83.75	86.43

Data augmentation through histogram equalization might reduce the recognition accuracy for iPhone and Samsung S7.

TABLE 10: The result of combining multiple data augmentation methods.

	iPhone (%)	Xiaomi (%)	Samsung (%)	Asus (%)	Avg. (%)
DA(1)(2)(3)	94.48	88.96	91.02	90.52	91.24
DA(1)(2)(3)(4)	93.33	89.06	90.31	89.06	90.44

TABLE 11: The result of combining multiple data augmentation methods.

	iPhone (%)	Xiaomi (%)	Samsung (%)	Asus (%)	Avg. (%)
Without DA	94.06	93.02	95.31	93.85	94.06
DA(1)(2)(3)	96.04	95.83	96.25	94.90	95.76
DA(1)(2)(3)(4)	95.63	95.52	96.88	94.58	95.65

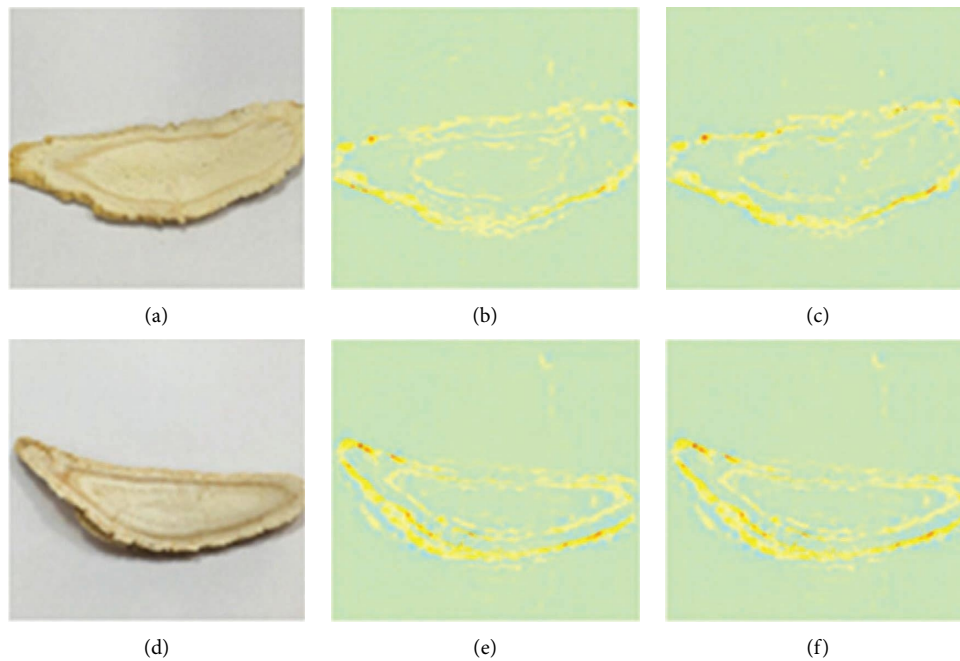


FIGURE 13: Visualization results using LRP for two easily confused herbs (C1 and C2) when CNN and hierarchical CNN are used. (a) Herb C1. (b) Herb C1 using CNN. (c) Herb C1 using hierarchical CNN. (d) Herb C2. (e) Herb C2 using CNN. (f) Herb C2 using hierarchical.

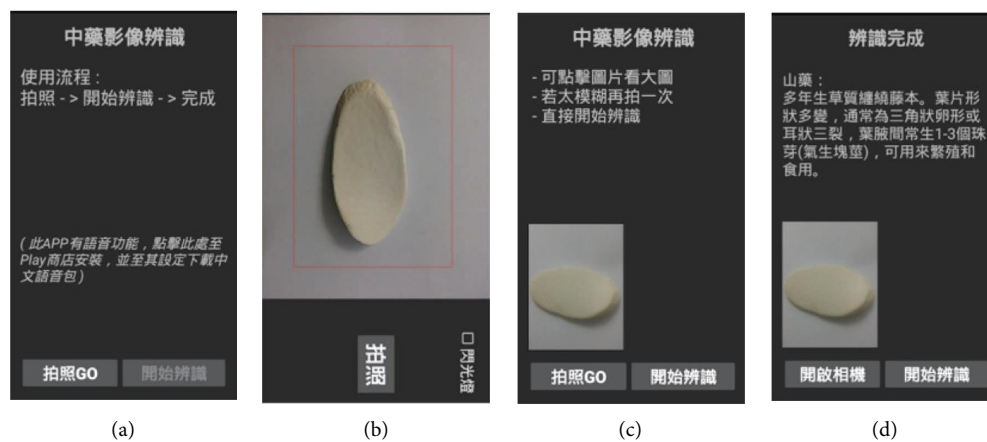


FIGURE 14: The user interface of the proposed system on smartphone. (a) The user instructions. (b) The camera screen. (c) and (d) Interface showing the recognition result and the corresponding information of the recognized herbs.

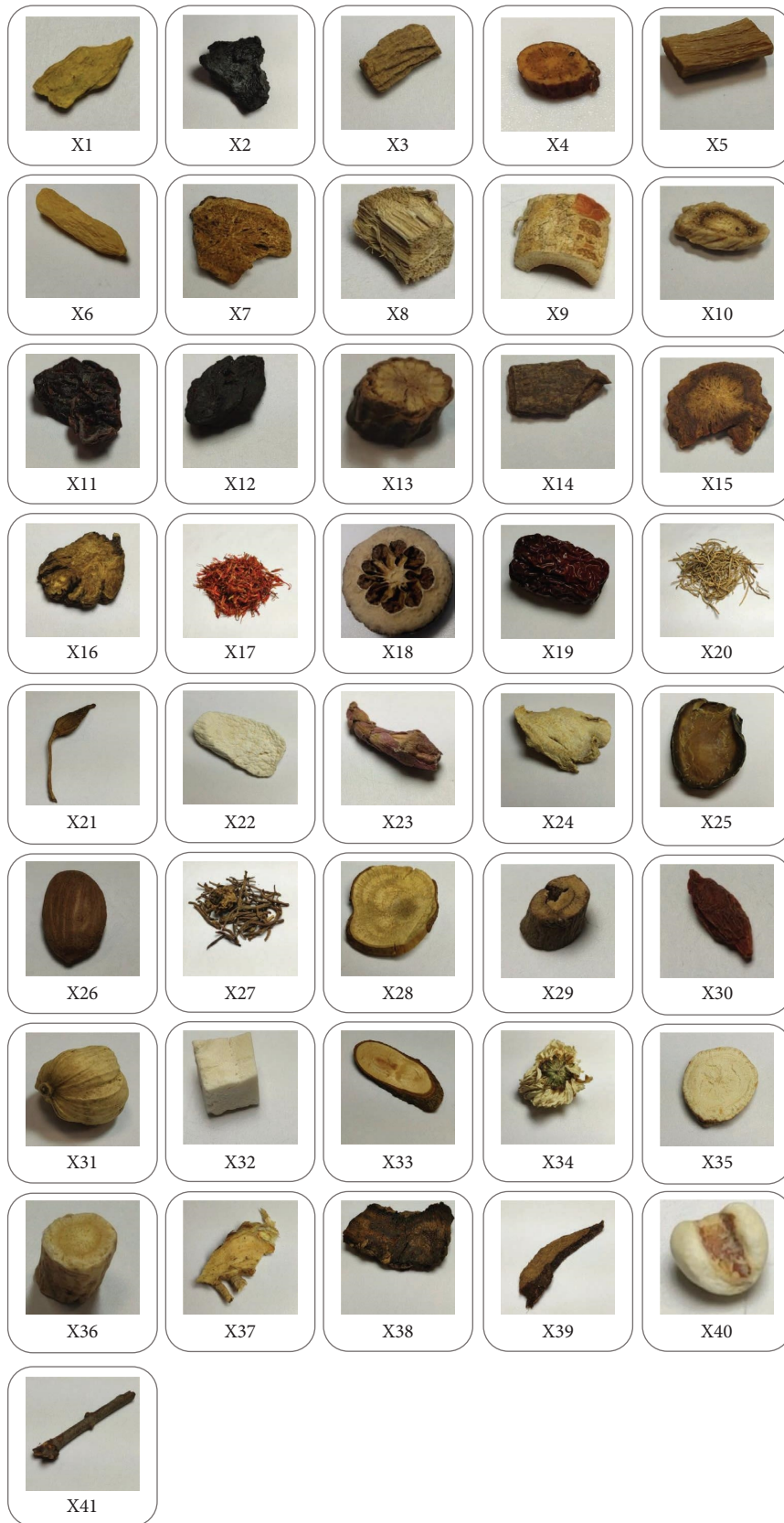


FIGURE 15: Images of additional 41 herbs.

TABLE 12: The name of additional 41 herbs.

Numbers	Names
X1	Scutellariae Radix
X2	Rehmanniae Radix Praeparata
X3	Codonopsis Radix
X4	Glycyrrhizae Radix et Rhizoma
X5	Achyranthis Bidentatae Radix
X6	Ophiopogonis Radix
X7	Atractylodis Macrocephalae Rhizoma
X8	Puerariae Radix
X9	Mori Cortex (桑白皮)
X10	Platycodonis Radix
X11	Corni Sarcocarpium
X12	Reynoutriae Multiflorae Radix
X13	Paeoniae Radix Rubra
X14	Cinnamomi Cortex
X15	Angelicae Sinensis Radix
X16	Chuanxiong Rhizoma
X17	Carthami Flos
X18	Aurantii Fructus Immaturus
X19	Jujubae Fructus
X20	Asari Radix
X21	Forsythiae Fructus
X22	Dioscoreae Rhizoma
X23	Farfae Flos
X24	Zingiberis Rhizoma
X25	Aconiti Lateralis Radix Praeparata
X26	Persicae semen
X27	Asteris Radix et Rhizoma
X28	Linderae Radix
X29	Moutan Radicis Cortex
X30	Lycii Fructus
X31	Myristicae semen
X32	Poria
X33	Cinnamomi Ramulus
X34	Chrysanthemi Flos
X35	Ginseng Radix et Rhizoma
X36	Astragali Radix
X37	Anemarrhenae Rhizoma
X38	Rehmanniae Radix
X39	Drynariae Rhizoma
X40	Coicis semen
X41	Taxilli Herba

input image. R_f is calculated by forward propagation; a pixel-wise relevance scores R_{il} is computed as follows:

$$R_i^l = \sum_j \frac{Z_{ij}}{\sum_{i'} Z_{i'j}} R_j^{l+1}, Z_{ij} = x_i^l w_{ij}^{l,l+1}, \quad (1)$$

where i is a neuron at layer l and P_j runs overall upper-layer neurons.

The results are shown as heatmaps in Figure 13. The pixels in yellow or red mean that they have higher LRP values (and the red pixel has a higher value than the yellow pixel) which are considered to have a strong influence on the classification results. Generally speaking, there are more circular layers (in yellow) in C2 than in C1 when either CNN or hierarchical CNN is used. These circular layers are slightly more observable when the proposed hierarchical CNN is used though.

5. Application

Based on the proposed hierarchical CNN, we implemented a smartphone App (currently only support Chinese) that can automatically recognize CHMs herbs, as shown in Figure 14.

To further validate the performance of our proposed system, in addition to the 24 easily confused herbs, we also collect another dataset which includes 41 herbs, as shown in Figure 15 and Table 12, and integrate these data into this herb recognition App system. We obtain similar results (around 98%) on the recognition accuracy for these additional herb data (the details are not discussed here due to the space limitation).

6. Discussion

In this work, we propose a system that can recognize easily confused TCM (traditional Chinese medicine) herbs on a smartphone with a high accuracy. As far as we know, this is the first smartphone-based system that considers recognition of easily- confused TCM herbs using deep learning techniques. Generally speaking, we observed that a deeper neural network performs better for herb recognition. In addition, we provide an explainable model to show what features in the herb image contribute most strongly to the final results of classification. We found that the recognition accuracy could be affected by the camera parameters (e.g., color histogram) of different brands of smartphones. Different data augmentation techniques were implemented to improve the system accuracy. Finally, we showed that the use of transfer learning is very beneficial where collecting large amount of herb data for training is difficult.

7. Conclusions and Future Work

In this work, we focus on the recognition of easily confused herbs by proposing a hierarchical clustering CNN method that uses affinity propagation to cluster similar herbs into groups. In each group, CNN is then used to extract representative features to distinguish similar herbs. As compared to CNN, our proposed method can improve the detection accuracy by almost 5%. In addition, we study the impact of different brands of smartphones on CHMs recognition accuracy. When the data augmentation is used with more data from different smartphones, we can improve the recognition accuracy from 86.82% to 95.76%. We are currently enriching our herb database so that our system can recognize more CHMs. In addition, we are exploring the use of generative adversarial networks (GANs) [32] to generate synthetic herb images for the data augmentation. Finally, in the future we plan to study the quality of CHMs by extending the App system we developed.

Abbreviations

CHMs:	Chinese herbal medicines
TCM:	Traditional Chinese medicine
HCNNs:	Hierarchical clustering convolutional neural networks

HCNN: Hierarchical clustering convolutional neural network
 VBM: Vision-based-measurement
 CNN: Convolutional neural network
 LBP: Local binary pattern
 HOG: Histogram of oriented gradients
 SIFT: Scale-invariant feature transform
 HD-CNN: Hierarchical deep CNN
 GTSRB: German traffic sign recognition benchmark
 CFC: CNN-oriented family clustering algorithm
 AP: Affinity propagation
 DA: Data augmentation
 GANs: Generative adversarial networks
 LRP: Layer-wise relevance propagation algorithm.

Data Availability

The data used to support in this study are available upon request from the corresponding author.

Conflicts of Interest

The authors declare that there are no conflicts of interest regarding the publication of this paper.

Authors' Contributions

Kun-chan Lan conceived and designed the experiments; Juei-Chun Weng, Jun-Xiang Zhang, and Tzu-Hao Tsai performed the experiments and analyzed the data; Min-Chun Hu helped on the interpretation of data; the acquisition of the herb data is provided by Yuan-Shiun Chang; both Kun-chan Lan and Tzu-Hao Tsai wrote the final version of this paper. All authors read and approved the final manuscript.

Acknowledgments

This research has received funding from Ministry of Science and Technology (MOST), Taiwan under the grant number 111-2221-E-006-120-.

References

- [1] X. Chengyong, W. Yuguo, F. Jian, Q. Li, X. Ran, and D. Yongqi, "Effect of optimal combination of Huangqi (Radix astragalus Mongolicus) and eZhu (rhizoma curcumae phaeocaulis) on proliferation and apoptosis of A549 lung cancer cells," *Journal of Traditional Chinese Medicine*, vol. 38, no. 3, pp. 351–358, 2018.
- [2] W. L. Zhang, R. C. Y. Choi, J. Y. X. Zhan et al., "Can Hedysari Radix replace Astragalus Radix in Danggui Buxue Tang, a Chinese herbal decoction for women's ailments?" *Phytomedicine*, vol. 20, no. 12, pp. 1076–1081, 2013.
- [3] M. J. Kim, H. Sung, and K. E. Hong, "Effects of Dioscorea rhizoma (SanYak) on peripheral neuropathy and its safety," *Journal of Pharmacopuncture*, vol. 16, no. 3, pp. 7–10, 2013.
- [4] E. Rivadeneyra-Domínguez and J. F. Rodríguez-Landa, "Preclinical and clinical research on the toxic and neurological effects of cassava (*Manihot esculenta* Crantz) consumption," *Metabolic Brain Disease*, vol. 35, no. 1, pp. 65–74, 2020.
- [5] Y. Yang, *Chinese Herbal Medicines: Comparisons And Characteristics*, Elsevier Health Sciences, London, UK, 2009.
- [6] S. Shirmohammadi and A. Ferrero, "Camera as the instrument: the rising trend of vision based measurement," *IEEE Instrumentation and Measurement Magazine*, vol. 17, no. 3, pp. 41–47, 2014.
- [7] O. Tao, Y. Zhang, Q. Chen, Y. Wang, and Y. Qiao, "Extraction of texture feature parameter of transverse section in Chinese herbal medicine by gray-level co-occurrence matrix," *World Science and Technology-Modernization of Traditional Chinese Medicine*, vol. 16, pp. 2531–2537, 2014.
- [8] O. Tao, Z. Lin, X. Zhang, Y. Wang, and Y. Qiao, "Research on identification model of Chinese herbal medicine by texture feature parameter of transverse section image," *World Science and Technology-Modernization of Traditional Chinese Medicine*, vol. 16, pp. 2558–2562, 2014.
- [9] G. Cai, Y. Zhao, H. Yuan et al., "Separation of Potentilla anserina active site (total saponin) and anti-DHBV DNA action in ducks," *Central South Pharmacy (China)*, vol. 1.
- [10] C. Liu, X. Wu, and W. Xiong, "Chinese herbal medicine classification based on BP neural network," *Journal of Software*, vol. 9, no. 4, pp. 938–944, 2014.
- [11] B. J. Frey and D. Dueck, "Clustering by passing messages between data points," *Science*, vol. 315, no. 5814, pp. 972–976, 2007.
- [12] D. Luo, D. Fan, H. Yu, and Z. Li, "A new processing technique for the identification of Chinese herbal medicine," in *Proceedings of the 2013 International Conference on Computational and Information Sciences*, pp. 474–477, IEEE, Shiyang, China, June 2013.
- [13] L. Dehan, W. Jia, C. Yimin, and G. Hamid, "Classification of Chinese Herbal medicines based on SVM," in *Proceedings of the 2014 International conference on information science, electronics and electrical engineering IEEE*, vol. 1, pp. 453–456, Sapporo, Japan, April 2014.
- [14] H. M. Zawbaa, M. Abbass, S. H. Basha, M. Hazman, and A. E. Hassenian, "An automatic flower classification approach using machine learning algorithms," in *Proceedings of the 2014 International conference on advances in computing, communications and informatics (ICACCI)*, pp. 895–901, IEEE, Delhi, India, September 2014.
- [15] M. A. Islam, M. S. I. Yousuf, and M. M. Billah, "Automatic plant detection using HOG and LBP features with SVM," *International Journal of Computer*, vol. 33, no. 1, pp. 26–38, 2019.
- [16] C. Narvekar and M. Rao, "Flower classification using CNN and transfer learning in CNN-Agriculture Perspective," in *Proceedings of the 2020 3rd International Conference on Intelligent Sustainable Systems (ICISS)*, pp. 660–664, IEEE, Thoothukudi, India, December 2020.
- [17] T. V. Janahiraman, L. K. Yee, C. S. Der, and H. Aris, "Leaf classification using local binary pattern and histogram of oriented gradients," in *Proceedings of the 2019 7th International Conference on Smart Computing & Communications (ICSCC)*, pp. 1–5, IEEE, Sarawak, Malaysia, June 2019.
- [18] P. Dhar, "A new flower classification system using LBP and SURF features," *International Journal of Image, Graphics and Signal Processing*, vol. 11, no. 5, pp. 13–20, 2019.
- [19] M. E. Pothen and M. L. Pai, "Detection of rice leaf diseases using image processing," in *Proceedings of the 2020 Fourth International Conference on Computing Methodologies and*

- Communication (ICCMC)*, pp. 424–430, IEEE, Erode, India, March 2020.
- [20] V. K. Jyothi, D. S. Guru, and Y. H. Kumar, “Classification of natural flower videos through sequential keyframe selection using SIFT and DCNN,” in *Proceedings of the International Conference on Recent Trends in Image Processing and Pattern Recognition*, pp. 305–318, Springer, Singapore, July 2018.
- [21] A. Krizhevsky, I. Sutskever, and G. E. Hinton, “Imagenet classification with deep convolutional neural networks,” *Communications of the ACM*, vol. 60, no. 6, pp. 84–90, 2017.
- [22] X. Sun and H. Qian, “Chinese herbal medicine image recognition and retrieval by convolutional neural network,” *PLoS One*, vol. 11, no. 6, Article ID 156327, 2016.
- [23] Z. Yan, H. Zhang, R. Piramuthu et al., “Hierarchical deep convolutional neural networks for large scale visual recognition,” in *Proceedings of the IEEE international conference on computer vision*, pp. 2740–2748, Cambridge, MA, USA, June 2015.
- [24] X. Mao, S. Hijazi, R. Casas, P. Kaul, R. Kumar, and C. Rowen, “Hierarchical CNN for traffic sign recognition,” in *Proceedings of the 2016 IEEE intelligent vehicles symposium (IV)*, pp. 30–135, IEEE, Gothenburg, Sweden, June 2016.
- [25] Y. Jia, E. Shelhamer, J. Donahue et al., “Caffe: convolutional architecture for fast feature embedding,” in *Proceedings of the 22nd ACM international conference on Multimedia*, pp. 675–678, New York, NY, USA, November 2014.
- [26] Y. Chang and Y. Ho, *Illustrations of Commonly Misused Chinese Crude Drug Species in Taiwan*, Ministry of Health and Welfare, Taipei, Taiwan, 1 edition, 2015.
- [27] C. C. Chang and C. J. Lin, “LIBSVM: a library for support vector machines,” *ACM transactions on intelligent systems and technology (TIST)*, vol. 2, no. 3, pp. 1–27, 2011.
- [28] K. Simonyan and A. Zisserman, “Very deep convolutional networks for large-scale image recognition,” 2014, <https://arxiv.org/abs/1409.1556>.
- [29] H. H. Bock, “Clustering methods: a history of k-means algorithms,” in *Selected contributions in data analysis and classification. Studies in Classification, Data Analysis, and Knowledge Organization*, P. Brito, G. Cucumel, P. Bertrand, and F. de Carvalho, Eds., Springer, Berlin, Heidelberg, pp. 161–172, 2007.
- [30] U. Von Luxburg, “A tutorial on spectral clustering,” *Statistics and Computing*, vol. 17, no. 4, pp. 395–416, 2007.
- [31] Y. Cheng, D. Wang, P. Zhou, and T. Zhang, “A survey of model compression and acceleration for deep neural networks,” 2017, <https://arxiv.org/abs/1710.09282>.
- [32] A. Aggarwal, M. Mittal, and G. Battineni, “Generative adversarial network: an overview of theory and applications,” *International Journal of Information Management Data Insights*, vol. 1, no. 1, pp. 100004–102021, 2021.
- [33] S. Bach, A. Binder, G. Montavon, F. Klauschen, K. R. Müller, and W. Samek, “On pixel-wise explanations for non-linear classifier decisions by layer-wise relevance propagation,” *PLoS One*, vol. 10, no. 7, Article ID 130140, 2015.

Research Article

A Comparison Study of Doctor-Patient Internet Interactions in Traditional and Modern Medicine: Empirical Evidence from Online Healthcare Communities

Song Cao ¹, Xiang Gao ², Shuzhen Niu ³, and Qian Wei ⁴

¹Nanyang Technological University, No. 50 Nanyang Avenue, Singapore 639798, Singapore

²Research Center of Finance, Shanghai Business School, No. 2271 West Zhong Shan Road, Shanghai 200235, China

³School of Business, Sanda University, No. 2727 Jinhai Road, Shanghai 201209, China

⁴School of International Economics and Trade, Guangxi University of Foreign Languages, No. 19 Wuhe Avenue, Qingxiu District, Nanning, Guangxi 530222, China

Correspondence should be addressed to Shuzhen Niu; nsz66@sina.com

Received 22 June 2022; Revised 8 September 2022; Accepted 19 September 2022; Published 7 October 2022

Academic Editor: Lei Jiang

Copyright © 2022 Song Cao et al. This is an open access article distributed under the Creative Commons Attribution License, which permits unrestricted use, distribution, and reproduction in any medium, provided the original work is properly cited.

Online healthcare platforms serve not just as a medical knowledge-sharing community but also bring about effective interactions between professional physicians and patients. However, it is unclear whether online technology adoption affects such interactions in the same way between traditional Chinese medicine and modern medical departments. By utilizing a large sample of online doctor-patient interaction information from 168,870 doctor-specific interactive webpages recorded in a famous Chinese online healthcare community, this paper studies the differences between 17,513 traditional medicine doctor homepages and 151,357 others from more than 100 different specialty areas. Our chosen platform is representative since it covers about 800,000 physicians working at over 10,000 hospitals across all major provincial regions in China. We document that online medical service users tend to accept and use online health care services. However, patients seeing Chinese medicine doctors exhibit the following unique characteristics. They still prefer choosing doctors according to third-party information and may be reluctant to pay for the current online service price level. This problem is hard to overcome by the platform in the short run. Patients need a long-term process to adapt to the upgraded medical environment gradually. Therefore, establishing a personalized doctor recommendation system has become the most urgent demand presently.

1. Introduction

As China chooses the urban-centered development route in the early stages of its economic and social growth plan, healthcare services and medical treatments, like other core resources, have experienced large urban-rural differences in distribution. Because of the dearth of quality hospitals, people in need of such care and consulting services are facing a series of problems with insufficient doctor-patient interaction, especially in the field of complementary, traditional, and alternative medicine [1]. In particular, patients with difficult, complicated, and miscellaneous diseases in remote areas often need to move around among multiple cities to finally obtain appropriate medical

assistance. It is common for patients to transfer from county-level hospitals to municipal ones and then to provincial hospitals. Besides, patients still face the problem of long queues for registration [2]. Although the application of the hospital's online appointment system has improved the doctor-patient relationship, patients' trust in doctors and hospitals still needs more open and transparent information system support [3].

With the development of Internet technologies, the online health care (OHC) community represented by the Good Doctor ("Hao Daifu" in Chinese) and the Dr. Clove ("Dingxiang Yisheng" in Chinese) platform has gradually emerged as a rising medical force in China [4], which significantly eases the pressure on the entire medical system

and effectively shortens the gap between urban and rural medical standards [5]. With the development of information and communication technology, many scholars have studied the impact of the Internet on the doctor-patient relationship and health outcomes [6]. Patients' acceptance of and willingness to pay for OHC services are both undoubtedly critical issues for the development of OHC platforms, especially when OHC appears to be a phenomenal application. Although OHC has become a hot topic in recent years, especially after the COVID-19 epidemic, and papers on the development of OHC have emerged in a huge stream, the question of whether complementary and traditional medicine are affected similarly in comparison to mainstream and modern medicine remains unanswered. This paper attempts to shed light on it.

Given the boom in China's online healthcare services, many people try to visit OHC websites for healthcare information and consultations [7]. The online medical care community can be defined as a medical career, which means attaining successful medical information exchange through remote electronic communication and providing treatment suggestions in conjunction with supporting and improving patients' clinical conditions [4]. Using texts and images, doctors can communicate their pieces of medical advice to patients and get feedback, which differs to a large extent from traditional face-to-face diagnosis and treatment. To meet complex needs, one may categorize OHCs into those having cure-oriented (i.e., functional) goals and those pursuing care-oriented (i.e., emotional) values [8]. The discussion presented in this paper mainly positions the analysis of comparing online traditional versus modern medical services in a cure-oriented OHC.

In regard to seeing a doctor online, there are essentially three types of doctor-patient interactive modes on the Internet that have been studied in the extant literature. The first involves making an appointment online and then meeting offline [9]. The second relates to selecting doctors online and consulting online too [10]. The third mode is mixed, including the online selection of and consultation with doctors, then switching to offline examinations if needed [11]. However, all the above three processes emphasize the same thing: choosing the right doctor. This has to be done either by word of mouth or by browsing each interested doctor's online web page.

As one kind of expert service, physicians' service inevitably leads to information asymmetry between doctors and patients [12]. In addition, because services are intangible, indivisible, and heterogeneous [13], it is hard for patients to judge the quality of the service they receive because doctors usually share much more professional knowledge than patients do [14]. In the highly centralized and miscellaneous OHCs, without mentioning the supervision of the platforms, patients actually take more risk and responsibility in how to choose the quality of doctor's service [10]. However, compared with offline hospitals, OHCs provide more useful information besides names and clinic titles [15], and users can even read the comments [10]. They found that patient-generated information, such as feedback, reviews, and ratings, will significantly affect patients' choices during their search stage. Besides, at the decision stage,

system-generated information, such as contribution, grade, and popularity, will play an important role along with patient-generated information, which effectively weakens information asymmetry. Cao et al. [16] also prove that patients' information processing affects their online health consulting intentions in the same way. Lu and Wu [17] found that word-of-mouth information about physicians reflects the physicians' service quality and exerts a positive effect on persuading patients to make appointments. They also claim that patients with severe illnesses are more motivated to seek high-quality medical services.

Our study is complementary to the strand of literature on utilizing online technology to deal with the challenges faced by promoting alternative and traditional medicine. On the one hand, several recent studies combine various aspects of Traditional Chinese Medicine (TCM) with new developments in technology, including the Internet tool. For example, Han et al. [18] considered the Internet hospital as a telehealth model in China and applied a systematic search and content analysis to explore its patterns. Wang et al. [19] focus on TCM and study its traceability system based on a lightweight blockchain. Zhang et al. [20] took a relevant but different perspective by evaluating the effectiveness of online courses on TCM for international students during the COVID-19 epidemic period.

On the other hand, quite a few Chinese studies also provided insights. Based on the survey data, Ding et al. [21] constructed the evaluation index system of the information service quality of Internet Chinese medicine hospitals by combining the main characteristics of the information service quality of domestic Internet Chinese medicine hospitals. Wang [22] analyzed the current status of TCM intelligent technology, Internet service, healthcare, and community hospitals, and discussed the new development model of community hospitals based on Internet and TCM intelligence, to better meet the health service needs of the public. As the COVID-19 epidemic era has significantly boosted the development of "Internet+" Chinese medicine medical treatment, a growing strand of literature can study various TCM topics under the background of "Internet+". For example, Cheng [23] explored how to optimize the effect of Chinese medicine in integrated family hospital management and the possible applications based on "Internet+" tools. Ma [24] proposed an "Internet+" Chinese medicine health management model to promote nursing treatment for elderly hypertensive patients. Cai et al. [25] argued that Internet medical technology can improve the treatment efficiency and accuracy of Chinese medicine acupuncturists by innovating the acupuncture treatment mode, optimizing the acupuncture treatment process, and improving patient health management. Sun and Ge [26] used the SWOT approach to analyze "Internet+ TCM nursing service," and discussed how to promote the innovation of TCM nursing health services and the associated risk issues. Tian and Gao [27] summarized the current situation of "Internet+" TCM medical development in China. Through analyzing the bottlenecks faced by the Internet TCM model, the authors make several suggestions, such as further enhancing the technology, educating personnel, and improving the medical

insurance policy and legal regulation. Therefore, our comparative study of the doctor-patient online communication between TCM departments and others can help deepen the understanding of this “Internet+” TCM notion, providing supportive evidence for bettering the education of TCM and cultivating the public’s online treatment habit in Chinese and alternative medicine.

When OHC became increasingly popular, related laws and regulations were gradually improved, and corresponding review mechanisms were also developed by well-known platforms. OHCs are gradually eliminating the barrier between patients and doctors. For example, the research results of Beaudoin and Tao [28] showed that the Internet can help cancer patients face disease, receive treatment, and seek support. Patients now not only have higher autonomy in choosing doctors but can also refer to more reliable information. Doctors with the ability and spare time can also create higher personal and social values while serving more patients [4]. Therefore, with the emergence of OHC, doctors can provide better and more personalized health care, and patients can get better health outcomes [29]. Although OHC is developing in full swing, its popularity, availability, and current acceptance, a.k.a., whether patients are willing to receive this kind of service and pay for it, still need further investigation. Based on this, we put forward the following three questions.

First, the telemedicine portal provides a wealth of personal information about doctors, but before the user’s browsing behavior occurs, the only information source available on the portal is the brief information on the doctor’s business card. Can this information fully induce the user’s browsing behavior? In other words, is the user’s browsing behavior purposeful or random? Based on this, we can judge the direction and extent of the actual effectiveness of Internet medical care. Second, the user’s behavior in paying for the OHC platform service can fully show the patient group’s preference for a certain type of doctor and enables us to make suggestions for better training of telemedicine service personnel. Third, there are great differences in the ways of interrogation and treatment between traditional Chinese medicine and modern medicine. Modern medicine often relies on high-end medical devices to assist in the completion of interrogation and treatment, while traditional Chinese medicine can often complete the treatment through the intuitive observation of the physiological characteristics of patients. In terms of drug treatment, traditional Chinese medicine should also be more convenient than modern medicine. Traditional Chinese medicine can often be easily purchased in local hospitals. Therefore, is there any difference in the convenience that telemedicine brings to the field of traditional and alternative medicine? In this regard, we start the analysis with the responses of Internet OHC user behavior to doctor information presented and practices delivered online.

2. Data and Empirical Method

2.1. Data Sources. Among the emerging Chinese OHC platforms, we collect data from the most representative

Good Doctor Internet hospitals. This platform was established in 2006 with the brand feature of “user-friendly”. As of June 2022, the platform includes 890,286 doctors from 10,096 hospitals across China. In this study, we used the public data of this platform, including doctors’ resumes and their evaluations by Internet patients, since they started an online service, which provided a rich set of data available for our research. In addition, as the most recognized and representative OHC platform in China, the Good Doctor website is chosen by many scholars to study various topics around the theme of OHC, which further reflects the reliability and availability of its data. All variables used in our research are listed and defined in Table 1.

The data were collected through web scraping between June 31st, 2019 and August 2nd, 2019, including three dimensions of records. First, the basic information on the doctor’s business card, including the doctor’s name, academic title, clinic title, employer, hospital, and department. Second, personal introduction, including their specialization and personal profile. Third, personal achievements, including page views, number of published articles, number of patients, number of reviews, number of thank letters and gifts received, search heat, recommended star, and the year of starting service. Given the availability of data, we used the data of 168,870 doctors who went online from 2008 to 2019. These doctors come from ten main departments, as shown in Figure 1. Among them, doctors from TCM departments account for 10.4% and doctors from modern medicine (MM) departments account for 89.6% of all doctors in our sample. No significant differences are found for the two categories regarding the percentages holding advanced clinic titles and academic titles, as shown in Figures 2 and 3. The online doctor resources on the Good Doctor website are quite high quality. 11.4% of the doctors have the academic title of professor, and 23.9% of the doctors have the practical title of chief physician.

2.2. Variable Construction. To compare the differences in online patient behaviors concerning the TCM department and other hospital departments, we employ two commonly used proxies suggested by scholars specializing in Chinese OHC research as our dependent variables. They are doctor web page visits and the number of medical service orders. In particular, we follow Yu et al.’s [30] research on the causal effect of honorary titles on the volume of services provided by physicians and Li et al.’s [11] research on patients’ decisions to switch from online to offline medical services. First, the volume of OHC users browsing a web page of a doctor, a.k.a. pageviews, is the result generated after patients decide to choose OHC and conduct a series of spontaneous searches. In essence, it is a direct reflection of the website’s communication power and recognition. However, the internal driving force of users’ browsing behavior should be to seek famous doctors rather than famous websites. It is also reasonable to believe that patients will check multiple platforms. Therefore, based on the data from the most representative and popular OHC platform, we think page view can show the impact and acceptance of

TABLE 1: Variable definition and description.

Variable	Definition
Page view	The number of visits to a doctor’s home page at the good doctor online platform in our sample
Order	The number of patients that the doctor has helped after paid medical service orders have been placed online (cumulative counts since the doctor has started his or her online services)
OCR	Order conversion ratio, which is calculated as the ratio of the number of orders placed to the doctor to the view volume of that doctor’s web page
Star	The degree of recommendation associated with the doctor rated by the good doctor website based on historical data (the rating is an integer from 0 to 5)
Hot	The degree of popularity assigned to the doctor by the Good Doctor website to a doctor based on historical data
Thank	The number of thank-you letters received by the doctor
Gift	The number of gifts received by the doctor
Article	The number of papers and articles published by the doctor
Review	Number of comments received by the doctor
Start year	The year that the doctor started online services on the platform
Desc_len	The length of the description of the doctor’s field of expertise
Intro_len	The length of the introduction to the doctor’s professional experience
City	Whether the hospital where the doctor works is located in the first-tier and second-tier cities (according to China business network, there are four first-tier cities (Beijing, Shanghai, Guangzhou, and Shenzhen) in China and their 30 second-tier cities are selected out of 337 Chinese cities at the prefecture level and above. The selection criteria encompass five dimensions based on commercial store data, user behavior data, etc.) in the corresponding province
Academic title (AT)	AT represents a series of dummy variables constructed based on the academic titles associated with the doctor, which include professor, associate professor, lecturer, teaching assistant, and none
Clinic title (CT)	CT represents a series of dummy variables constructed based on the clinic titles associated with the doctor, including chief physician, deputy chief physician, resident physician, attending doctor, attending examiner, attending physician, resident physician, and laboratory physician
Department	Department represents a series of dummy variables constructed based on hospital departments in which the doctor can be classified, including TCM, pediatrics, internal medicine, stomatology, surgery, obstetrics and gynecology, ophthalmology, oncology, orthopedic surgery, and other departments

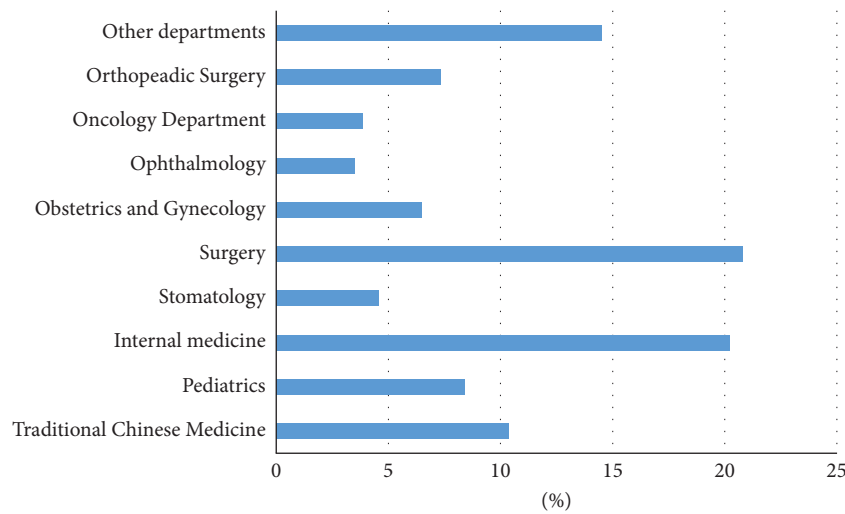


FIGURE 1: Proportion of doctors belonging to each hospital department.

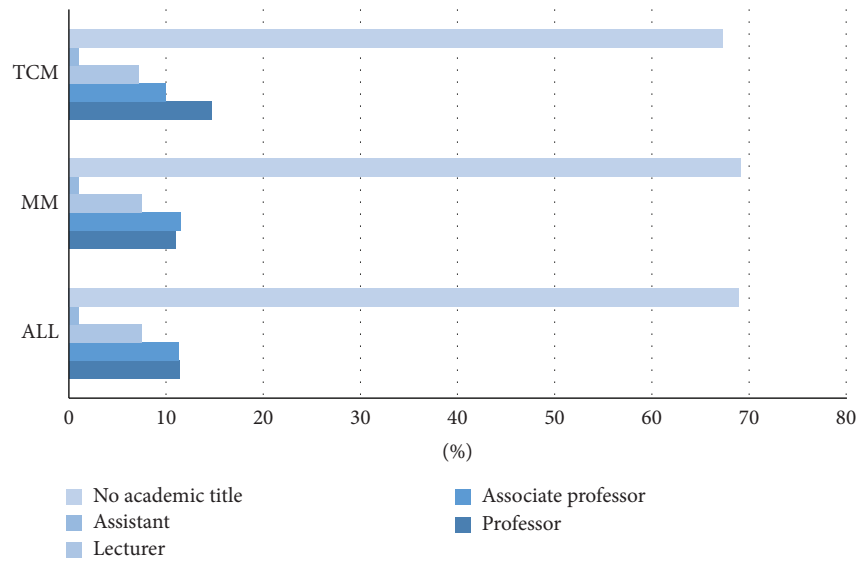


FIGURE 2: Proportion of doctors associated with each academic title in the TCM vs. MM department.

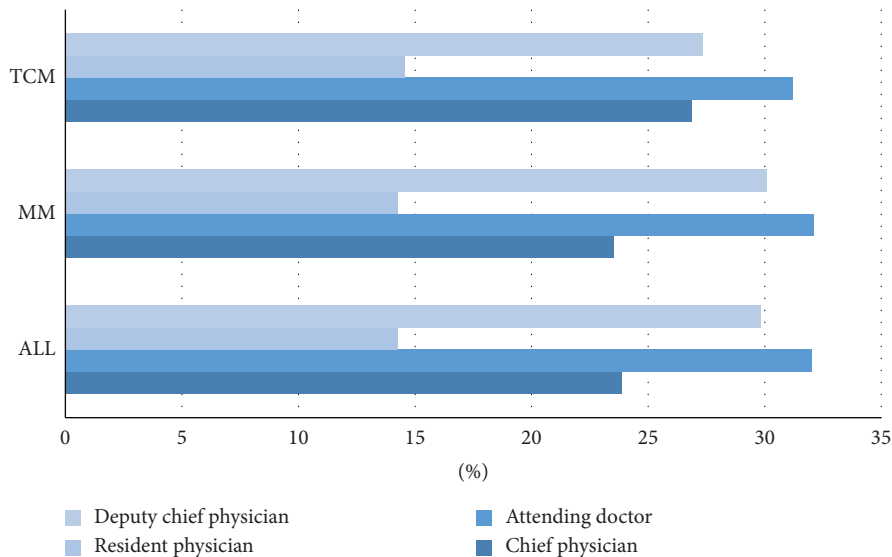


FIGURE 3: Proportion of doctors associated with each clinic title in the TCM vs. MM department. *Note.* The other four clinic titles together account for only a small proportion, hence not listed in the figure.

OHC. Since one of the purposes of our research is to study the logic of patients’ browsing behavior, it is understandable to use this simple but powerful indicator.

Turning to our second proxy of the volume of medical service orders, users placing orders and making payments will clearly reflect their preference for doctors as a direct result of browsing. Theoretically speaking, patients mainly use three information sources when selecting doctors: online reviews, comments, or feedback, family and friend recommendations; and doctor referrals [31]. The decision of patients to select doctors, that is, their order-placing behavior, is not only determined by the information provided by the platform but also by factors outside the system. However, the doctor’s profile and personal achievement information provided by the platform, as well as the scoring of doctors’

popularity and recommendations, can explain the uncertain factors caused by the differences in users’ reference checks to a certain extent. Therefore, using the criteria provided by the platform to study the behavior of placing orders, we should be able to accurately reflect the types of information that users value.

Staying in line with the decision-making process in Figure 4 for patients utilizing the information received, a variety of public information types provided by the Good Doctor website are selected as explanatory variables and control variables. As we have discussed previously, the existing studies found that the information provided by OHCs plays a role in affecting the selection of doctors for OHC patients. According to Wu and Lu [32], in which they studied patient satisfaction, these two authors mainly chose

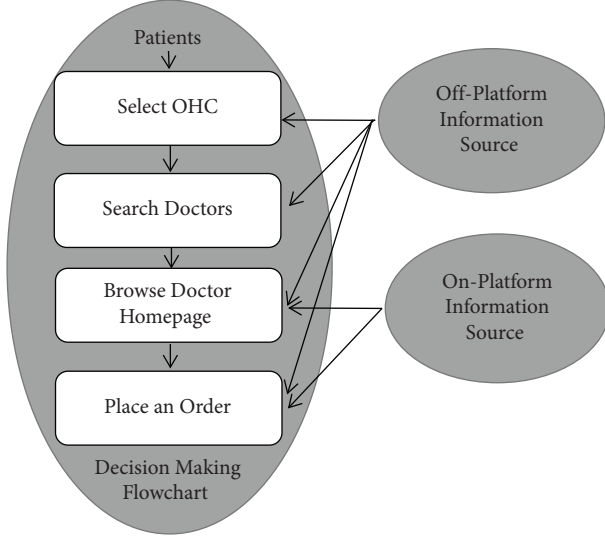


FIGURE 4: OHC user decision-making process.

explanatory variables from five dimensions of medical services: namely, service price, service provision, service quality, service criterion, and local economic development. The logic of selecting these variables is to intuitively reflect the judgments made by users after receiving services. Similarly, our model mainly relies on the predictions made by users before placing an order. Our variable selection mimics their choice of variables. The only difference is that the price factor is dropped in this paper because the price is not a directly observable factor in the process of the user searching and browsing on our platform. We only incorporate the information sources that can be gradually learned by OHC users as described by our setup.

2.3. Empirical Specification. Based on the information received by users when they perform corresponding behaviors on the website, we divided the samples, simulated the decision process, and established models based on the three different evaluation measures to analyze the development status of OHC and the differences between telemedicine in the fields of traditional Chinese medicine and modern medicine.

We begin by presenting the linear empirical regression of a decision model of page view volume determination. The general process of searching for doctors on the Good Doctor website is to select the target city and target department, and finally, browse the doctor's brief information and decide whether to enter the details page. When deciding whether to browse details, users first receive information about the doctor's name, academic title, clinic title, hospital name, corresponding department, specialized field description, popularity, hot, and online consultation price. It is worth noting that 90% of the online doctors who are good doctors come from lower-ranked hospitals. Therefore, we will mark the hospital level according to whether the city where the hospital is located belongs to the second-tier group of large cities in China instead of using the rankings of the hospitals themselves. In addition, we use the length of the detailed description to reflect the doctor's skills. Academic titles, clinic titles, and their departments are transformed into a series of dummy variables represented by vectors (marked as bold in the following equation).

$$\begin{aligned} \text{PAGEVIEW}_i = & \beta_0 + \beta_1 \cdot \mathbf{AT}_i + \beta_2 \cdot \mathbf{CT}_i + \beta_3 \\ & \cdot \mathbf{DEPARTMENT}_i + \beta_4 \times \text{HOT}_i + \beta_5 \\ & \times \text{DESC}_{\text{LEN } i} + \beta_6 \times \text{CITY}_i + \varepsilon_i, \end{aligned} \quad (1)$$

where i denotes the doctor's homepage in our sample, and all variables are as defined in Table 1. Following the similar decision rules stated above, we construct the next empirical specification to describe the number of orders placed with the detailed information provided on a doctor's OHC page. Compared with the above model, the new variables added include the doctor's resume, number of published articles, historical page views, number of thank-you letters and gifts received, and recommendation stars. Due to the high causal relationship between views and orders, this paper does not use orders as the explanatory variable of page views but uses page views as the explanatory variable of orders. We believe that multiple views can increase the probability of placing an order for that doctor's online service provided.

$$\begin{aligned} \text{ORDER}_i = & \beta_0 + \beta_1 \cdot \mathbf{AT}_i + \beta_2 \cdot \mathbf{CT}_i + \beta_3 \cdot \mathbf{DEPARTMENT}_i + \beta_4 \times \text{HOT}_i + \beta_5 \times \text{CITY}_i + \beta_6 \times \text{DESC}_{\text{LEN } i} \\ & + \beta_7 \times \text{ARTICAL}_i + \beta_8 \times \text{REVIEW}_i + \beta_9 \times \text{THANK}_i + \beta_{10} \times \text{GIFT}_i + \beta_{11} \times \text{INTRO}_{\text{LEN } i} \\ & + \beta_{12} \times \text{STARTYEAR}_i + \beta_{13} \times \text{PAGEVIEW}_i + \beta_{14} \times \text{STAR}_i + \varepsilon_i. \end{aligned} \quad (2)$$

3. Results and Discussion

3.1. Preliminary Inspection. We first present the descriptive statistics of our main variables in Table 2 across different samples (i.e., the full sample, the TCM observations, and all other non-TCM observations) and then compute the pairwise correlation coefficients between them in the

whole sample. As can be seen from Table 2, doctors from the TCM and those from other departments on average provide about the same number of paid online medical services, while doctors in the TCM department attract more than 20% higher attention than non-TCM doctors as measured by the mean number of page views. We find no significant and consistent difference for all other variables

TABLE 2: Descriptive statistics.

Variable	Whole sample: 168870				TCM sample: 17513				MM sample: 151357			
	Mean	Std. dev.	Min	Max	Mean	Std. dev.	Min	Max	Mean	Std. dev.	Min	Max
Page view	306001	1712036	671	167000000	411237.50	2786098	892.00	167000000	293824.50	1539700	671	138000000
Order	344.52	1334.86	0.00	73374.00	333.38	1472.95	0.00	59248.00	345.81	1317.95	0.00	73374.00
OCR	0.00	0.00	0.00	0.52	0.00	0.00	0.00	0.03	0.00	0.00	0.00	0.52
Star	0.16	0.64	0.00	5.00	0.09	0.47	0.00	5.00	0.17	0.65	0.00	5.00
Hot	3.61	0.31	0.00	5.00	3.75	0.28	0.00	5.00	3.60	0.31	0.00	5.00
Thank	8.18	33.90	0.00	1632.00	5.04	20.20	0.00	559.00	8.55	35.12	0.00	1632.00
Gift	20.86	115.54	0.00	9362.00	13.54	84.76	0.00	3353.00	21.71	118.56	0.00	9362.00
Article	7.32	28.15	0.00	313.00	15.24	51.05	0.00	313.00	6.41	21.77	0.00	78.00
Review	19.46	71.16	0.00	3187.00	13.94	48.70	0.00	1332.00	20.10	73.29	0.00	3187.00
Startyear	2014.28	2.92	2008	2019	2013.77	3.01	2008	2018	2014.33	2.91	2008	2019
Desc_len	31.98	17.97	1.00	162.00	35.09	17.70	2.00	145.00	31.61	17.97	1.00	162.00
Intro_len	211.78	383.94	38.00	27056.00	214.32	294.04	38.00	9966.00	211.04	393.00	38.00	27056.00
City	0.50	0.50	0.00	1.00	0.35	0.48	0.00	1.00	0.52	0.50	0.00	1.00

Note. Other dummy variable series, including the academic title, clinic title, and department, are not shown to save space.

TABLE 3: Correlation matrix of main variables.

	Page view	Order	OCR	Star	Hot	Thank	Gift	Article	Review	Start year	Intro_len
Order	0.81***										
OCR	0.01	0.12***									
Star	0.23***	0.44***	0.33***								
Hot	0.21***	0.35***	0.28***	0.48***							
Thank	0.47***	0.68***	0.14***	0.55***	0.47***						
Gift	0.56***	0.72***	0.07***	0.43***	0.35***	0.76***					
Article	0.36***	0.11***	0.01*	0.03***	0.03***	0.04***	0.06***				
Review	0.49***	0.72***	0.13***	0.55***	0.49***	0.98***	0.78***	0.05***			
Start year	-0.22***	-0.21***	0.19***	-0.08***	-0.20***	-0.18***	-0.15***	-0.03***	-0.21***		
Intro_len	0.15***	0.17***	0.01***	0.13***	0.27***	0.20***	0.15***	0.03***	0.21***	-0.26***	
Desc_len	0.12***	0.17***	0.14***	0.18***	0.33***	0.17***	0.12***	0.02***	0.18***	-0.22***	0.24***

Note. *** and * represent significance at the 1% and 10% levels, respectively.

across the two samples. Given that TCM doctors only account for about 10% of all doctors in our sample, the above observation crudely reveals that doctor-patient interactions can be more active for traditional medicine consultations in an Internet setup. Nevertheless, for all variables, the maximum values of the sample of modern hospital departments are noticeably higher than the corresponding values of the TCM sample. The same comparison relationship is also true for the values of variable standard deviations. In addition, almost all of our variables are significantly correlated with each other. Except for the year of being online, all explanatory variables have a positive association with both the proxies of our dependent variables, namely, page view and order. These facts imply that there exists a high degree of fluctuation in the potential explanatory variables within and across subsamples that allows us to identify the potential determinants of the higher number of web page visits to TCM doctors in the Internet hospital community. As a final check, Table 3 presents the pairwise correlation matrix. On an average, our concerned variables are significantly

correlated with a moderate level of correlation coefficient magnitude, except for the high associations among the three proxies of review, thank-you, and gift for physicians' online professional performance.

3.2. Comparative Regression Analysis. We first regress web page visits, a.k.a. page views, on doctor characteristics for making comparisons between TCM and other doctors. The results in Table 4 show that the information on the doctor's visiting card cannot significantly explain the user's browsing behavior, but after adding more detailed information, especially the doctor's evaluation information, the browsing behavior can be fully explained. This implies that the generation of page views may not be random and groundless, and users may have certain intrinsic motivations and clear directions when searching for doctors. Given that the main information channels for Chinese users to select doctors are online comments and doctor recommendations, as well as family and friend recommendations, patients will use different information sources when selecting different departments. For example, when selecting traditional Chinese

TABLE 4: The effects on page views for doctors in the TCM and MM departments.

Variables	(1) All Page view	(2) All Page view	(3) TCM Page view	(4) MM Page view
Desc_len	3.88*** (0.24)	1.50*** (0.19)	1.36* (0.81)	1.07*** (0.18)
Star	541.29*** (6.45)	-123.57*** (6.18)	-266.04*** (35.13)	-136.84*** (5.86)
City	104.45*** (8.20)	17.75*** (6.56)	-42.01 (27.35)	29.77*** (6.39)
Hot		-257.60*** (14.15)	-417.36*** (58.82)	-221.01*** (13.81)
Thank-you		-12.04*** (0.45)	23.51*** (2.76)	-11.37*** (0.43)
Gift		6.26*** (0.04)	15.75*** (0.27)	5.48*** (0.04)
Article		2.56*** (0.01)	2.32*** (0.02)	5.73*** (0.06)
Review		9.50*** (0.23)	-7.05*** (1.15)	9.34*** (0.22)
Start year		-62.64*** (1.24)	-66.14*** (4.98)	-59.05*** (1.21)
Intro_len		0.13*** (0.01)	0.38*** (0.05)	0.10*** (8.48)
Academic title dummies	Yes†	Yes†	Yes	Yes†
Clinic title dummies	Yes	Yes	Yes	Yes
Department dummies	Yes†	Yes†	Yes	Yes†
Constant	252.94 (1164.83)	127309.8*** (2643.47)	134057.7*** (10156.98)	119594.3*** (2443.94)
Observations	168870	168870	17513	151357
R-squared	0.075	0.452	0.621	0.428

Note. Page view is measured in thousands of web page visits. Standard errors are in parentheses. *** and * represent significance at the 1% and 10% levels, respectively. For all AT, CT, and department dummy variables included in the regression, we mark † only when more than half of the dummy coefficients turn out to be significant.

medicine, family and friend recommendations are the most dependent on patients. This finding explains the characteristics of browsing behavior to a certain extent. However, this behavioral logic also exposes the limited subjective initiative and limitations of OHC. That is, patients can learn about their condition through online doctors, but the excessive celebrity effect is likely to reduce the efficiency of medical resource redistribution, which may lead to a more serious occupation of cutting-edge doctor resources while middle- and low-end doctor resources are unoccupied to excess.

However, the behavior of patients' final choices can be significantly explained by the detailed information provided by doctors, especially by evaluative factors. We then replace the previous page view dependent variable with the order volume proxy and incorporate additional potential controls. Wang et al. [33] also found that doctors' online reputations will affect consumers' behavior in consultation. From the perspective of feedback, Yang and Zhang [34] discovered similar conclusions, and they further documented that the feedback of paid services has more reference value for patients. This implies that there exists a brand effect in the TCM field of OHC. Patients will try to find and choose doctors with good medical skills and reputations through various channels. Another crucial factor is the unintentional promotion of the website. Doctors with a large number of

orders completed will be ranked at the top of the list. Table 5 summarizes our findings by comparing the order number determination regressions in the TCM sample and the sample of non-TCM departments. It seems that online patients and OHC evaluations play a much larger role in increasing the number of TCM orders than other hospital departments. However, doctor-specific characteristics seem to possess no such power.

When comparing TCM with other MM departments, our finding is that when choosing modern medicine doctors on the Internet, users pay more attention to the degree of economic development of the doctor's residence city, while patients browsing TCM online content do not have such concerns. However, concerning placing medical service orders online, patients irrespective of TCM or MM collectively show great concern for regions. This phenomenon may be related to the better medical conditions of modern medicine in large cities. The academic titles of doctors in MM departments matter a lot to patients. However, titles seem to play a lesser role for TCM departments. In terms of goodness of fit, the browsing volume model with more regressors can explain the variations of the dependent variable much better for observations in the TCM department sample than in other departments. Besides, the order volume model also worked better in explaining the TCM department, which indicates that the online information about the TCM doctors is more

TABLE 5: The effects on the volume of doctor service orders in the TCM and MM departments.

Variables	(1) All Order	(2) TCM Order	(3) MM Order
Desc_len	1.13*** (0.11)	0.72*** (0.24)	1.11*** (0.13)
Star	193.91*** (2.72)	289.00*** (10.39)	189.62*** (2.80)
City	-39.14*** (2.73)	-23.63*** (7.91)	-39.52*** (2.90)
Hot	-41.82*** (6.21)	58.41*** (17.60)	-50.10*** (6.74)
Thank-you	-15.01*** (0.20)	-15.42*** (0.80)	-15.43*** (0.24)
Gift	1.22*** (0.01)	0.34*** (0.10)	1.30*** (0.01)
Article	-0.78*** (0.01)	-0.91*** (0.01)	-0.29*** (0.01)
Review	11.96*** (0.11)	11.07*** (0.32)	12.17*** (0.14)
Start year	6.44*** (0.53)	6.60*** (1.51)	6.60*** (0.64)
Intro_len	-0.01*** (0.01)	-0.09*** (0.01)	-0.03*** (0.01)
Page view	0.01*** (0.01)	0.01*** (0.01)	0.01*** (0.01)
Academic title dummies	Yes†	Yes	Yes†
Clinic title dummies	Yes	Yes	Yes
Department dummies	Yes†	Yes	Yes†
Constant	-12482.31*** (1137.22)	-13365.71*** (2985.30)	-13036.50*** (1150.92)
Observations	168870	17513	151357
R-squared	0.836	0.884	0.830

Note. Standard errors are in parentheses. *** and ** represent significance at the 1% and 5% levels, respectively. For all AT, CT, and department dummy variables included in the regression, we mark † only when more than half of the dummy coefficients turn out to be significant.

efficient and the extent to which patients receive and process these pieces of information is also large. In contrast, the information of interest to Internet users of other medical departments has been, to some extent, hidden in the constant terms of our empirical setup.

One last aspect that merits note is that the TCM doctor with more online reviews or comments has a lower volume of web page browsing. However, the number of medical

consulting orders placed is positively associated with the number of reviews. This might have something to do with the contents of the reviews. In the TCM field, it is very challenging to evaluate the effectiveness of a TCM treatment. As a result, both positive and negative reviews are more common for TCM doctors. Nevertheless, the number of orders and reviews should have a positive correlation in theory, regardless of good and bad comments. More orders will naturally lead to more views, but how many times a doctor's page has been viewed should be more related to the reputation of the doctor from a third-party perspective. We expect to dig deeper in this regard if detailed textual analysis can be performed on the comments.

3.3. Robustness Tests. Although the above empirical analysis preliminarily proves that the information provided by the website can help users make choices and well reflect the logic and preference of users' behavior, it is difficult to convincingly evaluate the acceptance of OHC and users' willingness to pay only by using simple quantitative variables. Moreover, either the number of page views or the number of orders placed for different doctors are not of the same degree of magnitude due to variations in their capability and popularity. Distortions in the estimate are likely to appear because of extreme values. For this reason, we use an alternative but relevant proxy to repeat our previous exercises as a robust test. In particular, we calculate the order conversion ratio to be the ratio of order volume to the number of page views. This is a standardized index, which can give us a unified evaluation standard to evaluate the ability and popularity of doctors with different attributes and more directly reflect the actual applicability of OHC. Compared with the single number of page views or orders, OCR contains more information, allowing us to analyze OHC acceptance and users' willingness to pay for OHC service in more dimensions. On the basis of the second model, we use OCR as the explained variable to establish the following model. Furthermore, because OCR is a positive number less than 1, we adopt the Probit model to analyze our results in addition to the baseline ordinary least squares (OLS) specification. The corresponding results are summarized in Table 6. It is demonstrated that the main findings of this article stay almost unchanged with alternative variable construction methods and alternative empirical estimation setups.

$$\begin{aligned}
 \text{OCR}_i = & \beta_0 + \beta_1 \cdot \text{AT}_i + \beta_2 \cdot \text{CT}_i + \beta_3 \cdot \text{DEPARTMENT}_i + \beta_4 \times \text{HOT}_i + \beta_5 \times \text{CITY}_i + \beta_6 \times \text{DESC}_{\text{LEN}}_i \\
 & + \beta_7 \times \text{ARTICAL}_i + \beta_8 \times \text{REVIEW}_i + \beta_9 \times \text{THANK}_i + \beta_{10} \times \text{GIFT}_i + \beta_{11} \\
 & \times \text{INTRO}_{\text{LEN}}_i + \beta_{12} \times \text{STARTYEAR}_i + \beta_{13} \times \text{STAR} + \varepsilon_i.
 \end{aligned} \tag{3}$$

When we focus on OCR, the interpretation effect of the information provided by the website is greatly reduced, which may be caused by individual differences in patient

behavior. Because the number of views generated by different patients is random, not all browsing behaviors will eventually lead to order placement. However, the previous

TABLE 6: Results of using alternative dependent variables and empirical specifications.

	(1) OLS all	(2) Probit all	(3) Probit TCM	(4) Probit MM
Variables	OCR	OCR	OCR	OCR
Desc_len	0.01*** (0.01)	0.01*** (0.01)	0.01*** (0.01)	0.01*** (0.01)
Star	0.01*** (0.01)	0.01*** (0.01)	0.01*** (0.01)	0.01*** (0.01)
City	-0.01*** (0.01)	0.02* (0.01)	0.01 (0.03)	0.01** (0.01)
Hot	0.01*** (0.01)	0.50*** (0.02)	0.49*** (0.07)	0.50*** 0.03
Thank-you	-0.01 (0.01)	0.19*** (0.01)	0.14*** (0.02)	0.19*** (0.01)
Gift	-0.01*** (0.01)	0.82*** (0.01)	0.76*** (0.03)	0.84*** (0.01)
Article	-0.01 (0.01)	0.10*** (0.01)	0.08*** (0.01)	0.10*** (0.01)
Review	-0.01*** (0.01)	0.04*** (0.01)	0.01** (0.01)	0.04*** (0.00)
Start year	0.01*** (0.01)	-0.04*** (0.01)	-0.04*** (0.01)	-0.04*** (0.01)
Intro_len	-0.01*** (0.01)	-0.01*** (0.01)	-0.01 (0.01)	-0.01*** (0.01)
Academic title dummies	Yes†	Yes†	Yes	Yes†
Clinic title dummies	Yes	Yes†	Yes	Yes
Department dummies	Yes†	Yes†	Yes	Yes†
Constant	-0.33*** (0.01)	82.01*** (3.8)	83.81*** (10.4)	79.75*** (4.1)
Observations	168870	157459	16840	140619
R-squared	0.262	0.347	0.315	0.352

Note. Standard errors are in parentheses. ***, **, and * represent significance at the 1%, 5%, and 10% levels, respectively. For all AT, CT, and department dummy variables included in the regression, we mark † only when more than half of the dummy coefficients turn out to be significant.

results are still valid, and the evaluation information about doctors is still the most important factor for users. The significant constant term and low fitting coefficient also show that the ordering behavior and browsing behavior are not unified in most cases, and the users' choice is disturbed by strong external factors.

By comparing traditional Chinese medicine with modern medicine, we find that "whether the hospital is located in large cities" is an irrelevant variable for the order conversion ratio of traditional Chinese medicine departments, but it is a significant variable for modern medical departments, which indicates that OHC gives full play to the resources for scheduling medical resources and promotes the redistribution of high-end medical resources to underdeveloped areas. At the same time, nonacademic TCM doctors have been exposed and visited more. In addition, in the process of browsing and placing orders, people who choose traditional Chinese medicine departments do not care about the academic and professional titles of doctors, but people who choose modern medicine will consider the academic title of doctors. This may also be determined by the traditional differences between TCM and modern medicine. Unlike the findings from the two previous models, the OCR determination specification performs less well in TCM than in other departments. Considering that we have far more than usual browsing and query data in TCM, we believe that this result is caused by the presence of excessive invalid browsing in TCM.

4. Further Discussion

According to the Department of Health and Human Services, more than 60% of medical institutions and 40% to 50% of hospitals in the United States already use some form of telemedicine [35]. It is worth mentioning that telehealth in the United States is not in the state of being relatively separated from the public medical system like in China, but is attached to the hospital where the doctor works, which is more similar to the expanded version of the online appointment system. Compared with China's OHC platforms, it lacks integration, but the regulatory responsibilities are mainly undertaken by the American Telemedicine Association and other industry groups [36], while not by private companies and general governance departments. Moreover, the acceptance of telemedicine by Americans is much higher than that of China. According to a report by Kaiser Permanente of Northern California, the telehealth service has exceeded in-person visits by Advisory Board [37]. It is not difficult to conclude that China's OHCs are still immature in promoting telemedicine services, and there is still a long way to go. In this regard, we propose the following three suggestions.

The latest research points out that the professional ability, integrity, online reputation, and patient group size of psychological counselors have a significant positive impact on patient initial trust. Initial trust and the efforts of

psychologists have a significant impact on sustained trust [38]. Whether this conclusion can be further extended to other departments still needs more experience. How to further promote telemedicine and help patients trust remote doctors? Providing more reliable information sources may be a worthwhile attempt. Therefore, a personalized doctor recommendation system is most needed at present. Secondly, the effective narrative turn of doctor-patient communication can be very useful to strengthen trust, improve the doctor-patient relationship, and increase the efficiency of treatment [39]. In the current narrative transformation of doctor-patient communication, in addition to necessary treatment and care for patients, more empathy and communication should be given in a narrative way [40]. The development of telemedicine also needs to consider this point of view. Last but not least, the platform should take more responsibility to avoid profit-making, false publicity, and promotion. This problem is much more serious in online traditional Chinese medicine departments. Although online TCM is theoretically more in line with the OHC diagnosis method, Chinese patients' long-standing habit of choosing doctors through offline interactions makes online TCM diagnosis results more of a reference. However, these facts also imply that TCM has a high degree of recognition in China and has a large room for exploring its potential applications in OHCs.

5. Concluding Remarks and Extensible Directions

Through the above analysis, it is easy to see that the current information provided by OHC is not enough to support or encourage patients to visit their doctors online, and patients often use third-party information actively or passively to make decisions. However, we are glad to see that users are happy to use the information on the OHC platform as a reference for medical treatment, especially when it is the most frequently browsed department, as represented by traditional Chinese medicine. Among these limited information sources, the factors that directly reflect the ability of doctors, such as the various achievements of doctors on the platform, have become the most recognizable by patients. Interestingly, the academic title is more persuasive in modern medicine than the doctor's clinical title. In addition, whether the hospital where the doctor works is located in a larger city or not turns out not to be a factor to consider. This coincides with the idea that Internet hospitals decrease the importance of geographical factors. On the one hand, it shows that the medical resources of the platform are of sufficient quality to believe, weakening the user's preference for developed cities. On the other hand, it also shows that OHC has overcome the geographical factors to a certain extent and realized the remote redistribution of medical resources by using the Internet.

The three proxies all reflect the same problem, that is, although users are gradually trying to accept and use OHC, they still tend to choose doctors according to third-party information and may have a low willingness to pay for the current OHC price level. This problem is difficult to

overcome by the platform in the short term. Patients need a long-term process to gradually adapt to the upgraded medical environment.

Regarding potential directions for future studies, our findings point out the following aspects. The volume of page views created by patients who want to see a doctor in TCM before selecting an OHC doctor is much larger than that of other departments, but the proportion of patients paying for diagnosis and treatment is much smaller than that of modern medical departments. The status quo of "view but no order" in TCM reflects the following potential problems. First of all, most of the patients who have completed the treatment of online TCM are attracted by the doctors' fame, but they will still actively check the cases and doctors for related information. Second, traditional Chinese medicine is the only alternative for patients. Although browsing occurs, they may eventually choose modern medicine. Third, some patients try to complete self-diagnosis through relevant comments because TCM often does not need CT, X-ray, and other precise examinations. Fourth, the price of online traditional Chinese medicine is relatively high for the low-income group, and patients will give up placing orders for OHC medical treatment. However, due to the purpose and scope of our research, we cannot make a specific conclusion. Future research may allow the analysis of a wider range of data to help identify and improve the development of Internet TCM.

Data Availability

The dataset used for this study is compiled from the publicly-available physicians' webpages on the Good Doctor website.

Conflicts of Interest

The authors declare that they have no conflicts of interest.

References

- [1] S. S. Guo, X. Guo, X. Zhang, and D. Vogel, "Doctor-patient relationship strength's impact in an online healthcare community," *Information Technology for Development*, vol. 24, no. 2, pp. 279–300, 2018.
- [2] J. N. Wang, Y. L. Chiu, H. Yu, and Y. T. Hsu, "Understanding a nonlinear causal relationship between rewards and physicians' contributions in online health care communities: longitudinal study," *Journal of Medical Internet Research*, vol. 19, no. 12, p. e427, 2017.
- [3] X. Zhang, L. Ma, Y. Ma, and X. Yang, "Mobile information systems usage and doctor-patient relationships: an empirical study in China," *Mobile Information Systems*, vol. 2021, Article ID 6684448, 11 pages, 2021.
- [4] Y. L. Chiu, J. N. Wang, H. Yu, and Y. T. Hsu, "Consultation pricing of the online health care service in China: hierarchical linear regression approach," *Journal of Medical Internet Research*, vol. 23, no. 7, Article ID e29170, 2021.
- [5] J. M. Goh, G. G. Gao, and R. Agarwal, "The creation of social value: can an online health community reduce rural-urban health disparities?" *MIS Quarterly*, vol. 40, no. 1, pp. 247–263, 2016.

- [6] H. S. Wald, C. E. Dube, and D. C. Anthony, "Untangling the web: the impact of internet use on health care and the physician-patient relationship," *Patient Education and Counseling*, vol. 68, no. 3, pp. 218–224, 2007.
- [7] N. Xiao, R. Sharman, H. R. Rao, and S. Upadhyaya, "Factors influencing online health information search: an empirical analysis of a national cancer-related survey," *Decision Support Systems*, vol. 57, pp. 417–427, 2014.
- [8] S. Van Oerle, A. Lievens, and D. Mahr, "Value co-creation in online healthcare communities: the impact of patients' reference frames on cure and care," *Psychology and Marketing*, vol. 35, no. 9, pp. 629–639, 2018.
- [9] G. Liu, L. Zhou, and J. Wu, "What affects patients' online decisions: an empirical study of online appointment service based on text mining," in *Smart Health*, H. Chen, Q. Fang, D. Zeng, and J. Wu, Eds., Springer, Berlin, Germany, 2018.
- [10] H. Yang, X. Guo, T. Wu, and X. Ju, "Exploring the effects of patient-generated and system-generated information on patients' online search, evaluation and decision," *Electronic Commerce Research and Applications*, vol. 14, no. 3, pp. 192–203, 2015.
- [11] Y. Li, Y. Song, W. Zhao, X. Guo, X. Ju, and D. Vogel, "Exploring the role of online health community information in patients' decisions to switch from online to offline medical services," *International Journal of Medical Informatics*, vol. 130, Article ID 103951, 2019.
- [12] D. Dranove, "Demand inducement and the physician/patient relationship," *Economic Inquiry*, vol. 26, no. 2, pp. 281–298, 1988.
- [13] A. Parasuraman, V. A. Zeithaml, and L. L. Berry, "A conceptual model of service quality and its implications for future research," *Journal of Marketing*, vol. 49, no. 4, pp. 41–50, 1985.
- [14] D. Dranove, *An economic model of the physician-patient relationship*, Ph.D Thesis, Stanford University, Stanford, CA, USA, 1983.
- [15] G. G. Gao, B. N. Greenwood, J. McCullough, and R. Agarwal, "A digital soapbox? the information value of online physician ratings," in *Proceedings of the Conference on Information Systems and Technology*, pp. 11–12, Washington, D.C., USA, October 2011.
- [16] X. Cao, Y. Liu, Z. Zhu, J. Hu, and X. Chen, "Online selection of a physician by patients: empirical study from elaboration likelihood perspective," *Computers in Human Behavior*, vol. 73, pp. 403–412, 2017.
- [17] N. Lu and H. Wu, "Exploring the impact of word-of-mouth about physicians' service quality on patient choice based on online health communities," *BMC Medical Informatics and Decision Making*, vol. 16, no. 1, p. 151, 2016.
- [18] Y. Han, R. K. Lie, and R. Guo, "The internet hospital as a telehealth model in China: systematic search and content analysis," *Journal of Medical Internet Research*, vol. 22, no. 7, Article ID e17995, 2020.
- [19] Z. Wang, L. Wang, F. Xiao, Q. Chen, L. Lu, and J. Hong, "A traditional Chinese medicine traceability system based on lightweight blockchain," *Journal of Medical Internet Research*, vol. 23, no. 6, Article ID e25946, 2021.
- [20] Q. Zhang, Y. J. He, Y. H. Zhu et al., "The evaluation of online course of traditional Chinese medicine for medical bachelor, bachelor of surgery international students during the COVID-19 epidemic period," *Integrative Medicine Research*, vol. 9, no. 3, Article ID 100449, 2020.
- [21] Y. Ding, X. Zhai, Q. Wang, J. Kou, and J. Tong, "Study on the construction of an index system for evaluating the quality of information services of internet Chinese medicine hospital," *Chinese Hospitals*, vol. 26, no. 5, pp. 23–27, 2022, in Chinese.
- [22] Y. Wang, "A brief exploration of the new development model of community hospitals based on internet-based TCM intelligence," *China's Naturopath*, vol. 30, no. 8, pp. 120–123, 2022, in Chinese.
- [23] Y. Cheng, "Application of traditional Chinese medicine in integrated family hospital management based on "internet+"," *Journal of Traditional Chinese Medicine Management*, vol. 30, no. 8, pp. 235–246, 2022, in Chinese.
- [24] Q. Ma, "Application of "internet+" Chinese medicine health management in the management of elderly patients with hypertension," *Journal of Traditional Chinese Medicine Management*, vol. 30, no. 8, pp. 235–246, 2022, in Chinese.
- [25] W. Cai, Y. Li, and W. Shen, "Practice and consideration of "internet+" acupuncture treatment in the post-epidemic era," *Journal of Traditional Chinese Medicine Management*, vol. 30, no. 8, pp. 221–222, 2022, in Chinese.
- [26] Y. Sun and Q. Ge, "SWOT analysis of the construction of Chinese medicine characteristic nursing in the context of "internet+"," *Journal of Traditional Chinese Medicine Management*, vol. 30, no. 5, pp. 86–90, 2022, in Chinese.
- [27] J. Tian and S. Gao, "Analysis of the constraints and countermeasures for the development of "internet+" Chinese medical treatment," *Health Economics Research*, vol. 39, no. 3, pp. 70–73, 2022, in Chinese.
- [28] C. E. Beaudoin and C.-C. Tao, "Benefiting from social capital in online support groups: an empirical study of cancer patients," *CyberPsychology and Behavior*, vol. 10, no. 4, pp. 587–590, 2007.
- [29] L. Yan and Y. Tan, "Feeling blue? go online: an empirical study of social support among patients," *Information Systems Research*, vol. 25, no. 4, pp. 690–709, 2014.
- [30] H. Yu, Y. Wang, J. N. Wang, Y. L. Chiu, H. Qiu, and M. Gao, "Causal effect of honorary titles on physicians, service volumes in online health communities: retrospective study," *Journal of Medical Internet Research*, vol. 22, no. 7, Article ID e18527, 2020.
- [31] S. Zhang, J. N. Wang, Y. L. Chiu, and Y. T. Hsu, "Exploring types of information sources used when choosing doctors: observational study in an online health care community," *Journal of Medical Internet Research*, vol. 22, no. 9, Article ID e20910, 2020.
- [32] H. Wu and N. Lu, "Service provision, pricing, and patient satisfaction in online health communities," *International Journal of Medical Informatics*, vol. 110, pp. 77–89, 2018.
- [33] Y. Wang, H. Wu, X. Lei, J. Shen, and Z. Feng, "The influence of doctors' online reputation on the sharing of outpatient experiences: empirical Study," *Journal of Medical Internet Research*, vol. 22, no. 12, Article ID e16691, 2020.
- [34] H. Yang and X. Zhang, "Investigating the effect of paid and free feedback about physicians' telemedicine services on patients' and physicians' behaviors: panel data analysis," *Journal of Medical Internet Research*, vol. 21, no. 3, Article ID e12156, 2019.
- [35] Office of Health Policy, *Report to Congress: E-Health and Telemedicine*, Office of the Assistant Secretary for Planning and Evaluation, Washington, D.C., USA, 2016.

- [36] R. V. Tuckson, M. Edmunds, and M. L. Hodgkins, "Telehealth," *New England Journal of Medicine*, vol. 377, no. 16, pp. 1585–1592, 2017.
- [37] Advisory Board, "A milestone: Kaiser now interacts more with patients virtually than in-person," 2016, <https://www.advisory.com/daily-briefing/2016/10/13/kaiser-telehealth>.
- [38] H. Wu, Z. Deng, and R. Evans, "Building patients' trust in psychologists in online mental health communities," *Data Science and Management*, vol. 5, no. 1, pp. 21–27, 2022.
- [39] B. Wu, "Patient continued use of online health care communities: web mining of patient-doctor communication," *Journal of Medical Internet Research*, vol. 20, no. 4, p. e126, 2018.
- [40] H. Zhang, "The shift in the narrative of doctor-patient communication and the cultivation of medical information exchange communication based on the information technology era," *Mobile Information Systems*, vol. 2022, Article ID 7121092, 11 pages, 2022.

Research Article

Deep Learning Multi-label Tongue Image Analysis and Its Application in a Population Undergoing Routine Medical Checkup

Tao Jiang ¹, Zhou Lu ^{1,2}, Xiaojuan Hu,³ Lingzhi Zeng,¹ Xuxiang Ma,¹ Jingbin Huang,¹ Ji Cui,¹ Liping Tu,¹ Changle Zhou,⁴ Xinghua Yao ¹, and Jiatio Xu ¹

¹Basic Medical College, Shanghai University of Traditional Chinese Medicine, 1200 Cailun Road, Shanghai 201203, China

²Department of Acupuncture and Moxibustion, Huadong Hospital, Fudan University, 221 West Yanan Road, Shanghai 200040, China

³Shanghai Collaborative Innovation Center of Health Service in Traditional Chinese Medicine, Shanghai University of Traditional Chinese Medicine, 1200 Cailun Road, Shanghai 201203, China

⁴School of Information Science and Engineering, Xiamen University, Xiamen 361005, China

Correspondence should be addressed to Xinghua Yao; xhyaosues@aliyun.com and Jiatio Xu; xjt@fudan.edu.cn

Received 12 March 2022; Revised 9 June 2022; Accepted 7 September 2022; Published 28 September 2022

Academic Editor: Vijaya Anand

Copyright © 2022 Tao Jiang et al. This is an open access article distributed under the Creative Commons Attribution License, which permits unrestricted use, distribution, and reproduction in any medium, provided the original work is properly cited.

Background. Research on intelligent tongue diagnosis is a main direction in the modernization of tongue diagnosis technology. Identification of tongue shape and texture features is a difficult task for tongue diagnosis in traditional Chinese medicine (TCM). This study aimed to explore the application of deep learning techniques in tongue image analyses. **Methods.** A total of 8676 tongue images were annotated by clinical experts, into seven categories, including the fissured tongue, tooth-marked tongue, stasis tongue, spotted tongue, greasy coating, peeled coating, and rotten coating. Based on the labeled tongue images, the deep learning model faster region-based convolutional neural networks (Faster R-CNN) was utilized to classify tongue images. Four performance indices, i.e., accuracy, recall, precision, and F1-score, were selected to evaluate the model. Also, we applied it to analyze tongue image features of 3601 medical checkup participants in order to explore gender and age factors and the correlations among tongue features in diseases through complex networks. **Results.** The average accuracy, recall, precision, and F1-score of our model achieved 90.67%, 91.25%, 99.28%, and 95.00%, respectively. Over the tongue images from the medical checkup population, the model Faster R-CNN detected 41.49% fissured tongue images, 37.16% tooth-marked tongue images, 29.66% greasy coating images, 18.66% spotted tongue images, 9.97% stasis tongue images, 3.97% peeled coating images, and 1.22% rotten coating images. There were significant differences in the incidence of the fissured tongue, tooth-marked tongue, spotted tongue, and greasy coating among age and gender. Complex networks revealed that fissured tongue and tooth-marked were closely related to hypertension, dyslipidemia, overweight and nonalcoholic fatty liver disease (NAFLD), and a greasy coating tongue was associated with hypertension and overweight. **Conclusion.** The model Faster R-CNN shows good performance in the tongue image classification. And we have preliminarily revealed the relationship between tongue features and gender, age, and metabolic diseases in a medical checkup population.

1. Introduction

Tongue inspection is the most common, intuitive, and effective diagnostic method of traditional Chinese medicine (TCM) [1]. Recent TCM researches have realized measurable and digitized color features of tongue images by means of color space parameters such as RGB, Lab, and HIS [2–4].

However, the quantification of the shape and texture of tongue images remains a difficult point in tongue diagnosis. Much attention has focused on the automatic recognition methods of the shape and texture of tongue images. Obafemi-Ajayi et al. [5] have proposed a feature extraction method for automated tongue image shape classification based on geometric features and polynomial equations. Yang et al. [6] extracted the cracks by applying the G component

of the false-color image in RGB color space, and the accuracy of detection was 82.00%. Douglas–Peucker algorithm was implemented to extract the number of features for tooth-marked tongue and achieved an accuracy of 80% [7]. Xu et al. [8] conducted an RGB color range and a gray mean value of acantha and ecchymosis in tongue patterns, and the overall accuracy of recognition was 77.10%. Wang et al. [9] realized the prickles extraction on the green tongue image, with an accuracy of 88.47%. Yet, due to the complex and diverse tongue features, classical image processing methods have some problems, such as space-time consumptive algorithm, difficulties in automated high-throughput processing, and weak migration ability in correlation research [10–12], which make the comprehensive analysis of tongue images unavailable.

Intelligent diagnosis based on images is a main direction of modernization of tongue diagnosis technology [13]. As the current mainstream technology, a convolutional neural network (CNN) has a powerful capability of feature extraction and representation [14, 15], which greatly improves the accuracy and efficiency of tongue image segmentation, and classification [16–20]. For example, Chen’s team has utilized the deep residual neural network (ResNet) to identify the tooth-marked tongue, with an accuracy of over 90% [21]. Xu et al. [22] have proposed a CNN model combining a u-shaped net (U-NET) and Discriminative Filter Learning (DFL) for classification and recognition of different types of tongue coating, achieving an F1-Score of 93%. The research on the recognition and classification of the tooth-marked tongue [23] and cracked tongue [24] has significantly improved the accuracy of tongue image identification.

However, tongue images have multi-label attributes (Figure 1(a)). Although the classical model CNN shows better recognition performance for single tongue features such as tooth marks or fissures (Figure 1(b)), the multi-CNN fusion model has no apparent superiority in the multi-label classification of tongue images with diverse features (Figure 1(c)). Under nonparallel conditions, multiple CNN models require huge space and time. The classical CNN model fails to accurately identify, locate and quantify complex and diverse fine-grained features of tongue images simultaneously, and it is difficult to achieve efficient detection and recognition of tongue images in parallel.

Object detection technology is considered as a method to find a specific object in an image and determine the specific position of the object. As one of the mainstream neural networks for object detection, faster region-based convolutional neural networks (Faster R-CNN) [25] can perform multi-label recognition with only one model, thus reducing the cost of training multiple models. Here, we utilized Faster R-CNN and fine-tune method to extract local features of tongue images, learning the high-level semantic features. Aiming at 7 categories of tongue shape and texture in TCM, ResNet [26] was used as the backbone network for feature extraction to construct a deep learning model.

In this research, we constructed a standard database for training, testing, and validation realized the efficient and accurate classification and recognition of local features of

tongue images and applied it to a population undergoing medical checkups with Chinese medicine, in order to reveal the association of tongue image features with diseases.

2. Materials and Methods

We proposed a deep learning multi-label tongue image model based on Faster R-CNN. A total of 8676 tongue images were collected to train and test the proposed model. The collected tongue images annotated by experts were divided into seven categories. Furthermore, this approach was applied to a population undergoing medical checkups with Chinese medicine. The specific process of this study is shown in Figure 2.

2.1. Tongue Image Collection and Preprocess. As shown in Figure 3, all the tongue images were acquired by using TFDA-1 and TDA-1 tongue diagnosis instruments designed by Xu’s team at Shanghai University of TCM. The instruments were equipped with unified CCD equipment, a standard D50 light source, a color temperature of 5003K, and a color rendering index of 97 [27]. Tongue images were obtained from September 2017 to December 2018 at Shuguang Hospital. The raw tongue image size was 5568×3711 pixels in JPG format. To reduce the amount of deep learning calculation and eliminate the interference of other regions except the tongue body, all tongue images were automatically cut to the size of 400×400 pixels by mask R-CNN.

2.2. Tongue Image Labeling and Datasets Construction. All tongue image labels were evaluated and screened by 10 TCM experts with normal vision and reported normal color vision [28]. To avoid the chromatic differences from the monitor, experts interpreted and screened under uniform conditions with 27 inches APPLE Cinema HD monitor. With reference to the diagnostic criteria of tongue image features [1, 29], tongue images were divided into seven categories. At least 8 out of 10 experts confirmed that the dataset contained the same labels, and all 8676 tongue images were annotated by two experts as seven different folders. Example samples of each typical tongue image were shown in Figure 2(b), and the other eight experts respectively checked the labeled folders. The images with the inconsistent diagnosis were excluded from this research.

The datasets for Faster R-CNN were with the MS COCO format, which was the most popular standard format in the field of object detection [30]. We used LabelImg (Version 1.8.1) to annotate the interest regions of shape and texture on the tongue image. The annotation was confirmed by experts and the process interface is shown in Figure 2(c). Then, the generated “XML” annotation files were transferred into the “JSON” format file using Python (Version 3.6).

2.3. Dataset Partition. The constructed datasets were randomly partitioned into 80% training set, 10% validation set, and 10% testing set. The number of the training datasets and labels in 7 categories used to build the Faster R-CNN model

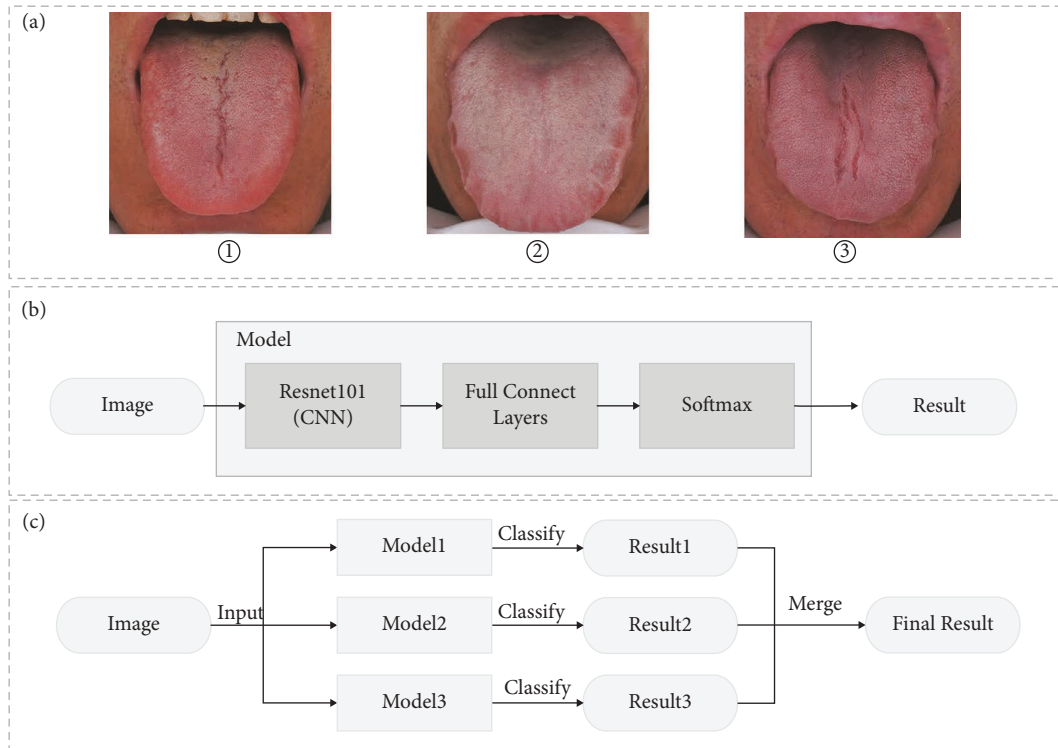


FIGURE 1: Deep learning methods for tongue diagnosis analyses. (a) Fissured tongue image, tooth-marked tongue image, and tongue image with fissures and tooth marks; (b) CNN method of single-object detection; (c) CNN method of multi-label detection in tongue images.

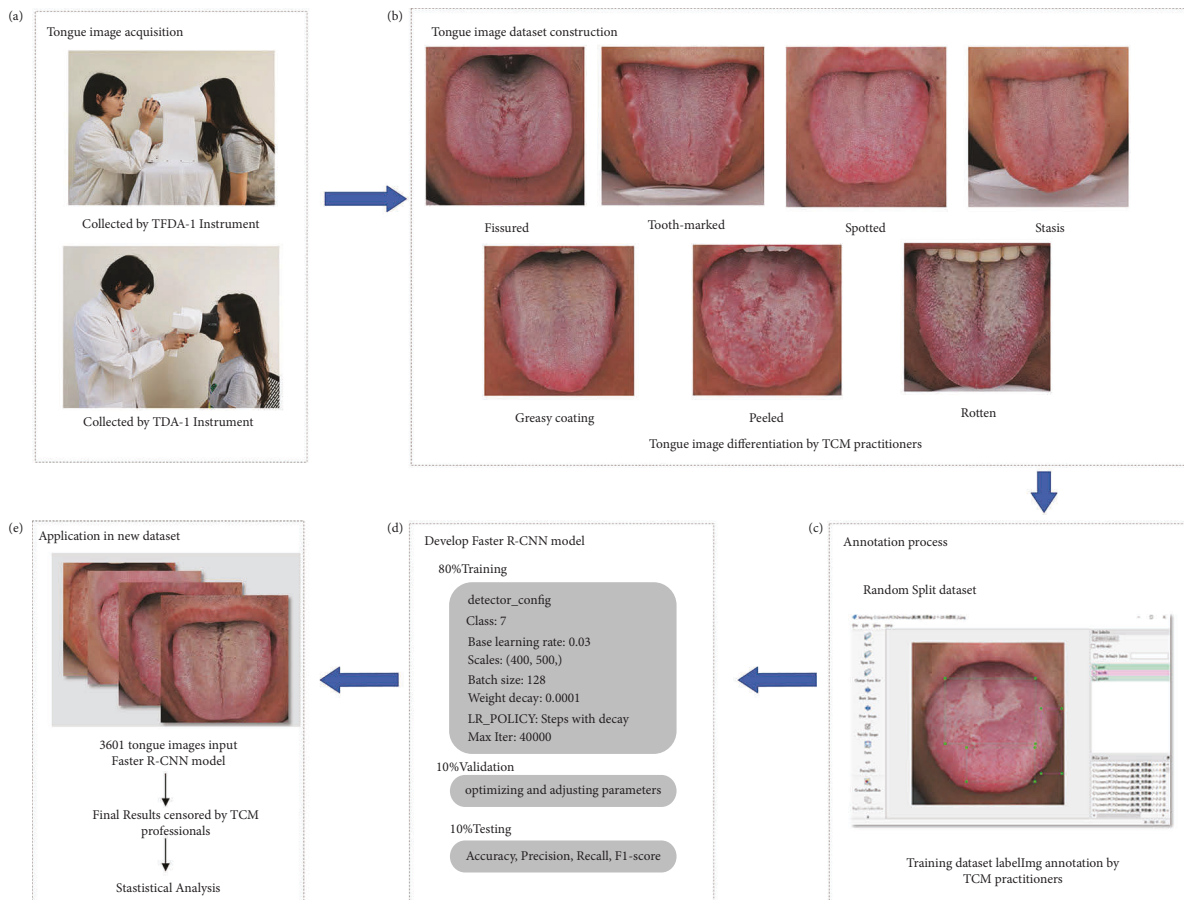


FIGURE 2: The workflow of the entire research. (a) Demonstration of the acquisition process of tongue image; (b) example samples of tongue image differentiation dataset calibrated by experts; (c) interest regions marked manually by TCM practitioners using the LabelImg software; (d) Faster R-CNN model trained by tongue images and object location of training set; (e) study on tongue image features of 3601 people undergoing medical checkup based on Faster R-CNN model.

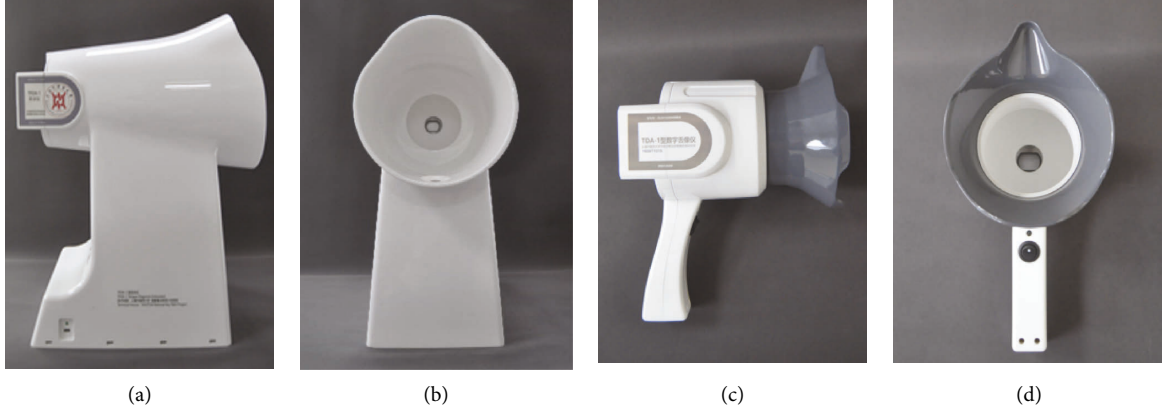


FIGURE 3: TFDA-1 and TDA-1 tongue diagnosis instrument. (a) Side view of TFDA-1; (b) front view of TFDA-1; (c) side view of TDA-1; (d) front view of TDA-1.

were shown in Table 1. In addition, the number of tongue images in each category included in the testing set was equal to the validation set.

2.4. Faster R-CNN Model Development for Recognizing Tongue Shape and Texture. Figure 4(a) shows the network architecture diagram of Faster R-CNN, mainly consisting of four parts: convolution layer, regional proposal network, the region of interest (ROI) pooling layer, and a layer of classifier and regressor [31]. The backbone convolution layer ResNet101, as shown in Figure 4(b), extracts feature maps from the input tongue images; the region proposal network (RPN) centers on each pixel of the feature maps, and generated anchor boxes with different scales in the tongue images by using nonmaximum suppression; the ROI pooling computes feature maps for region proposals; the final output feature maps of the ROI pooling layer are performed for classification. Finally, an average pooling is applied, and the features obtained from the pooling are used for classification and bounding box regression, respectively.

2.5. Model Training, Validation, and Testing. The Faster R-CNN model based on the Caffe framework was deployed in the Ubuntu operating system by using open-source code and was trained in a computing environment with 4 NVIDIA GTX 1080Ti GPUs, 12 Intel Core I7-6850K CPUs, and 128 GB DDR4 RAM.

The model training, validation, and testing were conducted according to the following steps: First, the Faster R-CNN network was fine-tuned on a tongue image dataset for 40000 iterations with an optimizer of stochastic gradient descent (SGD), the learning rate of 0.03, weight decay of 0.0001, the momentum of 0.9, gamma value of 0.1, and batch size of 128. Detailed initial parameters were shown in Table 2.

Then, the tongue image and the marked position information were fed into an integrated Faster R-CNN model for training. In each training iteration, features were extracted, labels and frame position were predicted, and losses (i.e., errors) between predicted frame position,

TABLE 1: The training set.

Tongue image categories	Training datasets	Labels
Fissured tongue	1570	1792
Tooth-marked tongue	1386	2589
Spotted tongue	746	920
Stasis tongue	1107	1942
Greasy coating	1559	1652
Peeled coating	478	639
Rotten coating	96	132
Total	6942	9666

Notes: one tongue image can contain multiple labels.

predicted labels, and object actual position and object actual label were calculated. The parameters were updated according to the backward error propagation. Complete the training and generate the object detection model of tongue image of TCM. At the end of the training, a well-trained object detection model for tongue images was achieved. Collect and observe results using a well-trained model with different hyper-parameters over the validation set. The operation of validation was performed during the training process. Based on the results over the validation set, the state of the model was checked, and the hyperparameters of the model were adjusted. When the results of accuracy in the validation do not increase, the training is stopped. The loss function for Faster R-CNN sums the classification loss and regression loss, as defined in the following equation [24]:

$$L(p_i, t_i) = \frac{1}{N_{\text{cls}}} \sum_i L_{\text{cls}}(p_i, p_i^*) + \lambda \frac{1}{N_{\text{reg}}} \sum_i p_i^* L_{\text{reg}}(t_i, t_i^*), \quad (1)$$

where N_{cls} and N_{reg} are the number of anchors in minibatch and number of anchor locations, λ and i mean the selected anchor box index and the balancing parameter; p_i and p_i^* represent the predicted probability and the ground truth of tongue feature; t_i and t_i^* represent the predicted bounding box and actual tongue feature label box. The accuracy results and the loss changes in the training are depicted in Figure 4(b).

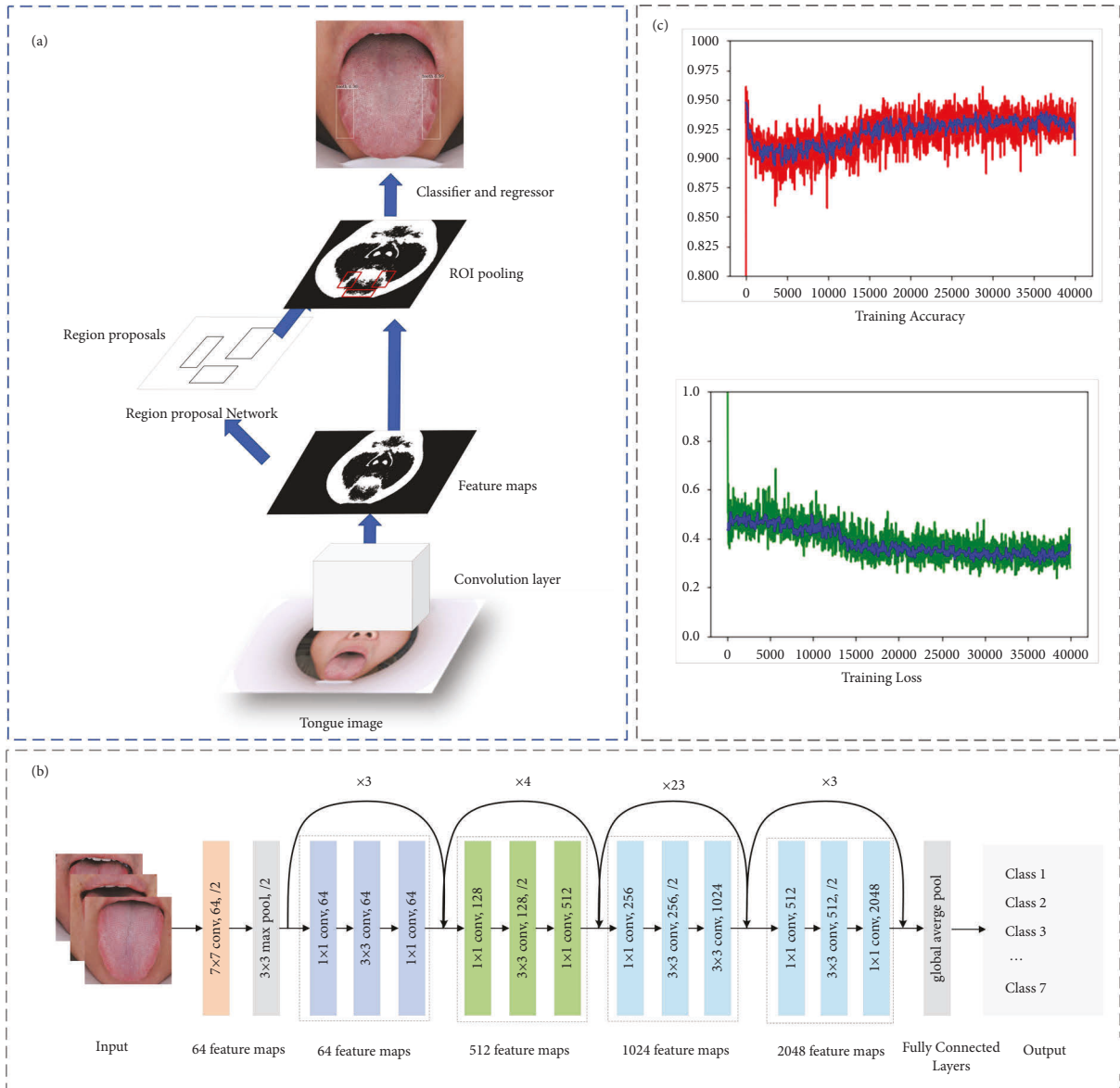


FIGURE 4: Faster R-CNN Model development for recognizing tongue shape and texture. (a) The workflow of Faster R-CNN; (b) the architecture of backbone feature extraction network ResNet101; (c) the accuracy and loss of model training.

Finally, by adjusting the initial learning rate and comprehensive comparison, the training model with a learning rate of 0.001 and iteration of 40000 was finally selected as the final object detection model. Then the trained model was applied to the testing set.

2.6. Strategies for the Prevention of Overfitting. In this study, the two means of regularization and dropout were deployed to prevent overfitting. In the process of the training model, the regularization of L2 was leveraged to constrain the weight estimates, so as to help in preventing overfitting [32]. In addition, the technique of dropout was applied for training the last several classification layers in the neural network of Faster R-CNN. By means of the dropout, convolution kernels were randomly deactivated in the

TABLE 2: Initial parameters of faster R-CNN model for training.

Parameters	Values
Base learning rate	0.03
Weight decay	0.0001
Momentum	0.9
Gamma value	0.1
Steps	(0, 13333, 26666)
Max iteration	40000
Scales	400, 500
Batch size	128

training process [33]. Furthermore, the importance of convolution kernels in the classification layers was dynamically balanced. Also, the overfitting phenomenon could be alleviated.

2.7. Indices for Model Evaluation. Based on the classification results of the model Faster R-CNN over the testing set, the five indices, including accuracy ((2)), recall ((3)), precision ((4)), and F1-score ((5)), were selected as metrics to evaluate the performance of Faster R-CNN in the multiclass classification of tongue images [34–37]. True positive (TP) means that the expert's conclusion and the result of object detection are the same, and false negative (FN) represents that the existing tongue feature category is not detected. False positive (FP) means if the tongue feature detection algorithm classifies those that are not in this category. True negative (TN) denotes that if the tongue image does not belong to a certain category, the tongue feature detection algorithm is the same as the expert conclusion. Macro averaged measures for the above indices are calculated for the model Faster R-CNN with respect to the 7-classes classification of tongue images.

$$\text{Precision} = \frac{\text{TP}}{\text{TP} + \text{FP}}, \quad (2)$$

$$\text{Recall} = \frac{\text{TP}}{\text{TP} + \text{FN}}, \quad (3)$$

$$\text{Accuracy} = \frac{\text{TP} + \text{TN}}{\text{TP} + \text{FP} + \text{TN} + \text{FN}}, \quad (4)$$

$$\text{F1 - score} = \frac{2 \times \text{Precision} \times \text{Recall}}{\text{Precision} + \text{Recall}}. \quad (5)$$

2.8. Application of Tongue Image Detection Model. The Faster R-CNN model obtained from the above training was applied to the population undergoing routine medical checkups with Chinese medicine to explore the association between tongue features and diseases. All samples were collected from January 2019 to December 2019. A total of 3601 subjects were included in the physical examination center of Eastern Hospital of Shuguang Hospital affiliated with Shanghai University of TCM. We excluded women who were pregnant or nursing; those who cannot cooperate with researchers. All volunteers signed informed consent, all subjects completed routine medical checkups and simultaneously used the TFDA-1 tongue diagnosis instrument to capture tongue images.

All tongue images were analyzed by a trained Faster R-CNN model. All analysis and test results were verified by experts for the second time, and the analysis results were unanimously confirmed. If they were inconsistent, comprehensive analysis results should be adopted. The indicators of shape and texture features of tongue images were classified into two categories. Doctors at the physical examination center of Shuguang Hospital affiliated with Shanghai University of TCM made a diagnosis with reference to the corresponding clinical guidelines for diseases, aiming at the common and multiple diseases in the medical checkup population.

2.9. Statistical Analysis Methods. Excel and Python3.6 were used for data matching, merging, and sorting. The tongue images were described by percentage (%) and were compared using the Pearson χ^2 test. Statistical analysis was

performed using the IBM SPSS Statistics for Windows, version 25 (IBM Corp., Armonk, N.Y., USA). All results were compared using the two-tailed t test and differences were considered statistically significant when $P < 0.05$.

A complex network by the improved node contraction method [38–40] is a weighted network that contains the degree and weight of edges based on the obtained node importance. The weight of the weighted network was defined as

$$\partial(WG) = \frac{1}{s \times l} = \frac{1}{\sum_i^n N_i \sum_{j \in N_i} W_{ij} \times \sum_{i \neq j \in V} d_{ij} / n \times (n - 1)}, \quad (6)$$

The visualization tool Python NetworkX [41] was used to store the constructed network in the form of the adjacency matrix and triple, and the complex network diagram was built with disease and tongue image features as nodes.

3. Results

3.1. Tongue Image Detection Over Testing Set. In our testing set, the average accuracy of the model achieved 90.67%, with a precision of 99.28%, recall of 91.27%, and F1 score of 95.00%, indicating that the model had a good detection effect and can accomplish the multiobject recognition task well, as shown in Table 3.

Our method detected tongue shape and texture features with different scales and ratios. Figure 5(a) shows a normal tongue image (without tooth marks, fissures, stasis, spots, greasy coating, peeled coating, and rotten coating), and there was no mark in the test result; Figures 5(b)–5(d) show tongue images with a single feature, (b) is a fissured tongue, (c) is a greasy coating (there are 2 spots), and (d) is a stasis tongue (there were 3 spots). Figures 5(e)–5(h) show a combination of two different tongue images, in which (e) is a tooth-marked tongue with fissures, (f) is a peeled tongue with fissures, (g) is a greasy tongue with fissures, and (h) is a greasy tongue with tooth marks. Figures 5(i)–5(l) show three or more different tongue-shaped features, in which (i) shows a greasy coating, tooth marks and stasis were detected simultaneously, (j) shows a greasy coating, tooth marks and spots were detected simultaneously, (k) shows a peeled coating, fissures and stasis were detected simultaneously, and (l) shows a greasy coating, tooth marks, fissures, and stasis were detected simultaneously.

3.2. Distribution of Tongue Image Features in the Medical Checkup Population. The tongue images were input into the established optimal Faster R-CNN intelligent tongue diagnosis analysis model, and 1494 cases (41.49%) of the fissured tongue, 1338 cases (37.16%) of the tooth-marked tongue, 1068 cases (29.66%) of greasy coating, 672 cases (18.66%) of the spotted tongue, 359 cases (9.97%) of stasis tongue, 143 cases (3.97%) of peeled coating, and 44 cases (1.22%) of rotten coating, as shown in Figure 6.

3.3. Statistics of Tongue Image Features on the Gender Factors and the Age Factors. It showed that the proportion of fissured tongue, tooth-marked tongue, and greasy

TABLE 3: Tongue images object detection results based on Faster R-CNN.

Tongue feature	Precision (%)	Recall (%)	F1-score (%)	Accuracy (%)
Fissured	99.49	99.49	99.49	98.97
Tooth-marked	100.00	98.84	99.42	98.84
Stasis	99.22	93.43	96.23	92.75
Spot	98.73	84.78	91.22	83.87
Greasy	99.44	90.72	94.88	90.26
Peel	98.11	88.14	92.86	86.67
Rot	100.00	83.33	90.91	83.33
Average	99.28	91.25	95.00	90.67

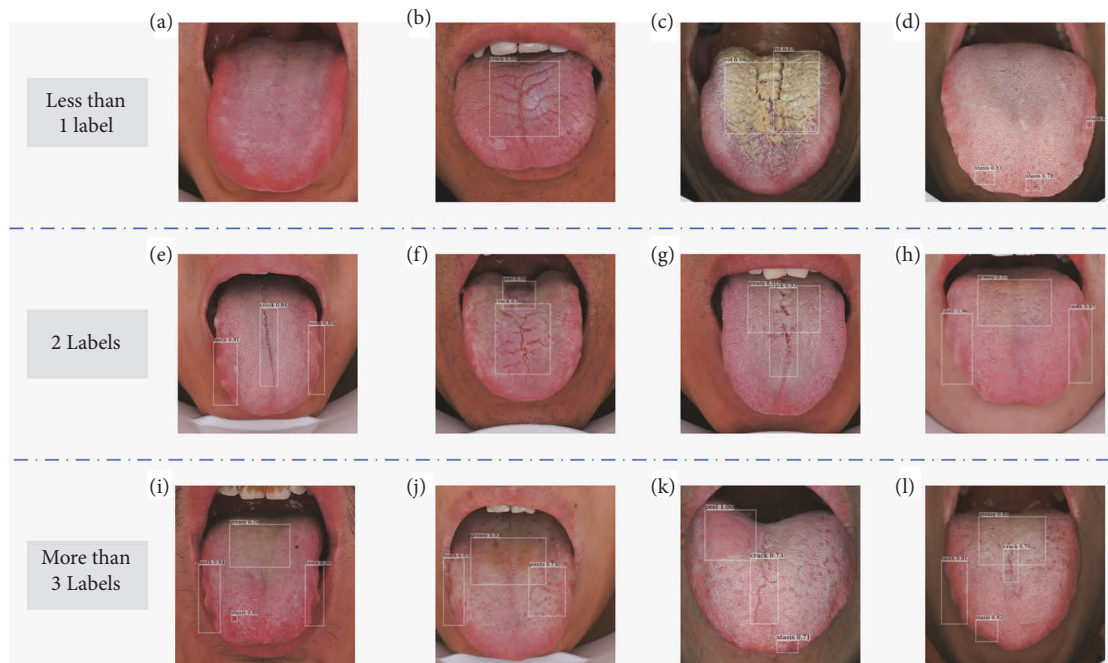


FIGURE 5: Examples of tongue image feature detection.

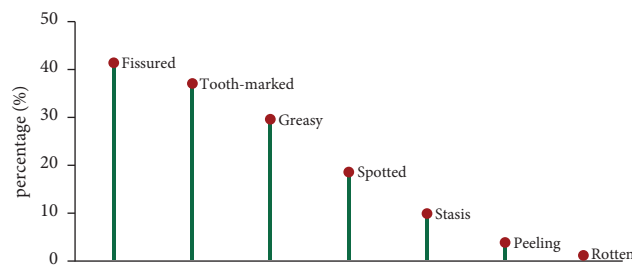


FIGURE 6: Distribution of different tongue shape and texture features.

coating in the male group was higher than that in the female group ($P < 0.001$), whereas the proportion of spotted tongue and stasis tongue in females was significantly higher than that in males ($P < 0.001$). There was no significant difference between the two groups in the proportion of peeled and greasy coating, as shown in Table 4, Figures 7(a) and 7(b).

The results from the above table illustrated that there were significant differences in the incidence of the

fissured tongue, tooth-marked tongue, spotted tongue, greasy coating, and rotten coating among the four age gradients, but there was no significant difference in the incidence of stasis tongue and peeled coating. Overall, with the increase of age, the incidence of fissured tongue and greasy coating increased gradually, while the incidence of spotted tongue and tooth-marked tongue decreased gradually, as shown in Table 5, Figures 7(c)–7(d).

TABLE 4: Comparison of tongue image features between different genders.

	Male ($n = 2006$)	Female ($n = 1595$)	χ^2	P
Fissure (yes)	978 (48.8%)	516 (32.4%)	98.475	<0.001
Tooth (yes)	794 (39.6%)	544 (34.1%)	11.405	<0.001
Spot (yes)	336 (16.7%)	336 (21.1%)	10.904	0.001
Stasis (yes)	92 (4.6%)	267 (16.7%)	146.223	<0.001
Greasy (yes)	569 (53.3%)	499 (46.7%)	3.632	0.057
Peel (yes)	84 (4.2%)	59 (3.7%)	0.556	0.456
Rot (yes)	37 (1.8%)	7 (0.4%)	14.544	<0.001

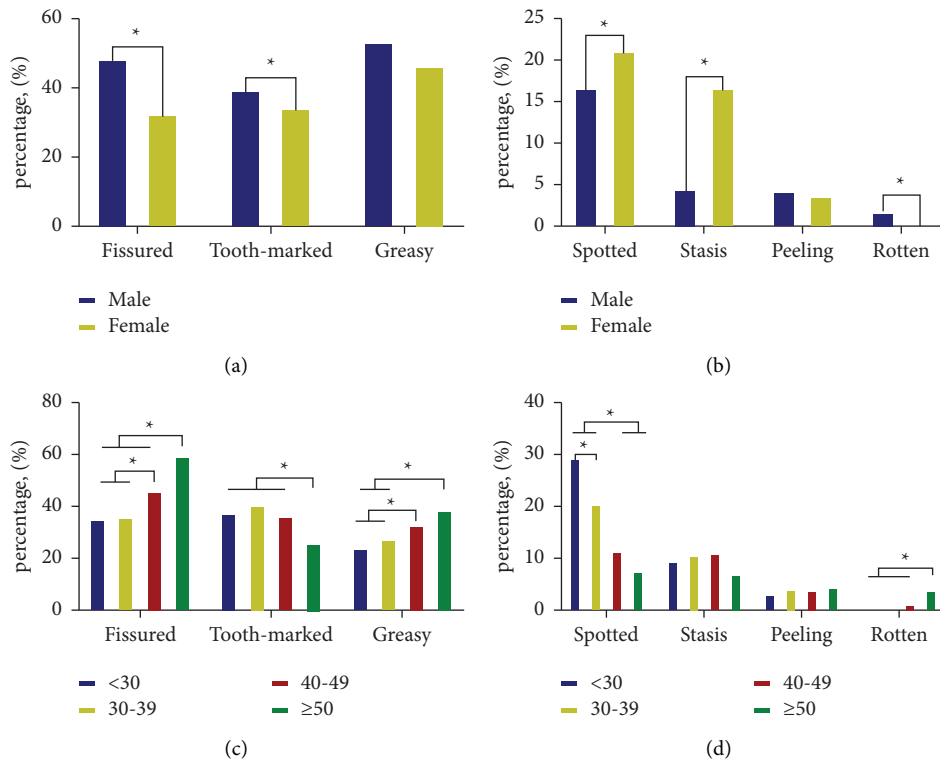


FIGURE 7: Comparison of tongue shape and texture features of different age ranges and genders.

TABLE 5: Comparison of tongue image features among different age ranges.

	<30 years ($n = 848$)	30–39 years ($n = 1418$)	40–49 years ($n = 826$)	≥50 years ($n = 509$)
Fissure (yes)	299 (35.3%)	510 (36.0%)	382 (46.2%)*#	303 (59.5%)*#▲
Tooth (yes)	321 (37.9%)	580 (40.9%)	302 (36.6%)	135 (26.5%)*#▲
Spot (yes)	249 (29.4%)	291 (20.5%)*	94 (11.4%)*#	38 (7.5%)*#
Stasis (yes)	81 (9.6%)	150 (10.6%)	92 (11.1%)	36 (7.1%)
Greasy (yes)	205 (24.2%)	391 (27.6%)	273 (33.1%)*#	199 (39.1%)*#
Peel (yes)	27 (3.2%)	60 (4.2%)	33 (4.0%)	23 (4.5%)
Rot (yes)	3 (0.4%)	13 (0.9%)	8 (1.0%)	20 (3.9%)*#▲

Note: * denotes significant difference compared to < 30 years old group, # denotes significant difference compared to 30–39 years old group, and ▲ denotes significant difference compared to 40–49 years old group.

3.4. Correlation Analysis among Tongue Features and Diseases Based on Complex Networks. Overall, the tongue features of diseases in medical checkups were mainly characterized by increased fissures, tooth marks, and greasy coating. Table 6 showed the top ten weights relationships between tongue features and diseases. Fissured tongue, tooth-marked tongue, and greasy coating are most closely related to

glucolipid metabolic diseases. Specifically, the fissured tongue had the highest weight in hypertension, reaching 0.974, and the weights for dyslipidemia, overweight, and NAFLD were 0.812, 0.799, and 0.775, respectively. For tooth-marked, the weights of hypertension, dyslipidemia overweight and NAFLD were 0.786, 0.649, 0.639, and 0.623, respectively. For greasy coating, the weights of hypertension

TABLE 6: Top 10 weight of tongue features and diseases in medical checkups.

Tongue feature	Disease	Weight
Fissured tongue	Hypertension	0.974
	Dyslipidemia	0.812
	Overweight	0.799
	NAFLD	0.775
Tooth-marked tongue	Hypertension	0.786
	Dyslipidemia	0.649
	Overweight	0.639
	NAFLD	0.623
Greasy coating	Hypertension	0.649
	Overweight	0.540

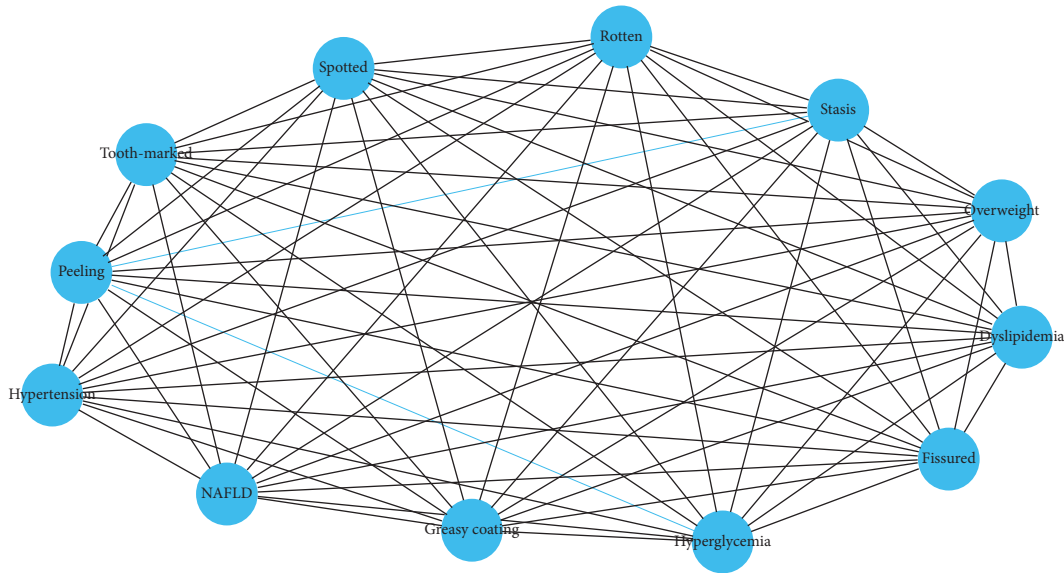


FIGURE 8: Correlation analysis between tongue features and diseases based on complex network.

and overweight were 0.649 and 0.540, respectively. As shown in Figure 8, greasy coating, tooth-marked tongue, and fissured tongue were more closely related to hypertension, dyslipidemia, NAFLD, and overweight.

4. Discussion

Intelligent tongue diagnosis is one part of the important content in clinical TCM diagnosis. The researchers have applied the tongue image features extracted by deep learning to diabetes mellitus [4, 42, 43], NAFLD [44], lung cancer-assisted diagnosis [45], and TCM constitution recognition [46–48] with good performance of disease classification [13, 49]. Professor Yang Junlin’s team [50] has applied the AI screening system for scoliosis developed and established by Faster R-CNN, and quantified the severity of scoliosis, with the accuracy reaching the average level of human experts. Tang et al. [51] have proposed a tongue image classification model based on multitask CNN, and the classification accuracy achieved 98.33%. However, due to the small sample size, the advantages of deep learning methods cannot be brought into full play, and the tongue features such as rotten, greasy, spotted, stasis, dryness, or thickness remain

unexplored [52]. Liu et al. [53] applied Faster R-CNN to identify tooth-marked tongues and fissured tongues, and the accuracy of identifying fissured tongues and tooth-marked tongues was 0.960 and 0.860, respectively. The research only involved tooth marks and fissures due to the small sample size, so the advantages of the deep learning multi-label object detection model were not fully exerted.

Compared with the tongue classification model constructed by the classical CNN, Faster R-CNN as a highly integrated and end-to-end model is still the mainstream object detection neural network at present [54–56].

In our research, we focused on the categories of the tongue image features, rather than the precise feature position, so we applied the method of object detection to the multiclass recognition problem of tongue features. Our tongue feature detection model based on Faster R-CNN had a good generalization ability. With the unique advantages of deep learning and transfer learning in the identification of shape and texture features of tongue images, it can realize automatic high-throughput processing, better solve the problems of local tongue image recognition, integrate the identification and annotation of tongue images, and has a good visualization effect. Our model accomplished the

multi-label object detection of 7 categories of tongue images, and the average accuracy achieved 90.67%, showing that Faster R-CNN had a good visualization effect in clinical TCM applications. In addition, the quantitative analysis of tongue features associated with diseases is an important link in the clinical diagnosis of tongue in TCM. The relationship between different features of tongue images, and the association of them with gender/age are not clear [57], and the correlations between them and the occurrence and progress of diseases are unknown. In this study, tongue feature diagnosis based on Faster R-CNN applied to a population undergoing routine medical checkup was a beneficial attempt to mine the implicit information of TCM tongue image and diseases through a complex network [40].

The intelligent diagnostic analysis was established to analyze 3601 physical examination population, and the results showed that the incidence of the fissured tongue was 41.49%, the tooth-marked tongue was 37.16%, the greasy coating was 29.66%, the spotted tongue was 18.66%, stasis tongue was 9.97%, the peeled coating was 3.97%, and the rotten coating was 1.22%, the incidence of fissures, tooth marks and greasy coating in men was higher than that in women, and the incidence of spotted tongue and stasis tongue in women was significantly higher than that in men, which may be related to deficiency of spleen qi, essence and blood in male subjects and excessive blood heat in female subjects. With age increasing, the incidence of fissured tongue and greasy coating increased, while the incidence of spotted tongue and tooth-marked tongue decreased, which may be related to the tendency of both qi and yin deficiency in the elderly and excess syndrome in the young. In the population with glucose and lipid metabolic diseases such as fatty liver and metabolic syndrome, fissures and greasy coating increased, which may be related to the pathogenesis of glucose and lipid metabolism, such as deficiency of qi and yin and dampness. These results were consistent with the clinical practice of TCM [58].

Although the method has some advantages, our model also has limitations.

Firstly, we will conduct further research on the multi-class classification of tongue images in the future. The performance of other neural network models such as VGGnet, ResNet, and DenseNet, will be explored in the task of tongue image classification.

Secondly, the tongue image object detection model has still to be optimized. Annotation of large samples requires a lot of labor cost. Tongue image data acquired by standardized technology has high stability, but the scalability is not strong. Regardless of the fact that the user visualization effect is good, it is still difficult to explain the extracted feature [59]. A more efficient model algorithm, such as unsupervised deep learning based on the flow generation model [60] and a self-attention mechanism based on end-to-end object detection with transformers [61], would be used to further optimize and establish a robust intelligent diagnosis and analysis model of tongue image.

Thirdly, our approach for the detection of tongue images is a qualitative model. However, the identification of tongue

images in TCM clinics is complicated, which is not only a binary problem but also a quantification of pathological change. The changes in tongue image features are also of great value in the diagnosis of disease symptoms, which will be the focus of our subsequent research.

5. Conclusions

This study was a cross-sectional study of healthy people with medical checkups. Furthermore, a case-control study will be carried out on patients with major chronic diseases in order to prove the value of tongue features in the diagnosis of disease. In addition, we will optimize the Faster R-CNN model with the respect to the precise location of objects in a tongue image. This paper presents a supervised deep learning method based on a large amount of labeled data. In the future, we will explore a more robust self-supervised deep learning model for the multiclassification of tongue features.

The model Faster R-CNN shows good performance in tongue image classification. And we have preliminarily revealed the relationship between tongue features and gender, age, and metabolic diseases in a medical checkup population.

Data Availability

The datasets used and/or analyzed in this study are available upon reasonable request from the corresponding author.

Ethical Approval

This study was reviewed and approved by the Institutional Research Ethics Committee of Shuguang Hospital affiliated to Shanghai University of TCM (No. 2018-626-55-01). The clinical trial has been registered at the Chinese Clinical Trial Registry with the registration number: <https://clinicaltrials.gov/ct2/show/ChiCTR1900026008>.

Consent

The patients/participants provided their written informed consent to participate in this study..

Conflicts of Interest

The authors declare that they have no conflicts of interest.

Authors' Contributions

T.J. and J.X. conceptualized the study; X.H. and X.Y. developed methodology; C.Z. designed software; X.H. and X.Y. validated the study; J.H. formally analyzed the study; L.T. investigated the study; J.C. collected resources; L.T. curated the data; T.J. and Z.L. wrote the original draft; T.J. and Z.L. reviewed and edited the manuscript; X.Y. visualized the study; C.Z. supervised the study; X.M. and L.Z. administered the project; J.X. and T.J. acquired funding. All authors have read and agreed to the published version of the manuscript. Tao Jiang and Zhou Lu contributed equally to this work.

Acknowledgments

The authors would like to thank all the involved professional TCM clinicians, nurses, students, and technicians for dedicating their time and skill to the completion of this study. This study was supported by the National Key Technology R&D Program of China (grant number: 2017YFC1703301), the National Natural Science Foundation of China (grant numbers: 82104736 and 82104738), Shanghai Science and Technology Commission (grant number: 21010504400), and Shanghai Municipal Health Commission (grant numbers: 201940117 and 2020JQ003).

References

- [1] D. Zhang, H. Zhang, and B. Zhang, *Tongue Image Analysis*, Springer, Singapore, 2017.
- [2] K. Tomooka, I. Saito, S. Furukawa et al., “Yellow tongue coating is associated with diabetes mellitus among Japanese non-smoking men and women: the toon health study,” *Journal of Epidemiology*, vol. 28, no. 6, pp. 287–291, 2018.
- [3] W. Jiao, X. J. Hu, L. P. Tu et al., “Tongue color clustering and visual application based on 2D information,” *International Journal of Computer Assisted Radiology and Surgery*, vol. 15, no. 2, pp. 203–212, 2020.
- [4] J. Li, P. Yuan, X. Hu et al., “A tongue features fusion approach to predicting prediabetes and diabetes with machine learning,” *Journal of Biomedical Informatics*, vol. 115, Article ID 103693, 2021.
- [5] T. Obafemi-Ajayi, R. Kanawong, X. Dong, L. Shao, and Y. Duan, “Features for automated tongue image shape classification,” in *Proceedings of the IEEE International Conference on Bioinformatics & Biomedicine Workshops*, pp. 273–279, Philadelphia, PA, USA, 2013.
- [6] Z. Yang, D. Zhang, and N. M. Li, “Kernel false-colour transformation and line extraction for fissured tongue image,” *Journal of Computer-Aided Design & Computer Graphics*, vol. 22, no. 5, pp. 771–776, 2010.
- [7] L. M. Zhumu, P. Lu, C. M. Xia, and Y. Q. Wang, “Research on douglas-peucker method in feature extraction from 55 cases of tooth-marked tongue images,” *Chinese Archives of Traditional Chinese Medicine*, vol. 32, no. 9, pp. 2138–2140, 2014.
- [8] J. Xu, Z. Zhang, Y. Sun, Y. M. Bao, and W. S. Li, “Recognition of Acantha and Ecchymosis in tongue pattern,” *Academic Journal of Shanghai University of Traditional Chinese Medicine*, vol. 4, pp. 38–40, 2004.
- [9] X. Wang, R. Wang, D. Guo, X. Z. Lu, and P. Zhou, “A research about tongue-prickled recognition method based on auxiliary light source,” *Chinese Journal of Sensors and Actuators*, vol. 29, no. 10, pp. 1553–1559, 2016.
- [10] L. L. Liu and D. Zhang, “Extracting tongue cracks using the wide line detector,” in *Lecture Notes in Computer Science*, pp. 49–56, Springer, Berlin, Germany, 2008.
- [11] B. Huang, J. S. Wu, D. Zhang, and N. M. Li, “Tongue shape classification by geometric features,” *Information Sciences*, vol. 180, no. 2, pp. 312–324, 2010.
- [12] X. Q. Li, D. Wang, and Q. Cui, “WLDF: effective statistical shape feature for cracked tongue recognition,” *Journal of Electrical Engineering and Technology*, vol. 12, no. 1, pp. 420–427, 2017.
- [13] X. Wang, X. Wang, and Y. Lou, “Constructing tongue coating recognition model using deep transfer learning to assist syndrome diagnosis and its potential in noninvasive ethnopharmacological evaluation,” *Journal of Ethnopharmacology*, vol. 285, Article ID 114905, 2021.
- [14] A. Esteva, B. Kuprel, R. A. Novoa et al., “Dermatologist-level classification of skin cancer with deep neural networks,” *Nature*, vol. 542, no. 7639, pp. 115–118, 2017.
- [15] J. Ker, L. Wang, J. Rao, and T. Lim, “Deep learning applications in medical image analysis,” *IEEE Access*, vol. 6, pp. 9375–9389, 2017.
- [16] M. C. Hu, K. C. Lan, W. C. Fang et al., “Automated tongue diagnosis on the smartphone and its applications,” *Computer Methods and Programs in Biomedicine*, vol. 174, pp. 51–64, 2019.
- [17] C. Zhou, H. Fan, and Z. Li, “Tonguenet: accurate localization and segmentation for tongue images using deep neural networks,” *IEEE Access*, vol. 7, pp. 148779–148789, 2019.
- [18] B. Lin, J. Xle, C. Li, and Y. Qu, “Deeptongue: tongue segmentation via resnet,” in *Proceedings of the 2018 IEEE International Conference on Acoustics, Speech and Signal Processing (ICASSP)*, pp. 1035–1039, IEEE, Calgary, Alberta, Canada, 2018.
- [19] Y. Cai, T. Wang, W. Liu, and Z. Luo, “A robust interclass and intra-class loss function for deep learning based tongue segmentation,” *Concurrency and Computation: Practice and Experience*, vol. 32, no. 22, p. e5849, 2020.
- [20] L. Li, Z. Luo, M. Zhang, Y. Cai, C. Li, and S. Li, “An iterative transfer learning framework for cross-domain tongue segmentation,” *Concurrency and Computation: Practice and Experience*, vol. 32, no. 14, p. e5714, 2020.
- [21] X. Wang, J. Liu, C. Wu et al., “Artificial intelligence in tongue diagnosis: using deep convolutional neural network for recognizing unhealthy tongue with tooth-mark,” *Computational and Structural Biotechnology Journal*, vol. 18, pp. 973–980, 2020.
- [22] Q. Xu, Y. Zeng, W. Tang et al., “Multi-task joint learning model for segmenting and classifying tongue images using a deep neural network,” *IEEE Journal of Biomedical and Health Informatics*, vol. 24, no. 9, pp. 2481–2489, 2020.
- [23] W. Tang, Y. Gao, L. Liu et al., “An automatic recognition of tooth-marked tongue based on tongue region detection and tongue landmark detection via deep learning,” *IEEE Access*, vol. 8, pp. 153470–153478, 2020.
- [24] H. Weng, L. Li, H. Lei, Z. Luo, C. Li, and S. Li, “A weakly supervised tooth-mark and crack detection method in tongue image,” *Concurrency and Computation: Practice and Experience*, vol. 33, no. 16, p. e6262, 2021.
- [25] S. Ren, K. He, R. B. Girshick, and J. Sun, “Faster R-CNN: towards real-time object detection with region proposal networks,” *IEEE Transactions on Pattern Analysis and Machine Intelligence*, vol. 39, no. 6, pp. 1137–1149, 2017.
- [26] K. He, X. Zhang, S. Ren, and S. Jian, “Deep residual learning for image recognition,” in *Proceedings of the IEEE Conference on Computer Vision & Pattern Recognition (CVPR)*, pp. 770–778, Seattle, WA, USA, 2016.
- [27] T. Jiang, X.-J. Hu, X.-H. Yao et al., “Tongue image quality assessment based on a deep convolutional neural network,” *BMC Medical Informatics and Decision Making*, vol. 21, no. 1, p. 147, 2021.
- [28] Z. Qi, L. P. Tu, and Z. Y. Luo, “Tongue image database construction based on the expert opinions: assessment for individual agreement and methods for expert selection,” *Evidence Based Complementary and Alternative Medicine*, vol. 2018, Article ID 8491057, 9 pages, 2018.

- [29] J. Xu, *Clinical Illustration of Tongue Diagnosis of Traditional Chinese Medicine*, Chemical Industry Press, Beijing, China, 2017.
- [30] T.-Y. Lin, M. Maire, S. Belongie et al., "Microsoft coco: common objects in context," in *European Conference on Computer Vision*, pp. 740–755, Springer, Berlin, Germany, 2014.
- [31] A. Zhang, Z. C. Lipton, M. Li, and A. J. Smola, "Dive into deep learning," 2021, <https://arxiv.org/abs/210611342>.
- [32] Y. Gu, Z. Li, and F. Yang, "Infrared vehicle detection algorithm with complex background based on improved faster R-CNN," *Laser & Infrared*, vol. 52, no. 4, pp. 614–619, 2022.
- [33] N. Srivastava, G. Hinton, A. Krizhevsky, I. Sutskever, and R. Salakhutdinov, "Dropout: a simple way to prevent neural networks from overfitting," *Journal of Machine Learning Research*, vol. 15, no. 1, pp. 1929–1958, 2014.
- [34] D. M. Powers, "Evaluation: from precision, recall and F-measure to ROC, informedness, markedness and correlation," 2020, <https://arxiv.org/abs/2010.16061>.
- [35] D. L. Olson and D. Delen, *Advanced Data Mining Techniques*, Springer Science & Business Media, Berlin, Germany, 2008.
- [36] A. Tharwat, "Classification assessment methods," *Applied Computing and Informatics*, vol. 17, no. 1, pp. 168–192, 2021.
- [37] D. Jurman and G. Jurman, "The advantages of the Matthews correlation coefficient (MCC) over F1 score and accuracy in binary classification evaluation," *BMC Genomics*, vol. 21, no. 1, p. 6, 2020.
- [38] T. Zhu, S. Zhang, R. Guo, and G.-C. Chang, "Improved evaluation method for node importance based on node contraction in weighted complex networks," *Systems Engineering and Electronics*, vol. 31, no. 8, pp. 1902–1905, 2009.
- [39] Y. Shi, X. Hu, and J. Cui, "Clinical data mining on network of symptom and index and correlation of tongue-pulse data in fatigue population," *BMC Medical Informatics and Decision Making*, vol. 21, no. 1, pp. 1–14, 2020.
- [40] C. Li, W. Wang, J. Li, J. Xu, and X. Li, "Community detector on symptom networks with applications to fatty liver disease," *Physica A: Statistical Mechanics and Its Applications*, vol. 527, Article ID 121328, 2019.
- [41] A. Hagberg, P. Swart, and D. S. Chult, "Exploring network structure, dynamics, and function using network," in *Proceedings of the 7th Python in Science Conference (SciPy 2008)*, T. V. G. Varoquaux and J. Millman, Eds., pp. 11–15pp. 11–, Pasadena, CA, USA, 2008.
- [42] S. Balasubramanian, V. Jeyakumar, and D. S. Nachimuthu, "Panoramic tongue imaging and deep convolutional machine learning model for diabetes diagnosis in humans," *Scientific Reports*, vol. 12, no. 1, p. 186, 2020.
- [43] B. Zhang, B. V. Kumar, and D. Zhang, "Detecting diabetes mellitus and nonproliferative diabetic retinopathy using tongue color, texture, and geometry features," *IEEE Transactions on Biomedical Engineering*, vol. 61, no. 2, pp. 491–501, 2014.
- [44] T. Jiang, X.-J. Guo, and L.-P. Tu, "Application of computer tongue image analysis technology in the diagnosis of NAFLD," *Computers in Biology and Medicine*, vol. 135, Article ID 104622, 2021.
- [45] J. Zhou, Q. Zhang, and B. Zhang, "An automatic multi-view disease detection system via collective deep region-based feature representation," *Future Generation Computer Systems*, vol. 115, pp. 59–75, 2021.
- [46] H. H. Li, G. H. Wen, and H. B. Zeng, "Natural tongue physique identification using hybrid deep learning methods," *Multimedia Tools and Applications*, vol. 78, no. 6, pp. 6847–6868, 2019.
- [47] G. Wen, J. Ma, Y. Hu, H. Li, and L. Jiang, "Grouping attributes zero-shot learning for tongue constitution recognition," *Artificial Intelligence in Medicine*, vol. 109, Article ID 101951, 2020.
- [48] J. Ma, G. Wen, C. Wang, and L. Jiang, "Complexity perception classification method for tongue constitution recognition," *Artificial Intelligence in Medicine*, vol. 96, pp. 123–133, 2019.
- [49] Y. Hu, G. Wen, and M. Luo, "Fully-channel regional attention network for disease-location recognition with tongue images," *Artificial Intelligence in Medicine*, vol. 118, Article ID 102110, 2021.
- [50] J. Yang, K. Zhang, H. Fan et al., "Development and validation of deep learning algorithms for scoliosis screening using back images," *Communications Biology*, vol. 2, no. 1, p. 390, 2019.
- [51] Y. Tang, L. Wang, X. He, P. Chen, and G. Yuan, "Classification of tongue image based on multi-task deep convolutional neural network," *Computer Science*, vol. 45, no. 12, pp. 255–261, 2021.
- [52] X. Zhang, Z. Chen, J. Gao, W. Huang, P. Li, and J. Zhang, "A two-stage deep transfer learning model and its application for medical image processing in Traditional Chinese Medicine," *Knowledge-Based Systems*, vol. 239, Article ID 108060, 2022.
- [53] M. Liu, T. Wang, and L. Zhou, "Study on extraction and recognition of traditional Chinese medicine tongue manifestation: based on deep learning and migration learning," *Journal of Traditional Chinese Medicine*, vol. 60, no. 10, pp. 835–840, 2019.
- [54] R. Girshick, "Fast R-CNN," in *Proceedings of the 2015 IEEE International Conference on Computer Vision (ICCV)*, pp. 1440–1448, Montreal, British Columbia, Canada, 2015.
- [55] L. Zheng, X. Zhang, J. Hu et al., "Establishment and applicability of a diagnostic system for advanced gastric cancer T staging based on a faster region-based convolutional neural network," *Frontiers in Oncology*, vol. 10, p. 1238, 2020.
- [56] Y. He, J. Tan, and X. Han, "High-resolution computer tomography image features of lungs for patients with type 2 diabetes under the faster-region recurrent convolutional neural network algorithm," *Computational and Mathematical Methods in Medicine*, vol. 2022, Article ID 4147365, 11 pages, 2022.
- [57] P.-C. Hsu, H.-K. Wu, Y.-C. Huang et al., "Gender-andage-dependent tongue features in a community-based population," *Medicine*, vol. 98, no. 51, p. e18350, 2019.
- [58] P. C. Hsu, Y. C. Huang, J. Y. Chiang, H. H. Chang, P. Y. Liao, and L. C. Lo, "The association between arterial stiffness and tongue manifestations of blood stasis in patients with type 2 diabetes," *BMC Complementary and Alternative Medicine*, vol. 16, no. 1, p. 324, 2016.
- [59] Z. I. Attia, P. A. Noseworthy, F. Lopez-Jimenez et al., "An artificial intelligence-enabled ECG algorithm for the identification of patients with atrial fibrillation during sinus rhythm: a retrospective analysis of outcome prediction," *The Lancet*, vol. 394, no. 10201, pp. 861–867, 2019.
- [60] D. P. Kingma and P. Dhariwal, "Glow: generative flow with invertible 1x1 convolutions," 2018, <https://arxiv.org/abs/03039>.
- [61] N. Carion, F. Massa, G. Synnaeve, N. Usunier, A. Kirillov, and S. Zagoruyko, "End-to-end object detection with transformers," in *European Conference on Computer Vision*, pp. 213–229, Springer, Berlin, Germany, 2020.

Review Article

The Psychological Recovery of Patients in the Context of Virtual Reality Application by a Complementary Medicine Scheme Based on Visual Art

Bolin Li ^{1,2} and Meilin Shen ³

¹Shanghai University, Shanghai Academy of Fine Arts, Shanghai, China

²Department of Publishing and Dissemination, Shanghai Publishing and Printing College, Shanghai, China

³Department of Film and Television Art, Shanghai Publishing and Printing College, Shanghai, China

Correspondence should be addressed to Bolin Li; libolinsppc@163.com

Received 27 June 2022; Revised 9 August 2022; Accepted 16 August 2022; Published 19 September 2022

Academic Editor: Lei Jiang

Copyright © 2022 Bolin Li and Meilin Shen. This is an open access article distributed under the Creative Commons Attribution License, which permits unrestricted use, distribution, and reproduction in any medium, provided the original work is properly cited.

Expressive art therapy, which originated from art therapy, uses visual art as a carrier and plays a complementary role in clinical medicine and psychological medicine in the healing process of mentally ill patients. With the rapid development of science and technology, expressive art therapy has also entered the field of technology-oriented virtual reality. This study aims to summarize the clinical psychology research of expressive art therapy based on virtual reality, to review the current state of the field, in order to provide detailed scientific research evidence summary for relevant content and complete knowledge reserve.

1. Introduction

As one of the complementary treatments, expressive art therapy with visual art as a carrier originated from art therapy and first appeared in 1942 [1]. American psychiatrist Margaret Naumburg proposed the concept of art therapy and promoted the art therapy model establishment. In the 1950s, psychologists encouraged patients to use various artistic media to express their inner fears, depression, and contradictions during psychotherapy. Since then, expressive art therapy has become basic psychotherapy [2]. In the 1970s, expressive art therapy had a further development, and researchers found that it could activate patients' self-awareness and communication, enhance creativity, adjust their emotional state, help release emotions, and help achieve physical and mental healing. After participating in experiential therapy groups, many people suggested that the experience of therapy did have a positive impact on their mental health and social relationships. Because of these characteristics, expressive art therapy is now used in various

fields, such as schools, hospitals, prisons, interventions, and rehabilitation training for special populations [1]. As a creative expression for therapy, expressive art therapy originates from the blending of art and psychotherapy. In a broad sense, it includes a variety of artistic means, such as painting, drama, and music., while in a narrow sense, it refers to painting-based visual art therapy, including sculpture, photography, and digital art [3, 4]. In this review, we focus on expressive art therapy in the form of visual arts.

2. Psychological Principles of Expressive Art Therapy

2.1. Principles of Psychoanalysis. The practice of art therapy emerged with the development of psychoanalytic theory. It combined free association, which is one of the main treatments of Freudian psychoanalysis, and the diagnosis and analysis of painting based on psychoanalytic theory [5]. It became an important theoretical basis for imagery connectivity in art treatment. Under the guidance of the theory

of unconscious repression and the theory of collective unconscious imagery, Margaret Naumburg proposed art psychotherapy [6]. She encouraged the use of spontaneous artistic expression of consciousness as a medium of self-therapy to directly express dreams, illusions, and other inner experiences in the form of images rather than verbal language to solve the transference relationship in therapy and to transfer the patient's dependence on the therapist to artwork attention. Edith Kramer proposed art behavioral therapy based on Freud's psychoanalytic theory, emphasizing the use of art as a tool to purify emotions to help patients convert primitive impulses and illusions into artwork. At the same time, she paid more attention to improve the emotional and behavioral problems of children with special needs with the aid of artistic means and believed that through the specific presentation method of art in the creative process, it can help individuals find and sublimate their inner real feelings and integrate reality and illusion and consciousness and unconsciousness, so as to achieve the effect of treatment [5].

2.2. Principles of Cognitive Development. With the development of cognitive behavioral therapy, cognitive behavioral art therapy with psychoeducation as the value orientation emerged, some scholars began to implement this cognitive behavioral therapy for patients with anxiety and panic disorders and proposed that psychological imagery can enhance patients' self-control, and emotional and behavioral problems can be improved in cognitive processes [7]. On the basis of child developmental psychology, Ron Field proposed that artistic expression has a positive effect on the emotional development of children with special needs and suggested that therapists design corresponding courses as needed from the perspective of children, so as to promote the development of their emotional functions, and proposed developmental extension from individual therapy to holistic rehabilitation education [5, 7].

2.3. Gestalt Psychology. Kurt Koffka proposed Gestalt theory and explained that human behavior is a kind of "field," and it is divided into two major systems: one is the environment and the other is the self, and the two are inseparable. Gestalt psychology emphasizes that organisms perceive entire patterns or configurations, not merely individual components [8]. Gestalt principles, such as proximity, similarity, figure-ground, continuity, closure, and connection, describe how humans perceive visuals in connection with different objects and environments [9]. On the basis of Gestalt theory, Janie Rhyne proposed "Gestalt painting therapy," which requires patients to perform a series of emotional experiences as complete Gestalt, such as abstract drawings on emotional experiences such as joy, fear, and anger [10], and each painting is not only a part of the whole but also a single Gestalt unit, and then by encouraging patients to illustrate, associate, and compare the similarities and differences of paintings, we find the crux of the painting and promote patient cognitive ability by review and discussion.

3. Advantages of Expressive Art Therapy

Expressive art therapy is a method that uses various media to help participants heal mental disorders, resolve conflicts, expand self-awareness, and thus achieve psychological healing [11]. In this safe, nonverbal healing environment, people's protective alertness is weakened, and participants' emotions can be soothed, resolved, and vented so that they can face themselves and others better and naturally express their inner feelings [12]. Therefore, expressive art therapy has the following advantages [13].

3.1. Nonverbal Communication. Expressive art therapy is not stressful for the participants, offers no restrictions on the participants' cognition, age, language, and art capabilities, enables self-creative expression in all possible ways, and has unique advantages for those unable to communicate or not good at talking [14].

3.2. Provide a Safe and Private Creative Healing Environment. This atmosphere helps reduce the psychological defense of the experiencer so that they can present the authentic self, while at the same time, it helps them present their inner thoughts and ideas through artistic expression on the artwork, which helps them recognize emotions and ideas, thereby promoting self-integration [15, 16].

3.3. The Function of Space-Time Integration. Through artistic expression, inner thoughts and emotions can be associated with different events at different times and places, and even contradictory emotions can be presented in the same work [17].

3.4. Easy and Effective Implementation. None of the materials and operating conditions required in the healing process are highly demanding, which can be carried out in all daily life situations, and they are intriguing and easy to operate [18].

4. Visual Art: An Important Carrier for Expressive Art Therapy

As the most important part of expressive art therapy, visual art focuses on the integration of thoughts and emotions, and the healing process is the expansion of consciousness. Humans can receive and feel external information through vision, smell, hearing, taste, and touch [19]. About 85% of external information is obtained through the eyes, that is, vision. Vision, as a dependent system, can only exhibit its healing properties when it has gained enough freedom. More and more exhibitions curated by museums now involve immersive experiences led by visual design. For example, the "Healing Art" theme exhibition held by Shanghai Liu Haisu Art Museum guides people to self-healing by various visual designs such as installation art, painting, and color so that art and design can soothe their emotions [20]. Based on the healing function of visual art and its gentle natural attributes,

visual art can be applied in some public welfare projects, such as photography, handicraft, video, painting, design, and other forms to provide services and help for mentally handicapped persons [21].

In visual art therapy, color and graphics are used as research priorities in treatment programs, especially in the treatment of children. The psychological effect of color begins with a vision and encompasses psychological processes such as perception, emotion, memory, and thought. Different colors can have different effects on people's emotions, which are linked to people's life experiences and memories, and are able to produce color associations, thus causing changes in mood. Usually, red represents enthusiasm and festivity, and yellow represents brightness and lightness [22]. Dark colors, such as black and gray, give people a heavy and sad feeling. Studies have shown that blue can inhibit excitement, red can make people active in mental activities, and green can relieve tension. Therefore, color can enable patients to express and vent their emotions, meet their psychological needs, and intervene in patients' emotions [23]. Graphics is another important point in visual art treatment. Because visual activities are active and highly selective, participants can directly identify objects when perceiving graphics, especially flat graphics, and the rich combination of graphics can stimulate imagination [24]. Presenting an individual's inner feelings through the multiple combinations of graphics, as well as the expressivity of colors, helps regulate stress and soothe emotions.

Artists reproduce trauma through artistic works to achieve self-reflection and self-confidence and achieve self-healing of the body and mind. American artist Louise Bourgeois achieved self-healing through self-confession art. Her works were presented to the audience in the form of autobiographical stories, which contain the artist's spiritual trauma. In 1974, she created a composite sculpture "the Destruction of the Father" (Figure 1). In the dark, small, den-like space, there were many orange balls of latex on the ceiling and floor (Bourgeois's father had mocked her femininity with oranges), surrounding a rectangular dining table with various shapes destroyed by violence. This was her encounter with shadows in her personality through her sculpture creation. She subconsciously exposed the scenes that reproduced and exaggerated the painful memories of her childhood and expressed her resentment against her father in this way. The creative method is a self-healing of childhood pain. Louise Bourgeois also created the huge sculpture "Maman" series (Figure 2), and she believed that spiders have characteristics of mothers, who work in repairing blankets and textiles to make money and raise their children, just as spiders spin webs to protect baby spiders. She deliberately enlarged the size of the spider to a shocking level, not only for emotional satisfaction and transfer but also for showing the strength of women and encouraging herself to become stronger and fight for and defend her own rights. Japanese artist Yayoi Kusama is the first artist to make a mirror house. She persistently used the dot pattern to extend the space through mirror reflection, giving people a feeling of infinite proliferation, like entering a fantasy world (Figure 3). The dots are a way for Yayoi Kusama to



FIGURE 1: Louise Bourgeois, the Destruction of the Father, 1974, Foto Lucie.



FIGURE 2: Louise Bourgeois, Maman Spider, 1999, Long Museum West Bund, Shanghai, 2018.

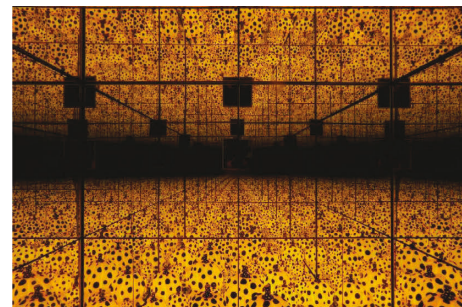


FIGURE 3: Yayoi Kusama, the Spirits of the Pumpkins Descended into the Heavens.

express her mind in her artworks. Mirrors, as a tool for infinite repetition and reproduction of dots, are an indispensable element in her spiritual self-healing process.

5. Making Art Therapy Virtual: Integrating Virtual Reality into Art Therapy

Virtual reality is a computer-advanced human-machine interface with immersion, interactivity, and conception as the basic characteristics [3, 25]. It integrated the use of computer graphics, simulation technology, multimedia technology, artificial intelligence technology, computer network technology, parallel processing technology, and multisensor technology to simulate the functions of human sense organs such as vision, hearing, and touch so that people can

immerse in the computer-generated virtual circle, interact with it in real time through natural ways such as language and gestures, and create an individualized and multidimensional information space [26]. Users can not only feel the immersive fidelity experienced in the objective physical world through the virtual reality system but also can break through space, time, and other objective constraints and feel the experience that cannot be experienced in the real world [27].

In recent years, some researchers have used VR as a psychotherapy tool and introduced it into expressive art therapy, especially for adolescents. Art therapy in VR can be thought of as a collage where images or selected parts of images are used, cut, and attached to new works that express different content, allowing people to re-express. Creation in VR combines elements of the painting (lines, patches, shapes, colors, and 2D), elements of the sculpture (3D), and novel elements supported by digital media [28]. This combination is similar to classical artwork but fundamentally different. The artwork itself is virtual and thus lacks concrete physicality and haptic feedback. The infinity, immersion, and dynamic environment of the virtual canvas can have a powerful impact on creators. Moreover, VR creation allows creators to observe the work from multiple angles, including from within the work itself [29]. VR creation requires a VR system (eg Oculus rift, HTC Vive) and a motion enclosure. Creators can move freely in the immersive 3D space, and the visual background of the environment can also be easily changed. Ohrius and Malchiodi studied the interaction and senses of digital media and argue that there is a clear difference between the sensory experience provided by digital technology and the traditional material approach, making digital media a viable alternative [30].

Instances of psychological recovery of patients in the context of virtual reality application by complementary medicine scheme based on visual art, Shamri Zeevi [25] used VR device, let participants wear a Head Mounted Display (HMD) and use Tilt Brush software by Google, also with two MOCAP, to create artwork in the virtual space, the participants faced to a 3D space meanwhile the therapist faced to a 2D monitor. The therapist and the participants had no eye contact but only while speaking, and the purpose of the therapy was to reproduce and shape the psychological process of the patient through the process of creating works in the virtual world. Hacmun [3] presented a similar clinical method but was more focused on presence and immersivity.

Overall, VR technology may be particularly beneficial for adolescents who are refractory to traditional art treatments. VR can also be a therapeutic option for patients who are afraid of committing mistakes and are unable to try, as it allows experiential exploration without any impact on the physical or real world. For patients who do not consider themselves imaginative, VR art therapy can help them broaden their specific ideas and find ways to express themselves.

Data Availability

There are no data used to support this study.

Conflicts of Interest

The authors declare that they have no conflicts of interest.

References

- [1] H. Vaartio-Rajalin, R. Santamäki-Fischer, P. Jokisalo, and L. Fagerstrom, "Art making and expressive art therapy in adult health and nursing care: a scoping review," *International Journal of Nursing Science*, vol. 8, no. 1, pp. 102–119, 2021.
- [2] J. L. Jamerson, "Expressive remix therapy: using digital media art in therapeutic group sessions with children and adolescents," *Creative Nursing*, vol. 19, no. 4, pp. 182–188, 2013.
- [3] I. Hacmun, D. Regev, and R. Salomon, "The principles of art therapy in virtual reality," *Frontiers in Psychology*, vol. 9, p. 2082, 2018.
- [4] A. Zubala, N. Kennell, and S. Hackett, "Art therapy in the digital world: an integrative review of current practice and future directions," *Frontiers in Psychology*, vol. 12, Article ID 595536, 2021.
- [5] J. Siegel, H. Iida, K. Rachlin, and G. Yount, "Expressive arts therapy with hospitalized children: a pilot study of Co-creating healing sock creatures," *Journal of Pediatric Nursing*, vol. 31, no. 1, pp. 92–98, 2016.
- [6] X. Liu, J. H. Ren, S. S. Jiang, Y. Tan, S. G. Ma, and Y. Huang, "Expressive arts therapy combined with progressive muscle relaxation following music for perioperative patients with gynecological malignancies: a pilot study," *Evidence-based Complementary and Alternative Medicine*, vol. 2022, Article ID 6211581, 9 pages, 2022.
- [7] B. Hoffmann, "The role of expressive therapies in therapeutic interactions; art therapy—explanation of the concept," *Trakia Journal of Science*, vol. 14, no. 3, pp. 197–202, 2016.
- [8] R. Basso, "Expressive arts in pediatric orientation groups," *Journal of Pediatric Nursing*, vol. 25, no. 6, pp. 482–489, 2010.
- [9] H. L. Stuckey and J. Nobel, "The connection between art, healing, and public health: a review of current literature," *American Journal of Public Health*, vol. 100, no. 2, pp. 254–263, 2010.
- [10] K. Collie, D. Spiegel, C. Malchiodi, and A. Backos, "Art therapy for combat-related PTSD: recommendations for research and practice," *Art Therapy*, vol. 23, no. 4, pp. 157–164, 2006.
- [11] G. Kaimal and K. Ray, "Free art-making in an art therapy open studio: changes in affect and self-efficacy," *Arts & Health*, vol. 9, no. 2, pp. 154–166, 2017.
- [12] V. G. Armstrong and R. Howatson, "Parent-infant art psychotherapy: a creative dyadic approach to early intervention," *Infant Mental Health Journal*, vol. 36, no. 2, pp. 213–222, 2015.
- [13] M. S. Walker, A. M. Stamper, D. E. Nathan, and G. Riedy, "Art therapy and underlying fMRI brain patterns in military TBI: a case series," *International Journal of Art Therapy*, vol. 23, no. 4, pp. 180–187, 2018.
- [14] P. Apotsos, "Art therapy in psychosocial rehabilitation of patients with mental disorders," *Psychiatriki*, vol. 23, no. 3, pp. 245–254, 2012.
- [15] G. Bar-Sela, L. Atid, S. Danos, N. Gabay, and R. Epelbaum, "Art therapy improved depression and influenced fatigue levels in cancer patients on chemotherapy," *Psycho-Oncology*, vol. 16, no. 11, pp. 980–984, 2007.
- [16] M. Chiang, W. B. Reid-Varley, and X. Fan, "Creative art therapy for mental illness," *Psychiatry Research*, vol. 275, pp. 129–136, 2019.

- [17] D. M. Crone, E. E. O'Connell, P. J. Tyson, F. Clark-Stone, S. Opher, and D. V. B. James, "Art Lift' intervention to improve mental well-being: an observational study from U.K. general practice," *International Journal of Mental Health Nursing*, vol. 22, no. 3, pp. 279–286, 2013.
- [18] D. Gussak, "The effectiveness of art therapy in reducing depression in prison populations," *International Journal of Offender Therapy and Comparative Criminology*, vol. 51, no. 4, pp. 444–460, 2007g.
- [19] Z. Jalambadani, "Art therapy based on painting therapy on the improvement of autistic children's social interactions in Iran," *Indian Journal of Psychiatry*, vol. 62, no. 2, pp. 218–219, 2020.
- [20] K. D. Ten Eycke and U. Müller, "Drawing links between the autism cognitive profile and imagination: executive function and processing bias in imaginative drawings by children with and without autism," *Autism*, vol. 22, no. 2, pp. 149–160, 2018.
- [21] D. Regev and L. Cohen-Yatziv, "Effectiveness of art therapy with adult clients in 2018-what progress has been made?" *Frontiers in Psychology*, vol. 9, p. 1531, 2018.
- [22] J. Hu, J. Zhang, L. Hu, H. Yu, and J. Xu, "Art therapy: a complementary treatment for mental disorders," *Frontiers in Psychology*, vol. 12, Article ID 686005, 2021.
- [23] A. Abbing, A. Ponstein, S. van Hooren, L. de Sonnevile, H. Swaab, and E. Baars, "The effectiveness of art therapy for anxiety in adults: a systematic review of randomised and non-randomised controlled trials," *PLoS One*, vol. 13, no. 12, Article ID e0208716, 2018.
- [24] S. Babaei, S. Fatahi Babani, M. Fakhri et al., "Painting therapy versus anxiolytic premedication to reduce preoperative anxiety levels in children undergoing tonsillectomy: a randomized controlled trial," *Indian Journal of Pediatrics*, vol. 88, no. 2, pp. 190–191, 2021.
- [25] L. Shamri Zeevi, "Making art therapy virtual: integrating virtual reality into art therapy with adolescents," *Frontiers in Psychology*, vol. 12, Article ID 584943, 2021.
- [26] D. Clus, M. E. Larsen, C. Lemey, and S. Berrouiguet, "The use of virtual reality in patients with eating disorders: systematic review," *Journal of Medical Internet Research*, vol. 20, no. 4, p. e157, 2018.
- [27] M. Dechant, S. Trimpl, C. Wolff, A. Muhlberger, and Y. Shiban, "Potential of virtual reality as a diagnostic tool for social anxiety: a pilot study," *Computers in Human Behavior*, vol. 76, pp. 128–134, 2017.
- [28] D. Freeman, S. Reeve, A. Robinson et al., "Virtual reality in the assessment, understanding, and treatment of mental health disorders," *Psychological Medicine*, vol. 47, no. 14, pp. 2393–2400, 2017.
- [29] J. L. King and G. Kaimal, "Approaches to research in art therapy using imaging technologies," *Frontiers in Human Neuroscience*, vol. 13, p. 159, 2019.
- [30] M. Bellani, L. Fornasari, L. Chittaro, and P. Brambilla, "Virtual reality in autism: state of the art," *Epidemiology and Psychiatric Sciences*, vol. 20, no. 3, pp. 235–238, 2011.

Research Article

Formation Mechanism of Microbial Diversity in Artificial Intelligence Devices due to Intermediate Disturbance by Low-Dose UV Radiation for Complementary Medicine

Junjie Ye,^{1,2} Yang Yang,³ Juanyi Wang,¹ Jingyu Han,¹ Lihong Zhang,⁴ Tianrun Gong,¹ Yi Zhang,¹ Xiaodong Xing,¹ and Chen Dong¹ 

¹Department of Health Service and Management, School of Sport Management, Shandong Sport University, Jinan 250102, China

²School of Graduate Education, Shandong Sport University, Jinan 250102, China

³Shandong Provincial Hospital, Jinan 250021, China

⁴Shandong Maternal and Child Health Hospital, Jinan 250014, China

Correspondence should be addressed to Chen Dong; dongchen@sdpei.edu.cn

Received 28 May 2022; Accepted 26 August 2022; Published 9 September 2022

Academic Editor: Wen Si

Copyright © 2022 Junjie Ye et al. This is an open access article distributed under the Creative Commons Attribution License, which permits unrestricted use, distribution, and reproduction in any medium, provided the original work is properly cited.

The development of artificial intelligence devices in the complementary medicine field is rapid and the surface microbial diversity pollution was found with periodic low-dose ultraviolet radiation (LDUVR). Since artificial intelligence devices do not have enough different types of substrates for microbial communities, it is unclear how the great microbial diversity can emerge and persist, as this clearly defies the competitive exclusion principle of ecology. In this study, the 5 most common genera in the artificial intelligence devices, *Escherichia*, *Pseudomonas*, *Streptococcus*, *Staphylococcus* and *Aeromonas* have been sampled without and with periodic LDUVR, respectively. A new hypothesis was put up to clarify the construction and maintenance process of high microbiological diversity in artificial intelligence devices by comparing and evaluating the variations between the dynamic response characteristics of their relative abundances in the two scenarios as follows: the periodic LDUVR can be regarded as an adverse factor with intermediate disturbance, causing stronger microbial stochastic growth responses (SGR) which would inevitably give rise to stronger random variation of the other important processes tightly correlated with SGR, such as intra- and interspecific competition process, and substrates production and consumption process, which could effectively diminish the auto- and cross-correlation of stochastic processes of microbial populations, alleviating the intra- and inter-specific competitions. In artificial intelligence devices with LDUVR, these crucial succession processes can propel the microbial communities to generate and sustain a high species diversity. Finally, thorough *Monte Carlo* simulations were used to thoroughly confirm the idea. This research can build the theoretical groundwork, offer fresh viewpoints, and suggest potential microbial prevention strategies for the succession of microbial communities in LDUVR.

1. Introduction

Microbial diversity in the medical treatment environment, such as operating room, sickroom, treatment room, and injection, is often at a lower level, and all sections of the environment need to be properly cleaned, disinfected, and maintained. However, microbial diversity with high richness and evenness has been currently found in the artificial intelligence devices where periodic ultraviolet (UV) ray disinfection was used extensively, because various kinds of

microbial species had been sampled and identified from the parts which were uneasily cleaned in the devices, such as screw, pulley, and backboard, where the microbial diversity is significantly higher than other parts of artificial intelligence devices. The microorganisms on the significant surface are killed by direct exposure to periodic high-dose UV radiation, nevertheless, those microorganisms colonized on the positions with a relatively long distance from the UV source can only receive periodic low-dose UV radiation (LDUVR) due to energy degradation [1, 2].

The indoor microorganisms are often combined with dust particles and exist in the form of aerosol suspending in the air and precipitating in artificial intelligence devices with periodic LDUVR [3]. The dust particles usually contain a small amount of macromolecular organic matters, which could be decomposed by the microbial community into monosaccharides, oligosaccharides, oligopeptides, amino acids, glycerol, fatty acids, and so on, which could be directly used as substrates for microbial growth and proliferation [4]. However, statistics show that the number of substrate types accessible for the microbial community in the medical treatment environment is about 10 at most, far less than the number of microbial species discovered in artificial intelligence systems with periodic LDUVR. Although only a few dominant species can coexist through substrate niche differentiation, the well-known competitive exclusion principle in ecology predicts that microbial species will compete fiercely over fewer varieties of substrates, making it impossible to create and maintain microbial diversity [5]. Although these phenomena were seen in artificial intelligence systems with periodic LDUVR, it is now unclear how the dynamic forces underpinning the microbial community succession work. The reason the microbiological variety can develop and persist in the artificial intelligence devices with periodic LDUVR is therefore still a mystery.

A negative disturbance for the microbial community succession in artificial intelligence devices could be the periodic LDUVR. The intermediate disturbance hypothesis has been put forth to suggest that species diversity will be higher in communities with moderate levels of perturbations than in communities with no perturbations or communities with rare or very frequent perturbations [6]. As is well known, ecosystem disturbance is defined as a relatively discrete event in time with frequency, intensity, and severity outside of a predictable range [7]. In a relatively simple environment with fluctuating temperature, for instance, many more species of phytoplankton have been observed to coexist, a phenomenon known as the “plankton paradox”. As an intermediate disturbance, fluctuating temperature may promote species diversity by reducing the pressure of dominant species on other species and allowing the latter to develop [8].

The periodic LDUVR can be viewed as an unfavorable factor with intermediate disturbance, causing microbial stochastic growth response (SGR) along with random variation of the crucial processes tightly correlated with SGR, such as intra- and inter-specific competition [8, 9]. This new dynamic mechanism is based on existing ecological investigations and drives microbial community succession with higher species diversity in artificial intelligence device with periodic LDUVR. In order to create and preserve high microbial diversity in artificial intelligence devices with periodic LDUVR, the periodic LDUVR may efficiently reduce the auto- and cross-correlation of stochastic processes of microbial populations.

In order to test the preceding hypothesis, in the research, the five most common genera, *Escherichia*, *Pseudomonas*, *Streptococcus*, *Staphylococcus*, and *Aeromonas* in artificial intelligence devices were periodically sampled and analyzed.

To describe the dynamic mechanisms causing microbial community successions in artificial intelligence devices with periodic LDUVR, highly valid kinetic models expressed by differential equations with kinetic parameters obeying different normal distributions were established based on the proposed assumptions, experimental phenomena, and data [9]. Additionally, a large number of microbial species and substrates were computer-generated. By using a significant amount of *Monte Carlo* simulations along with experimental data, the hypothesis was properly validated and proven. The findings of this study could create the theoretical groundwork for understanding the ecological impact of LDUVR on the succession of microbial communities and offer a practical advice on microbial prevention and control in the presence of LDUVR.

2. Materials and Methods

2.1. Source of the Samples. The selected artificial intelligence devices were located in the medical treatment environment, which was clearly divided into two functional areas, UV disinfection room and controlled room, with good ventilation, and annual keeping temperature and humidity, respectively, at 19–24°C and 40%–50% through the central air-conditioning system.

As an experimental group, the microorganisms were sampled by cotton swabs from the screw, pulley, and backboard of the UV disinfection room in the artificial intelligence devices, the effective sampling area was 10 cm × 20 cm. A germicidal lamp (Ushio Inc. Tokyo, Japan) emitting primarily 254 nm ultraviolet radiation (UV) was routinely utilized for sterilization with the disinfection time from 8 am to 8 pm every day. The sampling place was 6.18 m away from the germicidal lamp, and exposed to periodic LDUVR. As a control group, the microorganisms were sampled from the same area without UV disinfection in the artificial intelligence devices, the effective sampling area was also 10 cm × 20 cm.

The sampling time is 1 day which is relatively a short period to capture transient dynamic characteristics of microbial abundances, and the last is 100 days. Ecologically, the dynamic processes of microbial populations in the artificial intelligence devices must be stochastic processes, since they are mainly dependent on intrinsic growth rates of microbial species, intra- and inter-specific competitions, and random environmental disturbances. Based on the stochastic process theory, if a long-time observation and record for microbial populations have been carried out, the accurate statistical characteristics of their stochastic processes, such as the mean, variance, auto- and cross-correlation function, and power spectral density (PSD), can be obtained from time-series data [10]. Therefore, 100 days are long enough for stochastic processes of microbial populations to go through all possible states. According to the classic Lotka–Volterra competition model, however, the dynamic characteristics of a species population are totally dependent on the intrinsic growth rate, and intra- and inter-specific competition; hence, the auto- and the cross-correlation function can fully reflect the intra- and inter-specific relationships and

interactions, and disclose the dynamic mechanisms to drive microbial community succession in the artificial intelligence devices with periodic LDUVR. Therefore, only the auto- and the cross-correlation functions were calculated and used to analyze the stochastic process of microbial abundances [11, 12].

2.2. Analysis of Microbial Abundance and Diversity. The abundance of microbial samples was analyzed as the following steps:

- (1) Extracting microbial total DNA from the sample by using a powerful microbial DNA extraction kit (Power microbial® DNA Isolation Kit, MoBio)
- (2) High-throughput sequencing by means of an Illumina HiSeq platform using double-end sequencing
- (3) Performing quality control on preprocessed sequencing results using the DADA2 method
- (4) Dividing operational taxonomic units (OTUs) to assess the richness of the microbial community through the Chao1 Index
- (5) Annotating species for each sample and analyzing the composition of the microbial community abundance at the genus level
- (6) Calculating the microbial diversity based on the *Simpson index* and performing the overall α diversity analysis in conjunction with step (4)

The purified pooled sample was subjected to high-throughput sequencing analysis of bacterial rRNA genes utilizing the Illumina HiSeq 2500 platform (2250 paired ends) at Biomarker Technologies Corporation, Shanghai, China. These OTU sequences were classified taxonomically at various taxonomic levels using the RDP classifier and an 80 percent confidence criterion against the SILVA and UNITE databases.

2.3. Mathematical Modeling and Digital Simulations. Using the hypothesized theory, system dynamics, and experimental data, kinetic models of microbial community succession were created in this study [13]. Through digitally created *Monte Carlo* experiments, the microbial species and substrates were represented by model parameter vectors [14]. In order to simulate the scenario of microbial community succession in the controlled room and UV disinfection room with periodic LDUVR, respectively, the corresponding simulation models were established by MATLAB/Simulink based on these kinetic models. These stochastic parameters generated from the normal distribution would cause the stochastic processes of microbial populations to have different PSDs [15]. Digital simulations along with experimental data and phenomena were used to sufficiently validate and confirm the presented concept.

3. Results and Discussion

3.1. Dynamic Characteristics of Microbial Abundances. The microbial relative abundances of *Escherichia*, *Pseudomonas*, *Streptococcus*, *Staphylococcus* and *Aeromonas*, and

the corresponding *Simpson Diversity Index* of the microbial community were analyzed and quantified (Figure 1), after periodical sampling from UV the disinfection room and controlled room of the artificial intelligence devices, respectively.

Based on stochastic processes of relative abundances of the five most common genera, calculate the autocorrelation function of the relative abundances stochastic process of each microbial genus sampled from the controlled room (Figure 2) and UV disinfection room (Figure 3), respectively.

Furthermore, the cross-correlation function between two microbial genus-relative abundance stochastic processes was also calculated and illustrated in Figures 4 and 5, respectively.

From Figures 1, 2, and 4, the auto- and cross-correlation function of microbial abundances stochastic processes as well as the *Simpson Index* of microbial community sampled from the controlled room are relatively large. Based on the classic *Lotka-Volterra* competition model and stochastic process theory, the auto- and cross-correlation function can indicate the influence of intra- and inter-specific competition strength on species population. The larger auto- and cross-correlation functions would indicate that intra- and inter-specific competition strongly correlated to dynamic characteristics of the species population [16]. Microbes would compete fiercely over a limited range of substrates through intra- and inter-specific competition; as a result, only a small number of species could coexist, and the majority of microbial species would go extinct due to competitive exclusion. Hence the *Simpson Index* also indicated low species diversity in the microbial community sampled from the controlled room (Figure 1).

From Figures 1, 3, and 5, however, the situation is exactly reversed, which suggested both the intra- and inter-specific competition were alleviated and the dynamic characteristics were fundamentally independent on the microbial intra- and inter-specific competition [17], and the *Simpson Index* also signified high species diversity in the microbial community sampled from the UV disinfection room.

3.2. Hypothesis of Microbial Diversity in Artificial Intelligence Devices with Periodic LDUVR. Even though experimental phenomena and data can be directly observed and measured, the underlying dynamic mechanisms created by relationships and interactions between microbial species and their biotic/abiotic environments cannot be directly identified and recognized; instead, they can only be understood by hypotheses that have been developed based on microbial ecology, experimental phenomena, and data, and sufficiently investigated by mathematical modeling and digital simulations [18].

The competitive exclusion scenario in the controlled room of the artificial intelligence device without LDUVR could be imagined based on the following: microbial ecology, experimental data, and theoretical analyses. At the start of microbial community succession in the artificial intelligence devices, all populations grow exponentially. However, since substrate niches are regularly filled due to the quantity

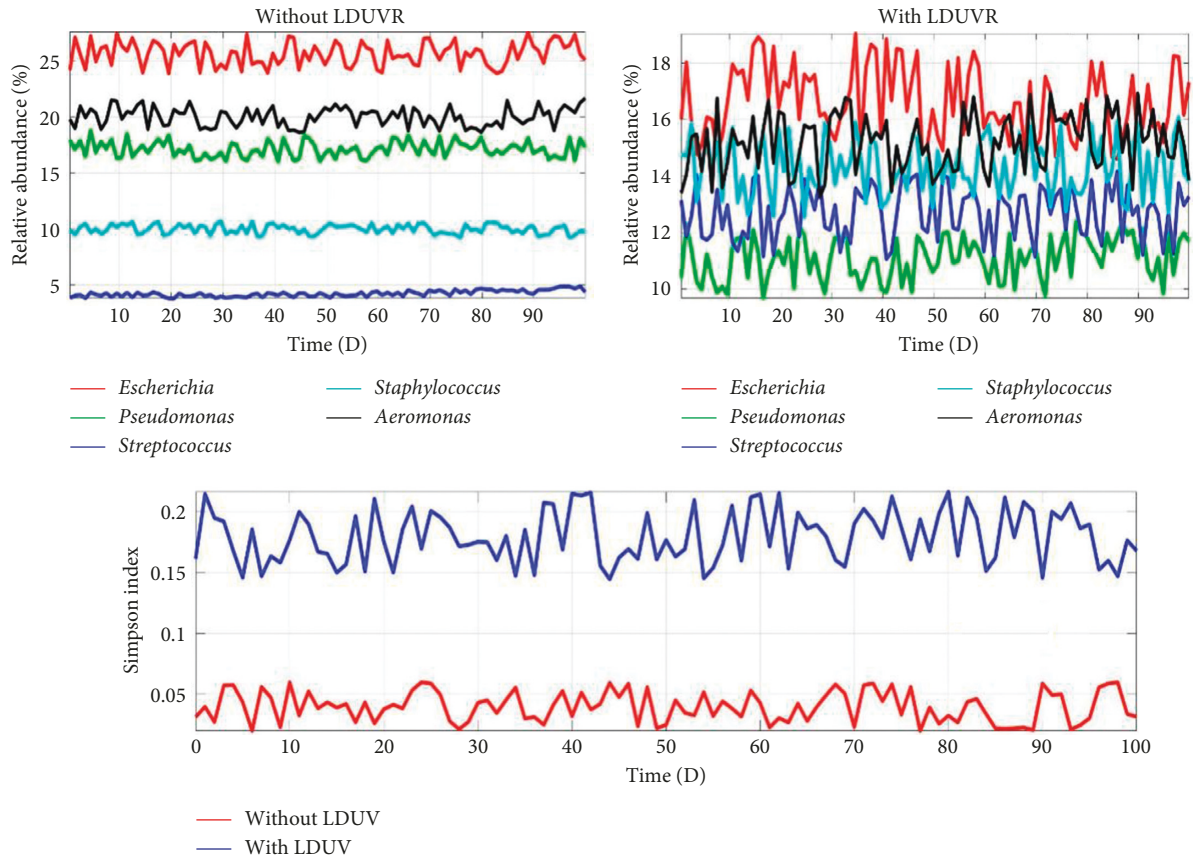


FIGURE 1: Stochastic processes of 5 genera abundances and the *Simpson Index* of microbial community respectively sampled from the controlled room and UV disinfection room.

and kind of substrates being limited, their development rates must inevitably slow down. Due to inter-specific variations in intrinsic growth rates, competitive abilities, carrying capacities, and other factors, a turning point will manifest sooner or later. Some species will eventually stop developing while others will continue to do so, eventually excluding the former and driving it to extinction [19]. In order to understand the succession of the microbial population in UV disinfection, a new dynamic mechanism must be proposed. The following new hypothesis of dynamic mechanisms driving microbial community succession in artificial intelligence devices with periodic LDUVR was put forth to interpret new relationships and interactions between microbial species and their biotic/abiotic environments based on microbial ecology, easily observed experimental phenomena, and data.

As an adverse factor, the periodic LDUV could generate intermediate disturbance to cause stronger microbial SGR determining the microbial population size directly, and inevitably gives rise to stronger random variations of other processes, such as the intra- and inter-specific competition process and the substrates production and consumption process. The stronger stochastic fluctuation of microbial populations could effectively weaken the auto- and cross-correlation of stochastic processes of microbial populations, greatly alleviating intra- and inter-specific competition and increasing the possibility of a wide spectrum of the microbial

species, according to the classic *Lotka–Volterra* competition model, which states that the intensity of microbial intra- and inter-specific competition only depends on the product of the species population size. As a result, a greater number of species can effectively cohabit under the intermediate disturbance induced by periodic LDUVR than that permitted under the competitive exclusion principle.

Instead, because of the relatively weak microbial populations' stochastic fluctuation caused by environmental background disturbances, which could lead to increased inter-specific competition and exclusion during microbial community succession in a controlled environment, the microbial diversity could not be formed or maintained at all.

3.3. Kinetic Model Derivation of Microbial Community Succession in Artificial Intelligence Device. The following rate equations were created to characterize the relationships and interactions between microbial species and their biotic/abiotic habitats in artificial intelligence devices based on the aforementioned premises and system dynamics.

3.3.1. Rate Equations of Microbial Population Growth. Consider the scenario where M types of microbial species were colonized in the artificial intelligence device and m types of substrates were produced for direct utilization, satisfying $M > m$ to mimic the scenario where M types of

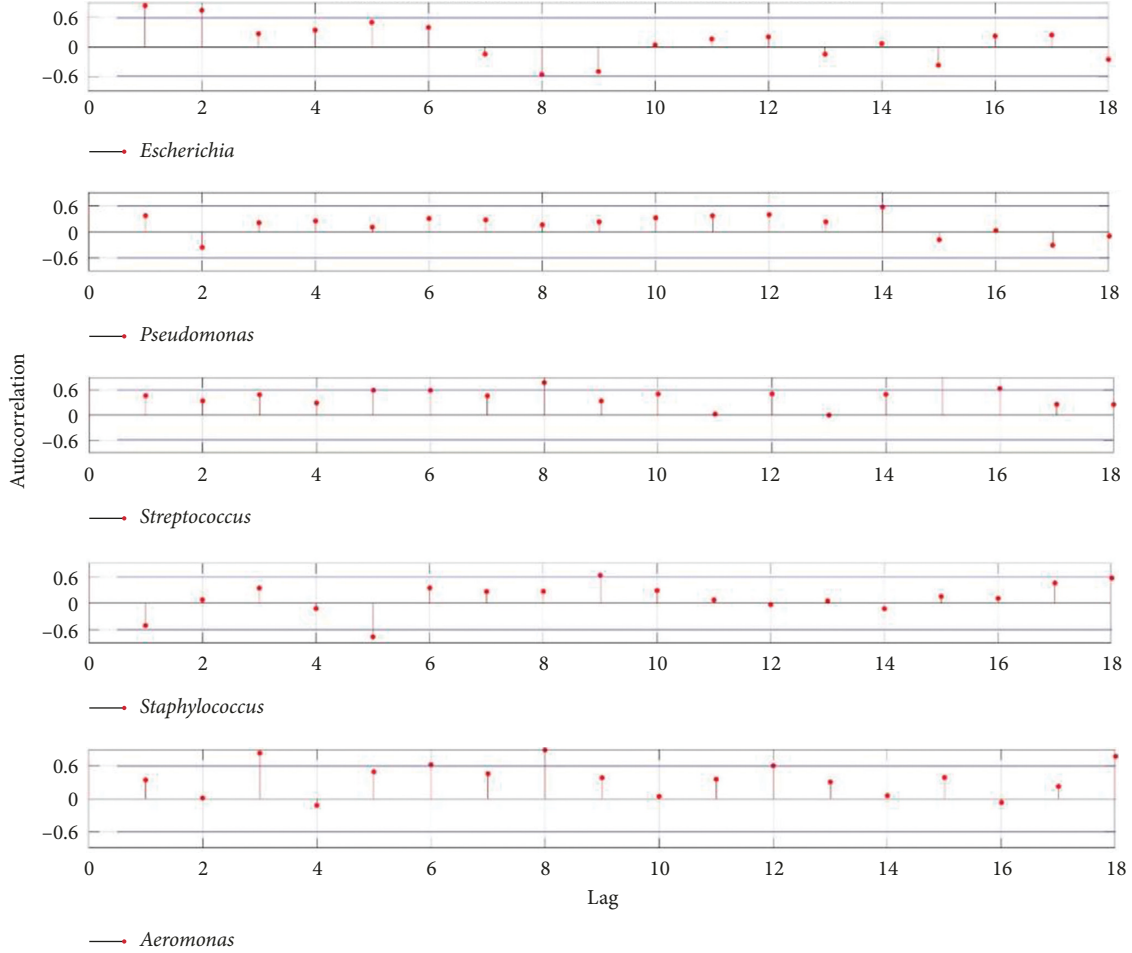


FIGURE 2: Autocorrelation function of the relative abundances stochastic process of each microbial genus sampled from the controlled room.

microbial species were much more numerous than m types of substrates in the artificial intelligence devices. The i -th microbial population (x_i) and the k -th substrate amount (S_k) produced by microbial breakdown were thus the state variables in the kinetic model. The i -th microbial population growth rate (v_{bi}) was formulated by Monod equations as follows:

$$v_{bi} = [\mu_i + \varepsilon_1(t)]x_i(t) \sum_{k=1}^m \frac{S_k(t)}{K_{ik} + S_k(t)}, \quad (1)$$

where K_{ik} is the half-saturation constant of the i -th microbial population growth on the k -th substrate, μ_i is the specific growth rate of the i -th microbial population, $\varepsilon_1(t)$ is normally distributed random numbers, and μ_i represents the environmental disturbance .

3.3.2. Rate Equations of Microbial Intra- and Inter-specific Competition. The traditional Lotka–Volterra competition model was used to develop the rate equations for intra-specific and inter-specific competition. The rates of intra-specific competition within the i -th microbial species (v_{ai}) were expressed as follows:

$$v_{ai} = [\alpha_i + \varepsilon_2(t)]x_i^2, \quad (2)$$

where α_i is the intraspecific competition inhibition coefficient of the i -th microbial species and $\varepsilon_2(t)$ is a set of randomly generated values with normal distribution and is a proxy for α_i environmental disturbance.

The following could be stated as the rates of inter-specific competition between the i -th and j -th microbial species (v_{ei}):

$$v_{ei} = \sum_{i \neq j}^M [\beta_{ij} + \varepsilon_3(t)]x_i(t)x_j(t), \quad (3)$$

where β_{ij} stands for the inter-specific competition inhibition coefficient of the j -th microbial population on the growth rate of the i -th microbial population and $\varepsilon_3(t)$ is a random number with a normal distribution and reflects β_{ij} environment.

3.3.3. Metabolism Rate of Microbial Population. The following could be used to express the metabolic rate of the i -th microbial population (v_{di}):

$$v_{di} = d_i x_i, \quad (4)$$

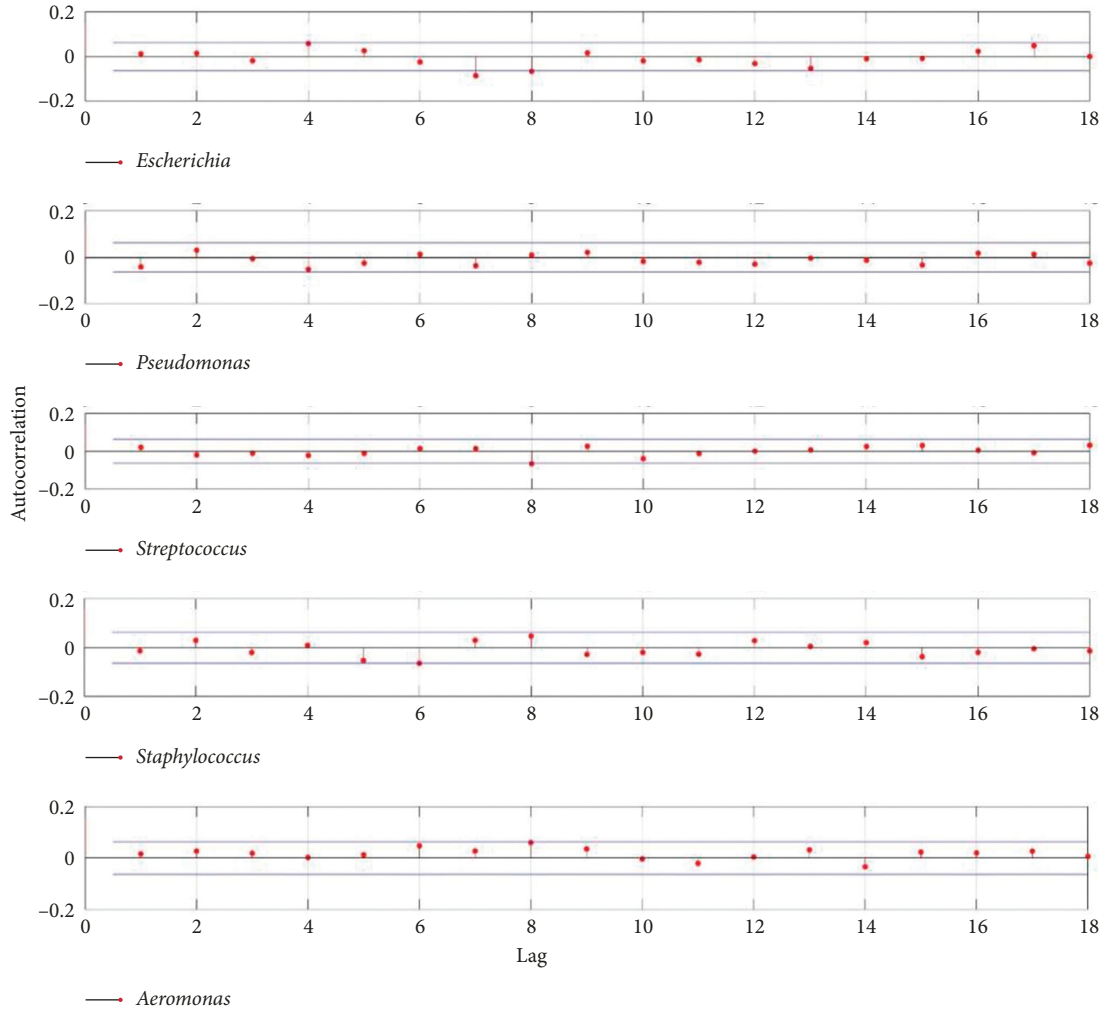


FIGURE 3: Autocorrelation function of the relative abundances stochastic process of each microbial genus sampled from UV disinfection room.

where d_i is the metabolism coefficient of the i -th microbial population.

3.3.4. Substrates Production and Consumption Rate. Furthermore, the production rate of the k -th substrate by the i -th microbial species through microbial decomposition (v_{pki}) could be specified as follows [20]:

$$v_{pki} = r_k \sum_{i=1}^M [c_i + \varepsilon_4(t)] \frac{x_i}{Z_i + x_i}, \quad (5)$$

where r_k is the proportion of the k -th substrate to the total substrates produced by microbial decomposition, c_i is the maximum rate of substrate production of the i -th microbial species with the half-saturation constant Z_i , and $\varepsilon_4(t)$ is normally distributed random numbers and represents the environmental disturbance to c_i .

Similarly, the consumption rate of the k -th substrate during the i -th microbial population growth (v_{cki}) could be specified as follows:

$$v_{cki} = h_k \sum_{i=1}^M [\gamma_i + \varepsilon_5(t)] v_{bi}, \quad (6)$$

where h_k is the ratio of the k -th substrate to the total number of substrates consumed by the microbial community, γ_i is the substrates consumption coefficient of the i -th microbial population, $\varepsilon_5(t)$ is normally distributed random numbers, and γ_i represents the environmental disturbance.

3.3.5. General Kinetic Model Obtained from Rate Equations. A top-down state-space model with $M+m$ first-order nonlinear ODEs of microbial community succession in the artificial intelligence devices was built based on the prior analysis and establishing rate equations [21].

The first-order kinetic equation of the i -th microbial population can be stated as follows, with reference to (1)–(4):

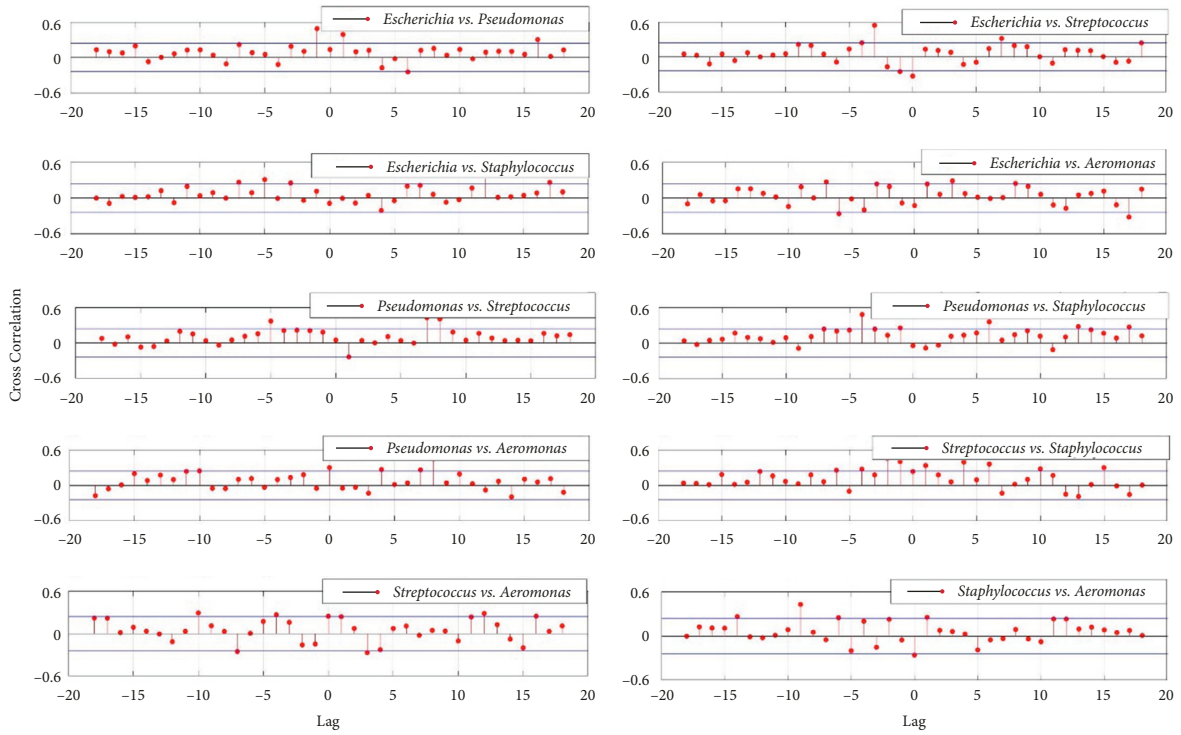


FIGURE 4: Cross-correlation function between two microbial genus-relative abundance stochastic processes from the controlled room.

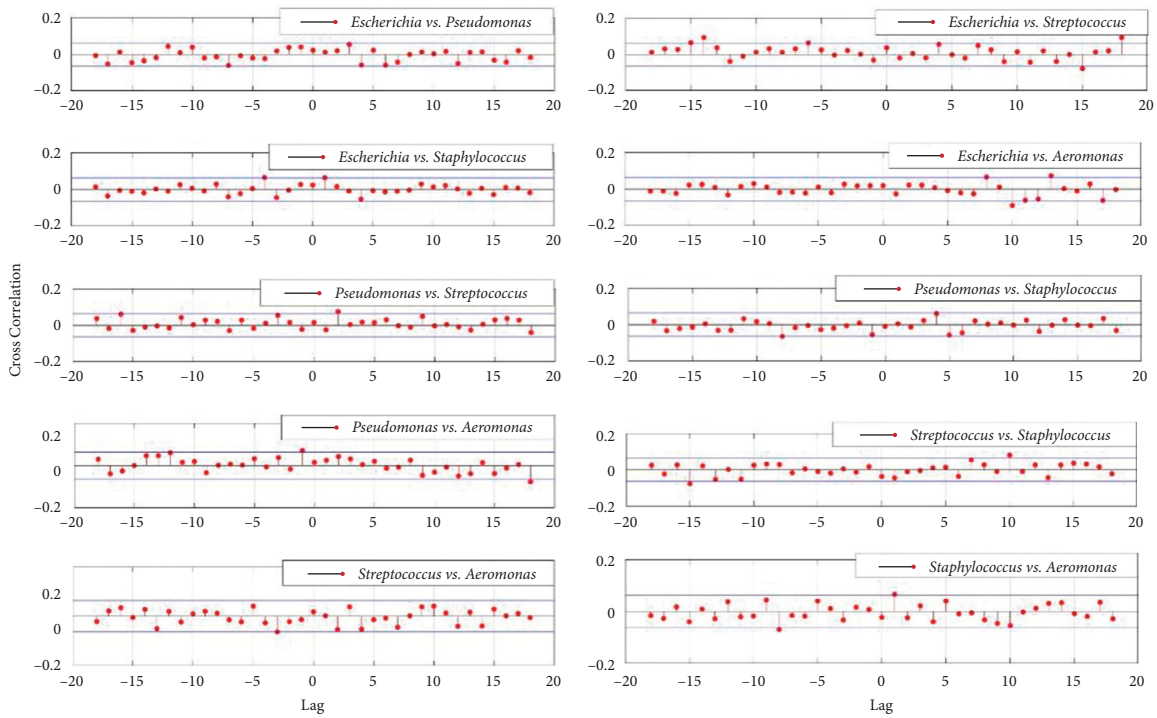


FIGURE 5: Cross-correlation function between two microbial genus-relative abundance stochastic processes from the UV disinfection room.

TABLE 1: Parametric intervals in the kinetic models.

Parameter	Unit	Parametric interval		Significance
		Without LDUVR	With LDUVR	
μ_i	h^{-1}	(0.24, 1.36)		The i -th microbial species' particular growth rate.
α_i	$(\log_{10} \text{CFU}^{-1}) \text{ml}\cdot\text{h}^{-1}$	(0.05, 1)		The i -th microbial species' intraspecific competition coefficient.
β_{ij}	$(\log_{10} \text{CFU}^{-1}) \text{ml}\cdot\text{h}^{-1}$	(0.16, 1)		The j -th microbial species' inter-specific competition coefficient on the i -th microbial species' growth rate.
c_i	$\text{mg}\cdot\text{h}^{-1}$	(136.23, 518.76)		The i -th microbial species' highest rate of substrate production
γ_i	$\text{mg} (\log_{10} \text{CFU})^{-1} \text{ml}$	(3.32, 12.55)		The consumption coefficient of substrates by the i -th microbial species
ε_1	$\text{W}\cdot\text{Hz}^{-1}$	(0, 2)	[2, 10]	Environmental disturbance to μ_i
ε_2	$\text{W}\cdot\text{Hz}^{-1}$	(0, 2)	[2, 10]	Environmental disturbance to α_i
ε_3	$\text{W}\cdot\text{Hz}^{-1}$	(0, 2)	[2, 10]	Environmental disturbance to β_{ij}
ε_4	$\text{W}\cdot\text{Hz}^{-1}$	(0, 2)	[2, 10]	Environmental disturbance to c_i
ε_5	$\text{W}\cdot\text{Hz}^{-1}$	(0, 2)	[2, 10]	Environmental disturbance to γ_i
K_{ik}	mg	(1.23·10 ⁵ , 1.82·10 ⁵)		The i -th microbial species' half-saturation constant while growing on the k -th substrate.
d_i	h^{-1}	(0.03, 0.58)		The i -th microbial species' metabolic coefficient.
Z_i	$(\log_{10} \text{CFU}) \text{ml}^{-1}$	(42, 177)		The substrates produced by the i -th microbial species' half-saturation constant.
r_k	%	(0, 80)		The percentage of all substrates generated by the microbial population to the k -th substrate.
h_k	%	(0, 80)		The proportion of the k -th substrate to total substrates consumed by microbial community.

$$\begin{aligned}
\frac{dx_i(t)}{dt} &= v_{bi} - v_{ai} - v_{ei} - v_{di} \\
&= [\mu_i + \varepsilon_1(t)]x_i(t) \sum_{k=1}^m \frac{S_k(t)}{K_{ik} + S_k(t)} - [\alpha_i + \varepsilon_2(t)]x_i^2 \\
&\quad - \sum_{i \neq j}^M [\beta_{ij} + \varepsilon_3(t)]x_i(t)x_j(t) - d_i x_i.
\end{aligned} \tag{7}$$

The first-order kinetic equation of the k -th substrate can be expressed as follows with reference to (1), (5), and (6):

$$\begin{aligned}
\frac{dS_k(t)}{dt} &= v_{pki} - v_{cki} = r_k \sum_{i=1}^M [c_i + \varepsilon_4(t)] \frac{x_i}{Z_i + x_i} \\
&\quad - h_k \sum_{i=1}^M [\gamma_i + \varepsilon_5(t)] [\mu_i + \varepsilon_1(t)] x_i(t) \sum_{k=1}^m \frac{S_k(t)}{K_{ik} + S_k(t)}.
\end{aligned} \tag{8}$$

3.4. Microbial Species and Substrates Computer-Generated for Simulation. The i -th microbial species could be represented by a parameter vector $(\mu_i, \alpha_i, \beta_{ij}, K_{ik}, d_i, c_i, \gamma_i, Z_i)$, and the k -th substrate could be denoted by a parameter vector (r_k, h_k) , as the parameters in kinetic models (equations (7) and (8)) of microbial community succession can embody specific biological and ecological characteristics tightly dependent on specific microbial genomes. These parameters could be acquired using parameter estimation uniformly and independently by random selection from defined parametric intervals [22] (Table 1).

In this study, the 5~15 different types of substrates and 20~50 different microbial species were produced stochastically by computers and inserted into kinetic models (equations (7) and (8)). This method allowed for the formulation of kinetic models with various dimensions for theoretical investigation of the succession of microbial communities in artificial intelligence devices and the validation of the hypothesis regarding the emergence and preservation of microbial diversity as a result of intermediate disturbance brought on by periodic LDUVR.

A large scale of *Monte Carlo* simulations was then carried out to confirm the proposed hypothesis on the formation and maintenance of microbial biodiversity in the artificial intelligence device with periodic LDUVR. Before digital simulation, simulation methods and other options were properly set [21], according to the complexity of kinetic models, accuracy, convergence speed, and computational cost.

3.5. Monte Carlo Simulations for Microbial Community Successions. The simulation model was correspondingly established on the Matlab/Simulink platform to conduct *Monte Carlo* simulations to support the proposed hypothesis on microbial community succession in artificial intelligence devices based on kinetic models (equation (7) and (8)) of microbial community succession in artificial intelligence devices (Figure 6) [23].

Figure 6 shows how the random number blocks were used to simulate environmental disturbances whose PSD was applied for assessments of the strength of disturbances. The PSD was set at reasonably mild values generated at random from the value range. The simulation results fully

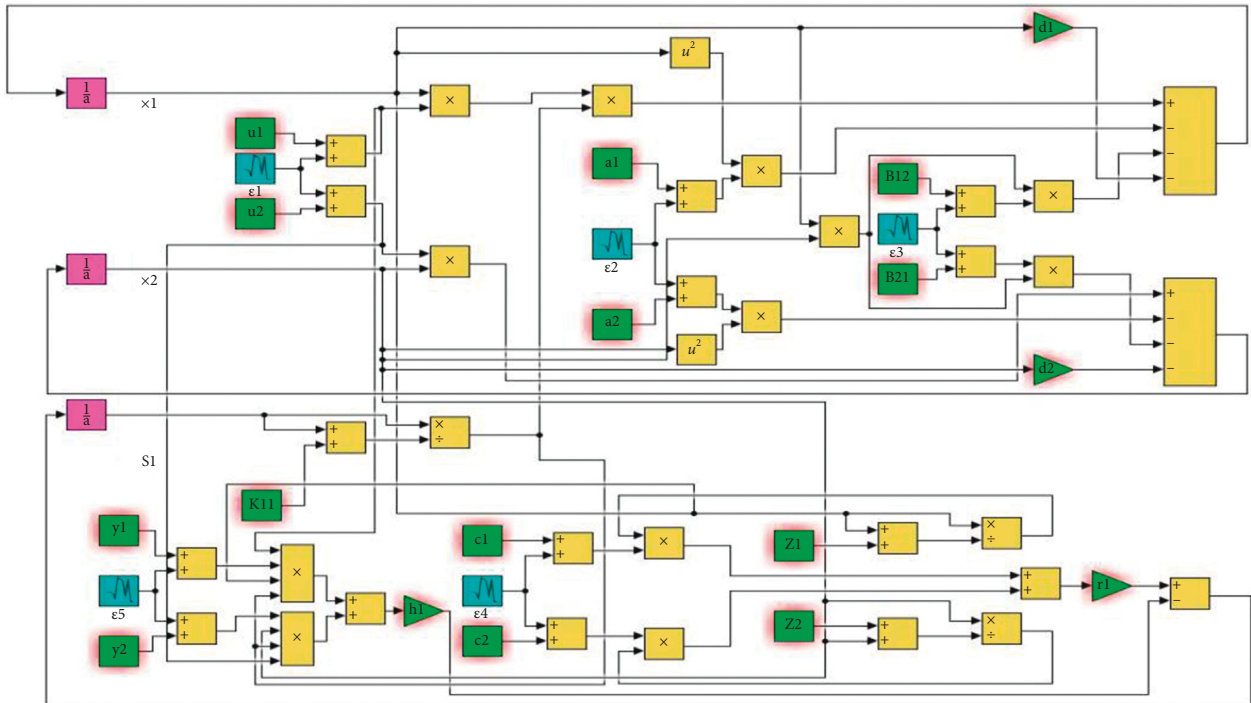


FIGURE 6: Part of the simulation model of microbial community succession in artificial intelligence devices.

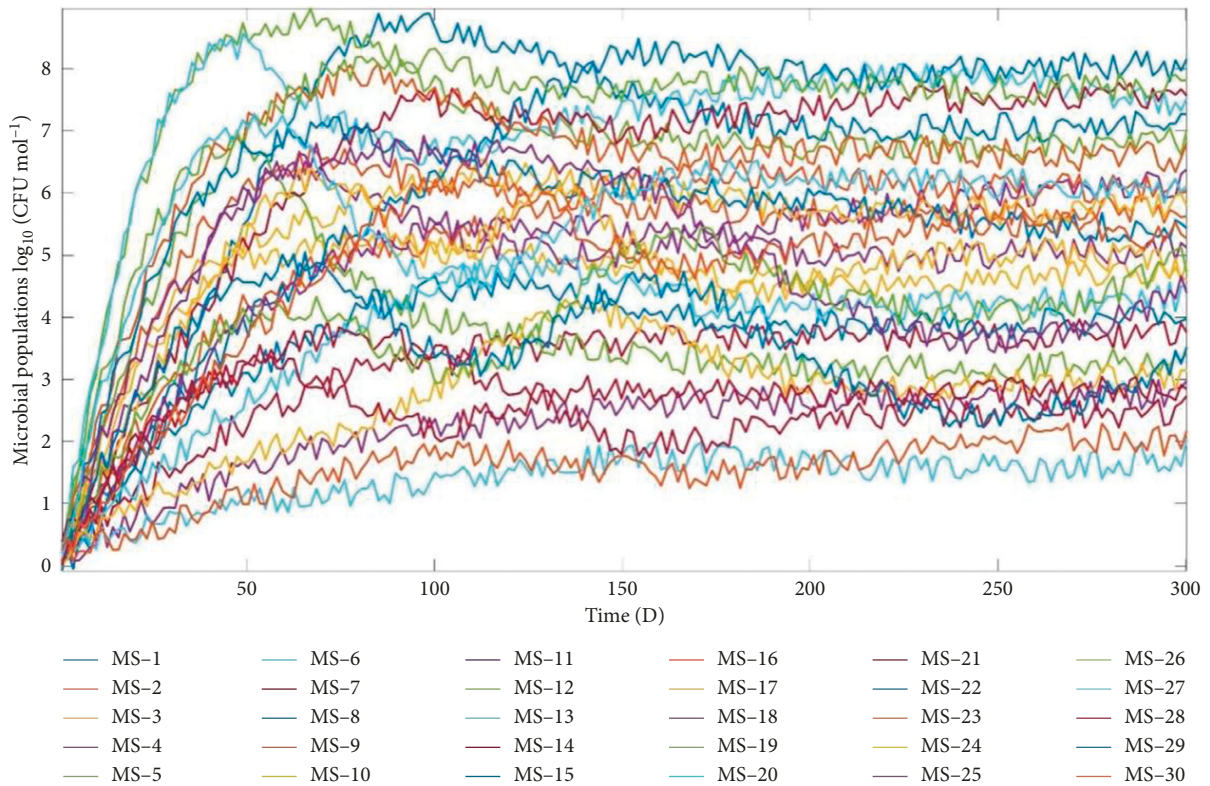


FIGURE 7: Microbial community succession pattern in artificial intelligence devices with periodic LDUVR.

demonstrated that the number of coexisting microbial species was far greater than the types of substrates produced by microbial decomposition, and the microbial populations generate almost independent stochastic processes via

desultorily transient responses (Figure 7). These dynamic behaviors could significantly reduce intra- and inter-specific competition [24, 25]. It will be advantageous for a large number of microbial species to dwell in artificial intelligence

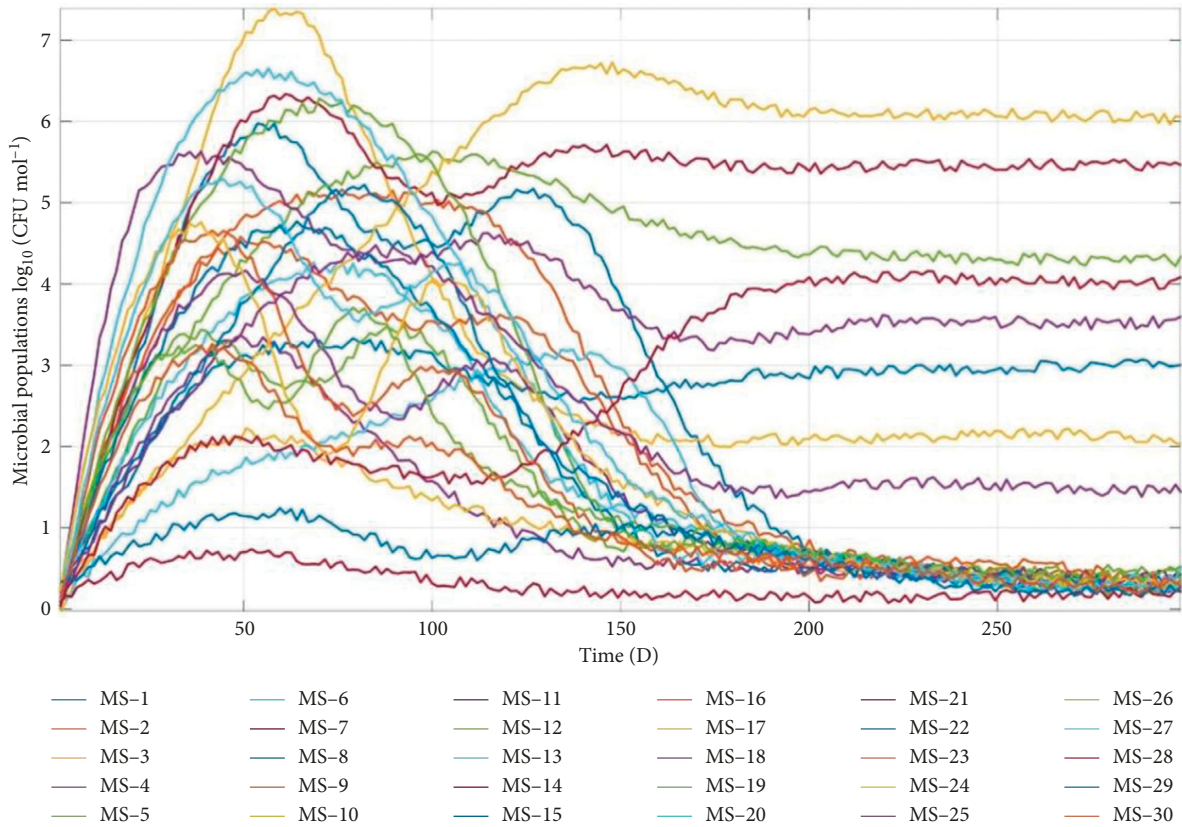


FIGURE 8: Microbial community succession pattern in artificial intelligence devices without LDUVR.

devices with periodic LDUVR to concurrently boost the richness and evenness of the microbial community.

It is important to note that the digital simulation results of the microbial community succession patterns that emerged in the artificial intelligence device with periodic LDUVR, as shown in Figure 7, are quite universal and general since these simulation results only depend on the structure of kinetic models, specifically the interactions and relationships between microbial populations and their biotic/abiotic environments in the artificial intelligence devices with periodic LDUVR.

Due to the PSD's modest setting, however, values chosen at random from the value range of the simulation results suggested that, subjected to competitive exclusion, the majority of microbial species would eventually go extinct, with only a few species whose number is no more than the substrate types produced by microbial decomposition being able to coexist (Figure 8), due to drastic intra- and inter-specific competition reflected in strong auto- and cross-correlation of stochastic without LDUVR to simulate the scenarios with weak disturbance caused by environmental background disturbances.

4. Conclusions

We theoretically provide a hypothesis on the production and preservation of microbial diversity in the artificial intelligence devices with intermediate disturbance brought on by periodic LDUVR based on microbial ecology, experimental phenomena, and data. The periodic LDUVR could produce intermediate disturbance that would lead to stronger microbial SGR

along with stronger random process variations of substrate production and consumption. This would significantly reduce the auto- and cross-correlation of microbial populations stochastic processes and effectively alleviate intra- and inter-specific competition to form and maintain a microbial community with higher richness. The hypothesized hypothesis was then quantified using a collection of kinetic models written by differential equations with parameters obeying various normal distributions. Finally, a significant number of *Monte Carlo* simulations were performed to sufficiently validate and confirm the proposed theory. The findings of this study could create the theoretical groundwork for understanding the ecological impact of LDUV on the succession of microbial communities and offer practical advice on microbial prevention and control in the context of LDUVR.

Data Availability

The data used to support the findings of this study are available from the corresponding author upon request.

Consent

Informed consent was obtained from all individual participants included in the study.

Conflicts of Interest

The authors declare that they have no conflicts of interest.

Acknowledgments

This work was supported by the Foundation for the Excellent Youth Scholars of Shandong Educational Committee (NO. 72).

References

- [1] J. A. Gilbert and B. Stephens, "Microbiology of the built environment," *Nature Reviews Microbiology*, vol. 16, no. 11, pp. 661–670, 2018.
- [2] A. Barberán, R. R. Dunn, B. J. Reich et al., "The ecology of microscopic life in household dust," *Proceedings of the Royal Society B: Biological Sciences*, vol. 282, no. 1814, pp. 212–220, 2015.
- [3] J. Y. Wakano, M. A. Nowak, and C. Hauert, "Spatial dynamics of ecological public goods," *Proceedings of the National Academy of Sciences*, vol. 106, no. 19, pp. 7910–7914, 2009.
- [4] G. Hardin, "The competitive exclusion principle," *Science*, vol. 131, no. 3409, pp. 1292–1297, 1960.
- [5] S. T. A. Pickett and P. S. White, "Natural disturbance and patch dynamics: an introduction," *Natural disturbance and patch dynamics*, 1985.
- [6] J. H. Connell, "Diversity in tropical rain forests and coral reefs: high diversity of trees and corals is maintained only in a nonequilibrium state," *Science*, vol. 199, no. 4335, pp. 1302–1310, 1978.
- [7] G. E. Hutchinson, "The paradox of the plankton," *The American Naturalist*, vol. 95, no. 882, pp. 137–145, 1961.
- [8] X. Yang, X. Xu, and D. Hu, "Succession mechanism of microbial community with high species diversity in nutrient-deficient environments with low-dose ionizing radiation," *Ecological Modelling*, vol. 435, Article ID 109270, 2020.
- [9] X. Yang, S. Li, G. Song, X. Xu, and D. Hu, "Microbial diversity formed and maintained through substrate feedback regulation and delayed responses induced by Low-Dose Ionizing Radiation," *Acta Astronautica*, vol. 188, pp. 239–251, 2021.
- [10] H. Ikehata and T. Ono, "The mechanisms of UV mutagenesis," *Journal of Radiation Research*, vol. 52, no. 2, pp. 115–125, 2011.
- [11] G. P. Pfeifer and A. Besaratinia, "UV wavelength-dependent DNA damage and human non-melanoma and melanoma skin cancer," *Photochemical and Photobiological Sciences*, vol. 11, no. 1, pp. 90–97, 2012.
- [12] W. Whitt, "Stochastic-process limits: an introduction to stochastic-process limits and their application to queues," *Space*, vol. 500, pp. 391–426, 2002.
- [13] S. M. Kay and S. L. Marple, "Spectrum analysis—a modern perspective," *Proceedings of the IEEE*, vol. 69, no. 11, pp. 1380–1419, 1981.
- [14] S. M. Ross, *Introduction to Probability models*, Academic Press, Cambridge, MA, USA, 2014.
- [15] G. John and M. R. Charles, *Algorithms for Statistical Signal processing*, Prentice-Hall, London, UK, 2002.
- [16] K. Ogata, *System dynamics*, Englewood Cliffs, Bergen, NY, USA, 1978.
- [17] M. Holyoak and M. Loreau, "Reconciling empirical ecology with neutral community models," *Ecology*, vol. 87, no. 6, pp. 1370–1377, 2006.
- [18] G. Kyliafis and M. Loreau, "Ecological and evolutionary consequences of niche construction for its agent," *Ecology Letters*, vol. 11, no. 10, pp. 1072–1081, 2008.
- [19] J. D. Oliver, "The public health significance of viable but nonculturable bacteria," *Nonculturable Microorganisms in the Environment*, ASM Press, Washington, DC, USA, 2000.
- [20] B. Descamps Julien and A. Gonzalez, "Stable coexistence in a fluctuating environment: an experimental demonstration," *Ecology*, vol. 86, no. 10, pp. 2815–2824, 2005.
- [21] X. Yang, G. Song, H. Liu, and D. Hu, "Microbial diversity formation and maintenance due to temporal niche differentiation caused by low-dose ionizing radiation in oligotrophic environments," *Life Sciences and Space Research*, vol. 31, pp. 92–100, 2021.
- [22] MathWorks, *MATLAB (R2020a) Simulink*, MathWorks Inc, Natick, MA, USA, 2020.
- [23] S. E. Jørgensen, S. N. Nielsen, and L. A. Jørgensen, *Handbook of Ecological Parameters and ecotoxicology*, Elsevier, Amsterdam, Netherlands, 1991.
- [24] D. Hu, H. Zhang, L. Li, R. Zhou, and Y. Sun, "Mathematical modeling, design and optimization of conceptual configuration of soil-like substrate bioreactor based on system dynamics and digital simulation," *Ecological Engineering*, vol. 51, pp. 45–58, 2013.
- [25] I. P. Marino, A. Zaikin, and J. Miguez, "A comparison of Monte Carlo-based Bayesian parameter estimation methods for stochastic models of genetic networks," *PLoS One*, vol. 12, no. 8, Article ID e0182015, 2017.

Research Article

Medication Regularity of Traditional Chinese Medicine in the Treatment of Aplastic Anemia Based on Data Mining

Nanxi Dong ¹, Xujie Zhang ², Dijiong Wu ¹, Zhiping Hu ¹, Wenbin Liu ¹,
Shu Deng ¹ and Baodong Ye ¹

¹The First School of Clinical Medicine, Zhejiang Chinese Medical University, Hangzhou, China

²The College of Control Science and Engineering, Zhejiang University, Hangzhou, China

Correspondence should be addressed to Baodong Ye; 13588453501@163.com

Received 19 May 2022; Revised 26 June 2022; Accepted 8 July 2022; Published 25 August 2022

Academic Editor: Lei Jiang

Copyright © 2022 Nanxi Dong et al. This is an open access article distributed under the Creative Commons Attribution License, which permits unrestricted use, distribution, and reproduction in any medium, provided the original work is properly cited.

Objective. Aplastic anemia (AA) is an uncommon disease, characterized by pancytopenia and hypocellular bone marrow, but it is common in the blood system. The medication rules of traditional Chinese medicine (TCM) in the treatment of AA are not clear, for which it is worth exploring the medication rules by data mining methods. **Methods.** This study used SPSS Modeler 18.0 and SPSS statistics to analyze the cases of AA from Zhejiang Provincial Hospital of Chinese Medicine (ZJHCM) from March 1, 2019, to March 1, 2022. Data mining methods, including frequency analysis, cluster analysis, and association rule learning, were performed in order to explore the medication rules for AA. **Results.** (1) A total of 859 prescriptions, which met the inclusion criteria, consisted of 255 herbs. In descending order of the frequency of herbal medicine, we have Danggui, Huangqi, Shudihuang, Fuling, Gancao, Shanyao, Shanzhuyu, Baizhu, Dangshen, and Xianhecao. (2) Frequency analysis of herb properties: the Four Qi of 255 kinds of TCMs are mainly warm and neutral medicines. The Five Flavors are mainly sweet medicines, followed by bitter medicines. The main meridians are the liver, spleen, and kidney. (3) Clustering of medications: TCMs with the top 20 frequencies are classified into 9 groups by cluster analysis. (4) Association rule analysis of high-frequency herbs: using the Apriori algorithm, the results showed that there were 3 herb pairs with support of over 0.3 and 12 herb pairs with confidence above 0.85. **Conclusion.** The basic pathogenesis of AA (Sui Lao) is spleen and kidney essence deficiency, Qi deficiency, and blood stasis. The main herbs have warm and neutral properties, sweet tastes, and liver, spleen, and kidney meridian tropisms, whose purpose is to tonify the kidney and invigorate the spleen, tonify Qi, and promote blood circulation.

1. Introduction

Aplastic anemia (AA) is a disease associated with bone marrow failure, which is mainly characterized by pancytopenia and infection due to decreased hematopoiesis in bone marrow [1, 2]. Patients with AA usually have a poor quality of life and high economic pressure. The treatment methods for AA include immunosuppressive therapy (IST), allogeneic hematopoietic stem cell transplantation (allo-HSCT), and supportive care [3]. Among patients who received first-line IST, 10-year overall survival (OS) and failure-free survival (FFS) rates were 55% and 40%, respectively [4]. In the National Institutes of Health (NIH) clinical trial of treating with IST, approximately one-third of

responding patients, either relapsed or required sustained cyclosporine administration to maintain their blood counts [5]. 30%–40% of patients showed no response to treatment with antithymocyte globulin (ATG), which will also consume platelets. Allo-HSCT is considered as the first-line treatment for young and adult patients who may have an HLA-matched sibling donor (MSD) [6–8]. A study conducted by the Severe Aplastic Anemia Working Party of the European Society for Blood and Marrow Transplantation (SAAWP-EBMT) showed that graft-versus-host disease-free, relapse-free survival (GRFS) of allo-HSCT for AA was only 69% over 5 years [9]. However, the remaining patients still have complications, such as graft-versus-host disease (GVHD) [10], virus infection [11], poor graft function [12],

and so on. Although the treatment of AA in Western medicine is developing rapidly, there are still many non-negligible clinical symptoms. With these treatments in patients with AA, the 5-year survival rate approaches 60–80% [13, 14]. A switch to a second-line regimen is recommended when there is treatment failure with first-line treatments. However, patients may face not only higher medical expenditure but also higher medical risk. In addition, the transfusion support will lead to a risk of iron overload [15–17]. Therefore, according to the different treatment stages of patients, the combination therapy of TCM is a common trend. The treatment strategies by integrative medicine could reduce the side effects and complications. It is noted that traditional Chinese medicine (TCM) treatment of AA medication rules is not clear, so it is necessary to carry out data mining on TCM treatment of AA.

The name “aplastic anemia” does not appear in the ancient Chinese classics, whose clinical manifestations tend to be “consumptive disease” or “hemorrhagic syndrome” in traditional Chinese concepts [18]. In the 1950s, AA was thought to be a deficiency of Qi and blood according to the clinical manifestations of the patients [19]. In the 1960s, on the basis of the syndrome differentiation of Qi and blood, the effects of Guipi Decoction and Bazhen Decoction were poor [20]. In the 1970s, according to the syndrome differentiation of yin and yang of viscera, the focus was shifted from the heart and spleen to the liver and kidney, and the efficacy of Zuoguiyin and Youguiyin in the treatment of AA was improved [21, 22]. In 1989, the Dalian National Symposium on Hematology of Integrated Traditional Chinese and Western Medicine associated the classification of AA with the kidney, which was analyzed by syndrome differentiation methods of zang-fu viscera and eight principles. Chronic aplastic anemia belongs to consumptive disease and blood insufficiency, which can be divided into kidney yin deficiency, kidney yang deficiency, and deficiency of both kidney yin and yang [21, 23]. In 2008, the China Association of Chinese Medicine issued guidelines for the diagnosis and treatment of common diseases in Chinese medicine, where the syndromes of spleen-kidney yang deficiency, liver-kidney yin deficiency, heat-toxin congestion, and blood heat syndrome were added [24]. In recent years, TCM has gained increasing attention in AA therapy. A previous study has shown that the hemocyte profile in the Shenlu granule combined treatment group was superior to the therapeutic effect in the western medicine alone group based on kidney reinforcing syndrome [25]. Another study suggested that potential mechanisms of Siwu Paste are to improve hematopoietic microenvironment and promote bone marrow hematopoiesis therapies [26]. However, these treatments are still limited in clinical application.

With the popularity of medical informatization, a large amount of medical data can be collected, stored, and analyzed, which also promotes the development of data mining in the medical field. Data mining technology [27] is a decision support process that can analyze data automatically, inductive reasoning, and mine potential patterns. The computer-based data mining technology employs algorithms to extract latent information embedded in a large

amount of medical data and provides valuable guidance for the treatment of diseases. At present, data mining can complete many tasks, mainly including association analysis, cluster analysis, classification, prediction, and so on [28], which makes it applicable to scenarios such as symptom and sign analysis [29], syndrome differentiation [30], and medication rule analysis [31]. To explore the medication rules for AA and provide integrated TCM-based treating suggestions, 859 prescriptions were adopted to obtain the medication rules from high-frequency Chinese medicine, Four Qi and Five Flavors of TCM, and their meridian tropism.

The treatment of AA in ZJHCM is characterized by integrated TCM and Western medicine. We also paid attention to adjusting zang-fu viscera, especially in kidney and spleen, and Qi, blood, and water. It is reported by ZJHCM that compared with treated with IST alone, standard IST for severe aplastic anemia (SAA) could improve hematologic responses, bone marrow hyperplasia, and clinical symptoms. [32]. It is also reported that treatment with the TCM may reduce the rate of graft failure and treatment-related mortality and improve the rate of (overall survival) OS in SAA patients with allo-HSCT [18]. Besides, a study revealed the TCM of Bushen Jianpi Quyu Formula in AA could alleviate myelosuppression by inhibiting the expression of the PI3K/AKT/NF- κ B signaling pathway [33]. It is a strong benefit for patients in various ways by TCM. However, research about current treatment patterns of AA in China reported that among the 352 enrolled patients, 43 patients (12.6% of all) received TCM, and only 3 of them used TCM as the main treatment regimen for AA [34]. Therefore, we analyzed the characteristics of TCM treatment of AA in ZJHCM by data mining.

2. Materials and Methods

Data mining can be composed of three main stages: first, data cleaning is performed on the collected data, which could remove noisy data so that the model can obtain more representative conclusions; next, the processed high-quality dataset could be used to construct a model, which extracts the relationship between the data; and finally, visualization technology can intuitively display the potential information extracted by the model, which is helpful for decision-makers to summarize and analyze.

2.1. Data Source and Processing. This study adopted a total of 1263 cases of AA from ZJHCM from March 1, 2019 to March 1, 2022. Including criteria are as follows: (1) compliance with diagnostic criteria for AA, (2) a complete TCM treatment prescription with at least one revisit. Excluding criteria are as follows: (1) patients with severe liver and kidney dysfunction, (2) TCM for external use, (3) prescriptions with more than 10 visits for the same patient, and (4) patients after HSCT and IST treatment. The screening process results in 859 prescriptions being collected. The herb names were standardized, where Shenghuangqi and Zhihuangqi were unified as Huangqi, as well as Shenggancao and Zhigancao

TABLE 1: Part of case prescriptions.

Date	No. (patient)	Herb name	Date	No. (patient)	Herb name
20190301	0001	Shengdihuang	20190304	0004	Bajitian
20190301	0001	Niuxi	20190304	0004	Cebaiye
20190301	0001	Shihu	20190304	0004	Guya
20190302	0002	Dangshen	20190304	0005	Baishao
20190302	0002	Baizhu	20190304	0005	Buguzhi
20190302	0002	Gancao	20190304	0005	Honghua
20190302	0003	Guizhi	20190304	0006	Shengshaishen
20190302	0003	Fuling	20190304	0006	Fuling
20190302	0003	Zexie	20190304	0006	Ganjiang

TABLE 2: Integrated prescriptions.

No. (prescription)	Herb 1	Herb 2	Herb 3	Herb 4	Herb 5	Herb 6	...
1	Shengdihuang	Niuxi	Shihu	Fangfeng	Dangshen	Danshen	...
2	Dangshen	Baizhu	Gancao	Danggui	Chenpi	Shanyao	...
3	Guizhi	Fuling	Zexie	Danshen	Longgu	Muli	...
4	Bajitian	Cebaiye	Guya	Biejia	Houpo	Taizishen	...
5	Baishao	Buguzhi	Honghua	Dangshen	Jixueteng	Taizishen	...
6	Shengshaishen	Fuling	Ganjiang	Gancao	Heshouwu	Baishao	...
7	Dangshen	Danggui	Honghua	Danshen	Taoren	Shengdihuang	...
8	Dangshen	Baizhu	Shudihuang	Danggui	Chaihu	Shanyao	...
9	Baishao	Shudihuang	Heshouwu	Danggui	Shanzhuyu	-	...

TABLE 3: Sparse matrix form of prescriptions.

No. (prescription)	Danggui	Huangqi	Fuling	Gancao	Shanyao	...
1	1	1	1	1	0	...
2	1	0	1	1	1	...
3	0	0	1	1	0	...
4	0	1	1	0	0	...
5	1	1	0	1	0	...
6	0	0	1	1	0	...
7	0	0	0	1	1	...

were unified as Gancao, and the information of properties, tastes, and meridian tropisms was complemented according to Chinese pharmacopoeia [35].

Some of the collected prescriptions are shown in Table 1, which need to be processed by *Python* to make them conform to the input form of SPSS. Then the prescriptions for a single visit were integrated, which obtained 859 prescriptions, involving 255 kinds of TCMs (Table 2). Finally, an all-zero matrix is created with the column name of the herb name, and its sparse matrix form (Table 3) is obtained by *Python* according to the integrated prescription (Table 2).

2.2. Frequency Analysis. Frequency analysis is a typical analytical method of descriptive statistics, which can be utilized to describe the statistical values of variables. Frequency analysis for TCMs has been widely used to extract prescription rules and to provide the basis for clinical forecasting and decision-making. It is beneficial to better understand the

nature of diseases and the typical methods of prevention or treatment. To analyze the characteristics of AA and to explore the preference of its herbal treatment, frequency analysis was applied to study the frequency of occurrence, properties, tastes, and meridian tropisms of all TCM involved. All frequency analyses were performed in Microsoft Excel 2016. The frequency of herbal medicine is calculated as follows:

$$\text{frequency}(a) = \left(\frac{a}{b}\right) \times 100\%, \quad (1)$$

where a means the usage times of a particular herbal medicine and b denotes the total number of prescriptions.

2.3. Cluster Analysis. As an important part of unsupervised learning, cluster analysis can automatically classify a variety of objects, such as herbs, with the same nature from the data itself when the category of objects is unknown. In the field of research on medication rules, cluster analysis can classify

various medicinal materials into regular groups, so as to reveal the potential combination rules of prescriptions. In order to discover and summarize reasonable herbal combinations for the treatment of AA, cluster analysis of the top 40 herbs was carried out by utilizing IBM SPSS Statistics. The hierarchical cluster method based on Pearson correlation coefficient was chosen as the data mining method to obtain cluster results with the calculated values standardized by Z scores for comparison [30]. Finally, the clustering results are displayed in the form of a dendrogram.

The calculation scheme of the hierarchical cluster method based on the Pearson correlation coefficient is offered as follows:

- (1) Set each sample as one class and calculate the Pearson distance between each two classes
- (2) Find the nearest two classes between each class and merge them into one class to reduce the total number of classes
- (3) Recalculate the similarity between the newly generated class and each old class
- (4) Repeat steps 2 and 3 until all sampling points are divided into 9 categories

The Pearson correlation coefficient is used to calculate the relationship between two variables X and Y as follows:

$$\rho_{X,Y} = \frac{\sum_{i=1}^n x_i y_i - (\sum_{i=1}^n x_i) \times (\sum_{i=1}^n y_i) / n}{\sqrt{(\sum_{i=1}^n x_i^2) - (\sum_{i=1}^n x_i)^2 / n} \times (\sum_{i=1}^n y_i^2) - (\sum_{i=1}^n y_i)^2 / n}} \quad (2)$$

where $X = (x_1, x_2, x_3, \dots, x_n)$ and $Y = (y_1, y_2, y_3, \dots, y_n)$. The correlation coefficient ranges from $[-1, 1]$, where the value 1 represents a perfect correlation, value 0 means no correlation, and value -1 represents negative correlation.

2.4. Association Rule Analysis. Association rule analysis is an unsupervised learning method, which reveals the internal structure of a dataset. It was first proposed to discover the relationship between different commodities in supermarket sales data to make better sales plans. In the study of medication rules, association rule analysis can also be used to explore the co-occurrence rules between herbs. To explore combinatorial rules for the treatment of AA, an SPSS modeler was adopted to perform association rule learning for all herbs in this study. The Apriori algorithm is chosen to obtain candidate item sets [36], where support and confidence are used to select important rules. The Apriori algorithm is chosen to obtain candidate item sets [37], where support and confidence are used to select important rules. Support refers to the probability that an itemset appears in all item sets. A high support value means that this association rule is very significant. Confidence is the ratio of the frequency that the antecedent and consequent items cooccur to the frequency that the antecedent item occurs individually, indicating the accuracy of the rule [38]. The support and confidence of rule is expressed as follows:

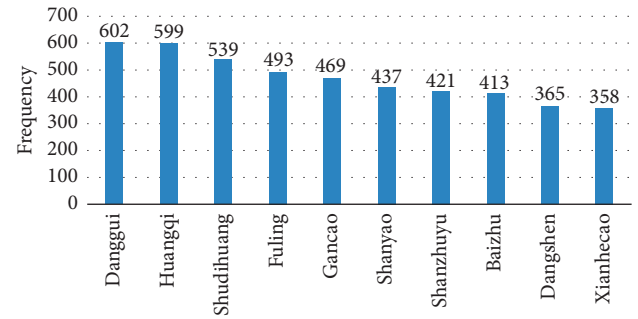


FIGURE 1: Frequency chart of Chinese herbs treating Aplastic anemia (top 10).

$$\text{support}(x \rightarrow y) = \text{support}(X \cup Y) = \frac{\text{count}(X \cup Y)}{\text{count}(D)},$$

$$\text{confidence}(X \cup Y) = \frac{\text{support}(X \cup Y)}{\text{support}(X)},$$

$$\text{lift}(X \rightarrow Y) = \frac{\text{confidence}(X \rightarrow Y)}{\text{support}(Y)}.$$

(3)

X and Y are examples of associations represented by association rules. For example, $X = \text{herb 1}$ and $Y = \text{herb 1}$, and $X \cap Y = \text{herb 1}$ are the set of all items in D . If the percentage of $X \cup Y$ in the dataset D is $a\%$, then the support of the association rule $X \rightarrow Y$ is $a\%$. In fact, the support is a probability value. The lift is the ratio of the probability of item Y appearing in the presence of X to the frequency of Y . Support and confidence are often used to eliminate meaningless combinations, and lift could show the validity of the rules.

To extract more representative rules, the minimum threshold of support was set to 0.20 and the minimum value of confidence was set to 0.8. Besides, the maximum number of antecedent items was set to 2.

3. Results

3.1. Frequency Analysis

3.1.1. Medication Frequency. After data collection and processing, the frequency of herbal medicine use (Figure 1) was calculated, involving a total of 255 herbs in 859 prescriptions. In this study, herbal medicines were ranked from high to low according to the usage frequency, and the cumulative total frequency of herb use was 16129. As shown in Figure 1, the top 10 most commonly used herbs were: Danggui (602 times, 70.08%), Huangqi (599 times, 69.73%), Shudihuang (539 times, 62.75%), Fuling (493 times, 57.39%), Gancao (469 times, 54.60%), Shanyao (437 times, 50.87%), Shanzhuyu (421 times, 49.01%), Baizhu (413 times, 48.08%), Dangshen (365 times, 42.49%), and Xianhecao (358 times, 41.68%).

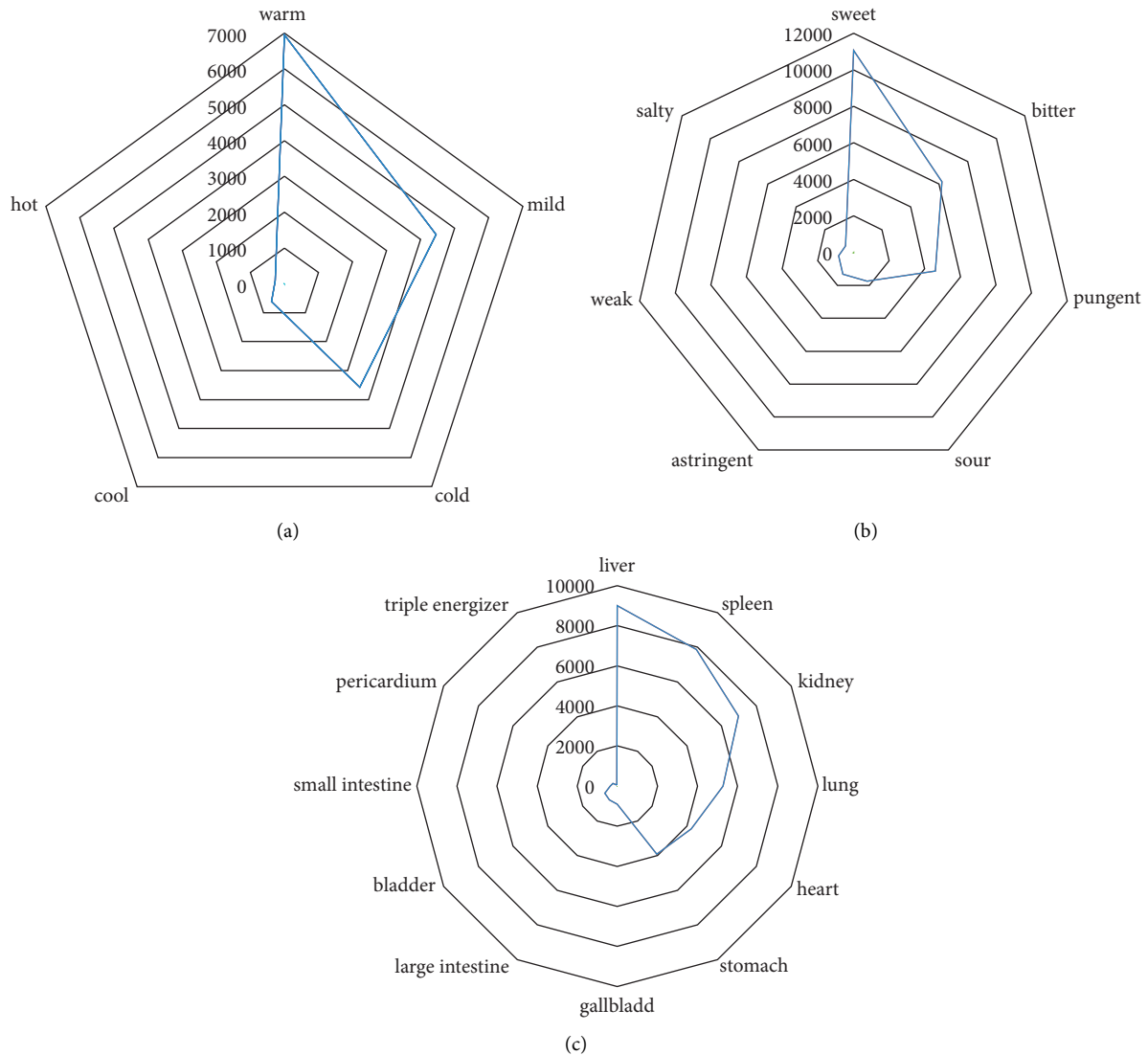


FIGURE 2: Four Qi, Five Flavors, and herb's Meridian Tropisms (a) Four Qi. (b) Five Flavors. (c) Meridian tropism of herbs. Four Qi, Five Flavors, and Meridian tropism of herbs were analyzed by a radar chart in Microsoft Excel.

Most of them belong to tonics, and others have the effect of promoting blood circulation and eliminating dampness.

3.1.2. Properties, Tastes, and Meridian Tropisms of Herbs.

The medicinal properties of TCM are divided into Yin and Yang. The "Four Qi" of TCM are as follows: cold, hot, warm, and cool. Besides, herbs with moderate effects are mild. Five flavors of TCM refer to the taste of herbs, including sour, bitter, sweet, pungent, and salty, which are commonly known as the most basic tastes. In addition, they are weak, astringent, etc. In order to correspond to the theory of the five elements in imperial China, astringency was attached to the sour and weakness attached to the sweet, with which all of them could be called Five Flavors. A medicine meridian denotes the site of drug action. Medicine meridian matches the effect of herbs with the theory of viscera and meridians to illustrate the selectivity of drug action to a certain site of the body.

It can be shown in g (c) that the herb's meridian tropisms are ranked as liver, spleen, kidney, lung, heart, stomach, gallbladder, large intestine, bladder, small intestine, pericardium, and triple energizer in descending order based on the frequency. The frequency of herb's meridian tropisms above 15% are liver, spleen, and kidney.

Figure 2(a) and 2(b) describe the distribution of herbs' Four Qi and Five Flavors. In descending order of frequency, the Four Qi of the herb are arranged as: warm, mild, cold, cool, and hot. The occurrence of warm herbs was 6950 times, and its frequency was up to 43.83%, which was much higher than other medicinal properties. The frequencies of the Five Flavors are ranked as sweet, bitter, pungent, sour, astringent, weak, and salty from high to low, where sweet medicines accounted for 42.05% of the total.

3.2. Cluster Analysis. The cluster analysis results of high-frequency herbs were obtained by SPSS statistics:

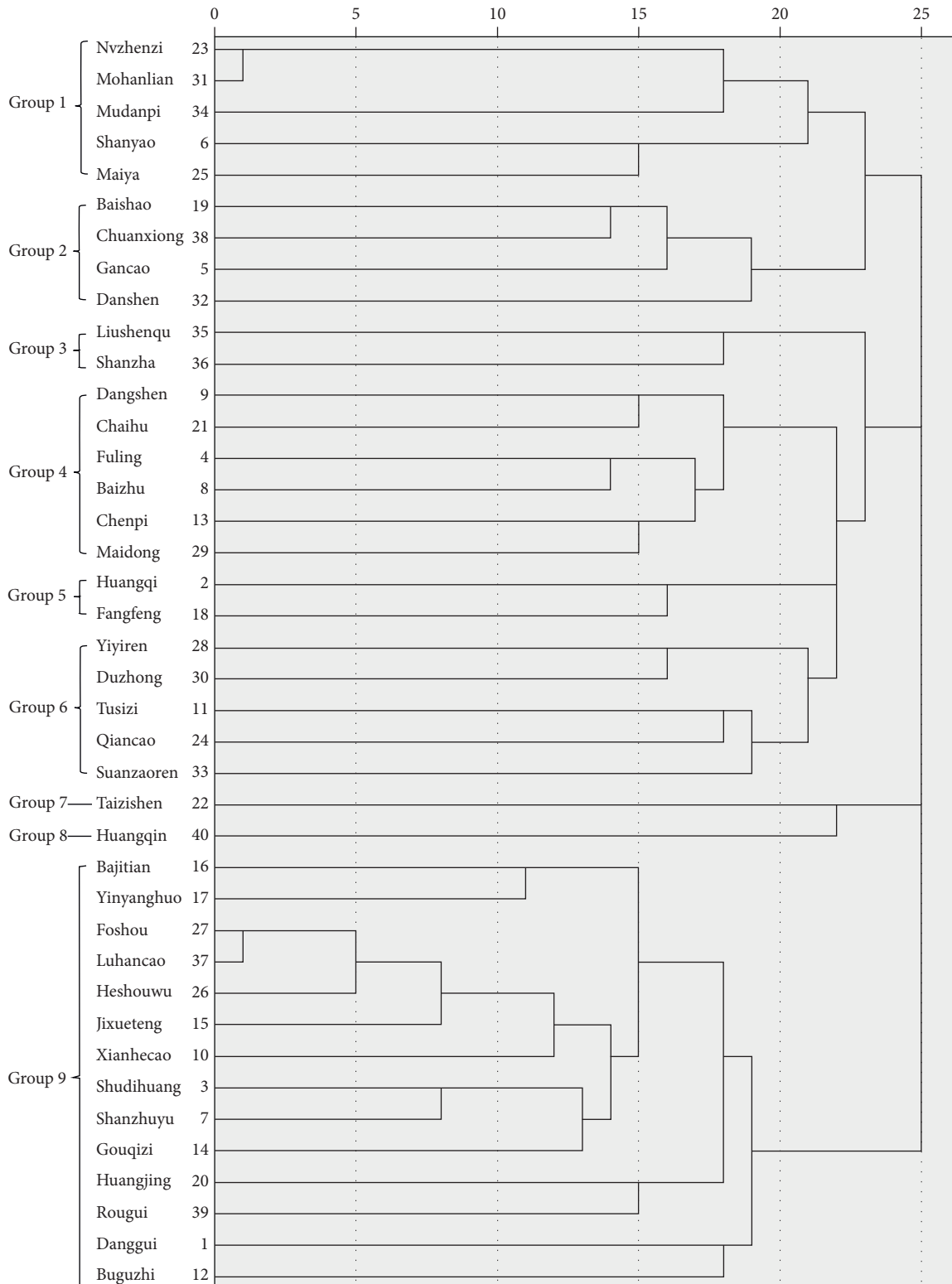


FIGURE 3: Results of cluster analysis.

- (1) Most herbs of Group 1 can be used to invigorate the kidney, cool the blood, and stop bleeding, except Maiya
- (2) In Group 2, Baishao and Chuanxiong belong to Chinese traditional Siwu decoction, and it was

- described by the ancients that the effect of Danshen is equivalent to that of Siwu Decoction
- (3) Herbs of Group 3 have the effect of improving indigestion

TABLE 4: Association rules.

No.	Consequent	Antecedent	Support (%)	Confidence (%)	Lift
1	Danggui	Jixueteng	36.06	80.26	1.172
2	Danggui	Yinyanghuo	33.72	82.70	1.207
3	Huangqi	Fangfeng	32.79	83.99	1.23
4	Danggui	Jixueteng, Huangqi	28.00	80.00	1.168
5	Shudihuang	Xianhecao, Shanzhuyu	27.65	80.17	1.532
6	Danggui	Xianhecao, Shanzhuyu	27.65	80.59	1.177
7	Shanzhuyu	Xianhecao, Shudihuang	26.72	82.97	1.689
8	Danggui	Xianhecao, Shudihuang	26.72	84.72	1.199
9	Fuling	Dangshen, Baizhu	26.02	81.61	1.436
10	Shudihuang	Yinyanghuo, Shanzhuyu	25.90	80.63	1.532
11	Danggui	Yinyanghuo, Shanzhuyu	25.90	86.04	1.256
12	Shanzhuyu	Yinyanghuo, Shudihuang	24.39	85.65	1.195
13	Danggui	Yinyanghuo, Shudihuang	24.39	84.69	1.221
14	Danggui	Jixueteng, Shudihuang	24.04	83.01	1.216
15	Danggui	Buguzhi, Shanzhuyu	23.69	80.79	1.179
16	Danggui	Baishao, Gancao	22.99	80.71	1.178
17	Shudihuang	Heshouwu	22.87	90.82	1.577
18	Danggui	Heshouwu	22.87	83.67	1.222
19	Shudihuang	Jixueteng, Xianhecao	22.64	80.41	1.467
20	Danggui	Jixueteng, Xianhecao	22.64	87.11	1.272

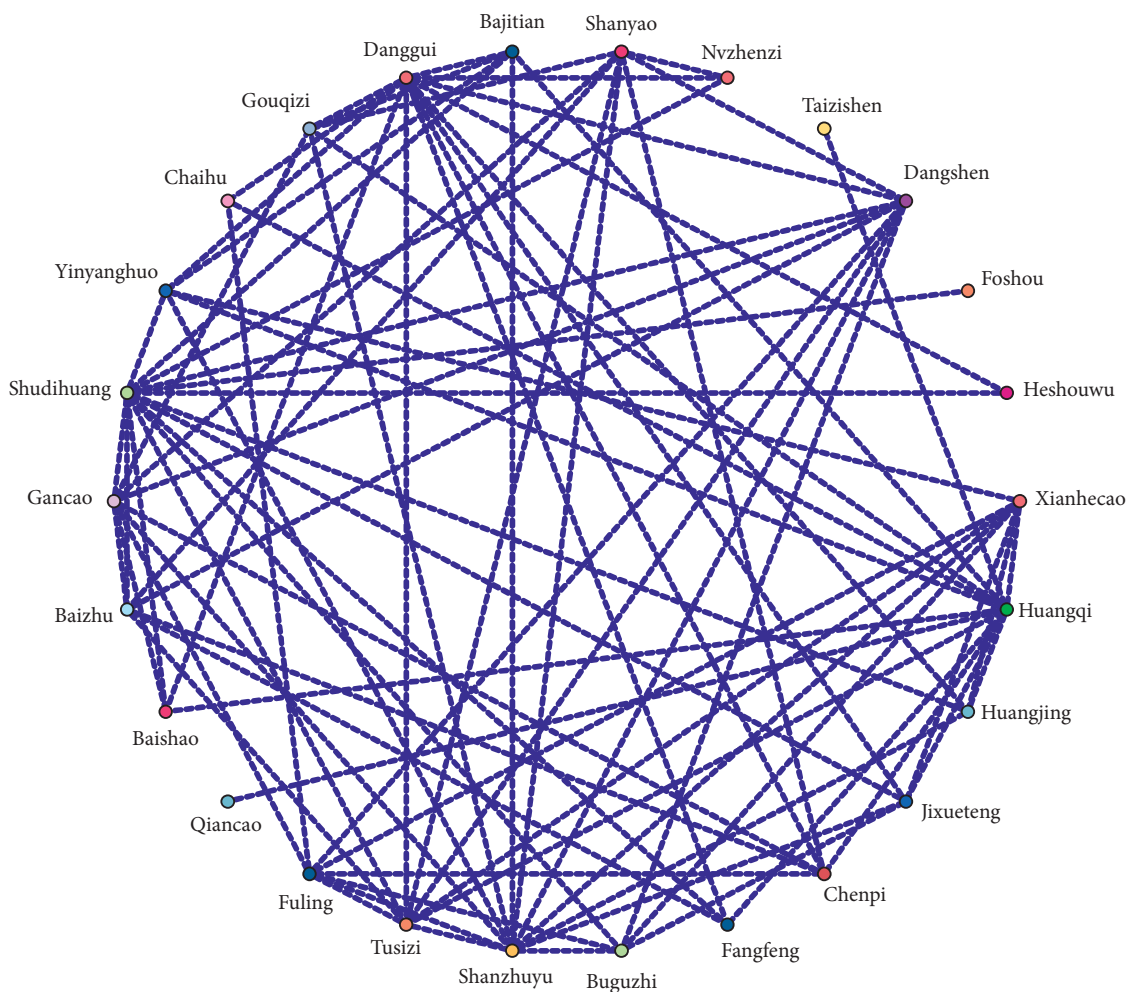


FIGURE 4: Network Diagram of core herbs.

- (4) Herbs of Group 4 can invigorate spleen to nourish original Qi
- (5) The goal of Group 5 is to tonify Qi and consolidate superficialities
- (6) Group 9 is contributing to nourishing kidney essence

The first six categories are meaningful in clinical prescription, and the results are shown in Figure 3.

3.3. Association Rule Analysis. The results of association rule analysis can mine the combination of potential core herbs from commonly used prescriptions. The results showed that there were three herb combinations with support over of 30% (“Danggui-Jixueteng,” “Danggui-Yinyanghuo,” and “Huangqi-Fangfeng”), whose objective is mainly to nourish blood, activate blood, and tonify the kidneys and Qi (Table 4). From the constructed network diagram (Figure 4), it can be seen that Danggui, Huangqi, and Fuling are the core herbs for treating AA, which is consistent with the conclusion of frequency analysis.

4. Conclusion

AA is a bone marrow hematopoietic dysfunction disease called “Suilao” or “Consumptive disease” in TCM. The main clinical symptoms of AA are hypodynamia, hemorrhage, and infection. In our center, we treated AA by integrating traditional Chinese medicine and western medicine, to reduce the clinical symptoms of patients, improve their quality of life, and alleviate their economic burden.

Based on data mining, we studied the regularity of TCM for the treatment of AA in our center. The top three herbs are Danggui (602 times, 70.08%), Huangqi (599 times, 69.73%), and Shudihuang (539 times, 62.75%). In terms of TCM, Danggui can replenish blood and activate blood. Besides, Danggui has an immunomodulatory effect [39]. Huangqi can nourish Qi and promote water metabolism. In clinical practice, Huangqi could enhance the nonspecific immune function of organisms, regulate humoral immunity, and normalize cellular immunity [40]. Shudihuang has the effect of invigorating the kidneys. A study indicates that there is an influence of the “bone marrow system” by the “kidney marrow” in TCM [41]. According to the results, Fuling, Gancao, Shanyao, Shanzhuyu, Baizhu, Dangshen, and Xianhecao follow. It revealed that the basic principle of treatment in AA was to strengthen the liver and kidney, as well as nourish Qi and blood. Moreover, herbs that promote water metabolism are often added to prescriptions, eliminating dampness and promoting hematopoiesis.

Ancient medical books called “Jingyue Quanshu” indicated that the therapy of TCM for patients with blood deficiency and stasis is enriching blood and promoting blood circulation, which is the origin of the method of Bushen Huoxue. According to experience, the Chinese medical pathogenesis of AA is generated by “deficiency”. However, it is found that “stasis” should be added to the pathogenesis. In our previous study [42], we found that the treatment of patients with AA can improve the engraftment of

hematopoietic stem cell transplantation by kidney-reinforcing, blood-activating, and stasis-removing. It has been reported that BUSHEN HUOXUE decoction could reduce the expression of IL-6 [18], which might affect the stability of the hematopoietic microenvironment in bone marrow [43]. In addition, about 61% of patients with AA were complicated by syndromes of “blood stasis” [19]. In this study, the “Danggui-Jixueteng” combo showed the highest statistical support in association rule analysis, which may indicate that dispelling blood stasis is as important as tonifying the kidneys in treating AA. Nonetheless, eliminating the dampness had possessed similar pharmacologic or pharmacodynamic action of removing blood stasis [44]. Fuling and Huangqi can eliminate the dampness, which appears in high-frequency drugs or association analysis pairs. Based on the prescription management platform of ZJHCM, using SPSS statistics and SPSS modeling, this study adopts a variety of data mining methods, such as cluster analysis and association rule analysis, to explore and analyze the medical record. This study has summarized the Chinese medication rules for treating AA, which can facilitate TCM diagnosis, treatment, and experimental research and would be helpful for AA patients. The results of the above data mining process show that the basic principle of AA’s therapeutic methods is strengthening kidney and liver, nourishing spleen Qi, and supplemented by the treatments of activating blood, and eliminating dampness. The focus of treatment is to improve the bone marrow microenvironment by tonifying the kidneys and promoting blood circulation. By analyzing Four Qi and Five Flavors of the sample herbs, we found out that sweet and warm are the top 2 most frequent properties, which could nourish Qi. However, heat-clearing herbs are also used when necessary. We focus on nourishing the liver, spleen, and kidney. The combination of Chinese and Western medicine in the treatment of AA alleviates the pain of patients. The conditions of patients change constantly, and we are continuing to explore and study.

Conflicts of Interest

The authors declare that they have no conflicts of interest.

Acknowledgments

This work was supported by the National Natural Science Foundation of China (nos. 82174138 and 81774092), Zhejiang Scientific Research Fund of Traditional Chinese Medicine (nos. 2020ZB085 and 2022ZA059), and Health Technology Plan of Zhejiang Province (no. 2022RC216).

References

- [1] N. S. Young and N. S. Young, “Aplastic anemia,” *New England Journal of Medicine*, vol. 379, no. 17, pp. 1643–1656, 2018.
- [2] P. Scheinberg, “Novel therapeutic choices in immune aplastic anemia,” *F1000Research*, vol. 9, p. 1118, 2020.
- [3] P. Scheinberg, “Acquired severe aplastic anaemia: how medical therapy evolved in the 20th and 21st centuries,” *British Journal of Haematology*, vol. 194, no. 6, pp. 954–969, 2021.

- [4] N. Yoshida, R. Kobayashi, H. Yabe et al., "First-line treatment for severe aplastic anemia in children: bone marrow transplantation from a matched family donor versus immunosuppressive therapy," *Haematologica*, vol. 99, no. 12, pp. 1784–1791, 2014.
- [5] N. S. Young, "Current concepts in the pathophysiology and treatment of aplastic anemia," *Hematology*, vol. 2013, no. 1, pp. 76–81, 2013.
- [6] Y. Zhu, Q. Gao, J. Hu, X. Liu, D. Guan, and F. Zhang, "Allo-HSCT compared with immunosuppressive therapy for acquired aplastic anemia: a system review and meta-analysis," *BMC Immunology*, vol. 21, no. 1, p. 10, 2020.
- [7] A. Bacigalupo, "Aplastic anemia: pathogenesis and treatment," *Hematology*, vol. 2007, no. 1, pp. 23–28, 2007.
- [8] Y. Zhu, Q. Gao, J. Hu, X. Liu, D. Guan, and F. Zhang, "Allo-HSCT compared with immunosuppressive therapy for acquired aplastic anemia: a system review and meta-analysis," *BMC Immunology*, vol. 21, no. 1, pp. 10–11, 2020.
- [9] R. Devillier, D. J. Eikema, P. Bosman et al., "Gvhd and relapse free survival (GRFS) after allogeneic transplantation for idiopathic severe aplastic anemia: an analysis from the saawp data quality initiative program of EBMT," *Blood*, vol. 136, no. Supplement 1, pp. 3–4, 2020.
- [10] Z. L. Xu and X. J. Huang, "Haploidentical stem cell transplantation for aplastic anemia: the current advances and future challenges," *Bone Marrow Transplantation*, vol. 56, no. 4, pp. 779–785, 2021.
- [11] K. Takenaka, Y. Onishi, T. Mori et al., "Negative impact of cytomegalovirus reactivation on survival in adult patients with aplastic anemia after an allogeneic hematopoietic stem cell transplantation: a report from transplantation-related complication and adult aplastic anemia working groups of the Japan Society for Hematopoietic Cell Transplantation," *Transplantation and Cellular Therapy*, vol. 27, no. 1, pp. 82.e1–82.e8, 2021.
- [12] A. Prabahran, R. Koldej, L. Chee, and D. Ritchie, "Clinical features, pathophysiology, and therapy of poor graft function post-allogeneic stem cell transplantation," *Blood Advances*, vol. 6, no. 6, pp. 1947–1959, 2022.
- [13] A. Tichelli, H. Schrezenmeier, G. Socié et al., "A randomized controlled study in patients with newly diagnosed severe aplastic anemia receiving antithymocyte globulin (ATG), cyclosporine, with or without G-CSF: a study of the SAA Working Party of the European Group for Blood and Marrow Transplantation," *Blood*, vol. 117, no. 17, pp. 4434–4441, 2011.
- [14] A. Bacigalupo, "Antithymocyte globulin and cyclosporin: standard of care also for older patients with aplastic anemia," *Haematologica*, vol. 104, no. 2, pp. 215–216, 2019.
- [15] S. B. Killick, N. Bown, J. Cavenagh et al., "& British Society for Standards in Haematology Guidelines for the diagnosis and management of adult aplastic anaemia," *British Journal of Haematology*, vol. 172, no. 2, pp. 187–207, 2016.
- [16] F. T. Shah, F. Sayani, S. Trompeter, E. Drasar, and A. Piga, "Challenges of blood transfusions in β -thalassemia," *Blood Reviews*, vol. 37, Article ID 100588, 2019.
- [17] A. Remacha, C. Sanz, E. Contreras et al., "Spanish society of blood transfusion, & Spanish society of haematology and haemotherapy Guidelines on haemovigilance of post-transfusional iron overload," *Blood transfusion = Trasfusione del sangue*, vol. 11, no. 1, pp. 128–139, 2013.
- [18] B. d Ye, X. Zhang, K. d Shao et al., "Combined use of Chinese medicine with allogeneic hematopoietic stem cell transplantation for severe aplastic anemia patients," *Chinese Journal of Integrative Medicine*, vol. 20, no. 12, pp. 903–909, 2014.
- [19] H. Hu, T. Chen, W. Liu et al., "Differentiation of yin, yang and stasis syndromes in severe aplastic anemia patients undergoing allogeneic hematopoietic stem cell transplantation and their correlation with iron metabolism, cAMP/cGMP, 17-OH-CS and thyroxine," *Journal of Blood Medicine*, vol. 12, pp. 975–989, 2021.
- [20] X. L. Wei, X. B. Dai, and Y. M. Zhou, "Retrospect and reflection on syndrome differentiation and treatment of aplastic anemia in TCM," *Shanghai Journal of Traditional Chinese Medicine*, vol. 46, no. 3, pp. 4–6, 2012.
- [21] N. Zhu, D. Wu, and B. Ye, "The progress of traditional Chinese medicine in the treatment of aplastic anemia," *Journal of Translational Internal Medicine*, vol. 6, no. 4, pp. 159–164, 2018.
- [22] M. H. Luo, L. M. Xia, L. L. Cui, Y. L. Jiang, and Z. Qin, "Meta-analysis of clinical efficacy of traditional Chinese medicine in the treatment of aplastic anemia," *World Journal of Traditional Chinese Medicine*, vol. 3, no. 4, p. 46, 2017.
- [23] W. Dijiong, S. Yiping, Y. Baodong et al., "Efficacy and advantages of modified Traditional Chinese Medicine treatments based on "kidney reinforcing" for chronic aplastic anemia: a randomized controlled clinical trial," *Journal of Traditional Chinese Medicine*, vol. 36, no. 4, pp. 434–443, 2016.
- [24] China Association of Chinese Medicine, *Guidelines for the Diagnosis and Treatment of Common Diseases in Chinese Medicine*, China Press of Traditional Chinese Medicine, Beijing, China, 2008.
- [25] Z. Feng, X. Hu, W. Qu et al., *Metabolomics-Based Clinical Efficacy of Compound Shenlu Granule, a Chinese Patent Medicine, in the Supportive Management of Aplastic Anemia Patients: A Randomized Controlled Pilot Trial*, Evidence-Based Complementary and Alternative Medicine, 2021.
- [26] D. He, W. Dan, Q. Du et al., "Integrated network pharmacology and metabolomics analysis to reveal the potential mechanism of Siwu Paste on aplastic anemia induced by chemotherapy drugs," *Drug Design, Development and Therapy*, vol. 16, pp. 1231–1254, 2022.
- [27] J. Yang, Y. Li, Q. Liu et al., "Brief introduction of medical database and data mining technology in big data era," *Journal of Evidence-Based Medicine*, vol. 13, no. 1, pp. 57–69, 2020.
- [28] M. K. Gupta and P. Chandra, "A comprehensive survey of data mining," *International Journal of Information Technology*, vol. 12, no. 4, pp. 1243–1257, 2020.
- [29] R. Kanawong, T. Obafemi-Ajayi, T. Ma, D. Xu, S. Li, and Y. Duan, "Automated tongue feature extraction for ZHENG classification in traditional Chinese medicine," *Evidence-based Complementary and Alternative Medicine*, vol. 2012, pp. 1–14, 2012.
- [30] N. L. Zhang, C. Fu, T. F. Liu et al., "A data-driven method for syndrome type identification and classification in traditional Chinese medicine," *Journal of integrative medicine*, vol. 15, no. 2, pp. 110–123, 2017.
- [31] J. Xuan, G. Deng, R. Liu, X. Chen, and Y. Zheng, "Analysis of medication data of women with uterine fibroids based on data mining technology," *Journal of infection and public health*, vol. 13, no. 10, pp. 1513–1516, 2020.
- [32] F. Y. Nie, T. Y. Dai, F. X. Li, C. Y. Zhang, and Z. P. Hu, "Clinical observation on the treatment of severe aplastic anemia with "cool-warm-hot" sequential therapy," *Zhejiang Journal of Integrated Traditional Chinese and Western Medicine*, vol. 30, no. 2, pp. 133–136, 2020.

- [33] H. Li, L. Ji, Y. Shen, D. Fu, D. Wu, and B. Ye, "Bushen Jianpi Quyu Formula alleviates myelosuppression of an immune-mediated aplastic anemia mouse model via inhibiting expression of the PI3K/AKT/NF- κ B signaling pathway," *Evidence-based Complementary and Alternative Medicine*, vol. 2022, pp. 1–10, 2022.
- [34] X. F. Zhu, H. L. He, S. Q. Wang et al., "Current treatment patterns of aplastic anemia in China: a prospective cohort registry study," *Acta Haematologica*, vol. 142, no. 3, pp. 162–170, 2019.
- [35] Chinese Pharmacopoeia Commission, *Chinese pharmacopoeia*, China Medical Science Press, Beijing, China, 2015.
- [36] V. M. Youroukova, D. G. Dimitrova, A. D. Valerieva et al., "Phenotypes determined by cluster analysis in moderate to severe bronchial asthma," *Folia Medica*, vol. 59, no. 2, pp. 165–173, 2017.
- [37] R. Agrawal, T. Imieliński, and A. Swami, "Mining association rules between sets of items in large databases," in *Proceedings of the 1993 ACM SIGMOD International Conference on Management of Data*, pp. 207–216, 1993.
- [38] N. Jayawickreme, E. Atefi, E. Jayawickreme, J. Qin, and A. H. Gandomi, "Association rule learning is an easy and efficient method for identifying profiles of traumas and stressors that predict psychopathology in disaster survivors: the example of Sri Lanka," *International Journal of Environmental Research and Public Health*, vol. 17, no. 8, p. 2850, 2020.
- [39] W. W. Chao and B. F. Lin, "Bioactivities of major constituents isolated from *Angelica sinensis* (Danggui)," *Chinese Medicine*, vol. 6, no. 1, 37 pages, 2011.
- [40] M. S. Wang, J. Li, H. X. Di et al., "Clinical study on effect of Astragalus Injection (黄芪注射液) and its immuno-regulation action in treating chronic aplastic anemia," *Chinese Journal of Integrative Medicine*, vol. 13, no. 2, pp. 98–102, 2007.
- [41] Y. Hijikata, T. Kano, and L. Xi, "Treatment for intractable anemia with the traditional Chinese medicines Hominis Placenta and Cervi Cornus Colla (deer antler glue)," *International Journal of General Medicine*, vol. 2, pp. 83–90, 2009.
- [42] Z. Sun, W. Su, L. Wang, Z. Cheng, and F. Yang, "Clinical effect of bushen huoxue method combined with platelet-rich plasma in the treatment of knee osteoarthritis and its effect on IL-1, IL-6, VEGF, and PGE-2," *Journal of Healthcare Engineering*, vol. 2022, pp. 1–8, 2022.
- [43] Y. F. Chen, Z. M. Wu, C. Xie, S. Bai, and L. D. Zhao, *Expression Level of IL-6 Secreted by Bone Marrow Stromal Cells in Mice with Aplastic Anemia*, International Scholarly Research Notices, New York, NY, USA, 2013.
- [44] J. Qin, M. H. Jin, J. H. Deng, H. Zhao, Z. Xu, and Z. Luo, "Clinical study of eliminating dampness and removing blood stasis in treating coronary heart disease-the summary about serial study of blood stasis due to dampness," *Chinese Journal of Integrated Traditional and Western Medicine*, vol. 17, no. 9, 1997.

Research Article

An Initial Study on Automated Acupoint Positioning for Laser Acupuncture

Kun-Chan Lan,¹ Chang-Yin Lee,^{2,3} Guan-Sheng Lee,¹ Tzu-Hao Tsai,¹ Yu-Chen Lee^{4,5} and Chih-Yu Wang⁶

¹Department of CSIE, National Cheng Kung University, Tainan 701, Taiwan

²The School of Chinese Medicine for Post-Baccalaureate, I-Shou University, Kaohsiung 824, Taiwan

³Department of Chinese Medicine, E-DA Hospital, Kaohsiung 824, Taiwan

⁴Graduate Institute of Acupuncture Science, China Medical University, Taichung 404, Taiwan

⁵Department of Acupuncture, China Medical University Hospital, Taichung 404, Taiwan

⁶Department of Biomedical Engineering, I-Shou University, Kaohsiung 824, Taiwan

Correspondence should be addressed to Chih-Yu Wang; crab@isu.edu.tw

Received 17 April 2022; Revised 24 June 2022; Accepted 26 July 2022; Published 22 August 2022

Academic Editor: Lei Jiang

Copyright © 2022 Kun-Chan Lan et al. This is an open access article distributed under the Creative Commons Attribution License, which permits unrestricted use, distribution, and reproduction in any medium, provided the original work is properly cited.

Acupuncture plays an important role in traditional Chinese medicine (TCM) and is one kind of an inexpensive and effective treatment. However, some people might be reluctant to receive acupuncture treatment due to fear of pain. Laser acupuncture, thanks to its painless and infection-free advantages, has recently become an alternative choice to traditional acupuncture. The accuracy of acupuncture point positioning has a decisive influence on the quality of laser acupuncture. In this study, built on top of our prior work, we proposed a low-cost automated acupoint positioning system for laser acupuncture. By integrating several machine learning algorithms and computer vision techniques, we design and implement a robot-assisted laser acupuncture system on top of a smartphone. Our contributions include the following: (a) development of an effective acupoint estimation algorithm with a localization error less than 5 mm; (b) implementation of a smartphone-controlled automated laser acupuncture system with lift-thrust function, as a point-of-care device, that can be used by patients to relieve their symptoms at home.

1. Introduction

Traditional Chinese medicine (TCM) is one kind of medicine based on more than 2000 years' clinical practice covering both diagnosis and treatment of diseases. In TCM, acupuncture plays a very important role and has unique advantages and significant clinical values. Its efficacy has been confirmed by many studies [1, 2]. Recently, thanks to its painless and noninvasive nature, laser acupuncture has become an alternative to traditional acupuncture and many studies have shown its effectiveness [3–6].

In our previous work, a novel laser acupuncture instruments with the lift-thrust function have been developed [7, 8]. Specifically, the lift-thrust function of laser acupuncture is implemented by moving the focused laser spot back and forth. The energy of the laser is concentrated at the

focused light spot, which is considered as the tip of an acupuncture needle. When the laser light enters the human body, the position of the focused light spot is mobile, as if the needle tip is moving through the acupuncture point, thereby realizing the lift-thrust function of the laser acupuncture.

We demonstrated that the laser acupuncture with the lift-thrust function performs better than the traditional laser acupuncture in our prior work [9]. In particular, the laser power used in our system is relatively lower compared with that in most of the commercially available laser acupuncture instruments. Lower power allows for a longer stimulating time, which is consistent with the practice of “needle retention” in traditional acupuncture. On the other hand, a longer stimulating time suggests that acupuncture practitioners have to hold the laser acupuncture instrument (which is much heavier than a steel needle) for a longer time,

which might not be convenient for clinical practice. Considering the physical labor paid by the acupuncturist, it is natural to restore to a robot to improve the efficacy of therapy. Motivated by this need, we propose a robot-assisted laser acupuncture system which consists of three parts: a smartphone-based chatbot, an acupuncture point database, and an acupoint positioning system. The chatbot app is implemented based on the popular BERT model [10]. For the acupoint database, we reuse a database we built in our previous study [11]. In this paper we focus on describing automated acupoints positioning which is the core of our proposed system.

To the best of our knowledge, this is the first prototype system that has been developed for smartphone-controlled automated laser acupuncture. The remainder of this paper is organized as follows: Section 2 discusses the related work. We describe our methods in Section 3. Section 4 discusses our experiments and results. Some observations are presented in Section 5. Finally, we conclude this paper in Section 6.

2. Related Work

Traditionally, TCM doctors rely on some methods such as bone measurements, body surface marker, and cun measurements to locate various acupoints [12]. However, it is difficult to remember the locations and corresponding therapeutic effects of all the acupoints (more than 400) without extensive training. On the other hand, acupoints are generally situated along meridians which are high-conductivity channels on the skin [13]. The Ryodoten, or electropermeable points (EPP), are a series of points with higher electrical conductivity than other areas of the skin [14]. These points are found to be close to the acupoints on meridians recognized in Chinese medicine. Inspired by this observation, many acupoint localization instruments were built based on the electrical characteristics of acupoints (i.e., looking for areas with a lower skin impedance to estimate the location of acupoints). However, such a contact-based acupoint searching method has some disadvantages such as a longer search time, inconvenient operation, and the inability to locate all the acupoints at the same time. In contrast to the method, based on skin conductivity, an image-based acupoint positioning method has the advantages of real-time localization, user-friendliness, and simultaneous positioning.

As far as we know, the image-based acupoint positioning system is currently still an underexplored area of research. Lin [15] used the landmark points on the back contour to localize the spine points based on the concept of barycentric coordinates. Given that the locations of acupoints on the back are relative to the positions of spine points, back acupoints can be localized once the positions of spine points are correctly identified. Jiang et al. proposed acu glass [12] for acupoint localization and visualization. They created a reference acupoint model for the frontal face, and the acupoint coordinates are expressed as a ratio to the face bounding box (computed by the face detector). The reference acupoints are rendered on top of the input face based

on the height and the width of the subject's face and the distance between the eyes, relative to the reference model. They used ORB feature descriptors to match feature points from the current frame and the reference frame, to get the estimated transformation matrix. Instead of scaling the reference acupoints such as the study in [12], Chang and Zhu [16] implemented a localization system based on cun measurement. Cun is a traditional Chinese unit of length (its traditional measure is the width of a person's thumb at the knuckle, whereas the width of two forefingers denotes 1.5 cun and the width of four fingers side-by-side is three cuns). They used the relative distance between landmarks to convert pixel into cun. The acupoint can be located based on its relative distance (in cun) from some landmark point. There are some issues with the abovementioned approaches for acupoint localization, such as that the differences of the body shape between different people are not considered. Recently, Chen et al. designed and implemented a system to localize facial acupoints on a smartphone by utilizing the 3D morphable model (3DMM) and achieved a localization error of 2.4 mm [17]. In this work, we adopt a similar approach as [17] for the acupoint point positioning in the image space.

Acupuncture is gaining increasing interests with the emergence of integrative medicine. Traditionally, acupuncture is performed by a licensed acupuncturist. It is natural to resort to a robot for such a labor-intensive job for its precision and endurance. In a robot-assisted acupuncture system, the camera and the robot arm are the main components. In such a system, one first determines the positions of acupoints in the image space, and then moves the robot arm to the position where the camera sees to perform the acupuncture. Therefore, it is important to know the relationship between the image space and the robot arm space. In literature, the problem of determining this relationship is referred to as the hand-eye calibration problem which is to solve a matrix equation of the form $Y = XM$ [18]. In our case, Y is the coordinate of the robot end-effector (in the robot arm space), X is the coordinate of an acupoint (in the image space), and M is the unknown transformation between the robot arm space and the image space. In robotics, this is a well-known problem and many approaches have been proposed [19, 20]. In practice, there are two different ways for hand-eye calibration depending on where the camera is placed: hand-in-eye and hand-to-eye calibrations. Hand-in-eye refers to the calibration where the camera is mounted on the robot arm and therefore the camera will move as the robot arm moves. Potentially, the viewing space of the camera will be limited by the operating range of the robot arm. On the other hand, hand-to-eye refers to the calibration where the camera is statically placed at a position independent of the movements of the robot arm. This generally will provide a macroscopic way of the environment. In this work, we design our system with the hand-to-eye method since that allows a viewing space of the camera which can cover the whole acupuncture area. In addition, we adopt the perspective transformation [21] to solve the hand-eye calibration problem.

Lifting and thrusting is an important manipulation method in traditional acupuncture. After piercing the skin to a certain depth, practitioners repeatedly move the tip of the

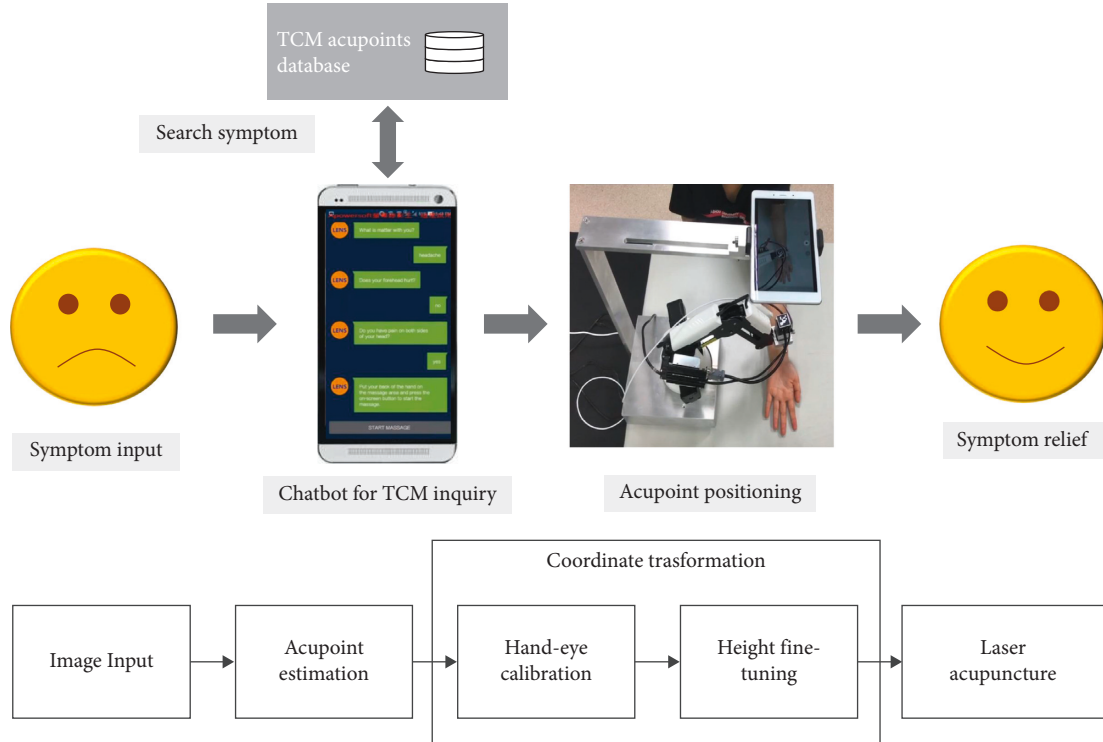


FIGURE 1: The architecture of the proposed system.

needle vertically at a specific frequency to stimulate the skin, fascia, fat, muscles, and other tissues [22]. With lift and thrust operation, specific effects such as reinforcement and reduction might be achieved during the acupuncture process. In our previous work, laser acupuncture instruments with the lift-thrust function have been developed [7, 8]. Furthermore, we also showed that laser acupuncture with lift-thrust operation enabled a more rapid, stable, and lasting temperature rise of the fingertip than that without the lift-thrust operation [9]. In those studies, the lift-thrust function of laser acupuncture is implemented by moving a focused laser spot back and forth with an electrical micro-activator and mobile lens. In the current study, we would like to emulate the lift and thrust operation by the moving robot arm (up and down) with a fixed focal length laser.

3. Methods

Our automated acupoint positioning system includes two parts: (A) image-based acupoints localization; (B) hand-eye calibration which consist of two processes: transformation matrix calculation and coordinate transformation. The purpose of transformation matrix calculation is to find the relationship between the camera space and the robot arm space. This process only needs to be performed once when initially setting up the system. As shown in Figure 1, the camera first reads an image as the input and passes it to the acupoint estimation process to get coordinates of the acupuncture points in the image space. Second, the obtained image coordinate is passed to the coordinate transformation process to get coordinates of the acupoints in the robot arm

space. Finally, the computed robot arm coordinate of the acupoint is used to position the robot arm to perform automated laser acupuncture.

3.1. Image-Based Acupoint Localization. In our previous work, we have established an image-based acupoint localization method for locating face acupoints with a smartphone camera [23]. In this work, we adopt a similar approach with some modification, as shown in Figure 2 (localization of hand acupoints is used here as an illustration for explaining our method). Specifically, to improve the speed and accuracy of the image recognition process, we replace the homography transformation (HOG) method [21] used in our prior work [23] with the convolutional neural network (CNN) technique [24], based on MobileNet [25], to detect the region of interest (ROI) area (i.e., the area that contains the acupoints). Furthermore, we implemented the constrained local Method (CLM) [26] for the landmark detection. The CLM methods, estimating landmark locations x based on the global shape patterns of objects as well as the independent local appearance information around each landmark, are comparatively faster than the regression tree method [27] used for landmark detection in our prior work [23]. As shown in Figure 3, our acupoint estimation procedure consist of two parts: an offline process and an online process, which are discussed next.

3.1.1. Offline Process. In the offline process, we first manually collect the 2D hand image data from different sides (front and back) of the hand using the smartphone camera.

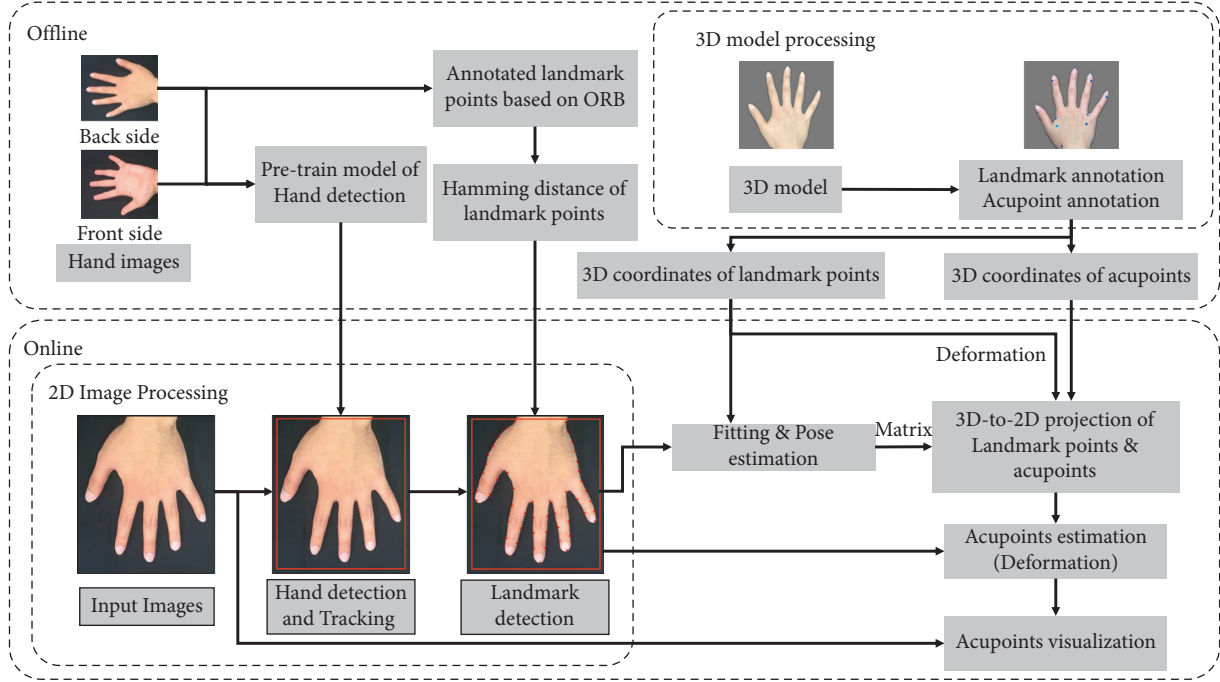


FIGURE 2: Flow chart of acupoints estimation.

These data will be used to train a MobileNet model as well as create a hand landmark model for the hand detection and landmark detection tasks in the online process later. In addition, we employ the 3D scanner to create a 3D hand model and annotate the landmark points and acupoints on this model to facilitate the pose estimation and acupoint estimation tasks in the online process. Conceptually, the aim of this offline process is to use the collected 2D/3D image data (from a number of subjects) to create a “virtual” acupuncture dummy model (in this case, for the hand) as a reference model, on which the acupoints are annotated. Therefore, in the online process we can match the input image (from the user) with this reference model to estimate the acupoints in the input image. This idea of matching the input image to the reference model is theoretically similar to the learning process of how a person finds the locations of acupoints on his/her body through an acupuncture dummy.

3.1.2. Online Process. The hardware components of our system consist of a smartphone and a robot arm. The smartphone is mounted above the robot arm as shown in Figure 1. The smartphone is used to localize the acupoint and direct the movement of the robot arm to the desired location for the laser stimulation.

In the online process, the hand in the input image is first detected by the pretrained MobileNet model from the offline process. The hand detection process will output a region in which the hand is located. The landmarks on the hand are then identified through a CLM method [26] based on ORB [28] and RANSAC [29]. The hand pose can then be estimated by matching the detected landmarks on the 2D input image and the annotated landmarks on the 3D model.

Once the hand pose is determined, the 3D model can be aligned with the 2D input image and projected to the 2D space. Finally, the acupoint estimation problem can be treated as an image deformation process [23]. In the process the detected landmarks (in the 2D input image) and the annotated landmarks (on the 3D model, and now projected to the 2D space) are used as the control points to estimate the acupoints in the input image by deforming the annotated acupoints on the 3D model (which are now projected to the 2D).

3.2. Hand-Eye Calibration. Once the coordinates of the acupoints are estimated, the next step is to move the robot arm (carrying the laser acupuncture device) to the located acupoint position. This involves converting a 2D coordinate in the image space to its corresponding 3D position in the robot-arm space, the so-called hand-eye calibration. In this work, we first move the robot arm to the position that corresponds to the calculated image coordinate on the x - y plane. Then, we move down (along the z -axis) the robot arm to reach the acupoint using a height sensor. Therefore, the transformation from an image coordinate to a robot-arm coordinate can be performed in 2D. Here the perspective transformation [21] is used in our system to transform coordinates between two 2D planes, which can be expressed by the following formulas:

$$\begin{aligned} X &= \frac{ax + by + c}{gx + hy + 1}, \\ Y &= \frac{dx + ey + f}{gx + hy + 1}. \end{aligned} \quad (1)$$

In the equation, (x, y) is the source coordinate (the image coordinate in our case) and (X, Y) is the target coordinate (i.e., the robot-arm coordinate). The eight parameters $(a-h)$ can be

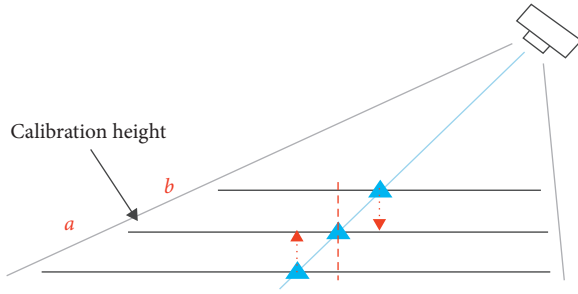


FIGURE 3: Errors caused by different heights.

estimated to control in-plane-rotation, out-plane-rotation, scaling, shearing, and translation between source and target coordinates. To balance the computation time and accuracy.

In this work we randomly selected 13 reference points (which were taken at a specific height) to solve the perspective transformation equation based on the least square method [30]. Here, we can model these estimated parameters (i.e., $a \sim h$) as a perspective matrix T so that $(X, Y) = T * (x, y)$.

Note that given that the reference points were selected from the x - y plane at a specific height (which is referred to as the “calibration height”) and the target acupoint could locate at a different height (i.e., higher or lower than the calibration height, as illustrated in Figure 3), errors will occur if we do not consider this height difference. We resolve this issue by performing another perspective transformation to convert the image coordinate obtained at height b to the image coordinate at height a , as shown in the equation (2), which is referred to as the “height fine-tuning process” in this paper. Here P_a'' is the image coordinate at height a , P_b'' is the image coordinate at height b , and F is the perspective matrix. To compute F , we collect another set of reference points from the x - y plane 1 cm higher than the calibration height to solve the linear equations. Finally, by combining the two perspective transformations described previously, we can now obtain an equation as shown in equation (3) to transform the estimated image coordinate of the acupoint to a robot-arm coordinate for positioning the laser acupuncture. Here p_i'' is the estimated image coordinate of the acupoint, p_i' is the robot-arm coordinate, and k is the height difference between the acupoint and the calibration height, which can be estimated by the height sensor.

3.3. Evaluation of the Proposed System. Several sources of errors could affect the performance of our proposed system in positioning the laser acupuncture. The contributing factors to the robot-arm positioning accuracy include the accuracy of estimating the acupoint coordinate (in the image space), the transformation from the image coordinate to the robot-arm coordinate, the height fine-tuning process, and the possible mechanical error of the robot arm.

3.3.1. Evaluation of the Accuracy of Acupoint Localization in the Image Space. In our experiment, 18 acupoint on the right hand were selected for evaluating the accuracy of acupoint estimation. The acupoints are listed as follows:

Back of the hand: LU-11, LI-1, LI-2, LI-3, LI-4, SJ-1, SJ-2, SJ-3, SI-1, SI-2, SI-3, SI-4, and HT-9

Palm: LU-10, PC-8, PC-9, HT-8, and HT-7

Ten young adults with ages ranging from 20 to 30 years are recruited and their data is used to train the AI models, as shown in Figure 3. The 18 selected acupoints are first marked with 5 mm diameter stickers served as the ground truth. Given that there is no consensus about the shape and the size of acupoint in the literature [31] (for example, a study examined the size of 23 acupoints and reported significant variability from 2.7 to 41.4 cm [32]), here, we follow the suggestion of some prior work [33–35] and conservatively choose the size of 5 mm which is smaller than most of the reported sizes from the literature. The smartphone is placed above the hand 30 cm from the hand. The estimation error is defined as the distance between the estimated position and the center of the sticker. This experiment was approved by the Institutional Review Board (IRB) of E-DA Hospital, Kaohsiung, Taiwan (IRB number. EMRP-105-005 (RIV)).

3.3.2. Evaluation of the Accuracy of Hand-Eye Calibration. To evaluate the errors introduced by the transformation from the image coordinate to the robot-arm coordinate, we placed a plate on a desk, randomly selected 9 points on this plate, and marked their positions with stickers. We then identified the image coordinates of these selected points, and they are as follows: (240,160), (320,160), (400,160), (240,240), (320,240), (400,240), (240,320), (320,320), and (400,320). Next, the image coordinate of the selected point was transformed into the robot arm coordinate using equation (1). The robot arm then moved to the computed coordinate. Finally, we calculate the distance between the tip of the robot arm and the sticker, and this distance is defined as the hand-eye calibration error.

3.3.3. Evaluation of the Accuracy of the Height-Fine-Tuning Process. To evaluate the accuracy of the height-fine-tuning process, the same test points discussed previously are used. Again, we first identified the image coordinates of the test points at different heights (from the plate) in advance as the ground truth. We then moved the robot arm to the computed coordinate based on equation (2). Finally, we compute the distance (in the image space) between the tip of the robot arm and the ground truth, and this is defined as the height-fine-tuning error.

3.3.4. Evaluation of the Accuracy of Localization of the Proposed Robot-Assisted System. The localization accuracy of the proposed robot-assisted system depends on the performance of the abovementioned three processes. For its evaluation, we further recruited five subjects (who are not included in our training data) to evaluate the accuracy of the proposed system.

3.3.5. Effect of Laser Acupuncture with Lift-and-Thrust Operation on Pulse Amplitude and Pulse Rate Variability (PRV). Based on the proposed robot positioning system, we now can emulate the lift-and-thrust operation [9] by moving the robot arm (up and down) with a fixed focal length laser. We compared the effects of traditional steel needle acupuncture

(performed manually) and laser acupuncture (with the aid of our proposed system) on the response of the human body. Three different acupuncture stimulation methods were compared: (a) laser acupuncture without lifting-thrusting function; (b) laser acupuncture with lifting-thrusting function; (c) traditional acupuncture stimulation (without lifting-thrusting operation).

The experiments were proceeded as follows: 10 healthy subjects (five males and five females) were recruited. Each subject received the abovementioned three types of stimulation for 5 minutes at Neiguan and Hegu points on both hands separately (at least 24 hours apart for each experiment). Photoplethysmography (PPG) signals (from the subject's wrist) were measured before and after the stimulation (the unit of PPG waveform is measured in mV). The PPG data were used to estimate the changes in pulse amplitude and pulse rate variability (PRV). Prior studies have found the changes of pulse amplitude and PRV can be associated with various diseases [36–40]. For example, changes in pulse amplitude and PRV have been found in patients with sleep apnea [36, 40]. The sampling rate of the PPG data is 25 Hz and the duration of the measurements is five minutes. To detect the pulse wave systolic peak (PWSP), we implemented an algorithm based on an event-related moving average [41]. Once the pulse wave peaks are identified, peak-to-peak (PP) intervals can then be computed and the power spectrum of the PP tachogram can be obtained. In this work, the PRV is computed as the power in the high frequency range (i.e., HF). The purpose of detecting the HF power is to observe the activity of the parasympathetic nerve, so as to know whether the autonomic nerve will be in a relatively relaxed state after laser acupuncture stimulation.

$$P_a'' = F * P_b'', \quad (2)$$

$$p_i' = T p_i'' (KF - K + 1). \quad (3)$$

4. Results and Discussion

In this section, we present the results for the evaluation of sources of errors that could affect the performance of our proposed system, including the accuracy of estimating acupoint coordinate (in the image space), the transformation from the image coordinate to the robot-arm coordinate, and the height fine-tuning process.

4.1. The Accuracy of Acupoint Estimation in the Image Space. As shown in Figure 4, the average error is about 2 mm. The variations in the estimation errors might be due to the fact that while the subjects were asked to open their fingers during the acupoint estimation process as shown in Figure 3, different subjects might open their hands with various degrees, which results in the variations in the landmark detection errors.

4.2. The Accuracy of Hand-Eye Calibration. Figure 5 shows the errors for various test points, and the average error is about 0.5~0.6 mm. The variations in errors for various test

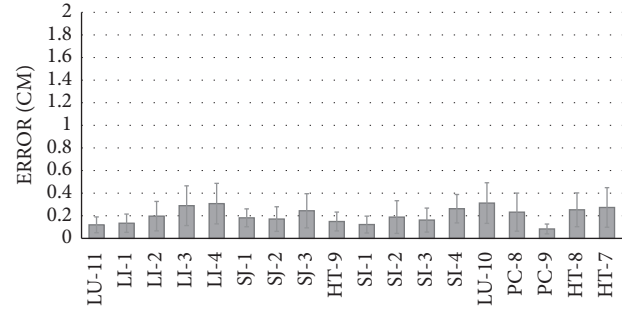


FIGURE 4: Estimation errors for various acupoints.

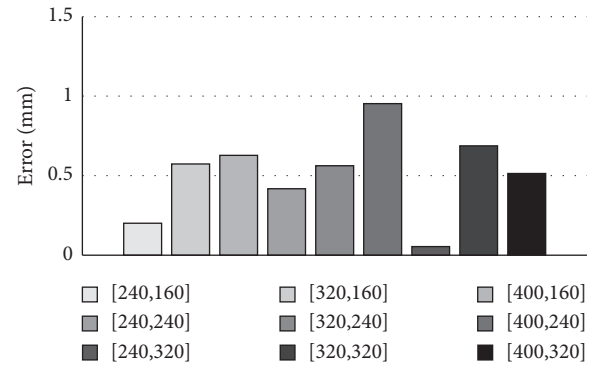


FIGURE 5: Hand-eye calibration errors for various test points.

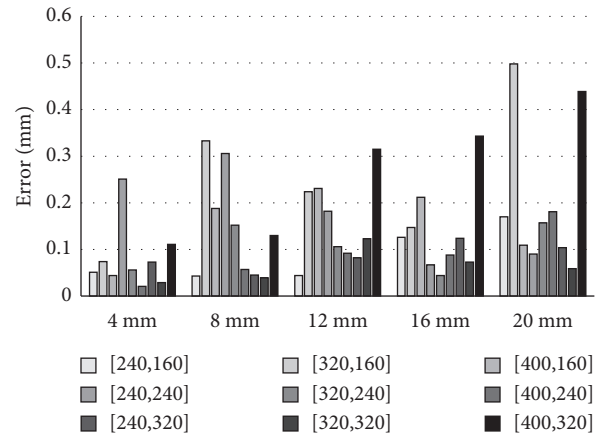


FIGURE 6: Height-fine-tuning error for various test points.

points might be due to the fact that our selected reference points are not evenly distributed in the image space.

4.3. The Accuracy of the Height-Fine-Tuning Process. As shown in Figure 6, the height-fine-tuning error is about 0.1~0.2 mm on average, which is comparatively much smaller than the errors introduced by the acupoint localization and coordinate transformation processes.

4.4. The Accuracy of Acupoint Positioning of the Proposed System. The average positioning error of our proposed

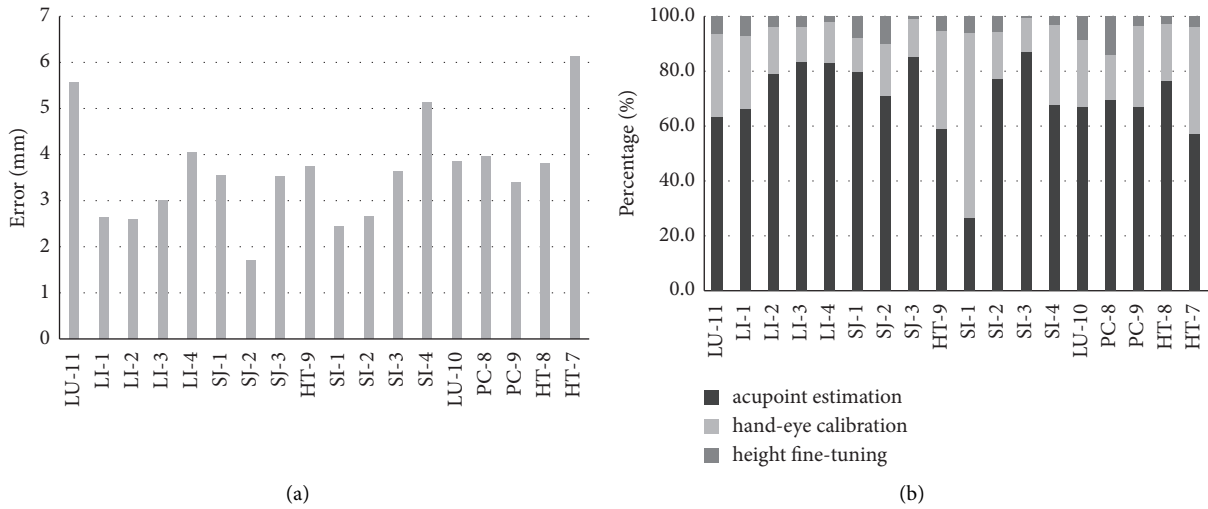


FIGURE 7: The positioning errors for each acupoint and the contribution by different sources of errors. (a) The positioning error for each acupoints. (b) The contribution by various sources of errors.

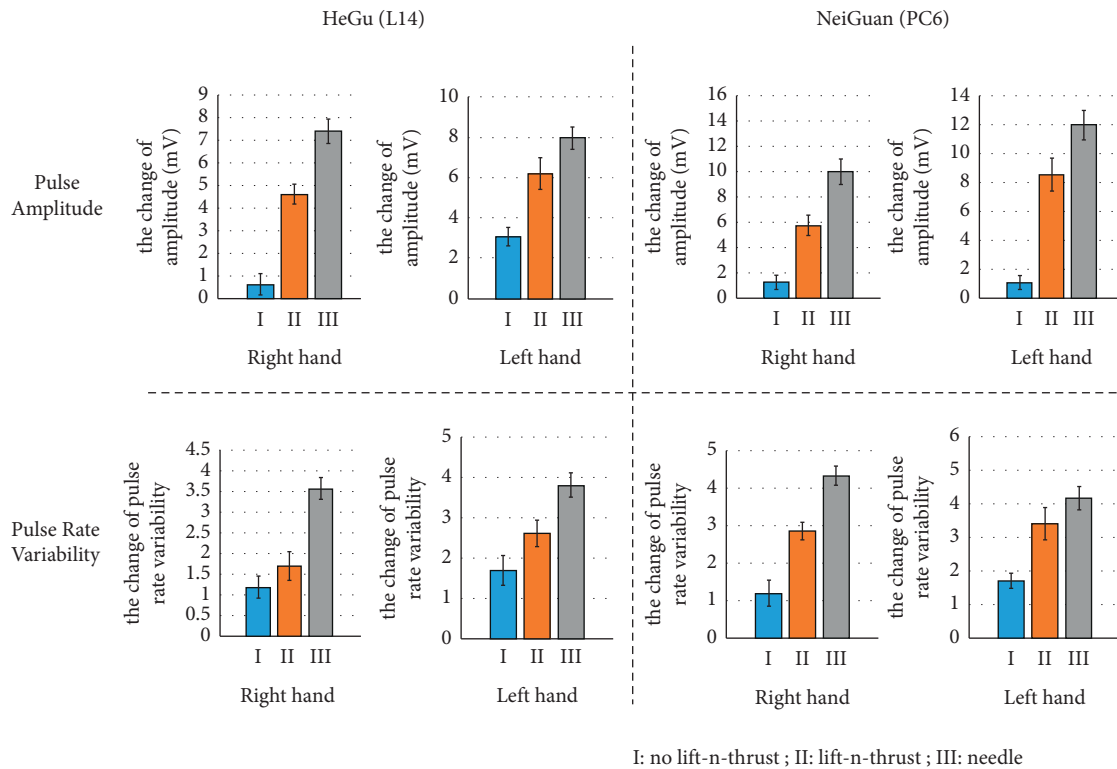


FIGURE 8: Changes in pulse amplitude and pulse rate variability (PRV), the unit (y-axis) of PRV is in 100 ms².

system is about 3.4 mm, as shown in Figure 7(a). In addition, we find that the acupoint estimation process accounts for most of the positioning error (>60%) for most acupoints, as shown in Figure 7(b). In addition, we observe that some of the selected acupoints (such as LU-11) appear to have a larger acupoint estimation error as compared to the results from the training data (as shown in Figure 4), which suggests a sign of overfitting (probably due to the small sample size of our training data). We plan to improve this in our future work.

4.5. *Effect of Laser Acupuncture with Lift-and-Thrust Operation.* Figure 8 shows the changes in pulse amplitude and PRV before and after needle and laser stimulation. Some observations are found as follows: (1) as compared to laser acupuncture, larger changes in both pulse amplitude and PRV have been observed for the needle acupuncture, for both Hegu and Neiguan acupoints.

(2) Laser acupuncture with lifting-thrusting function produced a larger increase in both pulse amplitude and PRV than that without the lifting-thrusting function. Note that in

most cases, our proposed automated laser acupuncture system (with lifting-thrusting operation) has a performance (demonstrated by the increase of pulse amplitude and PRV) close to that of needle acupunctures which were performed manually.

There are several limitations in this work. First, the sample size of test subjects is small in this study, which might not be able to cover the heterogeneity among people (e.g., skin color, body shape, etc.). Second, due to the limitation of time and space, in this paper, we only evaluate the positioning accuracy of hand acupoints. Third, given the increasing popularity of depth-camera-equipped smartphones, the height-tuning process could be removed from our positioning system when a depth-camera-enabled smartphone is employed. In addition, we currently detect the depth of the hand using a height sensor mounted on the robot arm. Such a sensor might not be necessarily needed when a depth camera is available. These limitations will be improved in our future work. In addition, we plan to conduct clinical research with the proposed system in the future and demonstrate the results of our research through medical statistical methods.

5. Conclusion

In this work, we proposed a smartphone-based automated acupoint positioning system for laser acupuncture with lifting-thrusting operation, based on the integration of several machine learning methods and computer vision techniques. There are three main contributions in the present research. First, we successfully implemented a mobile phone-controlled automatic laser acupuncture device based on a robotic arm. Second, the established system achieved an accuracy with a <5 mm of average acupoint positioning error. Third, it is verified that the automatic laser acupuncture combined with the lifting and thrusting function can significantly improve its efficacy in affecting the pulse amplitude and pulse rate variability compared with that without the lifting and thrusting function.

Data Availability

No data were used to support this study.

Conflicts of Interest

The authors declare that they have no conflicts of interest.

Acknowledgments

This study was financially supported by the Ministry of Science and Technology, Taiwan. (MOST 110-2221-E-214-008, MOST 107-2221-E-006-204-MY2).

References

- [1] B. Thompson and S. Bundell, "How electric acupuncture zaps inflammation in mice," *Nature*, 2021.
- [2] Y. He, X. Guo, B. H. May et al., "Clinical evidence for association of acupuncture and acupressure with improved cancer pain: a systematic review and meta-analysis," *JAMA Oncology*, vol. 6, no. 2, pp. 271–278, 2020.
- [3] G. Ton, L.-W. Lee, W.-C. Ho, C.-H. Tu, Y.-H. Chen, and Y.-C. Lee, "Effects of laser acupuncture therapy for patients with inadequate recovery from bell's palsy: preliminary results from randomized, double-blind, sham-controlled study," *Journal of Lasers in Medical Sciences*, vol. 12, no. 1, p. e70, 2021.
- [4] Y.-H. Shiao, Y.-C. Chen, Y.-C. Yeh, and T.-H. Huang, "Positive effects of laser acupuncture in methamphetamine users undergoing group cognitive behavioral therapy: a pilot study," *Evidence-based Complementary and Alternative Medicine*, vol. 2021, Article ID 5514873, 8 pages, 2021.
- [5] J.-H. Kim, C.-S. Na, M.-R. Cho, G.-C. Park, and J.-S. Lee, "Efficacy of invasive laser acupuncture in treating chronic non-specific low back pain: a randomized controlled trial," *PLoS One*, vol. 17, no. 5, Article ID e0269282, 2022.
- [6] R. F. de Oliveira, C. V. da Silva, J. T. de Paula, K. D. C. M. de Oliveira, S. R. D. T. de Siqueira, and P. M. de Freitas, "Effectiveness of laser therapy and laser acupuncture on treating paraesthesia after extraction of lower third molars," *Photobiomodulation, Photomedicine, and Laser Surgery*, vol. 39, no. 12, pp. 774–781, 2021.
- [7] C.-Y. Wang, S.-F. Yen, S.-C. Chang, Y.-H. Chiu, C.-C. Kuo, and C.-E. Wu, "Implementation of laser acupuncture with lifting-thrusting through the use of mechanically immobile components," *Applied Optics*, vol. 54, no. 28, pp. E129–E135, 2015.
- [8] S.-C. Chang, C.-C. Kuo, C.-H. Ni et al., "Emulated laser-acupuncture system," *Applied Optics*, vol. 53, no. 29, pp. H170–H176, 2014.
- [9] K.-C. Lan, C.-Y. Wang, C.-C. Kuo et al., "Effects of the new lift-thrust operation in laser acupuncture investigated by thermal imaging," *Evidence-Based Complementary and Alternative Medicine*, vol. 2019, Article ID 4212079, 2019.
- [10] N. Kanodia, K. Ahmed, and Y. Miao, "Question answering model based conversational chatbot using bert model and google dialogflow, 2021," in *Proceedings of the 31st International Telecommunication Networks and Applications Conference*, Sydney, Australia, 2021.
- [11] K. C. Lan, J. X. Zhang, and Y. H. Lin, "Visualizing the associations between acupoints based on diseases they treat, 2019," in *Proceedings of the IEEE 19th International Conference on Bioinformatics and Bioengineering*, Athens, Greece, 2019.
- [12] Y.-Z. Chen, C. Maigre, M.-C. Hu, and K.-c. Lan, "Localization of acupoints using augmented reality," in *Proceedings of the 8th ACM on Multimedia Systems Conference*, Taipei, Taiwan, 2017.
- [13] S. Silvério-Lopes and T. Silva, "Energy profile with ryodoraku electrodiagnosis of acupuncture in patients with spinal cord injury," *Journal of Acupuncture & Traditional Medicine*, vol. 3, 2020.
- [14] G. Kupperts, "The Ryodoraku method and the objective-possibility to differentiate neurosis from somatic illness," *The Japanese Journal of Ryodoraku Autonomic Nervous System*, vol. 30, no. 11, pp. 249–256, 1985.
- [15] J.-S. Lin, *Acupoint Localization from Video Images*, Institute of Computer and Communication Engineering, Chengkung University, Tainan, Taiwan, 2009.
- [16] M. Chang and Q. Zhu, "Automatic location of facial acupuncture-point based on facial feature points positioning," in *Proceedings of the 5th International Conference on Frontiers of*

- Manufacturing Science and Measuring Technology (FMSMT 2017)*, pp. 545–549, Atlantis Press, Taiyuan, China, 2017.
- [17] Y.-Z. Chen, C. Maigre, M.-C. Hu, and K.-C. Lan, “Localization of acupoints using augmented reality,” in *Proceedings of the 8th ACM on Multimedia Systems Conference*, pp. 239–241, ACM, Taipei, Taiwan, 2017.
- [18] R. Hartley and A. Zisserman, *Multiple View Geometry in Computer Vision*, Cambridge University Press, Cambridge, UK, 2nd edition, 2004.
- [19] H. Zhuang, Z. S. Roth, and R. Sudhakar, “Simultaneous robot/world and tool/flange calibration by solving homogeneous transformation equations of the form $AX=YB$,” *IEEE Transactions on Robotics and Automation*, vol. 10, no. 4, pp. 549–554, 1994.
- [20] J. Ha, D. Kang, and F. C. Park, “A stochastic global optimization algorithm for the two-frame sensor calibration problem,” *IEEE Transactions on Industrial Electronics*, vol. 63, no. 4, pp. 2434–2446, 2016.
- [21] “The Homography transformation,” https://www.corrmap.com/features/homography_transformation.php.
- [22] T. Y. Liu, H. Y. Yang, L. Kuai, and G. Ming, “Classification and characters of physical parameters of lifting-thrusting and twirling manipulations of acupuncture,” *Acupuncture Research*, vol. 35, no. 1, pp. 61–66, 2010.
- [23] K. C. Lan, M. C. Hu, Y. Z. Chen, and J. X. Zhang, “The application of 3D morphable model (3DMM) for real-time visualization of acupoints on a smartphone,” *IEEE Sensors Journal*, vol. 21, no. 3, pp. 3289–3300, 2021.
- [24] Y. LeCun, Y. Bengio, and G. Hinton, “Deep learning,” *Nature*, vol. 521, no. 7553, pp. 436–444, 2015.
- [25] G. Andrew and Z. Menglong, “Efficient convolutional neural networks for mobile vision applications, mobilenets,” 2017, <https://arxiv.org/abs/1704.04861>.
- [26] D. Cristinacce and T. F. Cootes, *Feature Detection and Tracking with Constrained Local Models*, 2006.
- [27] V. Kazemi and J. Sullivan, “One millisecond face alignment with an ensemble of regression trees,” in *Proceedings of the IEEE Conference on Computer Vision and Pattern Recognition*, pp. 1867–1874, Columbus, Ohio, USA, 2014.
- [28] E. Rublee, V. Rabaud, K. Konolige, and G. Bradski, *An Efficient Alternative to SIFT or SURF*, 2011 *International Conference on Computer Vision*, IEEE, Piscataway, NJ, USA, 2011.
- [29] M. A. Fischler and R. C. Bolles, “Random sample consensus: a paradigm for model fitting with applications to image analysis and automated cartography,” *Communications of the ACM*, vol. 24, no. 6, pp. 381–395, 1981.
- [30] S. Schaefer, T. McPhail, and J. Warren, *Image Deformation Using Moving Least Squares*, ACM SIGGRAPH, Vancouver, Canada, 2006.
- [31] F. Li, T. He, Q. Xu et al., “What is the Acupoint? A preliminary review of Acupoints,” *Pain Medicine*, vol. 16, no. 10, pp. 1905–1915, 2015.
- [32] A. F. Molsberger, J. Manickavasagan, H. H. Abholz, W. B. Maixner, and H. G. Endres, “Acupuncture points are large fields: the fuzziness of acupuncture point localization by doctors in practice,” *European Journal of Pain*, vol. 16, no. 9, pp. 1264–1270, 2012.
- [33] Y.-T. Ma and Z. H. Cho, *Biomedical Acupuncture for Pain Management-E-Book*, Elsevier Health Sciences, Amsterdam, Netherlands, 2004.
- [34] Y.-Q. Li, B. Zhu, P.-J. Rong, H. Ben, and Y.-H. Li, “Effective regularity in modulation on gastric motility induced by different acupoint stimulation,” *World Journal of Gastroenterology*, vol. 12, no. 47, pp. 7642–7648, 2006.
- [35] X. H. Yan, X. Y. Zhang, C. L. Liu et al., “Imaging study on acupuncture points,” *Journal of Physics: Conference Series*, vol. 186, Article ID 012100, 2009.
- [36] E. Gil, J. María Vergara, and P. Laguna, “Detection of decreases in the amplitude fluctuation of pulse photoplethysmography signal as indication of obstructive sleep apnea syndrome in children,” *Biomedical Signal Processing and Control*, vol. 3, no. 3, pp. 267–277, 2008.
- [37] D. N. Dutt and S. Shruthi, “Digital processing of ecg and ppg signals for study of arterial parameters for cardiovascular risk assessment, 2015,” in *Proceedings of the International Conference on Communications and Signal Processing (ICCSPP)*, pp. 1506–1510, IEEE, Chengdu, China, 2015.
- [38] M. Mueck-Weymann, T. Rechlin, F. Ehrengut et al., “Effects of olanzapine and clozapine upon pulse rate variability,” *Depression and Anxiety*, vol. 16, no. 3, pp. 93–99, 2002.
- [39] S.-z. Xin, S. Hu, V. P. Crabtree et al., “Investigation of blood pulse PPG signal regulation on toe effect of body posture and lower limb height,” *Journal of Zhejiang University-Science*, vol. 8, no. 6, pp. 916–920, 2007.
- [40] E. Constantin, C. D. McGregor, V. Cote, and R. T. Brouillette, “Pulse rate and pulse rate variability decrease after adenotonsillectomy for obstructive sleep apnea,” *Pediatric Pulmonology*, vol. 43, no. 5, pp. 498–504, 2008.
- [41] K.-C. Lan, G. Litscher, and T.-H. Hung, “Traditional Chinese medicine pulse diagnosis on a smartphone using skin impedance at acupoints: a feasibility study,” *Sensors*, vol. 20, no. 16, p. 4618, 2020.

Review Article

Application of Virtual Reality Technology in Clinical Practice, Teaching, and Research in Complementary and Alternative Medicine

Huifang Guan ¹, Yan Xu ², and Dexi Zhao ³

¹College of Traditional Chinese Medicine, Changchun University of Chinese Medicine, Changchun 130117, China

²College of Pediatrics, Henan University of Chinese Medicine, Zhengzhou 450000, Henan, China

³Department of Encephalopathy, The Affiliated Hospital of Changchun University of Chinese Medicine, No. 1478 Gong-Nong Road, Changchun, Jilin 130021, China

Correspondence should be addressed to Dexi Zhao; dexizhao1006@163.com

Received 27 May 2022; Accepted 8 July 2022; Published 11 August 2022

Academic Editor: Lei Jiang

Copyright © 2022 Huifang Guan et al. This is an open access article distributed under the Creative Commons Attribution License, which permits unrestricted use, distribution, and reproduction in any medium, provided the original work is properly cited.

Background. The application of virtual reality (VR) in clinical settings is growing rapidly, with encouraging results. As VR has been introduced into complementary and alternative medicine (CAM), a systematic review must be undertaken to understand its current status. **Aim.** This review aims to evaluate and summarize the current applications of VR in CAM, as well as to explore potential directions for future research and development. **Methods.** After a brief description of VR technology, we discuss the past 20 years of clinical VR applications in the medical field. Then, we discuss the theoretical basis of the combination of VR technology and CAM, the research thus far, and practical factors regarding usability, etc., from the following three main aspects: clinical application, teaching, and scientific research. Finally, we summarize and propose hypotheses on the application of VR in CAM and its limitations. **Results.** Our review of the theoretical underpinnings and research findings to date leads to the prediction that VR and CAM will have a significant impact on future research and practice. **Conclusion.** Although there is still much research needed to advance the science in this area, we strongly believe that VR applications will become indispensable tools in the toolbox of CAM researchers and practitioners and will only grow in relevance and popularity in the era of digital health.

1. Introduction

The rapid evolution of digital technology has allowed for novel and creative solutions across medical disciplines in recent years. Among these technologies, virtual reality (VR) has become a potentially powerful adjunct. VR affords the opportunity to create highly realistic, interactive, and systematically controlled stimulus environments that users can be immersed in and interact with for human testing, training, teaching, and treatment environments that allow for the precise control of complex, multisensory, and dynamic 3D stimulus presentations [1].

In recent years, complementary and alternative medicine (CAM) has become more popular worldwide, and the number and proportion of its uses continue to grow [2]. The combination of VR and CAM has received

extensive attention. Several recent studies, reviews, and meta-analyses have shown that VR plays a positive role in CAM treatments such as meditation, hypnosis, palliative therapy, tai chi (TC), qigong, acupoint sticking therapy, aromatherapy, and yoga [3–10]. In addition, VR has helped clinicians overcome barriers in education [11–24] and research [25, 26] during the coronavirus disease 2019 (COVID-19) pandemic. To some extent, VR opens the door to a new generation of application programs in CAM.

The COVID-19 pandemic has become one of the largest global health crises of our time [27]. Excessive pressure on health care systems has prompted medical resources around the world to be redirected to stop the spread of COVID-19 and treat severe cases. In fact, while there have been hundreds of millions of cases of COVID-19 worldwide, the

pandemic has brought about social problems and thus has forced the integration and development of VR technology in the field of CAM.

First, many patients have not been able to receive timely help due to the impact of COVID-19. Therefore, facilities offering services such as CAM have had to adapt their service offerings and develop virtual medicine strategies to ensure that their patients continue to receive necessary treatment.

Second, there is a high level of transmission of SARS-CoV-2, the virus that causes COVID-19; as a result, countries worldwide have imposed rigorous public health measures, such as quarantines. This has involved the suspension of medical school classes globally, resulting in students not being able to rotate at their institutions [28]. This results in medical students having less clinical experience, while varied and rich clinical experiences are the cornerstone of medical students' growth. This requires an unprecedented change in the way the medical education sector provides clinical instructions, in line with efforts aimed at prioritizing the safety and slowing the spread of the virus. Several studies have attempted to fill this gap by applying VR to medical education and training to support physician learning during social distancing [11, 13, 15, 18, 22, 23].

Third, COVID-19 has led to high levels of burnout and mental illness in medical students [29]. Mind-body interventions such as VR-based yoga [9] and mindfulness meditation [30] can be used as successful tools for stress management and the reduction of burnout rates and anxiety in resident physicians. VR can offer an immersive environment to enhance the user's experience and prevent distractions [31]. Research studies showed that 10 minutes of VR therapy was similar in effect to reducing work by 1.6 hours per week with regard to reductions in emotional exhaustion [30]. To this end, an important benefit of VR is the minimal time commitment necessary, allowing medical residents to benefit from decreased burnout without losing important educational opportunities [30].

Fourth, the application of VR has complemented strict preventive measures to reduce the infection rate of medical workers on the front lines of the COVID-19 pandemic.

Finally, during the COVID-19 pandemic, the burden on the medical system and medical costs have increased, which has become an emerging problem in the medical system. The application of VR in CAM can reduce the need for face-to-face consultation, thereby reducing the use and transportation of medical resources (such as protective clothing).

Even as countries and systems adapt to the new normal after the COVID-19 pandemic, many virtual systems built to meet short-term needs will eventually evolve into long-term trends and solutions. Therefore, a systematic review of the application of VR in the field of CAM can provide inspiration and reference for research on and development of related projects in the future.

Some systematic reviews have been published, but their scope only partially overlaps with that of this paper. For example, some systematic reviews examined only VR and meditation or VR and hypnosis, without a comprehensive review of VR and the entire field of CAM; other reviews were

published 5 years ago and therefore lack recent references. This paper expands on previous findings by providing a broader and updated overview of the potential of VR in CAM.

This review briefly presents evidence on how VR can be rationally used in conjunction with CAM in a range of settings, including clinical, educational, and scientific research settings. This article presents the potential advantages and disadvantages of using VR in CAM, as well as practical recommendations on how to incorporate VR into CAM.

2. What Is VR?

Before one can explore VR, it is useful to consider how it is defined. The term "virtual reality" itself is credited to Jaron Lanier, who, in 1989, developed a full-body suit of sensors for body movement recordings, a technique that is extensively used in film and game productions [32].

However, the technology was not sufficiently mature in the 1990s. As underlying VR-enabling technologies and methods (e.g., computational speed, computer graphics, panoramic video, audio/visual/haptic displays, natural user interfaces, tracking sensors, speech and language processing, artificial intelligence, virtual human agents, and authoring software) have continued to evolve [1], the definition of VR has also evolved alongside advancements in technical capabilities, from an early stage of large projection rooms to current consumer products that use high-resolution head-mounted displays (HMDs) [33]. Users of VR technology wear an HMD with a close-proximity screen that creates a sensation of being transported into lifelike, three-dimensional worlds [34], and the use of HMDs has three key characteristics: presence, immersion, and interactivity [35]. Presence mainly refers to the user's sense of immersion. The sense of immersion refers to the use of multiple senses, such as hearing, vision, touch, taste, and smell. Finally, interactivity is another key component of VR. Human-computer interaction allows people to operate VR systems at will and obtain the most realistic feedback from the environment during the operation. Multimodal stimulus control is important for inducing a sense of 'presence' in virtual environments, which is believed to be of crucial importance for the effectiveness of VR training [36]. The most commonly used forms of sensory stimulation are visual and auditory displays [36]. Additionally, VR systems may provide limited but compelling haptic feedback to simulate the sensation of forces, surfaces, and textures when users interact with virtual objects [36].

3. How Does VR Technology Work in a Medical Setting?

It is the abovementioned characteristics of VR technology that make it loved by many people and widely used in many fields, such as the medical field. To date, VR has successfully been applied in many clinical settings [1], such as helping to treat anxiety disorders [37, 38], alleviating fear [39], managing pain [33, 34, 40], supporting physical recovery [41], and preventing falls in elderly individuals [42]. Furthermore,

an interactive training system for public health emergency preparedness for major emerging infectious diseases based on VR should be established [43].

Likewise, VR has revolutionized medical education [44]. Opportunities for repeated exposure and hands-on experience are important for medical students. However, this puts patients at an increased risk. Therefore, VR is emerging as a necessary augmentation to conventional learning [45–47]. For example, VR can help train students in anatomy [48, 49], helping physicians optimize preoperative and intraoperative decision-making [50, 51]. For example, after VR simulation training in endoscopy, trainees were found to improve in areas such as the comprehensive assessment of technical and nontechnical skills and patient comfort [52].

In scientific research, the use of VR to create an integrative web-based VR system to explore the macromolecular structure is a new trend [53], and VR can be further used for novel drug development, such as drug discovery and rational drug design [54].

4. What Is CAM?

The term “complementary and alternative medicine” refers to interventions that are not part of conventional medical care but are provided alongside it as a supplement [55]. There is a broad range of interventions that fall under the realm of CAM, including ancient medicine traditions such as ayurvedic or traditional Chinese medicine, acupuncture, meditation, hypnotherapy, yoga, TC, and music intervention [55, 56]. Today, CAM has widespread use worldwide and is applied to various diseases and conditions, especially intractable diseases and conditions such as cancer, pain [57], and chronic diseases [58].

5. Clinical Application

5.1. Meditation. Meditation is a mental practice aiming to improve the psychological capacity of self-regulation regarding attention, awareness, and emotion [59]. Studies have found evidence of the positive effects of meditation on health and well-being, but the difficulty of learning and engaging in meditation practice has been identified as a major barrier [60]. VR technology may facilitate meditation practice by immersing users in a distraction-free and calming virtual environment [60]. Today, VR and meditation therapy have been applied to a range of disorders and conditions, including pain [60–62], depression [63], anxiety disorders [3, 63, 64], sleep disorders [65], posttraumatic stress disorder [66], and pressure [60].

Regarding pain management, clinical studies have validated the effectiveness of VR as a facilitator of meditation practice in patients with acute pain [62], chronic pain [60], and opioid tolerance or opioid use disorder [61, 62]. Further neurobiological research studies found that scores for pain, opioid craving, anxiety, and depression decreased after each intervention session (relative to before the session) [61]. In addition, salivary cortisol (but not CRP) levels were found to decrease from pre- to postsession [61]. Based on pre- to postintervention fMRI assessments, painful task-related left

postcentral gyrus (PCG) activation was found to decrease [61]. At baseline, the PCG showed positive connectivity with other regions of the pain neuromatrix, but this pattern changed postintervention [61]. The results of this feasibility study suggest that a VR-based meditation intervention is a promising approach for reducing pain scores and modulating pain neuromatrix activity and connectivity among patients with opioid use disorder [61].

The prolonged illness and recovery time of COVID-19, coupled with infection prevention measures that make on-site family visits or movement between hospital units difficult or contraindicated, present a range of challenges for patients hospitalized with COVID-19, such as social isolation, disability, neurologic sequelae, adjustment-related anxiety, depression, stress, sleep disorders, and posttraumatic stress disorder [67]. It has been suggested that novel VR-based meditation interventions could be used as a comprehensive recovery program for COVID-19 [3, 63–67] and as successful stress management tools to reduce burnout rates among residents [30].

5.2. Hypnosis. Hypnosis is defined as “a state of consciousness involving focused attention and reduced peripheral awareness characterized by an enhanced capacity for response to suggestion”. Hypnosis has been shown to be efficacious for a range of clinical conditions, such as relief of pain [68, 69]. However, there is a universal agreement that individual differences in hypnotizability exist, meaning that not all individuals are able to enter a hypnotic state, thereby limiting the clinical utility of this technique [70]. In fact, those lacking imaginative absorption-like traits have often shown little or no benefits in response to hypnosis in studies [10]. However, if the visual and auditory stimuli provided by VR can be experienced by individuals with low hypnotic susceptibility, these individuals have to rely less on their own imagination, which improves the intervention effect [10].

With attention mechanisms as a common denominator, the potential for synergy between these two modalities in VR and hypnosis is significant for several reasons. First, hypnotic suggestions may help an inhibited patient relax and immerse himself or herself in a virtual world. Furthermore, hypnotic suggestions can be used to deepen a patient’s sense of presence in the virtual world [71].

Currently, a new technique called VR hypnosis (VRH), which encompasses a combination of both tools combined with VR hardware/software and hypnosis induction [72], is regularly used to treat anxiety and pain [73]. This method immerses the patient in a relaxed, peaceful environment. It represents a noninvasive way to reduce preoperative stress levels without side effects and without the need for additional medical or support staff. In parallel experiments, the combined effect of hypnotic analgesia and VR pain distraction was stronger than that of VR distraction alone [74]. The combination of hypnosis and VR can be used to treat a variety of types of pain, such as pain following traumatic injuries [75] or spinal cord injury-associated neuropathic pain [76]; this combination has been widely used to relieve preoperative anxiety in preoperative patients, such as

beforehand surgery under axillary plexus block [77] or cardiac surgery [78]. In a review that included 8 studies on VRH, short-term results showed significant reductions in pain intensity, unpleasant pain, time spent thinking about pain, anxiety, and opioid craving levels, and improved short-term quality of life in patients [72]. In contrast, the Violeta Enea study found that although hypnosis + VR had the same efficacy as hypnosis alone and VR alone, it appeared that their combination did not have an additive effect and that the two interventions might even interfere with each other [79].

5.3. Palliative Care. During COVID-19, strict inpatient visitation restrictions to prevent infection have meant that many people have died alone in hospitals [80]. With limited resources and a rapidly increasing number of patients, the desperate race to fight to preserve life has understandably but regrettably led to inattention to those dying [81]. Existential pain and psychological barriers for patients and their families may last a lifetime [81]. To help meet this challenge, several institutions have used VR as a supplement to palliative care during the COVID-19 pandemic [81]. Using VR to have conversations with relatives of patients in palliative care at the end of life makes the patient and family feel like they are in the same room, promotes connection between patients and their families, and creates opportunities for final contact before death [5, 82, 83]. Virtual palliative care can also help address challenges and barriers to providing such care, including geographic barriers, clinician staffing, and outreach to underserved populations [84]. Some health systems have introduced virtual palliative care to meet growing demands [85, 86] and to expand their insurance coverage during the COVID-19 pandemic [87].

During the COVID-19 crisis, a New York City hospital virtually trained hospitalists practicing remotely to partner with on-site clinicians to meet the high demand for its palliative care services [88]. The plan addressed multiple challenges posed by the surge in COVID-19 cases: high numbers of severely ill patients, limitations on personal protective equipment, increased communication needs due to visitor restrictions and uncertainty about the novel disease, and restrictions on doctors' in-person field visits [88].

With aging populations and advances in science and technology, an increasing number of people diagnosed with life-limiting diseases will face longer periods of palliative care, which may require health care support for a period from six months to a year [89]. Some patients with terminal cancer wish to go to a memorable place or return home. However, owing to various symptom burdens and physical dysfunction, these wishes are difficult for them to realize [90]. VR can simulate physical locations and can hence be employed in facilitating a good death by allowing patients to have experiences on their "bucket list", such as visiting the North Pole to see the aurora [90]. Likewise, as most patients do not wish to die in a hospital and would prefer the comfort of their home and company of their loved ones, patients can choose their ideal location of care during their last days using VR [90]. Research has shown that such virtual tours can

improve spiritual wellbeing, physical and psychological symptoms, and blood pressure measurements in patients with advanced cancer [91].

There is growing evidence that VR is a positive psychological intervention for patients with advanced cancer receiving palliative care [92], with excellent analgesic effects [93]. Studies have demonstrated that this approach positively impacts the quality of life, mood, and health of adults receiving palliative care [94, 95], with significant improvements in pain, depression, anxiety, wellbeing, and shortness of breath [96]. The combination of VR and palliative care is not just for adults; it is also a way to help pediatric patients with serious medical conditions virtually leave their rooms while undergoing palliative care and improve their feelings of isolation [97]. This not only improves their nausea and headaches but also improves their mood [97].

In conclusion, virtual palliative care consultation is a promising resource that can help safeguard our health system's ability to address unmet palliative care needs for critically ill patients, especially during a pandemic [85].

5.4. Tai Chi. TC is a popular Chinese mind-body exercise [7]. Several studies have demonstrated the positive effect of TC in individuals, such as reducing the risk of cardiovascular disease [98] or preventing falls among elderly people at high risk of falls [99]. The ongoing COVID-19 pandemic has confined seniors most at risk of infection to their homes, reducing their opportunities for physical activity and worsening their physical performance [100]. Motivated by these public health challenges, some studies have explored the possibility of combining VR with TC, hoping to help elderly individuals reduce falls and improve balance and mobility through the program [100]. In a previous study, the authors attempted to apply the VR technique with TC to induce and enhance concentration, learning ability, fun, and feedback for older adults with cognitive impairment [7]. The results showed that VR-based TC exercise had protective effects on cognitive and physical function and that a higher degree of program participation was associated with greater improvements in cognitive performance [7]. The rapid conversion of TC programs from face-to-face to virtual classes has been feasible during the COVID-19 pandemic [101].

5.5. Qigong. Qigong is a mind-body therapy that has been widely used for health promotion and disease prevention in ancient China and India for thousands of years [102]. VR technology can be used to show the specific details of qigong movements in a complete view so that the recipient can observe more clearly and learn [8]. In VR, the actions of the recipient in the VR scene can be recorded and played back. This function allows the communicator to accurately assess whether the recipient's actions are standard through the recipient's specific actions and the data of the computer system and improve the teaching quality of online courses [8]. In addition, VR can affect the sensory system through sight, touch, hearing, etc. It can help individuals concentrate on life and achieve an optimal state in which the body, qi, and spirit are unified [8].

5.6. Acupoint Sticking Therapy. Acupoint sticking therapy is a treatment that works through the external application of a herbal paste, which is made from different materials according to the treatment purposes [103]. A study found that the use of acupoint sticking therapy combined with VR in children after circumcision effectively relieved their anxiety, diverted their attention, improved their pain perception threshold, and reduced their feelings of pain while also being noninvasive [6]. Acupoint sticking uses external treatment based on traditional Chinese medicine to relieve the physical discomfort of children, and VR uses three-dimensional dynamic vision and an interactive virtual world to divert the attention of children and provide a pleasant spiritual experience [6]. The two methods are easy to operate and are inexpensive. Due to the pleasant spiritual experience, the children in the intervention group were more cooperative in the follow-up nursing procedures, which not only improved the parents' and children's satisfaction with nursing care but also facilitated routine postoperative nursing procedures [6].

5.7. Aromatherapy. Aromatherapy, also known as essential oil therapy, is a complementary treatment that uses ingredients from different parts of plants, such as leaves, flowers, and seeds, to yield aromatic essential oils using different extraction techniques. Aromatherapy is widely used clinically in the treatment of postoperative nausea and vomiting [104] and dementia [105]. Research shows that the combination of 3D VR and hands-on aromatherapy allows for a powerful learning experience and facilitates the construction of a 3D space for aromatherapy products [4]. After 9 weeks of intervention, older subjects showed significant post-intervention improvements in comparison with the control group in terms of the scores for happiness, perceived stress, sleep quality, meditation experience, and life satisfaction [4]. Additionally, this approach was found to increase the social participation and interpersonal communication of elderly people and reduce the waste of materials from hands-on activities [4].

5.8. Yoga. Yoga is a mind-body intervention that incorporates physical postures, breathing, and meditation to increase flexibility and strength, relaxation, and body awareness [106, 107]. Research found that VR-based yogic pranayama and meditation among health care workers was feasible during the COVID-19 pandemic and helped them feel more at peace, hopeful, and relaxed after the practice [9]. In a pilot study, participants preferred to engage in virtually delivered yoga interventions over face-to-face yoga, likely because it eliminated travel barriers and the risk of COVID-19 infection [108].

5.9. Comprehensive Application. Mind-body interventions such as relaxation, hypnosis, meditation, and music interventions for cancer patients who experience pain, fatigue, and sleep disturbances helped patients manage all symptoms in a group with a single treatment strategy [109].

In one study, subjects were offered mind-body group therapy sessions in fitness, meditation, yoga, dance, TC, and music using Zoom video conferencing during a COVID-19 outbreak [110]. The high utilization of and satisfaction with these virtual mind-body services demonstrate the significant potential of remote delivery to facilitate patient access to services [110]. A similar pilot study conducted in palliative care, where patients created a personalized soundtrack with a music therapist and then paired the soundtrack with a 360° VR environment, was well-rated by most participants, who described pleasant emotional and physical responses [111].

In summary, during a pandemic, a positive attitude and regular exercise are considered a strategy to strengthen the immune system to fight COVID-19 infection [112]. People can use VR systems combined with TC, qigong, yoga, etc., to facilitate exercise. Similarly, people can use VR with meditation, hypnosis, music therapy, and aromatherapy to help themselves relieve anxiety and panic caused by long-term isolation. At the same time, the combination of VR and meditation, hypnosis, palliative therapy, and acupuncture has become a necessary addition in CAM.

6. Teaching

6.1. Virtual Ward Rounds and Hospital Rotations. The COVID-19 pandemic has resulted in unprecedented public health measures. A survey of UK medical students showed that the impact on medical student education has been significant, particularly affecting the transition from a student to a doctor [113]. Limited exposure to medical school specialties has been shown to increase the likelihood of future medical mismanagement and misdiagnosis [114]. Therefore, given the uncertainty about the duration of the pandemic and the possibility of additional quarantine periods in the future, educational innovations are needed to ensure that medical students continue to be immersed in clinical settings.

Given the uncertainties about COVID-19, it is expected that students will continue to be excluded from evaluating COVID-19 patients in the near future. However, the COVID-19 pandemic has provided important teaching moments. How can educators provide medical students with first-hand knowledge of caring for COVID-19 patients while mitigating the risk of infection and addressing concerns about limited supplies of PPE [13]? Hoffman et al. explored the use of virtual ward rounds for medical students to observe and interact with COVID-19 patients successfully educate students about the diagnosis and treatment of COVID-19 while eliminating the risk of infection [13].

During the COVID-19 pandemic, many universities and hospitals around the world, including the University of California, Los Angeles [22], Baylor College of Medicine [23], the University of Chicago [18], the Columbia University Irving Medical Center [15], and the University of Pennsylvania [11], have conducted similar experiments. After virtual hospital practicums, students appreciated the interactive nature of the course, felt that the instruction and rotation provided sufficient experience and confidence to

understand internal medicine in a hospital setting, and expressed that they cherished this exposure to future career opportunities [11, 15, 18, 22, 23].

While helping students gain clinical knowledge, the virtual practicum approach reduces the burden on the health care system [115]. For example, Imperial College London uses this model to provide an effective triage system [16]; Harvard Medical School has developed the use of a virtual medical student response team of 500 students to educate or help a community or health care team [19]. Because of their positive role in helping during a pandemic, students report feeling empowered and enthusiastic, and they felt a sense of purpose during uncertain times. Additionally, the project promotes teamwork skills and indirectly increases students' knowledge and awareness of COVID-19.

Virtual practicums are a novel and successful model to help students familiarize themselves with the clinical environment, understand the mechanics of medical procedures, and help reduce health care burdens as COVID-19 continues to evolve. New interactive forms of virtual teaching are being developed to enable students to interact with patients from their homes. Open-access teaching with medical experts has enabled students to remain abreast of the latest medical advancements and to reclaim knowledge lost due to the suspension of university classes and clinical attachments [116]. At the same time, this virtual traineeship mitigates high rotation costs and removes financial barriers for all students [22]. Therefore, as COVID-19 continues to evolve and health systems respond, virtual internships and rotations are reasonable alternatives to in-person clinical rotations.

However, to some extent, inequalities in virtual teaching services worldwide are also noted to cause differences in medical education [116]. In developed countries such as the United Kingdom and the United States, the virtual teaching of medical students is a highly respected teaching method [16, 19]. In stark contrast, due to insufficient funds and infrastructure for virtual learning, some developing countries are yet to develop these teaching methods.

6.2. Teaching in Acupuncture. Acupuncture treatment, a traditional Chinese medical technology, is an extensive and rich practice, and teaching of acupuncture includes the teaching of human medicine, traditional medicine, acupuncture treatment methods, and clinical pain treatment [117]. In Chinese medicine, acupuncture points are of great significance to the human body and are an important part of learning acupuncture treatment techniques. The acupuncture points of the human body are identified through long-term observation and practice. They are special points on the surface of human organs, which serve as stimulation sites during acupuncture treatment. The acupoints of the human body are not only on the body's surface; their locations are deeply connected with the internal tissues and organs and are closely connected throughout the body [117].

At present, in most lessons on the position of acupoints, teachers use two-dimensional models such as pictures and multimedia software or use auxiliary teaching aids such as meridian and acupoint human models. Practical teaching

regarding the position of acupoints generally includes finding the anatomical location of the acupoints on the body and drawing the direction of the meridians, etc., mainly relying on the students to practice on each other as operation subjects. However, the details cannot be viewed, and accuracy is lacking, which complicates the entire learning process [117]. The application of modern human anatomy knowledge in acupuncture makes the positioning of acupoints more standardized, but all Chinese medical schools have limited cadaveric resources, which has an impact on the development and quality of teaching. In the practice of acupuncture and moxibustion, in addition to practicing on themselves or other students, students often practice with paper balls, cotton balls and other substitutes [17]. This approach has no advantage in the three-dimensional sense of the meridians in the teaching display, and the students' experience is not strong in practice.

In response to these difficulties, some researchers have combined VR technology with anatomy [12, 24, 48] and applied it to the field of acupuncture teaching, aiming to create a virtual three-dimensional space to show the anatomical structure of acupuncture points to beginners in acupuncture and moxibustion, to realistically imitate the acupuncture process and to provide acupuncture points for these practices. This provides a safe and solid foundation to improve the efficacy of clinical acupuncture.

In a teaching experiment at Guangzhou University of Traditional Chinese Medicine, teachers used a virtual acupuncture teaching system to display the outline of the fourteen meridians and the local anatomy of the key points of each meridian (bones, blood vessels, nerves, muscles, and epidermal texture) [17]. When teaching acupuncture and moxibustion procedure courses, the virtual acupuncture teaching system can be used to construct intelligent three-dimensional animations, which vividly display the needle insertion level of each acupoint and the danger of an incorrect acupuncture procedure [17]. When students practice the operation, the system displays the hierarchical anatomical structure according to the needle insertion level in virtual acupuncture. If the acupuncture is wrong, the system will give a prompt response, and the score of the operation will be displayed after the acupuncture procedure is completed [17]. This fun and interactive learning method not only improves test scores but also improves students' enthusiasm for learning [17].

In VR, adding tactile feedback to simulate the sense of touch in the real world to visual feedback can greatly enhance the operator's sense of reality [14]. Through a force-feedback device, Jiang Jun et al. collected acupuncture experts' Fengchi acupuncture techniques, integrated them into a digital virtual human body, and used VR technology to build a virtual Fengchi acupuncture force-feedback simulation system so that the operator could achieve one-to-one acupuncture. The advanced simulation learning effect can simulate the visual, tactile, and force sensation of needle insertion to achieve the purpose of rapidly improving the learner's acupuncture skills, which helps in transferring traditional Chinese medicine skills from a virtual anatomical person to a real physical person [14].

6.3. Teaching in Palliative Care. Dying patients are a reality in medicine [20]. As the population ages, more knowledge, skills, and experience in palliative care are needed to manage end-of-life patients. Medical students, however, feel unprepared to effectively navigate the complex end-of-life management issues of dying patients and want increased experiential learning in palliative care [20]. In teaching students in palliative care, VR technology proves to be an effective teaching tool that may help address the need to add formal palliative care experience to medical school training programs [20, 21].

Palliative care, on the other hand, is often delivered by an interdisciplinary team through different hospital stages to address the needs of patients and families; the team often includes advanced practice nurses, physicians, registered nurses, social workers, and spiritual or religious counselors. The team may also include members from other health care professions, including nutrition, physical therapy, and occupational therapy [118]. The use of VR technology could be an important way for palliative care courses to effectively and conveniently help students from different majors meet on a certain day, time and place, bringing interprofessional learners together [26].

7. Scientific Research

7.1. Virtual Diagnosis. Using an online virtual diagnostic model to determine the association between the diagnostic model and the designated acupoints is a new research method for acupoints. In one study [26], acupuncture practitioners were asked to participate in a virtual diagnosis process, a method employed in previous studies to evaluate the performance of doctors and medical students [119, 120]. According to the model data, the model could evaluate the commonality and specific treatment prescription of various acupoint selections and explore the core acupoints for specific diseases [26]. Kyung Hee University also conducted a similar study [25]. Based on the virtual diagnoses of currently practicing doctors, the results suggested a relationship between symptom indications and acupoint prescriptions in Korean medicine and revealed clear patterns of acupoints commonly prescribed across various diseases, as well as acupoints used in specific cases [26].

This study had several limitations that should be considered [26]. First, due to the nature of the experiment, the validity of virtual diagnoses could not be assessed, and it is necessary to review other types of data to support this [121]. Second, prospective studies should include a larger sample including physicians from around the globe to cover the wide range of different skills among physicians [121].

8. Advantages of Using VR for CAM

There are numerous benefits of using VR over traditional methods. In determining whether the combination of VR and CAM is ready for widespread use, we need to consider what capabilities VR offers that make it particularly suitable for clinical practice, teaching, and scientific use in the field of

CAM. On a very broad level, VR can facilitate the development of individual therapies in the field of CAM. These aids can be summed up simply as follows.

First, this review found convincing evidence that VR has widespread clinical use. VR eliminates a potential barrier for patients who may experience difficulty imagining or visualizing. VR can enhance therapy by enhancing sensory immersion (e.g., VR combined with meditation therapy can help patients maximize immersion, and VR provides compelling visual and auditory stimuli in people with low hypnotic susceptibility). Simultaneously, virtual locations can be simulated to transport the patient to where he or she wants to go. For example, VR can help patients who are receiving palliative care to fulfill their wishes to travel or return home. It can also help people practicing yoga, qigong, TC, etc., at home to pretend they are in a classroom. These exercises are embedded in sports or games and are more engaging than staying home all the time. Moreover, interactivity should be used to help palliative care patients in hospitals make real-world connections with loved ones.

Second, in teaching, VR can help medical students with virtual medical practice during the COVID-19 pandemic. In some special disciplines, such as acupuncture and palliative care, VR plays an irreplaceable role. More importantly, VR can provide behavioral performance capture and retrospective and intuitive post hoc evaluation. Safe testing and training environments minimize the risks due to errors.

Third, VR introduces a new method and opens new avenues for overcoming boundaries in scientific CAM research.

Fifth, from a research perspective, the use of VR could facilitate data collection during the COVID-19 pandemic to monitor progress, providing policymakers with valuable information such as factors affecting the disease course, infectivity, and disease severity.

Sixth, VR can reduce infection rates and health care burdens. Especially for patients with reduced mobility, a VR headset can be used safely in the patient's home, which can reduce the need for hospital visits [122]. In teaching, the use of VR may allow simple tasks in clinical practice to be repeated multiple times in an immersive environment without constant supervision by medical staff, which could significantly reduce the cost of training facilities and trained medical staff [122].

In conclusion, the application of VR in CAM has great scientific, practical, and socioeconomic implications that can help people stay healthy and reduce the burden on the health care system.

9. Limitations of VR-Based CAM and Recommendations for How to Improve

Unfortunately, many challenges need to be overcome before this vision of clinical VR can be achieved. Setting up VR systems in clinical settings remains technically challenging and costly, requiring ongoing technical assistance, skill development, and infrastructure investment, which is especially challenging in resource-constrained settings [123].

While the initial cost of using VR continues to be a potential disadvantage, prices have decreased over time. As VR-enabling technologies and methods continue to evolve, the widespread adoption of VR in the CAM space will likely involve more advanced, less expensive systems and will be generally welcomed.

While conducting scientific research in CAM with VR, problems have been noted, including small sample sizes, a lack of methodological rigor, and lack of comparison groups. When designing a VR study, the use of a control condition and large enough sample sizes for sufficient power to detect an effect while considering possible treatment drop-out rates and projected attrition over all follow-up assessments are recommended [38]. A need exists for more well-powered and controlled studies comparing VR-based treatments to other treatments, including real-world medical records, randomized clinical trial data, and traditional medical texts.

10. Summary and Outlook

We previously assessed the acceptability of VR for hospitalized patients and found that most patients found the use of VR to be a positive and pleasurable experience, relieving anxiety and providing a form of escape from the confines of distressing illness experiences. Most patients reported that they would be willing to use VR again if given the opportunity.

The COVID-19 pandemic has accelerated the implementation of video- and audio-capable telemedicine infrastructures around the world. The advancement and widespread acceptance of these virtual communication technologies is a clear trend in the current pandemic. Clinicians, medical students, and researchers have had to adapt quickly to using a combination of VR and clinical applications, and in most cases, it works well.

As we have discussed, VR enables the better development of CAM in dynamic, complex, and realistic situations. VR methods continue to accrue validating results. This trend should continue as these methods become widely adopted and are extended to the study of different areas and a wider range of therapies.

However, despite rapid development, this relatively new field calls for replication and standardization as part of a theoretical framework to facilitate reflective, purposeful progress that is not driven solely by technology [33]. Training programs in CAM should also encourage students to consider how VR and other technological advances can better help us serve our patients and the public.

Going forward, we should continue to build on the positive contribution of VR to the field of CAM.

Conflicts of Interest

The authors declare that they have no conflicts of interest.

Authors' Contributions

All authors read and approved the final manuscript.

Acknowledgments

This study was supported by Disciplinary Layout Project of Natural Science Foundation of Jilin Province (No. 20200201412JC).

References

- [1] A. S. Rizzo and S. T. Koenig, "Is clinical virtual reality ready for primetime," *Neuropsychology*, vol. 31, no. 8, pp. 877–899, 2017.
- [2] M. J. Uddin and C. Zidorn, "Traditional herbal medicines against CNS disorders from Bangladesh," *Natural Product of Bioprospect*, vol. 10, no. 6, pp. 377–410, 2020.
- [3] L. J. Chavez, K. Kelleher, N. Slesnick et al., "Virtual reality meditation among youth experiencing homelessness: pilot randomized controlled trial of feasibility," *JMIR Mental Health*, vol. 7, no. 9, Article ID e18244, 2020.
- [4] V. Y. W. Cheng, C. M. Huang, J. Y. Liao et al., "Combination of 3-dimensional virtual reality and hands-on aromatherapy in improving institutionalized older adults' psychological health: quasi-experimental study," *Journal of Medical Internet Research*, vol. 22, no. 7, Article ID e17096, 2020.
- [5] J. L. Frydman, E. W. Choi, and E. C. Lindenberger, "Families of COVID-19 patients say goodbye on video: a structured approach to virtual end-of-life conversations," *Journal of Palliative Medicine*, vol. 23, no. 12, pp. 1564–1565, 2020.
- [6] Q. Gao, J. H. Chen, Y. Liu, F. Yang, and L. Q. Dai, "Acupoint application combined with virtual reality technology to relieve pain after circumcision in children," *Zhonghua Nan ke Xue*, vol. 27, no. 3, pp. 236–239, 2021.
- [7] C. C. Hsieh, P. S. Lin, W. C. Hsu et al., "The effectiveness of a virtual reality-based tai chi exercise on cognitive and physical function in older adults with cognitive impairment," *Dementia and Geriatric Cognitive Disorders*, vol. 46, no. 5–6, pp. 358–370, 2018.
- [8] H. Xiaowei, "The Research on the Regulation and Objective Expression of the Human Life Optimized Condition of TCM," *Traditional Chinese Medicine*, Chinese Ph.D. thesis, 2021.
- [9] S. Narayanan, J. Tennison, L. Cohen, C. Urso, B. Subramaniam, and E. Bruera, "Yoga-based breathing techniques for health care workers during COVID-19 pandemic: interests, feasibility, and acceptance," *Journal of Alternative & Complementary Medicine*, vol. 27, no. 8, pp. 706–709, 2021.
- [10] T. Thompson, T. Steffert, A. Steed, and J. Gruzelier, "A randomized controlled trial of the effects of hypnosis with 3-D virtual reality animation on tiredness, mood, and salivary cortisol," *International Journal of Clinical and Experimental Hypnosis*, vol. 59, no. 1, pp. 122–142, 2010.
- [11] T. N. Chao, A. S. Frost, R. M. Brody et al., "Creation of an interactive virtual surgical rotation for undergraduate medical education during the COVID-19 pandemic," *Journal of Surgical Education*, vol. 78, no. 1, pp. 346–350, 2021.
- [12] J. Chen, L. Xiao, L. P. Hu, X. Cao, S. Z. Li, and J. Y. Xie, "Application of the interaction teaching mode integrated with virtual anatomy platform in teaching Meridian and Acupoints," *Zhongguo Zhen Jiu*, vol. 39, no. 11, pp. 1235–1238, 2019.
- [13] H. Hofmann, C. Harding, J. Youm, and W. Wiechmann, "Virtual bedside teaching rounds with patients with COVID-19," *Medical Education*, vol. 54, no. 10, pp. 959–960, 2020.

- [14] J. Jiang, F. B. Wang, H. D. Guo et al., "Study on force feedback of acupuncture at Fengchi (GB 20)," *Zhongguo Zhen Jiu*, vol. 33, no. 10, pp. 939–942, 2013.
- [15] E. J. Margolin, R. J. Gordon, C. B. Anderson, and G. M. Badalato, "Reimagining the away rotation: a 4-week virtual subinternship in urology," *Journal of Surgical Education*, vol. 78, no. 5, pp. 1563–1573, 2021.
- [16] A. Mian and S. Khan, "Medical education during pandemics: a UK perspective," *BMC Medicine*, vol. 18, no. 1, p. 100, 2020.
- [17] X. D. Rao, H. B. Yu, J. H. Wu, W. Z. Zhong, and X. X. Huang, "Practical experience of virtual acupuncture and moxibustion teaching system in the operation teaching course of Acupuncture Sciences," *Zhongguo Zhen Jiu*, vol. 40, no. 8, pp. 877–879, 2020.
- [18] J. Saltzman, B. McGrath, K. White et al., "A student in my pocket: development of a virtual internal medicine hospital rotation during the COVID-19 pandemic," *Academic Medicine*, vol. 96, no. 11S, pp. S195–S196, 2021.
- [19] D. Soled, S. Goel, D. Barry et al., "Medical student mobilization during a crisis: lessons from a COVID-19 medical student response team," *Academic Medicine*, vol. 95, no. 9, pp. 1384–1387, 2020.
- [20] A. Tan, S. P. Ross, and K. Duerksen, "Death is not always a failure: outcomes from implementing an online virtual patient clinical case in palliative care for family medicine clerkship," *Medical Education Online*, vol. 18, no. 1, Article ID 22711, 2013.
- [21] M. Taubert, L. Webber, T. Hamilton, M. Carr, and M. Harvey, "Virtual reality videos used in undergraduate palliative and oncology medical teaching: results of a pilot study," *BMJ Supportive & Palliative Care*, vol. 9, no. 3, pp. 281–285, 2019.
- [22] S. Villa, H. Janeway, K. Preston-Suni et al., "An emergency medicine virtual clerkship: made for COVID, here to stay," *Western Journal of Emergency Medicine*, vol. 23, no. 1, pp. 33–39, 2021.
- [23] S. Wendt, Z. Abdullah, S. Barrett et al., "A virtual COVID-19 ophthalmology rotation," *Survey of Ophthalmology*, vol. 66, no. 2, pp. 354–361, 2021.
- [24] K. Yammine and C. Violato, "A meta-analysis of the educational effectiveness of three-dimensional visualization technologies in teaching anatomy," *Anatomical Sciences Education*, vol. 8, no. 6, pp. 525–538, 2015.
- [25] C. H. Kim, D. E. Yoon, Y. S. Lee, W. M. Jung, J. H. Kim, and Y. Chae, "Revealing associations between diagnosis patterns and acupoint prescriptions using medical data extracted from case reports," *Journal of Clinical Medicine*, vol. 8, no. 10, p. 1663, 2019.
- [26] A. L. Lee, M. DeBest, R. Koeniger-Donohue, S. R. Strowman, and S. E. Mitchell, "The feasibility and acceptability of using virtual world technology for interprofessional education in palliative care: a mixed methods study," *Journal of Interprofessional Care*, vol. 34, no. 4, pp. 461–471, 2020.
- [27] P. C. Doherty, "What have we learnt so far from COVID-19," *Nature Reviews Immunology*, vol. 21, no. 2, pp. 67–68, 2021.
- [28] H. Ahmed, M. Allaf, and H. Elghazaly, "COVID-19 and medical education," *The Lancet Infectious Diseases*, vol. 20, no. 7, pp. 777–778, 2020.
- [29] C. G. Ahlers, V. Lawson, J. Lee et al., "A virtual wellness and learning communities program for medical students during the COVID-19 pandemic," *Southern Medical Journal*, vol. 114, no. 12, pp. 807–811, 2021.
- [30] R. E. Weitzman, K. Wong, D. M. Worrall et al., "Incorporating virtual reality to improve otolaryngology resident wellness: one institution's experience," *The Laryngoscope*, vol. 131, no. 9, pp. 1972–1976, 2021.
- [31] E. Seabrook, R. Kelly, F. Foley et al., "Understanding how virtual reality can support mindfulness practice: mixed methods study," *Journal of Medical Internet Research*, vol. 22, no. 3, Article ID e16106, 2020.
- [32] D. E. Burt, "Virtual reality in anaesthesia," *British Journal of Anaesthesia*, vol. 75, no. 4, pp. 472–480, 1995.
- [33] Z. Trost, C. France, M. Anam, and C. Shum, "Virtual reality approaches to pain: toward a state of the science," *Pain*, vol. 162, no. 2, pp. 325–331, 2021.
- [34] B. Spiegel, G. Fuller, M. Lopez et al., "Virtual reality for management of pain in hospitalized patients: a randomized comparative effectiveness trial," *PLoS One*, vol. 14, no. 8, Article ID e0219115, 2019.
- [35] J. Mütterlein, "The three pillars of virtual reality? Investigating the roles of immersion, presence, and interactivity," in *Proceedings of the 51st Hawaii International Conference on System Sciences*, Hawaii, USA, 2018.
- [36] C. J. Bohil, B. Alicea, and F. A. Biocca, "Virtual reality in neuroscience research and therapy," *Nature Reviews Neuroscience*, vol. 12, no. 12, pp. 752–762, 2011.
- [37] N. Bruining, P. A. Cummins, and P. P. de Jaegere, "Addressing interventional periprocedural anxiety with virtual reality," *EuroIntervention*, vol. 16, no. 12, pp. e963–e965, 2020.
- [38] J. L. Maples-Keller, B. E. Bunnell, S. J. Kim, and B. O. Rothbaum, "The use of virtual reality technology in the treatment of anxiety and other psychiatric disorders," *Harvard Review of Psychiatry*, vol. 25, no. 3, pp. 103–113, 2017.
- [39] M. Andreatta and P. Pauli, "Contextual modulation of conditioned responses in humans: a review on virtual reality studies," *Clinical Psychology Review*, vol. 90, Article ID 102095, 2021.
- [40] C. Small and H. Laycock, "Are we near to making virtual reality the new reality in pain medicine," *Anaesthesia*, vol. 76, no. 5, pp. 590–593, 2021.
- [41] S. Bond, D. R. Laddu, C. Ozemek, C. J. Lavie, and R. Arena, "Exergaming and virtual reality for health: implications for cardiac rehabilitation," *Current Problems in Cardiology*, vol. 46, no. 3, Article ID 100472, 2021.
- [42] N. Masclet, L. Delbes, A. Voron, J. J. Temprado, and G. Montagne, "Acceptance of a virtual reality headset designed for fall prevention in older adults: questionnaire study," *Journal of Medical Internet Research*, vol. 22, no. 12, Article ID e20691, 2020.
- [43] Y. Luo, M. Li, J. Tang et al., "Design of a virtual reality interactive training system for public health emergency preparedness for major emerging infectious diseases: theory and framework," *JMIR Serious Games*, vol. 9, no. 4, Article ID e29956, 2021.
- [44] B. M. Kuehn, "Virtual and augmented reality put a twist on medical education," *JAMA*, vol. 319, no. 8, pp. 756–758, 2018.
- [45] S. G. Izard, J. A. Juanes, F. J. García Peñalvo, J. M. G. Estella, M. J. S. Ledesma, and P. Ruisoto, "Virtual reality as an educational and training tool for medicine," *Journal of Medical Systems*, vol. 42, no. 3, p. 50, 2018.
- [46] A. Pourmand, S. Davis, D. Lee, S. Barber, and N. Sikka, "Emerging utility of virtual reality as a multidisciplinary tool in clinical medicine," *Games for Health Journal*, vol. 6, no. 5, pp. 263–270, 2017.

- [47] F. J. Real, A. Meisman, and B. L. Rosen, "Usability matters for virtual reality simulations teaching communication," *Medical Education*, vol. 54, no. 11, pp. 1067-1068, 2020.
- [48] S. G. Izard, J. A. Juanes Méndez, and P. R. Palomera, "Virtual reality educational tool for human anatomy," *Journal of Medical Systems*, vol. 41, no. 5, p. 76, 2017.
- [49] R. Kurul, M. N. Ögün, A. Neriman Narin, Ş Avci, and B. Yazgan, "An alternative method for anatomy training: immersive virtual reality," *Anatomical Sciences Education*, vol. 13, no. 5, pp. 648-656, 2020.
- [50] M. Casanova, A. Clavreul, G. Soulard et al., "Immersive virtual reality and ocular tracking for brain mapping during awake surgery: prospective evaluation study," *Journal of Medical Internet Research*, vol. 23, no. 3, Article ID e24373, 2021.
- [51] G. Quero, A. Lapergola, L. Soler et al., "Virtual and augmented reality in oncologic liver surgery," *Surgical Oncology Clinics of North America*, vol. 28, no. 1, pp. 31-44, 2019.
- [52] T. Mahmood, M. A. Scaffidi, R. Khan, and S. C. Grover, "Virtual reality simulation in endoscopy training: current evidence and future directions," *World Journal of Gastroenterology*, vol. 24, no. 48, pp. 5439-5445, 2018.
- [53] K. Xu, N. Liu, J. Xu et al., "VRmol: an integrative web-based virtual reality system to explore macromolecular structure," *Bioinformatics*, vol. 37, no. 7, pp. 1029-1031, 2021.
- [54] X. H. Liu, T. Wang, J. P. Lin, and M. B. Wu, "Using virtual reality for drug discovery: a promising new outlet for novel leads," *Expert Opinion on Drug Discovery*, vol. 13, no. 12, pp. 1103-1114, 2018.
- [55] H. J. West, "Complementary and alternative medicine in cancer care," *JAMA Oncology*, vol. 4, no. 1, 2018.
- [56] A. M. Gallegos, H. F. Crean, W. R. Pigeon, and K. L. Heffner, "Meditation and yoga for posttraumatic stress disorder: a meta-analytic review of randomized controlled trials," *Clinical Psychology Review*, vol. 58, pp. 115-124, 2017.
- [57] K. Gasteratos, M. Papakonstantinou, A. Man, E. Babatsikos, A. Tamalonis, and J. Governan, "Adjunctive non-pharmacologic interventions for the management of burn pain: a systematic review," *Plastic and Reconstructive Surgery*, vol. 149, no. 5, pp. 985e-994e, 2022.
- [58] B. V. McConnell, M. Applegate, A. Keniston, B. Kluger, and E. H. Maa, "Use of complementary and alternative medicine in an urban county hospital epilepsy clinic," *Epilepsy and Behavior*, vol. 34, pp. 73-76, 2014.
- [59] T. Brandmeyer, A. Delorme, and H. Wahbeh, "The neuroscience of meditation: classification, phenomenology, correlates, and mechanisms," *Progress in Brain Research*, vol. 244, pp. 1-29, 2019.
- [60] K. Liu, E. Madrigal, J. S. Chung et al., "Preliminary study of virtual-reality-guided meditation for veterans with stress and chronic pain," *Alternative Therapies in Health & Medicine*, 2021.
- [61] M. M. Faraj, N. M. Lipanski, A. Morales et al., "A virtual reality meditative intervention modulates pain and the pain neuromatrix in patients with opioid use disorder," *Pain Medicine*, vol. 22, no. 11, pp. 2739-2753, 2021.
- [62] J. L. Hargett, S. D. McElwain, M. E. McNair, M. J. Palokas, B. S. Martin, and D. L. Adcock, "Virtual reality based guided meditation for patients with opioid tolerance and opioid use disorders," *Pain Management Nursing*, vol. 22, no. 3, 2022.
- [63] T. L. Ong, M. M. Ruppert, M. Akbar et al., "Improving the intensive care patient experience with virtual reality-A feasibility study," *Critical Care Explorations*, vol. 2, no. 6, Article ID e0122, 2020.
- [64] J. H. Kwon, N. Hong, K. K. Kim, J. Heo, J. J. Kim, and E. Kim, "Feasibility of a virtual reality program in managing test anxiety: a pilot study," *Cyberpsychology, Behavior, and Social Networking*, vol. 23, no. 10, pp. 715-720, 2020.
- [65] S. Y. Lee and J. Kang, "Effect of virtual reality meditation on sleep quality of intensive care unit patients: a randomised controlled trial," *Intensive and Critical Care Nursing*, vol. 59, Article ID 102849, 2020.
- [66] D. Mistry, J. Zhu, P. Tremblay et al., "Meditating in virtual reality: proof-of-concept intervention for posttraumatic stress," *Psychological Trauma: Theory, Research, Practice, and Policy*, vol. 12, no. 8, pp. 847-858, 2020.
- [67] L. Kolbe, A. Jaywant, A. Gupta, W. M. Vanderlind, and G. Jabbour, "Use of virtual reality in the inpatient rehabilitation of COVID-19 patients," *General Hospital Psychiatry*, vol. 71, pp. 76-81, 2021.
- [68] M. Billot, P. Jaglin, P. Rainville et al., "Hypnosis program effectiveness in a 12-week home care intervention to manage chronic pain in elderly women: a pilot trial," *Clinical Therapeutics*, vol. 42, no. 1, pp. 221-229, 2020.
- [69] M. P. Jensen, M. E. Mendoza, D. M. Ehde et al., "Effects of hypnosis, cognitive therapy, hypnotic cognitive therapy, and pain education in adults with chronic pain: a randomized clinical trial," *Pain*, vol. 161, no. 10, pp. 2284-2298, 2020.
- [70] M. J. Batty, S. Bonnington, B. K. Tang, M. B. Hawken, and J. H. Gruzelier, "Relaxation strategies and enhancement of hypnotic susceptibility: EEG neurofeedback, progressive muscle relaxation and self-hypnosis," *Brain Research Bulletin*, vol. 71, no. 1-3, pp. 83-90, 2006.
- [71] S. W. Askay, D. R. Patterson, and S. R. Sharar, "Virtual reality HYPNOSIS," *Contemporary Hypnosis*, vol. 26, no. 1, pp. 40-47, 2009.
- [72] F. Rousseaux, A. Bicego, D. Ledoux et al., "Hypnosis associated with 3D immersive virtual reality technology in the management of pain: a review of the literature," *Journal of Pain Research*, vol. 13, pp. 1129-1138, 2020.
- [73] D. R. Patterson, J. R. Tinenenko, A. E. Schmidt, and S. R. Sharar, "Virtual reality hypnosis: a case report," *International Journal of Clinical and Experimental Hypnosis*, vol. 52, no. 1, pp. 27-38, 2004.
- [74] D. R. Patterson, H. G. Hoffman, G. Chambers et al., "Hypnotic enhancement of virtual reality distraction analgesia during thermal pain: a randomized trial," *International Journal of Clinical and Experimental Hypnosis*, vol. 69, no. 2, pp. 225-245, 2021.
- [75] D. R. Patterson, M. P. Jensen, S. A. Wiechman, and S. R. Sharar, "Virtual reality hypnosis for pain associated with recovery from physical trauma," *International Journal of Clinical and Experimental Hypnosis*, vol. 58, no. 3, pp. 288-300, 2010.
- [76] B. Chi, B. Chau, E. Yeo, and P. Ta, "Virtual reality for spinal cord injury-associated neuropathic pain: systematic review," *Annals of Physical and Rehabilitation Medicine*, vol. 62, no. 1, pp. 49-57, 2019.
- [77] N. Touil, A. Pavlopoulou, M. Momeni et al., "Evaluation of virtual reality combining music and a hypnosis session to reduce anxiety before hand surgery under axillary plexus block: a prospective study," *International Journal of Clinical Practice*, vol. 75, no. 12, Article ID e15008, 2021.
- [78] F. Rousseaux, M. E. Faymonville, A. S. Nyssen et al., "Can hypnosis and virtual reality reduce anxiety, pain and fatigue among patients who undergo cardiac surgery: a randomised controlled trial," *Trials*, vol. 21, no. 1, p. 330, 2020.

- [79] V. Enea, I. Dafinoiu, D. Opriş, and D. David, "Effects of hypnotic analgesia and virtual reality on the reduction of experimental pain among high and low hypnotizables," *International Journal of Clinical and Experimental Hypnosis*, vol. 62, no. 3, pp. 360–377, 2014.
- [80] U. Münch, H. Müller, T. Deffner et al., "Recommendations for the support of suffering, severely ill, dying or grieving persons in the corona pandemic from a palliative care perspective: recommendations of the German society for palliative medicine (DGP), the German interdisciplinary association for intensive and emergency medicine (DIVI), the federal association for grief counseling (BVT), the working group for psycho-oncology in the German cancer society, the German association for social work in the healthcare system (DVSG) and the German association for systemic therapy, counseling and family therapy (DGSF)," *Schmerz, Der*, vol. 34, no. 4, pp. 303–313, 2020.
- [81] S. S. Wang, W. Z. Teo, W. Z. Teo, and Y. W. Chai, "Virtual reality as a bridge in palliative care during COVID-19," *Journal of Palliative Medicine*, vol. 23, no. 6, p. 756, 2020.
- [82] J. R. Hanna, E. Rapa, L. J. Dalton et al., "A qualitative study of bereaved relatives end of life experiences during the COVID-19 pandemic," *Palliative Medicine*, vol. 35, no. 5, pp. 843–851, 2021.
- [83] J. R. Hanna, E. Rapa, L. J. Dalton et al., "Health and social care professionals' experiences of providing end of life care during the COVID-19 pandemic: a qualitative study," *Palliative Medicine*, vol. 35, no. 7, pp. 1249–1257, 2021.
- [84] B. A. Calton, M. W. Rabow, L. Branagan et al., "Top ten tips palliative care clinicians should know about telepalliative care," *Journal of Palliative Medicine*, vol. 22, no. 8, pp. 981–985, 2019.
- [85] L. Aspreco, C. D. Blinderman, A. Berlin et al., "Virtual interinstitutional palliative care consultation during the COVID-19 pandemic in New York city," *Journal of Palliative Medicine*, vol. 24, no. 9, pp. 1387–1390, 2021.
- [86] A. Taylor, T. French, and S. Raman, "Developing design principles for a Virtual Hospice: improving access to care," *BMJ Supportive & Palliative Care*, vol. 8, no. 1, pp. 53–57, 2018.
- [87] J. A. Ouellet, E. H. Prsic, R. A. Spear et al., "An observational case series of targeted virtual geriatric medicine and palliative care consults for hospitalized older adults with COVID-19," *Annals of Palliative Medicine*, vol. 0, no. 0, pp. 0–6306, 2021.
- [88] K. Bloom-Feshbach, R. E. Berger, R. P. Dubroff, M. L. McNairy, A. Kim, and A. T. Evans, "The virtual hospitalist: a critical innovation during the COVID-19 crisis," *Journal of General Internal Medicine*, vol. 36, no. 6, pp. 1771–1774, 2021.
- [89] M. Robertson, "Experiences of time: a qualitative inquiry into experiences of time as described by palliative care inpatients," *Palliative & Supportive Care*, vol. 13, no. 1, pp. 67–73, 2015.
- [90] K. Niki, Y. Okamoto, I. Maeda et al., "A novel palliative care approach using virtual reality for improving various symptoms of terminal cancer patients: a preliminary prospective, multicenter study," *Journal of Palliative Medicine*, vol. 22, no. 6, pp. 702–707, 2019.
- [91] M. Kabir, J. L. Rice, S. H. Bush et al., "A mixed-methods pilot study of 'LIFEView' audiovisual technology: virtual travel to support well-being and quality of life in palliative and end-of-life care patients," *Palliative Medicine*, vol. 34, no. 7, pp. 954–965, 2020.
- [92] R. M. Baños, M. Espinoza, A. García-Palacios et al., "A positive psychological intervention using virtual reality for patients with advanced cancer in a hospital setting: a pilot study to assess feasibility," *Supportive Care in Cancer*, vol. 21, no. 1, pp. 263–270, 2013.
- [93] P. D. Austin, P. J. Siddall, and M. R. Lovell, "Feasibility and acceptability of virtual reality for cancer pain in people receiving palliative care: a randomised cross-over study," *Supportive Care in Cancer*, vol. 30, no. 5, pp. 3995–4005, 2022.
- [94] T. Johnson, L. Bauler, D. Vos et al., "Virtual reality use for symptom management in palliative care: a pilot study to assess user perceptions," *Journal of Palliative Medicine*, vol. 23, no. 9, pp. 1233–1238, 2020.
- [95] A. Lloyd and E. Haraldsdottir, "Virtual reality in hospice: improved patient well-being," *BMJ Supportive & Palliative Care*, vol. 11, no. 3, pp. 344–350, 2021.
- [96] S. Moscato, V. Sichi, A. Giannelli et al., "Virtual reality in home palliative care: brief report on the effect on cancer-related symptomatology," *Frontiers in Psychology*, vol. 12, Article ID 709154, 2021.
- [97] K. Weingarten, F. Macapagal, and D. Parker, "Virtual reality: endless potential in pediatric palliative care: a case report," *Journal of Palliative Medicine*, vol. 23, no. 1, pp. 147–149, 2020.
- [98] A. W. K. Chan, S. Y. Chair, D. T. F. Lee et al., "Tai Chi exercise is more effective than brisk walking in reducing cardiovascular disease risk factors among adults with hypertension: a randomised controlled trial," *International Journal of Nursing Studies*, vol. 88, pp. 44–52, 2018.
- [99] F. Li, P. Harmer, K. Fitzgerald et al., "Effectiveness of a therapeutic tai ji quan intervention vs a multimodal exercise intervention to prevent falls among older adults at high risk of falling: a randomized clinical trial," *JAMA Internal Medicine*, vol. 178, no. 10, pp. 1301–1310, 2018.
- [100] F. Li, P. Harmer, J. Voit, and L. S. Chou, "Implementing an online virtual falls prevention intervention during a public health pandemic for older adults with mild cognitive impairment: a feasibility trial," *Clinical Interventions in Aging*, vol. 16, pp. 973–983, 2021.
- [101] L. M. Sawyer, L. M. Brown, S. Y. Lensing et al., "Rapid conversion of Tai Chi classes from face-to-face to virtual during the COVID-19 pandemic: a quality improvement project," *Nursing Forum*, vol. 57, no. 3, pp. 491–496, 2022.
- [102] C. C. Wang, K. Li, A. Choudhury, and S. Gaylord, "Trends in yoga, tai chi, and qigong use among US adults, 2002–2017," *American Journal of Public Health*, vol. 109, no. 5, pp. 755–761, 2019.
- [103] S. J. Xiang, M. H. Li, C. O. Chan et al., "Altered metabolites in Guinea pigs with allergic asthma after acupoint sticking therapy: new insights from a metabolomics approach," *Phytomedicine*, vol. 54, pp. 182–194, 2019.
- [104] S. Hines, E. Steels, A. Chang, and K. Gibbons, "Aromatherapy for treatment of postoperative nausea and vomiting," *Cochrane Database of Systematic Reviews*, vol. 3, no. 3, Article ID CD007598, 2018.
- [105] E. L. Ball, B. Owen-Booth, A. Gray, S. D. Shenkin, J. Hewitt, and J. McCleery, "Aromatherapy for dementia," *Cochrane Database of Systematic Reviews*, vol. 8, no. 8, Article ID CD003150, 2020.
- [106] H. Cramer, R. Lauche, P. Klose, S. Lange, J. Langhorst, and G. J. Dobos, "Yoga for improving health-related quality of life, mental health and cancer-related symptoms in women

- diagnosed with breast cancer,” *Cochrane Database of Systematic Reviews*, vol. 1, no. 1, Article ID CD010802, 2017.
- [107] L. S. Wieland, N. Skoetz, K. Pilkington, R. Vempati, C. R. D’Adamo, and B. M. Berman, “Yoga treatment for chronic non-specific low back pain,” *Cochrane Database of Systematic Reviews*, vol. 1, no. 1, Article ID CD010671, 2017.
- [108] R. Knoerl, A. Giobbie-Hurder, J. Berfield et al., “Yoga for chronic chemotherapy-induced peripheral neuropathy pain: a pilot, randomized controlled trial,” *J Cancer Surviv*, vol. 16, no. 4, pp. 882–891, 2021.
- [109] K. L. Kwekkeboom, C. H. Cherwin, J. W. Lee, and B. Wanta, “Mind-body treatments for the pain-fatigue-sleep disturbance symptom cluster in persons with cancer,” *Journal of Pain and Symptom Management*, vol. 39, no. 1, pp. 126–138, 2010.
- [110] K. M. Trevino, N. Raghunathan, S. Latte-Naor et al., “Rapid deployment of virtual mind-body interventions during the COVID-19 outbreak: feasibility, acceptability, and implications for future care,” *Supportive Care in Cancer*, vol. 29, no. 2, pp. 543–546, 2021.
- [111] A. Brungardt, A. Wibben, A. F. Tompkins et al., “Virtual reality-based music therapy in palliative care: a pilot implementation trial,” *Journal of Palliative Medicine*, vol. 24, no. 5, pp. 736–742, 2021.
- [112] S. Shahrbanian, S. Alikhani, M. Ahmadi Kakavandi, and A. C. Hackney, “Physical activity for improving the immune system of older adults during the COVID-19 pandemic,” *Alternative Therapies in Health & Medicine*, vol. 26, no. S2, pp. 117–125, 2020.
- [113] B. Choi, L. Jegatheeswaran, A. Minocha, M. Alhilani, M. Nakhoul, and E. Mutengesa, “The impact of the COVID-19 pandemic on final year medical students in the United Kingdom: a national survey,” *BMC Medical Education*, vol. 20, no. 1, p. 206, 2020.
- [114] M. Paci, G. Mini, M. Marchettini, and F. Ferrarello, “The Salford Gait Tool: does the clinical experience of the raters influence the inter-rater reliability,” *Developmental Neuro-rehabilitation*, vol. 21, no. 2, pp. 131–132, 2018.
- [115] S. Chandra, C. Laoteppitaks, N. Mingioni, and D. Papanagnou, “Zooming-out COVID-19: virtual clinical experiences in an emergency medicine clerkship,” *Medical Education*, vol. 54, no. 12, pp. 1182–1183, 2020.
- [116] R. J. Wilcha, “Effectiveness of virtual medical teaching during the COVID-19 crisis: systematic review,” *JMIR Medical Education*, vol. 6, no. 2, Article ID e20963, 2020.
- [117] W. Huang, Y. Yang, L. Yang, and M. Yan, “Application of acupuncture acupoint visual teaching system by neural regulation,” *World Neurosurgery*, vol. 138, pp. 619–628, 2020.
- [118] T. L. Griebing, “Sexuality and aging: a focus on lesbian, gay, bisexual, and transgender (LGBT) needs in palliative and end of life care,” *Current Opinion in Supportive and Palliative Care*, vol. 10, no. 1, pp. 95–101, 2016.
- [119] J. Bateman, M. E. Allen, J. Kidd, N. Parsons, and D. Davies, “Virtual patients design and its effect on clinical reasoning and student experience: a protocol for a randomised factorial multi-centre study,” *BMC Medical Education*, vol. 12, no. 1, p. 62, 2012.
- [120] I. Pantziaras, U. Fors, and S. Ekblad, “Innovative training with virtual patients in transcultural psychiatry: the impact on resident psychiatrists’ confidence,” *PLoS One*, vol. 10, no. 3, Article ID e0119754, 2015.
- [121] Y. S. Lee, Y. Ryu, D. E. Yoon et al., “Commonality and specificity of acupuncture point selections,” *Evidence-based Complementary and Alternative Medicine*, vol. 2020, pp. 1–10, 2020.
- [122] A. W. K. Yeung, A. Tosevska, E. Klager et al., “Virtual and augmented reality applications in medicine: analysis of the scientific literature,” *Journal of Medical Internet Research*, vol. 23, no. 2, Article ID e25499, 2021.
- [123] Y. Chávarri-Guerra, W. A. Ramos-López, A. Covarrubias-Gómez et al., “Providing supportive and palliative care using telemedicine for patients with advanced cancer during the COVID-19 pandemic in Mexico,” *The Oncologist*, vol. 26, no. 3, pp. e512–e515, 2021.

Research Article

Establishing a Regulatory Science System for Supervising the Application of Artificial Intelligence for Traditional Chinese Medicine: A Methodological Framework

Ying He ¹, Qian Wen ¹, Ying Wang ², Juan Li,³ Ning Li,¹ Rongjiang Jin,³ Nian Li ², and Yonggang Zhang ^{4,5}

¹Department of Integrated Traditional and Western Medicine, West China Hospital, Sichuan University, Chengdu, China

²Department of Medical Administration, West China Hospital, Sichuan University, Chengdu, China

³School of Health Preservation and Rehabilitation, Traditional Chinese Medicine of Chengdu University, Chengdu, Sichuan, China

⁴Department of Periodical Press, West China Hospital, Sichuan University, Chengdu, Sichuan, China

⁵Department of Evidence-based Medicine and Clinical Epidemiology, West China Hospital, Sichuan University, Chengdu, China

Correspondence should be addressed to Nian Li; linian@wchscu.cn and Yonggang Zhang; jebm_zhang@yahoo.com

Received 18 March 2022; Accepted 11 May 2022; Published 2 June 2022

Academic Editor: Lu Zhang

Copyright © 2022 Ying He et al. This is an open access article distributed under the Creative Commons Attribution License, which permits unrestricted use, distribution, and reproduction in any medium, provided the original work is properly cited.

In this study, we reported a methodological framework for the development of a guideline for establishing a regulatory science system for supervising the application of artificial intelligence for traditional Chinese medicine (TCM). It introduced all of the key steps for developing the guideline as follows: the composition of the guideline expert groups, summary steps, agency, purpose, targeted population, writing, publishing, updating, dissemination, dynamic monitoring, and evaluation. The guideline will provide the basis for national authorities to effectively regulate artificial intelligence technology and enrich the supervisory system for TCM, and it will be of great significance to TCM.

1. Introduction

Traditional Chinese medicine (TCM) is a medical and pharmaceutical system with a long history, unique theory, and technical methods, which made great contributions to human health [1]. As a result of dissemination of TCM, domestic and foreign scholars have conducted many scientific research studies, and its influence has gradually expanded [2, 3]. Many landmark research studies have been published in top journals, including Journal of the American Medical Association (JAMA), Annals of Internal Medicine, and JAMA Internal Medicine [4–6]. Thus, the academic influence of TCM has greatly improved. However, its international influence is still encountering challenges, which are mainly reflected in the reluctance of some disciplines to accept the validity of the recognition of TCM [7, 8].

As a result of the development of computer science, the application of artificial intelligence (AI) can effectively transform the combined online and offline medical model to achieve multidisciplinary integration, multipath diagnosis, and treatment of the wisdom of the Internet medical, which can improve the efficiency of diagnosis, treatment, and management [9, 10]. In recent years, interest in AI has increased in the application of data mining, computer-aided diagnosis, intelligent decision therapy, and intelligent rehabilitation of TCM [11]. AI can convert TCM's classical ancient books and clinical treatment experience into data and establish an extremely large TCM database to provide a basis for scientifically explaining TCM treatments. Doing this can greatly improve the overall service level of TCM, reduce the number of medical resources required, and promote the development of TCM [12, 13].

As a result of the wide application of AI technology in the construction of an evaluation system, disease model construction, medical device innovation, and public health crisis response, the establishment of a regulatory science system for supervising the application of AI has become a potential research topic [14, 15]. Until now, no such study has been conducted in this field, and no such guideline has been developed, and it is urgent to develop a guideline in this field. Thus, we will develop such a guideline. In order to make the guideline transparent [16, 17], we reported the current methodological framework. It will help to establish a regulatory science system and to help in the application of AI technology to TCM. It will also fill research gaps and help TCM serve human health [18].

2. Methods

2.1. Summary Steps of Developing Guideline. The guideline's development will follow the latest definitions of guidelines provided by the United States Institute of Medicine [19], which are based on the methodology developed by the World Health Organization standard guidance [20] and the six major areas of the Appraisal of Guidelines for Research and Evaluation (AGREE II) [21]. We will also use the Reporting Items for Practice Guidelines in Healthcare (RIGHT) [22] and other international standards to help us develop the guideline [23–26]. The key steps of the guideline are shown in Figure 1.

The development of the guideline consists of four phases (Figure 1). In phase 1, we will form the guideline groups and construct the problems and outcomes. Additionally, we will survey experts from universities and scientific research institutions. In phase 2, we will conduct a systematic review of all available guidelines, documents, and papers on supervising the application of AI to TCM and provide evidence for developing items of the guideline. In phase 3, first, we will draft the initial version of the guideline based on the results from the Delphi method and consensus meeting. Subsequently, we will modify, validate, and finalize the guideline through multiple steps. In phase 4, we will establish the regulatory scientific evidence base, dynamic update, and evaluation protocol.

2.2. Explanations of the Terms. TCM [27]: traditional Chinese medicine (TCM) is an alternative medical practice drawn from traditional medicine in China. It includes various forms of herbal medicine, acupuncture, cupping therapy, Guasha, massage (Tuina), bonesetter (Die-Da), exercise (Qigong), and dietary therapy.

AI [28]: artificial intelligence (AI) is a broad umbrella term used to encompass a wide variety of subfields dedicated to creating algorithms to perform tasks that mimic human intelligence. It combines human abilities of learning, reasoning, perception, and an understanding of natural language through computer programs.

Regulatory science [29]: regulatory science is the science of developing new tools, standards, and approaches derived from various scientific disciplines to assess the safety,

efficacy, quality, and performance of all Food and Drug Administration (FDA)-regulated products.

Living guideline [30]: A living guideline is a novel approach that operates through, for example, dynamic monitoring, timely inclusion of new evidence, and live updates of recommendations to effectively improve the timeliness of clinical guidelines by periodically obtaining clinical evidence and updating the results of systematic reviews in a timely manner.

2.3. Ethics and Dissemination. The guideline will not require ethical approval because no data linked to individual patient information will be used in our study. Additionally, the findings will be disseminated through peer-reviewed journals or conferences.

2.4. Agency of the Guideline. The guideline will be developed by members from editorial boards of the Journal of Evidence-Based Medicine and the Chinese Journal of Evidence-Based Medicine, in collaboration with a large number of institutions in China, and we will invite experts from multiple units outside of China.

2.5. Guideline Teams. The guideline teams consist of a guideline steering committee, guideline expert group, guideline secretariat group, and external review group. To ensure the authority and comprehensiveness of the guideline, the guideline teams will include experts from main cities around China. Additionally, we will invite regulatory science experts from countries out of China to participate. Members of the guideline steering committee, guideline expert group, guideline external review group, and secretariat group should complete a declaration of interest and declare any conflict of interests before formally participating in the work related to the development of the guideline. All members' statements of interest will be reported in the final guideline document.

2.6. Patient and Public Involvement Statement. The current study is a methodological study, and patient and public involvement is not needed.

2.7. Purpose and Targeted Population of the Guideline. The purpose of the guideline is to establish a regulatory science system for supervising the application of AI to TCM. The guideline will focus on the scientific regulatory approach, comprehensive evaluation, and dynamic updating of the application of AI to TCM. This guideline applies to personnel at all levels who conduct regulatory science research on the application of AI to TCM, including policy-makers, medical device managers, clinicians, nurses, computer scientists, and journal editors.

2.8. Clarify the Guideline Questions. Guiding questions will be designed by the guideline steering committee using the relevant literature and study objectives. A three-round Delphi

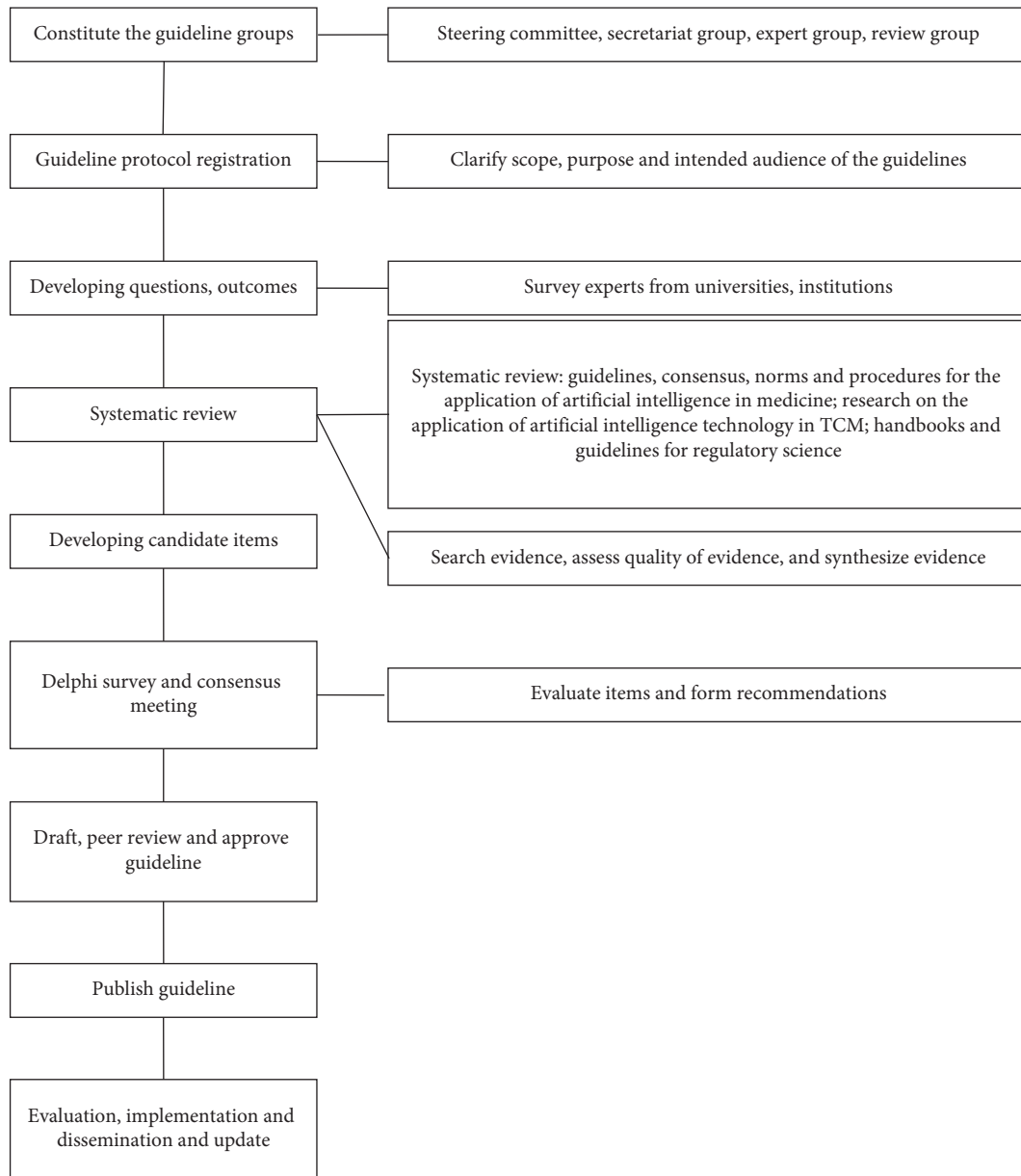


FIGURE 1: Key steps of methodology of the guideline.

study will be conducted to determine the issues that refer to the guidance and the development method of the regulatory scientific system. Each item will be rated by using a five-point Likert scale (not important, of little importance, neutral, important, and very important). The mean value (X), standard deviation (SD), coefficient of variation (CV), and R value will be calculated for each attribute.

2.9. Search Strategy. The search databases will include PubMed, the Cochrane Library, Embase, Chinese Biomedical Literature Service System, China National Knowledge Infrastructure, WanFang Data, China Science and Technology Journal Database, UptoDate, Guideline Central, National Guideline Clearinghouse, Guidelines International Network, and the National Institute for Health and Care Excellence. The

following databases will also be searched: NHS Economic Evaluation Database and Health Technology Assessment. Additionally, information will be obtained from official websites, such as the health authorities' official websites of the international and local organizations and universities, Food and Drug Administration, and the official website of the health insurance department or relevant industry association. Finally, we will search Google, Baidu, and other search engines to obtain other literature. According to the retrieval strategy formulated in advance, articles from the above databases will be imported into the Endnote X9 software.

Subject words and text words will be searched. Search terms will include guideline, consensus, standard, process, artificial intelligence, machine learning, traditional Chinese medicine, TCM, regulatory science, and handbook. There will be no limitation to the types of included studies. The

languages will be limited to English and Chinese. The search will be performed in May 2022, and the search will be updated when necessary.

2.10. Survey of Problems. We will conduct a survey of problems from TCM universities and research institutions regarding the application of AI to TCM. It will help us to understand the current scenario and problems regarding the application of AI to TCM.

2.11. Literature Screening and Data Extraction. To achieve the stability and consistency of literature retrieval, pre-retrieval will be performed to achieve a unified standard. The inclusion criteria will be as follows: any study that is helpful to establish a regulatory science system for the application of artificial intelligence in TCM, including guideline, consensus, standard, process, article, or review. The exclusion criteria will be as follows: the study does not report the clear method for establishing a guideline; it does not involve a regulatory science system. When necessary, the criteria will be revised. Two researchers will independently select and screen the studies according to inclusion criteria and exclusion criteria. A third researcher will be consulted to resolve the disagreement. These two researchers will independently extract data, and discrepancies will be resolved by consensus. If information cannot be retrieved, the corresponding author will be contacted.

2.12. Systematic Review. The quality of the included studies will be assessed according to the types of studies. The risk of bias (ROB) will be assessed using ROB 2.0 for RCTs [31]. The Newcastle–Ottawa Scale [32] will be used to assess the quality of cohort studies or case-control studies. The AGREE II will be used to assess the quality of guidelines [33]. A Measurement Tool to Assess Systematic Reviews 2 (AMSTAR 2) will be used to assess the quality of systematic reviews and meta-analyses [34]. The process will be performed by two independent researchers. Disagreement will be discussed or consulted by a third researcher. A systematic review will be performed to assess the potential studies and to provide evidence to develop the guideline. It will also help to provide recommendations for the guideline.

2.13. Generation of a List of Candidate Items. The candidate items in the guideline will be developed using the Delphi method. We will develop the candidate items before sending them the questionnaire. A two-round Delphi questionnaire and a final consensus meeting will be employed [35, 36]. An item will be recommended if the votes are above 50%. The remaining scenarios will be considered if no consensus is reached, and recommendations with no consensus will be subjected to the next round of voting. A subsequent review of the results will be conducted by the steering committee to identify statements where a consensus is almost reached. With the agreement of two-thirds of the members of the consensus expert group, the steering committee may revise and improve

important issues existing in the recommendations, and the guideline secretariat group will faithfully record the entire revision process.

2.14. Writing, Publishing, and Updating the Guideline. Once the recommendations are approved, the guideline steering committee will write the guideline according to the RIGHT (<http://right-statement.org>) reporting standard. The draft guideline will be submitted to the steering committee for review and approval. Then, the introduction and announcement of the guideline will be published. The guideline will also be presented and discussed at relevant professional society academic meetings and through publication in scientific journals. We will establish the regulatory scientific evidence systematic based on the guideline. The guideline will be updated according to the feedback on the actual operation of the guideline and the latest research results in relevant fields.

3. Discussion

Developing a guideline for establishing a regulatory science system for supervising the application of AI to TCM is urgent because the development of AI is so fast. The future guideline will be developed by a multidisciplinary team of experts. To help the guideline, opinions will be obtained from experts, policy-makers, and users. The guideline developers will establish an update and evaluation process to update the guideline and finally help supervise the application of AI in TCM. The guideline will not only track new evidence in real time, promote the practical application of the best research evidence, and implement scientific regulation but also save a large number of resources and optimize the guideline formulation and evaluation process. The guideline will be a new innovation in TCM.

In conclusion, the current study describes the steps of formulating a guideline for the application of AI to TCM. The guideline will be developed in strictly accordance with the standards of an evidence-based guideline. The results will be used as a context for analyzing general strengths and gaps in the current quality of evidence in the application of AI to TCM.

Data Availability

The data used to support this study are included within the article and available from the corresponding author upon request.

Disclosure

The funding bodies did not play roles in study design, data collection, analysis, interpretation of results, and the manuscript.

Conflicts of Interest

The authors declare that they have no conflicts of interest.

Authors' Contributions

Yonggang Zhang provided ideas and designed the manuscript. Ying He and Yonggang Zhang wrote the first draft of the manuscript. Qian Wen, Ying Wang, Juan Li, Nian Li, and Ning Li revised the manuscript. All authors approved the submitted version. Ying He and Qian Wen contributed equally to this work.

Acknowledgments

The authors thank Maxine Garcia, PhD, from Liwen Bianji (Edanz) (<https://www.liwenbianji.cn/>), for editing the English text of a draft of this manuscript. The authors have registered the methodological framework for this guideline on the Global Practice Guidelines Registry Platform (registration number: IPGRP-2021CN297). This study was supported by the National Natural Science Foundation of China (82174227).

References

- [1] G. Tian, C. Zhao, X. Zhang et al., "Evidence-based traditional Chinese medicine research: two decades of development, its impact, and breakthrough," *Journal of Evidence-Based Medicine*, vol. 14, no. 1, pp. 65–74, 2021.
- [2] H. Liu and Z. g. Ma, "Analysis on situation of traditional Chinese medicine development and protection strategies in China," *Chinese Journal of Integrative Medicine*, vol. 26, no. 12, pp. 943–946, 2020.
- [3] W. Y. Wang, H. Zhou, Y. F. Wang, B. S. Sang, and L. Liu, "Current policies and measures on the development of traditional Chinese medicine in China," *Pharmacological Research*, Article ID 105187, 2020.
- [4] L. Zhao, D. Li, H. Zheng et al., "Acupuncture as adjunctive therapy for chronic stable Angina: a randomized clinical trial," *JAMA Internal Medicine*, vol. 179, no. 10, pp. 1388–1397, 2019.
- [5] J. W. Yang, L. Q. Wang, X. Zou et al., "Effect of acupuncture for postprandial distress syndrome: a randomized clinical trial," *Annals of Internal Medicine*, vol. 172, no. 12, pp. 777–785, 2020.
- [6] D. L. Hershman, J. M. Unger, H. Greenlee et al., "Effect of acupuncture vs sham acupuncture or waitlist control on joint pain related to aromatase inhibitors among women with early-stage breast cancer: a randomized clinical trial," *Journal of the American Medical Association*, vol. 320, no. 2, p. 167, 2018.
- [7] Y. Yang, K. Tian, G. Bai, X. Zhu, X. Yu, and L. Shi, "Health technology assessment in traditional Chinese medicine in China: current status, opportunities, and challenges," *Global Health Journal*, vol. 3, no. 4, pp. 89–93, 2019.
- [8] A. X. Lin, G. Chan, Y. Hu et al., "Internationalization of traditional Chinese medicine: current international market, internationalization challenges and prospective suggestions," *Chinese Medicine*, vol. 13, no. 1, p. 9, 2018.
- [9] S. Vollmer, B. A. Mateen, G. Bohner et al., "Machine learning and artificial intelligence research for patient benefit: 20 critical questions on transparency, replicability, ethics, and effectiveness," *BMJ*, vol. 368, Article ID l6927, 2020.
- [10] X. Liu, S. C. Rivera, D. Moher, M. J. Calvert, and A. K. Denniston, "Reporting guidelines for clinical trial reports for interventions involving artificial intelligence: the CONSORT-AI extension," *The Lancet Digital Health*, vol. 2, no. 10, Article ID m3164, 2020.
- [11] H. Zhang, W. Ni, J. Li, and J. Zhang, "Artificial intelligence-based traditional Chinese medicine assistive diagnostic system: validation study," *JMIR Medical Informatics*, vol. 8, no. 6, Article ID e17608, 2020.
- [12] X. Chu, B. Sun, Q. Huang, S. Peng, Y. Zhou, and Y. Zhang, "Quantitative knowledge presentation models of traditional Chinese medicine (TCM): a review," *Artificial Intelligence in Medicine*, vol. 103, Article ID 101810, 2020.
- [13] G. Arji, R. Safdari, H. Rezaeizadeh, A. Abbassian, M. Mokhtaran, and M. Hossein Ayati, "A systematic literature review and classification of knowledge discovery in traditional medicine," *Computer Methods and Programs in Biomedicine*, vol. 168, pp. 39–57, 2019.
- [14] H. D. Marble, R. Huang, S. N. Dudgeon et al., "A regulatory science initiative to harmonize and standardize digital pathology and machine learning processes to speed up clinical innovation to patients," *Journal of Pathology Informatics*, vol. 11, no. 1, p. 22, 2020.
- [15] D. B. Kramer and A. S. Kesselheim, "Trust and transparency in medical device regulation," *BMJ*, vol. 365, Article ID l4166, 2019.
- [16] Q. Wang, N. Li, J. Li et al., "A protocol of a guideline to establish the evidence ecosystem of acupuncture," *Frontiers of Medicine*, vol. 8, Article ID 711197, 2022.
- [17] Y. He, J. Li, Y. Li et al., "Strengthening the quality of clinical trials of acupuncture: a guideline protocol," *BMJ Open*, vol. 12, no. 1, Article ID e053312, 2022.
- [18] Z. Liang, Y. Lai, M. Li et al., "Applying regulatory science in traditional Chinese medicines for improving public safety and facilitating innovation in China: a scoping review and regulatory implications," *Chinese Medicine*, vol. 16, no. 1, p. 23, 2021.
- [19] IOMU Trustworthy and C. P. Guidelines, *Clinical Practice Guidelines We Can Trust*, National Academies Press, Washington, DC, USA, 2011.
- [20] D. Sinclair, R. Isba, T. Kredon, B. Zani, H. Smith, and P. Garner, "World health organization guideline development: an evaluation," *PLoS One*, vol. 8, no. 5, Article ID e63715, 2013.
- [21] Mc Brouwers, K. Kerkvliet, and K. Spithoff, "The AGREE reporting checklist: a tool to improve reporting of clinical practice guidelines," *BMJ*, Article ID i1152, 2016.
- [22] Y. Chen, K. Yang, A. Marušić et al., "A reporting tool for practice guidelines in health Care: the RIGHT statement," *Annals of Internal Medicine*, vol. 166, no. 2, p. 128, 2017.
- [23] P. O. Vandvik and L. Brandt, "Future of evidence ecosystem series: evidence ecosystems and learning health systems: why bother?" *Journal of Clinical Epidemiology*, vol. 123, pp. 166–170, 2020.
- [24] I. Boutron, P. Créquit, H. Williams, J. Meerpohl, J. C. Craig, and P. Ravaud, "Future of evidence ecosystem series: 1. Introduction evidence synthesis ecosystem needs dramatic change," *Journal of Clinical Epidemiology*, vol. 123, pp. 135–142, 2020.
- [25] E. A. Akl, N. R. Haddaway, G. Rada, and T. Lotfi, "Future of evidence ecosystem series: evidence synthesis 2.0: when systematic, scoping, rapid, living, and overviews of reviews come together," *Journal of Clinical Epidemiology*, vol. 123, pp. 162–165, 2020.
- [26] P. Ravaud, P. Créquit, H. C. Williams, J. Meerpohl, J. C. Craig, and I. Boutron, "Future of evidence ecosystem series: 3. from an evidence synthesis ecosystem to an evidence ecosystem," *Journal of Clinical Epidemiology*, vol. 123, pp. 153–161, 2020.

- [27] C. Liu and M. Gu, "Protecting traditional knowledge of Chinese medicine: concepts and proposals," *Frontiers of Medicine*, vol. 5, no. 2, pp. 212–218, 2011.
- [28] G. S. Collins and K. G. M. Moons, "Reporting of artificial intelligence prediction models," *The Lancet*, vol. 393, no. 10181, pp. 1577–1579, 2019.
- [29] G. A. FitzGerald, "Regulatory science: what it is and why we need it," *Clinical Pharmacology & Therapeutics*, vol. 89, no. 2, pp. 291–294, 2010.
- [30] E. A. Akl, J. J. Meerpohl, J. Elliott, L. A. Kahale, and H. J. Schunemann, "Living systematic reviews: 4. Living guideline recommendations," *Journal of Clinical Epidemiology*, vol. 91, pp. 47–53, 2017.
- [31] K. Slim, E. Nini, D. Forestier, F. Kwiatkowski, Y. Panis, and J. Chipponi, "Methodological index for non-randomized studies (minors): development and validation of a new instrument," *ANZ Journal of Surgery*, vol. 73, no. 9, pp. 712–716, 2003.
- [32] A. Stang, "Critical evaluation of the Newcastle-Ottawa scale for the assessment of the quality of nonrandomized studies in meta-analyses," *European Journal of Epidemiology*, vol. 25, no. 9, pp. 603–605, 2010.
- [33] J. Lang and K. Haines, "Clinimetrics: appraisal of guidelines, research and evaluation II," *Journal of Physiotherapy*, vol. 65, no. 3, p. 176, 2019.
- [34] B. J. Shea, B. C. Reeves, G. Wells et al., "AMSTAR 2: a critical appraisal tool for systematic reviews that include randomised or non-randomised studies of healthcare interventions, or both," *BMJ*, Article ID j4008, 2017.
- [35] P. Alonso-Coello, H. J. Schünemann, and J. Moberg, "GRADE evidence to decision (EtD) frameworks: a systematic and transparent approach to making well informed healthcare choices. 1: Introduction," *BMJ*, vol. 353, 2016.
- [36] P. Alonso-Coello, A. D. Oxman, J. Moberg et al., "GRADE evidence to decision (EtD) frameworks: a systematic and transparent approach to making well informed healthcare choices. 2: clinical practice guidelines," *BMJ*, vol. 353, Article ID i2089, 2016.